Characterising the Emissions, Occurrence and Fate of Tyre Wear Particles in Urban Rivers

Victoria Gutierrez Dominguez

PhD

University of York

Environment and Geography

October 2023

Abstract

Tyre and road wear particles (TRWP), generated from the interaction between road surfaces and tyres, are increasingly recognized for their role in microplastic pollution of freshwater systems. The release of these particles into the environment poses potential toxicological risks to aquatic organisms due to both the chemicals added during manufacturing and the adsorption of environmental contaminants. Although annual TRWP emissions have been estimated for various countries, studies simulating TRWP transport through surface runoff to freshwater systems, particularly at high spatial and temporal resolutions, remain limited.

This thesis aims to determine the emissions and exposure of urban aquatic systems to TRWPs at high spatial and temporal resolutions. Firstly, a temporally and spatially resolved model was used to estimate TRWP emissions in the City of York, UK. The exposure modelling used data on tyre particle generation rates, local weather patterns, land cover composition, and wastewater treatment plant characteristics to estimate emissions to different points in York's river system at a daily resolution.

Secondly, a method was developed for the analysis of TRWPs in environmental samples using Py-GC-MS, focusing on pre-treatment procedures to mitigate matrix interferences. The method involved organic matter digestion and TRWP extraction by density separation, which was then tested by analysing sediment samples collected from regions characterized by significant traffic influence.

Lastly, the proposed methodology was employed to investigate the spatio-temporal distribution of TRWP concentrations in York's river sediments. The analysis of sediment samples revealed a wide range of TRWP concentrations attributed to differences in river size, depositional characteristics, and monthly precipitation fluctuations. This study underscores the significance of extended sampling periods for a comprehensive assessment of TRWP and microplastic contamination in the environment, as well as the value of employing multiple methods for the analysis of TRWPs (i.e., microscopy and Py-GC-MS) to cross-reference results and reduce uncertainties.

List of contents

List of contents

List of tables

List of figures

List of Figures

List of Figures

List of Figures

Acknowledgements

First and foremost, I would like to express my sincere gratitude to my supervisors, Prof Alistair Boxall and Dr Colin McClean, who provided guidance and support throughout my entire PhD journey. I want to extend special thanks to Alistair for all his patience and encouragement during a difficult time in my life, where his compassion and understanding made it possible for me to finish.

A big thank you to CONACyT for allowing me to study this PhD, without the financial support, this would not have been possible.

I would also want to thank Prado and Antonia for their time and guidance on the modelling work, as well as all the lab technicians Debs, Rebecca, Blaine, Luke and Emma, whose assistance, especially on my first days in the laboratory, was incredibly helpful.

A special mention to Raymond and Charlotte at the BDC, for all their support during my time working there. It was a real pleasure working with you and I am very grateful for everything I have learnt.

I would also like to express my appreciation to Ale, James, Alizee, Isla, and Luke for their help with my fieldwork, where you transformed hard and long days into enjoyable and fun experiences. In addition, to past and current PhD fellows, Ruochan, Alizee, Ale, Isla, Harriet, Katie and Talia, thank you for your friendship and encouragement, especially during challenging times.

I want to thank my family, especially my mom, Arcelia, for her constant support, unconditional love, and unwavering belief in me. Thank you for providing me with all the necessary tools to achieve everything I have ever wanted in life. I also want to extend my thanks to my second family, Caroline and Alan, for always being there for me and for preparing those delicious meals that made a struggling student very happy.

Acknowledgements

To the most important person in my life, thanks to my loving husband, Ben, who not only drove me to each and every one of my field trips but has been an incredible support during the write-up of this thesis. I will forever be grateful to you for everything you have done to make this goal of mine possible.

Lastly, I would like to dedicate this thesis and all my hard work to my dad, Dr Enrique Gutierrez as he liked to introduce himself, you left us too soon but I hope you are smiling proud from wherever you are.

Declaration

I declare that this thesis is a presentation of original work and I am the sole author. This work has not previously been presented for a degree or other qualification at this University or elsewhere. All sources are acknowledged as references.

Chapter 1. Introduction and literature review

The global generation of plastics (synthetic organic polymers) began in the 1960s (Alves *et al.,* 2023; Blair *et al*., 2019; Duis and Coors, 2016) and since then production has increased exponentially due to the high level of consumption (e.g., in packaging, and single-use products) (Rogers, 2018; Hamid *et al*., 2018). It is the durability and resistance properties of plastics that makes them an environmental concern. This is because plastics will be discarded as waste and accumulate in landfills (Wright *et al*., 2019) where their degradation processes can be very slow, making them available to reach freshwater and marine ecosystems (Blair *et al*., 2019; Horton *et al*., 2017; Dominik, 2015). It has been estimated that the ocean is the final destination of about 4 and 12 million tonnes of plastic per year, which represents almost 5% of the total plastic production in the world (Fig. 1.1) (Rogers, 2018).

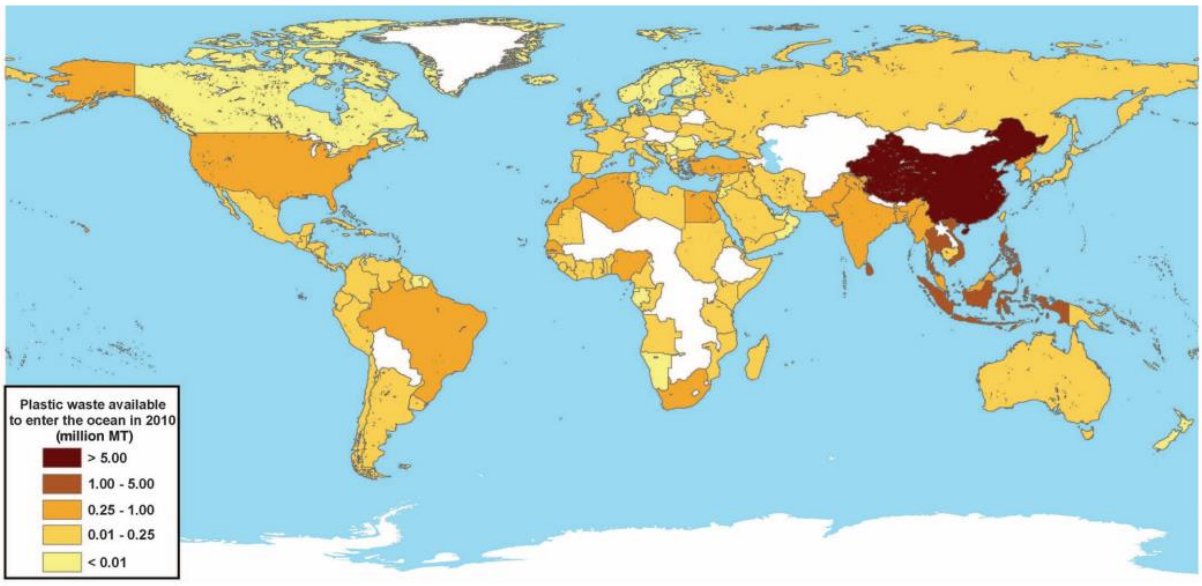

Figure 1.1. Map representing the estimated mass of mismanaged plastic waste available to enter the oceans in 2010. Source: taken from (Jambeck et al., 2015).

Environment contamination by large pieces of plastic has received increasing attention from the scientific community (Blair *et al*., 2019). Even in the most distant and isolated locations, researchers have observed contamination by plastics, including in the Arctic (Emberson-Marl *et al*., 2023; Bergmann and Klages, 2012),

deep sea habitats (Ferreira *et al*., 2023; Schlining *et al*., 2013), the open ocean gyres (Pereira *et al.*, 2023; Dominik, 2015; Cózar *et al*., 2014), and remote islands (Ranborges *et al.,* 2023; Eerkes-Medrano *et al*., 2015; Heskett *et al*., 2012). Most work has focused on marine systems with only a few studies exploring the problem of plastic pollution in freshwater systems even though it has been shown that rivers are heavily contaminated due to their proximity to urban areas and wastewater treatment outflows, which makes them an important source of marine litter (Pogojeva *et al*., 2023; Blair *et al*., 2017; Dris *et al*., 2015).

1.1 Urban contributions of microplastics

Microplastics are defined as plastic particles smaller than 5 mm in size (Forrest and Vermaire, 2023; Compa *et al*., 2018; Gajšt *et al*., 2016; Vandermeersch *et al*., 2015). There are two main sources of microplastics a) primary microplastics, which are particles (< 5 mm) manufactured and produced to be used in domestic and industrial products such as, exfoliating facial-cleansers, cosmetics, toothpastes and resin pellets (Leads and Weinstein, 2019; van der Hal *et al*., 2017) and b) secondary microplastics, which originate from the fragmentation of larger plastic items due to biological, physical and chemical degradation in the environment (Forrest and Vermaire, 2023; Carbery *et al*., 2018). For example, the breakdown of mismanaged plastic litter, release of synthetic fibres from clothes every time they are washed (Blair *et al*., 2019), and wear of road markings, vehicle tyres and paints (Wright *et al*., 2019; Bye and Johnsen, 2019).

Within cities, primary microplastics will enter the environment primarily through point sources (i.e., sources with specific locations from which pollutants are emitted) (Domercq, 2019). In this case, effluents from industrial and municipal wastewater treatment plants are the main point sources in urban environments (Leads and Weinstein, 2019). Additionally, fluxes from combined sewer overflows, that are discharged untreated to surface water during periods of heavy rainfall or when the wastewater treatment system is not functioning correctly, are also a potential significant input of microplastics into rivers (Klein *et al*., 2018).

On the other hand, secondary microplastics will mainly enter the environment from diffuse emission sources (with the exception of fibres from clothes and textiles), which will mainly consist of the particles entering adjacent water bodies through rainfall-induced runoff (Domercq, 2019).

Diffuse inputs are more complex to characterise than that of point sources (Klein *et al*., 2018). This is because they occur over a wider area and there are fundamental gaps of information regarding the process of plastics degradation, which is influenced by several factors such as polymer type and environmental exposure conditions (Blair *et al*., 2019; Burns *et al*., 2018). For instance, the amount of fragmented secondary microplastics will only increase over time due to their continued degradation into ever smaller fragments, resulting in nano-sized particles. This could be the reason why they have evaded focus in the scientific community so far (Burns *et al*., 2018). Nevertheless, findings from monitoring studies, involving microplastic characterization, have consistently shown a higher prevalence of secondary microplastics (e.g., fibres from clothing or fragments of larger plastic items) in the environment compared to primary microplastics (Burns *et al*., 2018).

Siegfried *et al*., (2017) developed a global modelling approach to analyse the principal sources of microplastics entering European river systems and their transport to the sea. As a result, 42% of the microplastics exported by rivers to the seas constituted tyre wear particles, while textile fibres shed during laundry activities occupied the second position with a 29% contribution, both considered to be of secondary origin. In comparison, synthetic polymers in household dust and microbeads present in personal care products were found to account for 19% and 10% of the total exports, respectively (Siegfried *et al*., 2017). This significant variation in the proportion of microplastic emissions could be the result of the reduction and banning of microbeads in self-care products (cosmetics and scrubs) across many developed countries, such as the Netherlands, Canada, the United States, the United Kingdom and New Zealand (Jessieleena *et al*., 2023; Burns *et al*., 2018; Browne *et al*. 2011). Therefore, more attention should be given to understanding the sources, abundance, fate and

impact of secondary microplastics on the environment, mainly in freshwater systems (Horton *et al*., 2017).

1.2 Environmental concerns of microplastics

The small size of microplastics, their transportation processes and durability within the aquatic environment makes them available for ingestion by a wide range of aquatic organisms (Troost *et al*., 2018; van der Hal *et al*., 2017). Several studies both in the natural environment and in laboratory conditions have confirmed the presence of microplastics in the digestive system of marine organisms such as zooplankton, lugworms, mussels, shrimps and fish (Pellini *et al*., 2018). Similar results have been observed in freshwater organisms (Blair *et al*., 2017). Research conducted by Hamid *et al*., (2018) reported that microplastics were found in 30% higher concentrations in fish from urban river environments compared to those from non-urbanized areas. However, research on microplastic debris in freshwaters is still in its infancy (Blair *et al*., 2017).

The effects of microplastic ingestion are thought to be similar to those observed for macroplastics and may include gastrointestinal obstruction, reduced growth rate, laceration, reproductive complications and false satiation resulting in reduced food intake (Jahan *et al.,* 2023; Vandermeersch *et al*., 2015). In addition, these small particles can have toxicological effects on marine and freshwater biota (Jahan *et al.,* 2023; Faure *et al*., 2015). This is due to the incorporation of chemical additives during the manufacturing process (Compa *et al*., 2018) as well as the adsorption and subsequent accumulation of contaminants existing within the surrounding environment (Carbery *et al*., 2018). Contaminants known to sorb to microplastics include persistent organic pollutants (POPs), polychlorinated biphenyls (PCBs), polycyclic aromatic hydrocarbons (PAHs), dichloro-diphenyl-trichloroethane (DDT), and heavy metals (Panti *et al*., 2015). Consequently, these pollutants can be transferred throughout the food web and become a major threat to human health (Jahan *et al*., 2023; Clark *et al*., 2016).

1.3 Characterization of microplastics from road vehicle tyres

Research on microplastics has been mainly directed to thermoplastics (polyethylene (PE), polypropylene (PP), polyamide (PA), polyethylene terephthalate (PET) and polystyrene or styrofoam (PS)) (Wagner *et al*., 2018; Kole *et al*., 2017) and it was not until very recently that rubber was also considered a class of plastic (Kole *et al*., 2017). While there has been ongoing discussion within the scientific community regarding this classification, it is now generally accepted that plastic and rubber, composed of synthetic polymers and various additives, can generate solid particles through degradation or abrasion processes. Hence, both materials are widely acknowledged as potential contributors to microplastic pollution (Baensch-Baltruschat *et al.*, 2021; Klein *et al*., 2018; Verschoor, 2015). There are two types of rubber: natural rubber and synthetic rubber, in general, almost 27 million tonnes of rubber are sold worldwide and 70% of the total consumption goes into tyre production (Kole *et al*., 2017).

1.3.1 Tyre materials

The tyre manufacturing process involves the complex assembly of many elements implementing a wide variety of raw materials (Jekel, 2019; Wagner *et al*., 2018) (Fig. 1.2). When the tyres were first produced, their only ingredient was natural rubber, which was mainly extracted from the Brazilian rubber tree (*Hevea brasiliensis)* (Kole *et al*., 2017). Nowadays, the composition of the rubber compounds might vary according to their application and the manufacturer (Bye and Johnsen, 2019). The exact details on their formulation are unknown due to commercial confidentiality reasons. Therefore, the percentages of different components present in tyres can only be estimated (Verschoor *et al*., 2016).

Estimates suggest that a passenger car tyre will consist mainly of a mixture of natural and synthetic rubber (40%), fillers (30%), reinforcing materials (15%) and, to a lesser extent, accelerators, processing aids, retarders and activators (1 or <1%) (Bye and Johnsen, 2019; Verschoor *et al*., 2016). Every individual component in the tyre will undergo meticulous development to fulfil specific needs in relation to flexibility,

durability, and grip. Furthermore, long links of both metal and synthetic cable are also used (Garg *et al*., 2000).

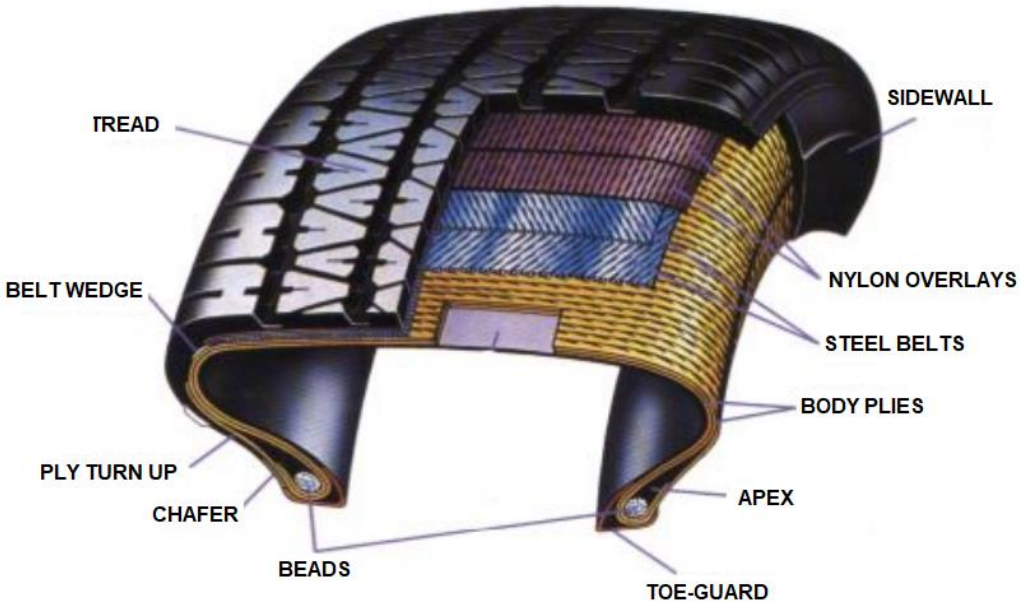

Figure 1.2. Illustration of the composition of a passenger vehicle tyre. Source: taken from (Bye and Johnsen, 2019).

The vulcanisation process is an integral part of tyre production, as it is where the sulphur incorporated into the rubber compounds forms bonds between the polymer chains and gives the tyre its desired shape, size and tread design (Wagner *et al.,* 2018; Wik and Dave, 2009). During this process accelerators are used to increase the number of links (between sulphur bridges and polymer chains), activators will help trigger the accelerators (Zinc oxide is generally used as activators) (Baensch-Baltruschat *et al.*, 2020; Councell *et al*., 2004), and retarders will prevent oxygen or heat from degrading the rubber (Pant and Harrison, 2013; Wik and Dave, 2009). Moreover, carbon black is a very common filler used to improve tyre strength and make them resistant to UV light degradation; however, sometimes it has been replaced by silica to reduce road resistance (Sommer *et al*., 2018; Verschoor *et al*.,

2016). Finally, aromatic oil is added to improve the tyre flexibility and wet grip performance (Table 1.1) (Kole *et al*., 2017).

Road vehicle tyre tread refers to the part of the tyre that makes contact with the road surface (Wik, 2008) and its composition can be different from that of the whole tyre (Verschoor *et al*., 2016). Treads mainly consist of blends of natural rubber (NR), styrene-butadiene rubber (SBR), and polybutadiene (PBD) (Sommer *et al*., 2018; Pant and Harrison, 2013; Wik, 2008).

The composition of a tyre varies based on its intended application. For example, tyres used on trucks and buses typically consist of 80% natural rubber (NR). This is due to the fact that the vulcanization process involving raw natural rubber, sulfur, and carbon black filler results in exceptional elasticity and flexibility, providing the tear strength and heat resistance required for heavy-duty vehicles (Wagner *et al*., 2018). In contrast, passenger car tyres predominantly contain styrene-butadiene rubber (SBR) as the primary component, with only 15% being natural rubber (NR) (Eisentraut *et al*., 2018; Verschoor *et al*., 2016).

Table 1.1. Composition of passenger tyre tread. Source: adapted from (Bye and Johnsen, 2019; Wik and Dave, 2009; Wik, 2008).

Component/additive	**Ingredients**	**Content (wt-%)**
Rubber/Elastomer	Synthetic and natural rubbers: Poly-butadiene (BR), styrene-butadiene (SBR), neoprene isoprene (NR), and polysulphide	40-60
Reinforcing agent (filler)	Carbon black and silica	20-35
Process oils/extender oils	Mineral oils: High aromatic oils rich in poly aromatic hydrocarbons (PAHs)	15-20
Vulcanisation agents	S, Se, Te, thiazoles, organic peroxides, and nitro-compounds	1-2
Vulcanisation activators	Zinc oxide Stearic acid	1.5 1
Vulcanisation accelerators	Lead, magnesium, zinc, calcium oxides and sulphur compounds	0.5

Protective agents	Preservatives (halogenated cyanoalkanes), anti-oxidants (amines, phenols), anti-ozonants (diamines and waxes) and desiccants (calcium oxides)	1
Processing aids	Peptizers, plasticizers (synthetic organic oils and resins), and softeners	<1

1.3.2 Tyre and road wear particles generation

Road traffic emissions are one of the main contributors of particulate matter (PM) concentrations into the environment, especially in densely populated areas (AQEG, 2019; Pant and Harrison, 2013). PM emissions can be classified into two main categories: exhaust and non-exhaust emissions. Exhaust emissions originate from the incomplete combustion of fuel that is emitted through the tailpipe. On the other hand, non-exhaust emissions are produced through abrasion processes, which involve the tear and wear of various vehicle parts such as, tyres, brakes, clutches, and road surfaces (AQEG, 2019; Grigoratos and Martini, 2015; Pant and Harrison, 2013).

Previous research has mainly focused on fine particles (PM < 2.5 μm) within exhaust emissions, which have been strongly associated with respiratory diseases through inhalation, including conditions like emphysema, bronchitis and asthma (Verschoor *et al*., 2016). As a consequence, over the past few decades, many regulations and technological improvements have been implemented to reduce emissions from vehicle exhaust pipes (Verschoor *et al*., 2016; Pant and Harrison, 2013).

Conversely, non-exhaust emissions have been associated to the release of coarse particles (>PM10), that become trapped in the pavement. However, there are still some knowledge gaps regarding their physicochemical characteristics, emission factors, transport processes and their potential effects on aquatic organisms (Grigoratos and Martini, 2015). In addition, it has been demonstrated that fine and ultrafine particles also originate from non-exhaust emissions. Despite the fact that exhaust emissions can be significantly reduced in the future, it is estimated that over

80% of total road traffic emissions in the fine and coarse modes will still arise from non-exhaust sources (Sommer *et al*., 2018; Pant and Harrison, 2013).

Tyre wear particles are generated through the abrasion that occurs when the tread surface of the tyre interacts with the road pavement while the tyre is rolling (Jekel, 2019; Bye and Johnsen, 2019; Verschoor *et al*., 2016). This is a complex physicochemical process that leads to the generation of particles with varying sizes and composition (Jekel, 2019). A small fraction of the tyre wear (less than 5%) becomes airborne, while the majority is deposited on the road surface or within close proximity to the roadside (approximately around 30 meters) (Baensch-Baltruschat *et al*., 2020; Wik and Dave, 2009). The amount of tyre wear and therefore formation of tyre wear particles will depend on several factors such as, weather conditions, driving style, and tyre and road surface characteristics (Table 1.2) (Verschoor *et al*., 2016; Wik and Dave, 2009; Councell *et al*., 2004). For instance, studies have indicated that roads made of concrete contribute to higher tyre wear emissions compared to asphalt pavements. Moreover, the wear rate increases in urban areas compared to rural regions due to the frequent acceleration and braking cycles that occur in city environments (Verschoor *et al*., 2016; Wik, 2008). In general, a tyre may experience a loss of roughly 10% of its total mass during its lifetime (Pant and Harrison, 2013).

Table 1.2. Factors influencing the composition of tyre wear. Source: adapted from (Jekel, 2019; Panko et al. 2018; Verschoor et al., 2016).

Factor	**Characteristics**
Tyre	Size (radius/width/depth), tread depth, construction, pressure and temperature, contact patch area, chemical composition, accumulated mileage and alignment

Vehicle	Weight, distribution of load, location of driving wheels, engine power, electronic braking systems, suspension type, state of maintenance, power/unassisted steering, and type of vehicle (light good vehicle or heavy good vehicle)
Road surface	Road material (asphalt/concrete), aggregate rocks, binder (bitumen, cement), texture pattern and wavelength, road dust loading in surface texture, porosity, condition, wetness and surface dressing
Vehicle operation	Speed, linear acceleration, radial acceleration, frequency and extent of braking and cornering

Tyre wear particles are composed not only of the pure tyre material but also include contributions from the tyre tread, the pavement, and other particles deposited on the road (Unice *et al*., 2013). These hetero-aggregates of worn material are termed tyre and road wear particles (TRWPs) (Klöckner *et al*., 2019). According to Unice *et al*., (2013) TRWPs are composed of 50% tread polymer and 50% mineral encrustations from the roadway (Table 1.3) (Unice *et al*., 2013). Due to interactions with other particulate matter, TRWPs behave differently than other microplastics and can be difficult to detect and quantify in environmental matrices (Bye and Johnsen, 2019; Kole *et al*., 2017).

Table 1.3. General composition analysis of particles as determined by thermogravimetric analysis (% mass). Source: taken from (Verschoor et al., 2016; Kreider et al., 2010).

	Outdoor tyre and road wear particle (RP)[1]	**Laboratory tyre and road wear particle[2]**	**Tread composition[3]**
Plasticizers and oil (%)	13	10	19
Polymers (%)	23	16	46
Carbon blacks (%)	11	13	19
Minerals (%)	53	61	16

[1]Tyre and road wear particles: collected during outdoor driving, which contain contributions from tyres, as well as other sources (i.e., fuel, brakes, pavement, atmospheric deposition, etc.): [2]Tyre wear particles: collected on a simulated laboratory driving course; [3]Tread particles: cryogenically ground from pieces of unused tread.

Laboratory studies, whether conducted for ecotoxicological investigations or the analysis of physicochemical properties of tyre wear particles, have used materials generated through various methods. For example, these methods include: 1) replicating "real" on-road driving conditions, accounting for the enrichment of tread particles with mineral encrustations and pre-existing road dust from the pavement surface; 2) employing a road simulator within a laboratory setting; or 3) manually generating wear particles from a used tyre using a steel brush or sandpaper (Wagner *et al*., 2018). Consequently, the size, shape and composition of the produced particles might differ from each other (Wagner *et al*., 2018). Therefore, careful consideration should be given to the chosen technique for the study, as only the first method truly replicates driving conditions.

There is a concern that TRWPs could be highly toxic and potentially serve as a carrier for other substances, such as heavy metals, in the environment (Baensch-Baltruschat *et al*., 2020; Pant and Harrison, 2013). Furthermore, TRWPs found in soil and aquatic systems contribute to the leaching of polycyclic aromatic hydrocarbons (PAHs) and other harmful additives, posing a risk to organisms due to their teratogenic and mutagenic properties (Verschoor *et al*., 2016). As a result, minimizing non-exhaust emissions from tyre wear becomes crucial (Eisentraut *et al*., 2018; Verschoor *et al*., 2016).

1.3.3 Physical properties of tyre and road wear particles

1.3.3.1 Size

Tyre and road wear particles will have complex shapes and different size distributions, which will determine their fate in the environment (Wagner *et al*., 2018). According to Wagner *et al*., (2018) TRWP can be classified into ultrafine (PM0.1), fine (PM2.5) and coarse (PM10) particles. It is estimated that a small fraction, approximately 0.1 to 5%, will be emitted as fine/ultrafine particles, while the majority of the abraded rubber is likely to be released in the form of larger particles that will be deposited onto the road surface (Wik and Dave, 2009). Differing from PM10 particles, fine particles from tyre and road wear are primarily composed of carbon, while ultrafine particles appear to be made up of minerals, oils, and fillers (Wagner *et al*., 2018).

According to Verschoor *et al*. (2016), the coarse fraction of TRWP released into the environment typically falls within the size range of 10 and 400 µm. This particle size distribution depends on a variety of factors, including road material, (i.e., concrete or asphalt), temperature, wetness, speed and the age of the tyre (Kole *et al*., 2017). Additionally, the reported size ranges in a given study are also influenced by the method employed for the tyre particles formation (i.e., cryogenically ground tyre particles), the conditions under which sampling occurs, and the specific analytical equipment used (Fig. 1.3) (Jekel, 2019). For example, if the lower limit for particle detection is 10 µm, then the smaller fraction may be lost (passing the pores of filters), therefore, the reported size distributions would not be representative of all worn particles (Jekel, 2019). Furthermore, Kreider *et al*. (2010) conducted an analysis on the sizes of TRWPs resulting from the interaction between various passenger car tyres and asphalt-based pavements within a road simulator. Their study demonstrated the variation in the size distribution of these particles, highlighting the influence of the method of analysis used. For instance, when laser diffraction is used, the size distributions ranged from 5 µm to 220 µm, centred around a mode of 75 µm. In comparison, volume size distributions as determined by transmission optical microscopy varied from 4 µm to 350 µm, with a mode centred at 100 µm. Overall, the

size pattern of TWP showed a bimodal distribution, characterized by peaks at approximately 5 µm and 25 µm (with a range of 4 - 350 µm) (Kreider *et al*., 2010).

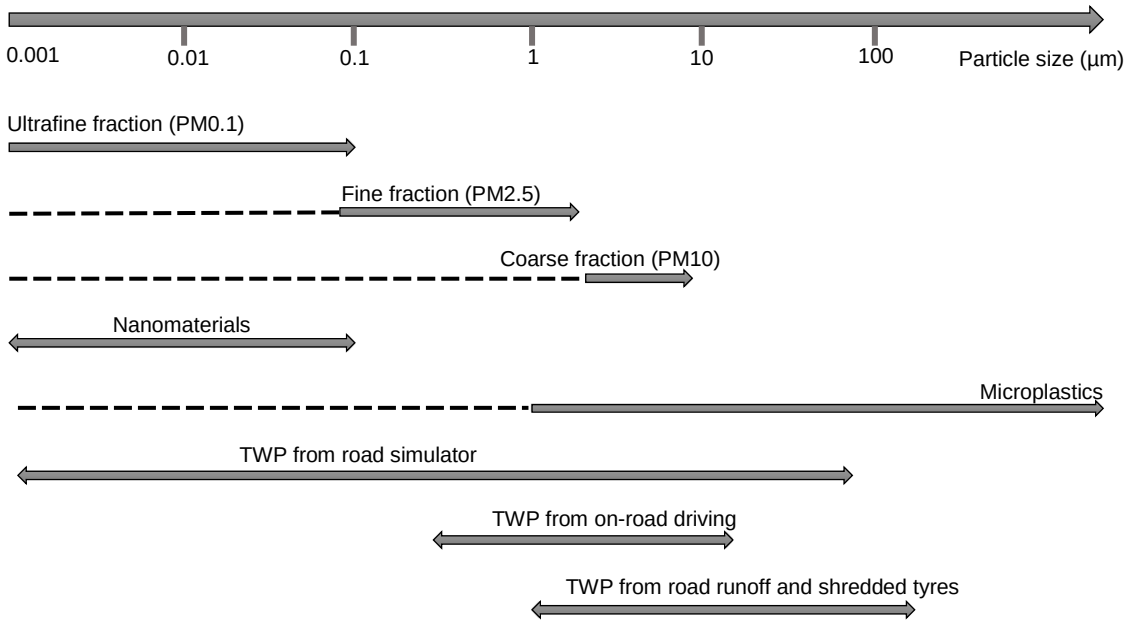

Figure 1.3. Particle size ranges and obtained TWP size distributions. Source: taken from (Wagner et al., 2018).

In addition Kovochich *et al*., (2021b) reported different size ranges for various environmental sample types through the application of single particle analysis (SPA), a methodology that involves employing chemical mapping techniques. Their investigation revealed that TRWPs from tunnel dust samples displayed an average particle size of 54 µm by number and 94 µm by volume (ranging from 8 to 315 µm), while road dust exhibited an average TRWP particle size of 158 µm by number and 224 µm by volume (ranging from 6 to 649 µm). Conversely, environmental sediment TRWPs presented an average particle size of 267 µm by number and 506 µm by volume (ranging from 11 to 1588 µm) (Kovochich *et al*., 2021b).

Unice *et al*., (2019) developed a modelling methodology to estimate TRWP fate and transport in the Seine (France) watershed. Here they established that the mean

diameter (size) of TRWPs for direct emissions to soil and water was 105 µm (with a lower and upper limit of 0.5 – 200 µm, respectively). In the process of conducting sensitivity analysis on the model, it was determined that the proportion of tyre and road wear particles transported to the estuary exhibited increased sensitivity to changes in TRWP diameter and density values. Furthermore, the potential influence of biofilms on facilitating the transport of TRWPs to the estuary aligned with the inherent uncertainty surrounding TRWP size (Unice *et al*., 2019b).

Based on these studies, it becomes evident that existing literature shows a pronounced diversity in the size distribution of tyre and road wear particles. As such, further investigation is necessary to comprehensively characterize TRWP size distributions across different environmental compartments. This holistic understanding of particle sizes generated under authentic driving conditions is essential for enhancing the accuracy in predicting the fate and transportation of TRWP within the environment (Kole *et al*., 2017).

1.3.3.2 Morphology

The morphology of TRWP has been described in many scientific publications as an elongated “sausage-like” shape with rough surfaces (due to the mineral incrustations from the road) (Fig. 1.4) (Jekel, 2019; Pant and Harrison, 2013; Kreider, 2010). The presence of carbon black in the tread particle gives the TRWP its dark colour, making its visual detection challenging as it can easily blend in with other dark particles in the environment (Bye and Johnsen, 2019). As mentioned above, the morphological characteristics of TRWPs are complex and will be influenced by many external factors, for example, the methodology used for their generation (Table 1.4).

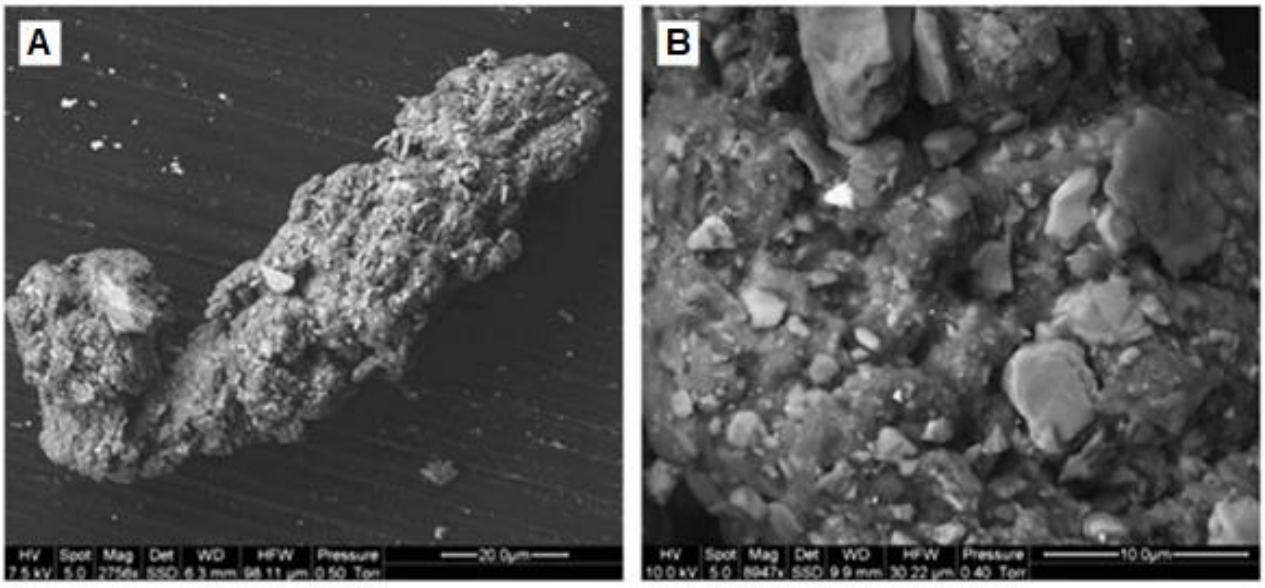

Figure 1.4. Scanning electron microscope images of TRWP. Mineral incrustations are evident in the photo magnification (B). Source: taken from (Kreider et al., 2010).

Table 1.4. Morphologies of tyre materials obtained under various sampling conditions. Source: taken from (Wagner et al., 2018).

Sampling conditions	**Morphology**	**Reference**
Road runoff, road simulator, shredded tyres	Elongated, circularity 0.83, aspect ratio 0.64	(Kreider *et al*., 2010)
Road simulator	Jagged, droplets, granules	(Gustafsson *et al*., 2008)
Road simulator, road runoff	Warped, porous	(Camatini *et al*., 2001)
Road runoff	Irregular	(Wang *et al*., 2017)
Road simulator	Near spherical, elongated	(Dahl *et al*., 2006)

Kreider *et al*. (2010) examined the physical properties of tyre and road wear particles produced using different techniques, including the simulation of driving conditions in a laboratory, collection of particles from “real” on-road driving, and cryogenic generation of tread particles. The comparison of the TRWPs generated through the three methodologies revealed that the TRWPs from laboratory generation and on-road collection exhibited nearly identical morphologies, characterized by an

elongated shape and the presence of minerals. In contrast, the cryogenically generated tread particles displayed a more irregular shape (Jekel, 2019; Kreider *et al*., 2010). Similarly, the morphologies of TRWPs observed within different environmental matrices, including road dust, tunnel dust and sediment, presented elongated shapes with an aspect ratio greater than 1.5 (Kovochich *et al*., 2021b).

In addition, Kim and Lee, (2018) analysed the characteristics of pure tyre wear particles produced by a tyre simulator setup (i.e., comprising sandpaper, a drum and a tyre). Their study concluded that larger TRWPs (in the micron-size range) had an elongated morphology, while submicron-sized TWPs inclined towards a predominantly round or irregular shape (Kim and Lee, 2018).

1.3.3.3 Density

Plastics exhibit a wide range of densities influenced by their composition and manufacturing processes (Stride *et al.*, 2024). Among commonly produced plastic polymers such as PE, PP, PVC, PS, PA, PET, densities typically range from 0.88 to 1.4 g/cm^3 (Stride *et al.*, 2024). However, most studies analysing microplastic pollution in surface waters primarily focus on lower density microplastics, typically ranging from 0.88 to 1.02 g/cm^3, due to their tendency to float in aquatic environments (e.g., Carbery *et al*., 2018; Pedrotti *et al*., 2016). In comparison, the density of TRWPs is considered to be much higher due to their hetero-aggregated material (road particles and minerals) (Klöckner *et al*., 2019). Tyre rubber has a density of approximately 1.15 g/cm^3, whereas the density of cement and asphalt roadway pavement materials is estimated to be 2.4 g/cm^3 (Bye and Johnsen, 2019). Additionally, the density of quartz is anticipated to align closely with that of mineral particles at 2.65 g/cm^3 (Klöckner *et al*., 2019). Consequently, the density of tyre and road wear particles collected from the road surface will depend on their final composition (i.e., the fraction of mineral encrustation), resulting in a density range from 1.7 to 2.1 g/cm^3 (Vogelsang *et al*., 2019).

In a recent investigation conducted by Unice *et al*. (2019) to assess the transport of TRWPs within the Seine basin, the density of TRWPs was estimated to be 1.8 g/cm^3.

This value was determined based on the assumption, as documented in literature sources, that TRWPs comprise an equal proportion of 50% tread material and 50% mineral particles originating from the pavement (Unice *et al*., 2019). Furthermore, Klöckner *et al*. (2019) provided additional validation for the density estimate of 1.8 g/cm³. They achieved this by isolating TRWP from road runoff sediment using a sodium polytungstate (SPT) solution with a density of 1.9 g/cm³, demonstrating that over 90% of the TRWP present in the sample exhibited a density below 1.9 g/cm³.

The density of TRWPs plays an important role in their dispersion within the environment (Verschoor *et al*., 2016). With the higher densities of tyre wear particles relative to water (ranging from 0.9 to 1 g/cm^3), it is reasonable to deduce their tendency to settle and accumulate within sediment, particularly when undergoing heteroaggregation with other suspended particulate matter (Van Cauwenberghe *et al*., 2015). Nonetheless, during periods of elevated flow rates and turbulence in the river, tyre particles might also be present in the water column facilitating their transportation over extended distances (Verschoor *et al*., 2016). Furthermore, due to the constituents of rubber and carbon black, it is projected that TRWPs, once introduced into the environment, exhibit persistence and undergo a slow degradation process over time (Wagner *et al*., 2018).

1.3.4 Chemical composition of tyre and road wear particles

Their formation processes, leading to a different composition from the makeup of the original tyre material, will define the chemical constitution of TRWPs. The particle size fraction will play an important role in determining its final chemical composition (Table 1.5) (Wagner *et al*., 2018). For example, a study conducted by Kwak *et al*. (2013) investigated the chemical composition of tyre wear particles produced under various driving conditions, differentiating between the coarse and fine modes. The results indicated elevated levels of Zn, Fe, and Ca in the coarse fraction emitted during constant speed and cornering events. In contrast, the fine fraction emitted under similar conditions exhibited higher concentrations of Fe, Ca, Ti, Ba, and Sb (Kwak *et al*., 2013).

Due to their chemical composition, TRWPs released into aquatic environments pose a potential risk to organisms. This threat can arise from the direct presence of TRWPs as particulate entities or from the potential leaching of toxic substances that could migrate into the aqueous phase (Wagner *et al*., 2018). The principal substances capable of leaching from TRWPs include heavy metals (Zn, Cu, Cd, Cr, and Pb), organic compounds such as PAHs and benzothiazoles, and their transformation products such as 6PPD and 6PPD-quinone (Khan *et al*., 2024; dos Santos *et al*., 2019; Pant and Harrison, 2013; Bian and Zhu, 2009; Gualtieri *et al*., 2005). Aquatic organisms, including *Daphnia magna,* have been shown to be negatively affected following exposure to organic additives found in tread particles, which may contain antidegradants of phenylenediamine types, benzothiazolic accelerators, or specific process oils (Wik and Dave, 2009). Refer to section 1.8 for further details on how TRWPs impact aquatic biota.

Table 1.5. Chemical characterization of wear particles. Source: taken from (Wagner et al., 2018).

	$PM_{2.5}$	**$PM_{2.5-10}$**	**Wear particles**
Brake wear	Transition metals (Cu, Fe), Sb (III, V), Sn, Ba, Zr, Al, S	FeO, Fe_2O_3, Cu oxides, Sb (III), Sb (V), Sn, Ba, Zr, Al	Cu, Fe, Sb (III, V), Sn, Ba, Zr, Al, S, PAHs, n-alkanes, n-alkanoic acids, benzaldehydes
Tyre wear	Zn, organic Zn, Cu, S, Si, Organic compounds, Al	Zn, organic Zn, Cu, Si, Fe, Ba, Sb, Ti	Zn, Fe, Ca, Cu, S, Si, PAHs, benzothiazoles, natural resins, n-alkanes, n-alkanoic acids, natural resins

Several studies have underscored the significant toxicity of zinc at elevated concentrations and its extensive presence in the environment (Bye and Johnsen, 2019; Councell *et al*., 2004). Zinc emissions into the air and aquatic environments originate from many sources, such as break wear, tyre wear, combustion exhaust, galvanized parts, fuel and oil (Councell *et al*., 2004). Nevertheless, among all traffic-related sources, it has been recognized that tyre wear is the main contributor to zinc emissions (Harrison *et al*., 2012). In a study carried out by Schauer *et al*., (2006), a

Chemical Mass Balance Model was used to determine the contribution of three sources to zinc emissions: exhaust emissions (gasoline tailpipe), brake wear and tyre wear. The outcome revealed that the predominant share of zinc emissions was associated with tyre wear. This compares closely with the results obtained in other studies, where it was found that approximately 60% of the total Zn load present in sediment samples originated from tyre-wear particles (Councell *et al*., 2004).

In Great Britain alone, the annual release of zinc from tyre particles is expected to be 1,435 g Zn/km (Councell *et al*., 2004). On the other hand, emissions of PAHs to the environment are mainly attributed to sources other than tread wear, including asphalt, automobile exhaust and fuel combustion products (Kumar *et al*., 2013). In fact, Kreider *et al*., (2010) reported that road particles and TRWPs exhibited significantly higher PAH concentrations, up to 95%, compared to tread particles. In addition, in January 2010 a new European regulation was enforced to encourage the use of low-PAH alternatives in the tyre industry, aiming to reduce oils with high PAH content. Consequently, new tyres are anticipated to incorporate these low-PAH options (Wik and Dave, 2009).

1.4 Estimation of TRWP emissions from automobile traffic

TRWP emissions at the global and regional scale have been calculated using two different approaches (Kole *et al*., 2017). One approach uses vehicle kilometres travelled, total mileage and emission factors (EF) (Luhana *et al*., 2004; Baumann and Ismeier, 1998). An emission factor is considered the mass of tyres released from the wear process per unit time/distance travelled (Pant and Harrison, 2013). Emission factors for TRWP are usually expressed in milligrams per kilometre (Klein *et al*., 2018).

The characterization of tyre and road wear emissions can lead to the calculation of emission factors, however, results can vary depending on sampling conditions, traffic intensity and the methodology used for the study (i.e., dynamometer, roadway tunnel, and remote sensing) (Pant and Harrison, 2013). Consequently, the emission factors reported in several studies cover a wide range, as shown in Table 1.6 (Wagner *et al*., 2018). For example, TRWP emission factors for passenger cars can range between

53 to 200 mg/km, while for lorries, the range extends from 105 to 900 mg/km and for heavy good vehicles from 1000 to 1500 mg/km (Hillenbrand *et al*., 2005). This leads to the estimation of significantly varied tyre wear emissions, making comparisons between studies unfeasible. For this reason, it is essential to standardize the emission factors for each type of vehicle and road. Emission factors for road transport will be differentiated by vehicle category and road type. The first has to do with the weight of the vehicle and the number of tyres. For example, articulated lorries that weigh more than 20 tonnes and have approximately 12 tyres will generate more TRWPs than passenger cars whose weight averages 1,302 kg and only have four tyres (Klein *et al*., 2018). Therefore, the emission factor of articulated lorries will be higher. Furthermore, a road classification is also made when determining the specific EF of the vehicle class. Urban areas, rural roads and highways will contribute differently to tyre and road wear emissions due to differences in speed limits and driving conditions. As a result, roads in cities have higher emission factors due to the constant acceleration and braking cycles and cold starts associated with systems with multiple traffic lights (Klein *et al*., 2018).

The emission factor per vehicle-km approach has been used in most of the available studies on tyre wear. The following annual TRWP emissions have been reported using this method: Netherlands 8,834 tonnes/year (Verschoor *et al*., 2016), Sweden 11,619 tonnes/year (Magnusson *et al*., 2016), Norway 7,520 tonnes/year (Sundt *et al*., 2014), Denmark 7,660 tonnes/year (Lassen *et al*., 2015), Germany 111,420 tonnes/year (Hillenbrand *et al*., 2005) and USA 1,524,740 tonnes/year (Kole *et al*., 2017). It is worth noting that the calculation of TRWP emissions has primarily focused on European countries, among which the Netherlands stands out with the lowest per capita emission of TRWP at 0.52 kg/year. On the other hand, the United States exhibits significantly higher per capita emissions compared to the other countries, with a value of 4.7 kg/year, where 66% of its total emissions were attributed to urban areas (Kole *et al*., 2017; Wagner *et al*., 2018).

Table 1.6. Comparison of the emission factors (EF) used to calculate the generation of TRWP in urban roads.

	Emission Factor (mg/Km)									
Vehicle type	(Kole *et al.*, 2015) Netherlands	(Verschoor *et al.*, 2016) Netherlands	(Magnusson *et al.*, 2016) Sweden	(Sundt *et al.*, 2014) Norway	(Luhana *et al.*, 2004) Norway	(Lassen *et al.*, 2015) Denmark	(Kole *et al.*, 2017) Denmark	(Hillenbrand *et al.*, 2005) Germany	(Baumann and Ismeier, 1998) Germany	(Kole *et al.*, 2017) China
Moped		13						22.54		7
Motorcycle		60						45		7
Passenger car	100	132	50	132	100	132	100	90	80	132
Van		159								132
Lorry	495	850	700					700	189	
Truck		658								
Bus		415	700					700	192	
LGV		159				204	204	180	180	204
HGV	600	850		712	712	712	712	1200	270	1068

The second method for calculating the emissions of tyre wear involves the number of discarded tyres and their weight loss during use (Lassen *et al*., 2015). This approach can only be implemented in regions where worn out tyres have been collected and processed by the manufacturer, as is the case of many European countries (Kole *et al*., 2017). For example, in 1996, the Environmental Agency of the United Kingdom (UK) made an estimation regarding tyre wear based on the weight of the 37 million tyres discarded during that year. They approximated the amount to be around 380,000 tonnes, taking into account the assumption that a car tyre typically experiences a weight loss of approximately 10-20% during its usage. By employing this calculation method, the annual TRWP emission for UK was within the range of 38,000-76,000 tonnes (Kole *et al*., 2017). Other countries that have calculated TRWP emissions using the tyre number weight loss approach are Italy and Japan, where the total amount of tyre wear calculated was 50,000 tonnes/year and 239,762 tonnes/year, respectively. (Yamashita and Yamanaka, 2013; Milani *et al*., 2004).

1.5 Pathways of TRWP into the environment

Once TRWP are generated, their relevant pathways are classified into: atmospheric dispersion, retention on the road surface, roadside soil deposition, runoff to sewerage systems (WWTP) and release into surface water (Fig. 1.5) (Furuseth and Rødland, 2020; Wagner *et al*., 2018).

Fine particles are commonly released into the atmosphere and are susceptible to dispersion by airflows (Kole *et al*., 2017). In contrast, larger particles tend to settle onto road surfaces, with a percentage of them becoming entrapped and others being washed-off by rainwater runoff, ultimately finding their way into soils, sewers, or surface waters (Kole *et al*., 2017). In urban settings, rainwater can flow directly into surface waters without undergoing any treatment *via* separate sewers, or it can enter combined sewers, potentially reaching wastewater treatment facilities (Jekel, 2019). The implications of climate change include increased rainfall frequency and intensity, resulting in combined sewer overflows (CSOs), thus leading to an increase in the number of spills (Jekel, 2019). These spills involve the uncontrolled release of untreated sewage and stormwater directly into aquatic ecosystems, representing a significant source of water pollution. On the other hand, in rural areas and along highways, runoff management involves the implementation of swales and ditches, and stormwater treatment systems, respectively (Jekel, 2019).

TRWPs that are transported to roadside soils become intricately integrated into the soil matrix, acting as an important sink and potential sites for degradation processes (Jekel, 2019). A previous study, which examined TRWP concentrations in sediment samples and roadside soil across three watersheds, indicated that when samples were categorized by population density, concentrations in roadside soil averaged around 70% higher compared to sediment levels. Furthermore, these elevated concentrations in surface soils were particularly registered within a distance of less than 3 meters from the road compared to greater distances (Unice *et al*., 2013).

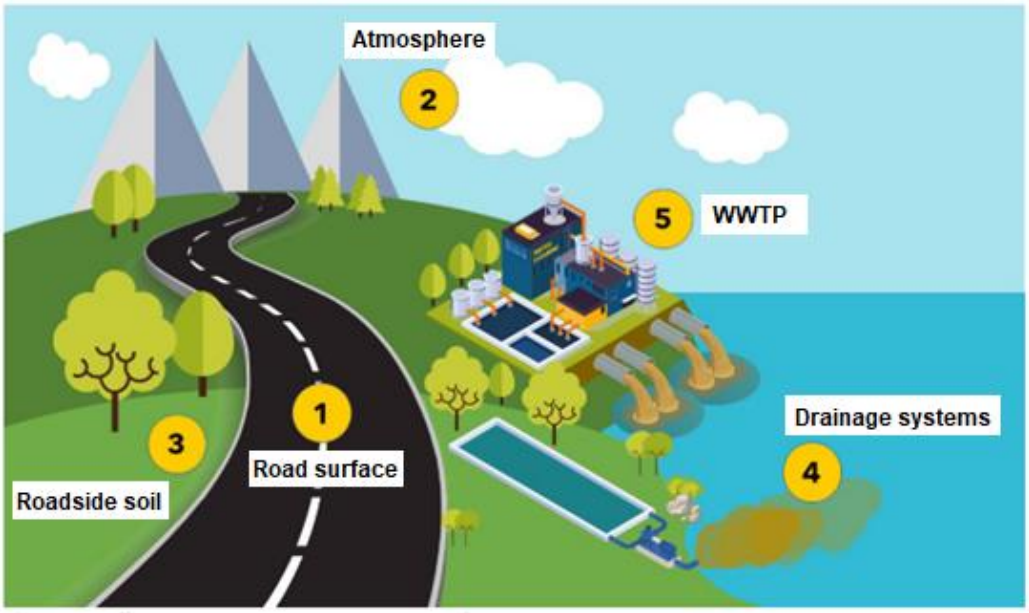

Figure 1.5. Illustration of the five main pathways for tyre particles from the road surface to the environment Source: adapted from (Furuseth and Rødland, 2020).

1.6 Analytical methods to determine concentrations of TRWP in the environment

The recognition of the occurrence of TRWPs across various environmental matrices, along with the potential environmental risks they pose, has resulted in the development of robust analytical techniques aimed at their detection and quantification. However, the task of reliably determining TRWP concentrations in environmental samples remains an ongoing challenge (Mattonai *et al*., 2022).

Several studies have confirmed that spectroscopic methods commonly employed for the detection of microplastics in environmental samples, such as Fourier-transform infrared (FTIR) and Raman techniques, are not suitable for the analysis of tyre wear particles (Eisentraut *et al*., 2018). This is attributed to their small particle size and the absorption of IR light caused by the dark colour of the particles resulting from the inclusion of carbon black as a filler component. Consequently, a distinct ATR spectrum is generated, characterized by a downward slope (Leads and Weinstein, 2019; Eisentraut *et al*., 2018). For this reason, alternative approaches for the analysis of TRWP in the environment have been explored, including indirect methodologies

focused on the use of markers (Wagner *et al*., 2018). Various tyre components have been employed as markers. Examples include elements resulting from the vulcanization process such as zinc and sulphur, as well as organic molecules generated as by-products during vulcanization, including benzothiazoles, 2-(4-morpholinyl) benzothiazole (24MoBT) and N-cyclohexyl-2-benzothiazolamine (NCBA) (Mattonai *et al*., 2022; Wik and Göran, 2009).

Kovochich *et al*., (2021a) developed a methodology to identify TRWPs originating from road simulators, employing a combination of different analytical techniques such as X-ray spectroscopies (SEM-EDX) and time-of-flight secondary ion mass spectrometry (ToF-SIMS) mapping. This approach consisted of evaluating distinct aspects of TRWPs, encompassing their morphological attributes (including elongated/round shapes with mineral encrustations), elemental surface characteristics (highlighting the presence of S + Zn/Na ± Si, K, Mg, Ca, and Al) and organic markers (specifically C6H5 + and C7H7 +). The same authors also employed this protocol for the analysis of TRWPs in road dust, tunnel dust, and sediment environmental samples (Kovochich *et al*., 2021b). Furthermore, Klöckner *et al*. (2019) devised a technique to assess TRWP levels in samples collected from road environments by using Zn as the elemental marker. Their methodology involved segregating the zinc present within the organic component of TRWP from the denser inorganic road dust, which is unrelated to tyre wear, *via* density separation before conducting ICP-MS analysis. Quantification of TRWP concentrations was achieved by measuring the mass of Zn in the buoyant fraction, considering that tyres typically contain 8.7% Zn and assuming that TRWP consist of 50% tyre material (Klöckner *et al*., 2019).

Despite the advancements achieved through the methodologies mentioned above, which have enhanced the accuracy of elemental markers through approaches like density separation or cross-validation *via* multiple analytical techniques, the potential for overestimating TRWP concentrations remains. This is due to the non-specificity of several markers, including Zn, S, and C7H7 +, to rubber polymers (Kovochich *et al*., 2021a; Panko *et al*., 2018; Hillenbrand *et al*., 2005). For instance, various sources

such as oil, combustion exhaust, deicing salts, road barriers, and galvanized street furniture contribute to the presence of Zn in urban environments, making them components of runoff water as well (Baensch-Baltruschat *et al*., 2020; Klöckner *et al*., 2019; Unice *et al*., 2013). On the other hand, molecular markers like NCBA and 24MoBT might lead to an underestimation of TRWP concentrations due to their susceptibility to degradation and leaching in the environment. Additionally, their presence in tyres could exhibit variability depending on the manufacturer (Mattonai *et al*., 2022).

Given the inherent limitations of previous markers, recent research has focused on the use of polymeric markers for the quantification of TRWP concentrations. These markers are considered more reliable due to their high specificity to tread, high abundance in tyre wear particles and stability in the environment (Unice *et al*., 2013). Advance thermo-analytical techniques have been reported in the literature for the detection of the main decomposition products of rubber materials employed in tyre production (Mattonai *et al*., 2022; Wik and Göran, 2009). For example, Unice *et al*. (2013) calculated tyre and road wear particle concentrations in sediments from three different watersheds (France, Japan and the United States) using Pyrolysis coupled to gas chromatography and mass spectrometry (Py-GC-MS) analysis. The markers used were dipentene for natural rubber (NR) and vinylcyclohexene for styrene-butadiene rubber (SBR) and butadiene rubber (BR). They also incorporated a deuterated polymer internal standard to account for potential matrix effect. The assumption of a 15% market average styrene content for SBR+BR used in treads was adopted to convert the overall polymer concentration to tread polymer concentration. Moreover, polymer proportions of 44%, 45%, and 50% were taken into account for SBR, NR, and SBR+BR+NR, respectively. This led to the identification of TRWPs in 97% of the 149 sediment samples collected (Unice *et al*., 2013).

Furthermore, Eisentraut *et al*. (2018) introduced an automated thermal extraction desorption gas chromatography−mass spectrometry system (TED−GC−MS) capable of swiftly identifying and quantifying thermoplastic polymers and tyre wear particles, all with minimal sample preparation. The analysis resulted in the identification of

various marker compounds for tyre tread particles (Fig. 1.6). Among these, SBR, the main constituent in passenger car tyres, emerged as the most abundant marker, demonstrating exceptional sensitivity and specificity attributed solely to tyres, without any other environmental sources. Conversely, while NR, the primary elastomeric compound found in truck tyres, was detected across all samples, the study concluded that assessing NR in environmental samples is not advisable due to the interference of decomposition products from environmental matrix compounds (such as plant material) (Eisentraut *et al*., 2018).

Peak Assignment	Structure	Substance	Characteristic fragment ions	Retention time in min	Parental Elastomer
	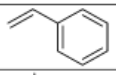	Styrene	104, 78, 51	7.2	SBR
	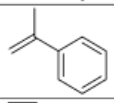	Methylstyrene	118, 103, 78	9.6	
	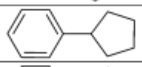	Cyclopentylbenzene	117, 104, 146, 91	16.6	
		Cyclopentenylbenzene	144, 129, 115	17.8	
SB		Cyclohexenylbenzene	104, 158, 129, 115	19.6	
SBB		Phenyl-[4.4.0]bicyclodecene	104, 91, 156, 212	26.8	
But2	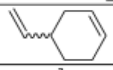	Vinylcyclohexene	79, 54, 93, 108	5.6-6.4	SBR, BR
But3	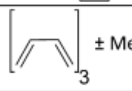	Trimers of Butadiene & Homologues	91, 148, 162, 176	13.1-21.7	BR
Iso2	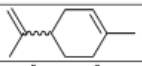	Dipentene	68, 93, 121, 136	11.0	NR
Iso3	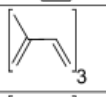	Trimers of Isoprene	119, 162, 189, 204	21.5-23.3	
Iso4	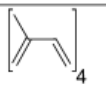	Tetramers of Isoprene	121, 93, 134, 272	31.0-36.0	

Figure 1.6. Summary of identified decomposition products for elastomer and tyre materials using TED−GC−MS. Source: taken from (Eisentraut et al., 2018).

1.7 Modelling approaches of tyre and road wear particles

Microplastics are commonly transported from rivers to the marine environment, constituting a significant pathway for marine contamination. Nonetheless, there exists

a general lack of knowledge concerning the emissions, fate, and transport of microplastics within freshwater systems (Besseling *et al*., 2017). Several different modelling approaches have been developed in the last 10 years for engineered nanoparticles (ENPs) in marine and freshwater systems (e.g., Domercq *et al*., 2018; Praetorius *et al*., 2012; Gottschalk *et al*., 2013; Gottschalk *et al*., 2010; Gottschalk *et al*., 2011; Dale *et al*., 2015a; Dale *et al*., 2015b; De Klein *et al*., 2016; Kumar *et al*., 2011; Markus *et al*., 2016; Meesters *et al*., 2016; Nowack, 2017; Sun *et al*., 2015), as well as nano- and microplastics in the marine environment (e.g., Ballent *et al*., 2012; Enders *et al*., 2015; Everaert *et al*., 2018; Critchell and Lambrechts, 2016; Chubarenko *et al*., 2016; Griffin *et al*., 2018; Lebreton *et al*., 2012; Siegfried *et al*., 2017) and nano- and microplastics in rivers (e.g., Unice *et al*., 2019; Besseling *et al*., 2017; Nizzetto *et al*., 2016; Meesters *et al*., 2014; Siegfried *et al*., 2016; van Wezel *et al*., 2015) (Table 1.7). Nevertheless, among the riverine models, only the frameworks introduced by Nizzetto *et al*. (2016) and Besseling *et al*. (2017) have demonstrated the capability to replicate the transport of plastic debris within freshwater rivers at high spatial and temporal resolution. However, it is important to note that these models have not yet undergone validation using empirical data for nano- and microplastics (Wagner and Lambert, 2018).

Table 1.7. Comparison of the main features of the currently existing plastic debris models for freshwater systems. Source: table taken from (Wagner and Lambert, 2018).

Type of Model	**Plastic size range**	**Media included**	**Processes included**	**Spatial Resolution**	**Temporal Resolution**	**Reference**
Mass flow model	Microplastics	Effluents	Emissions (personal care products), plastic removal in WWTP	Zero-D	Steady state	(van Wezel et al., 2015)
Global modeling	Microplastics	Water	Emissions (personal care products, fibres and car tyres), plastic removal in WWTP, during river transport and by water abstraction	1° latitude by 1° longitude (input) and basis totals (output)	Annual totals	(Siegfried et al., 2016)

Multimedia models	Nanoplastic (<100 µm), microplastic	Air, water, soil, sediment	Assumed emissions (1,000 t)	Zero-D	Steady state	(Meesters et al., 2014)
Spatiotemporally explicit models	Microplastic, 0.005 – 0.5, separated in five size classes	Soil, effluents, water, sediment	Emissions from sewage sludge, surface runoff, WWTP effluents, advection, settling, resuspension, store depletion	10,000 km^2 divided in eight segments	Daily, simulation for 2008 - 2014	(Nizzetto *et al*., 2016)
Spatiotemporally explicit model	Nano- and microplastics	Water, sediment	Assumed emissions upstream, advection, dispersion, biofouling, aggregation, degradation, settling, resuspension, burial	40 km river stretch divided in 477 segments of on average 87.7 m	0.01 day, modeled until steady state was reached	(Besseling et al., 2017)

Only a few recent modelling studies have estimated tyre and road wear particle emissions and fate in freshwater systems. For example, Unice *et al*., (2019) developed an integrated model approach, which is the first study so far to estimate the transport of TRWPs from their terrestrial generation to their export to the estuary. The temporally and geospatially resolved mass balance modelling methodology account for TRWP emissions and their transport into different environmental compartments (atmosphere, roadside soils, and surface waters). Once TRWPs reach freshwater systems, transport processes such as particle heteroaggregation, degradation and sedimentation are considered. Results for the Seine watershed in France showed a TRWP emission of 27,607 tonnes/year and per capita of 1.8 kg/year. This represents 18% of the total emissions in the area (75,291 tonnes/year). Furthermore, only 2% of the TRWPs discharged into the river were exported to the marine environment, where the Seine was attributed a capture efficiency of 90% (Unice *et al*., 2019).

Another recent study that estimated the emissions of tyre wear particles on German roads was conducted by Baensch-Baltruschat *et al*., (2021). To calculate TRWP emissions two sets of different emission factors and the vehicle-km approach were used. Environmental pathways such as air, soils and surface water were considered, as well as the sewerage system in urban areas. As a result, it was estimated that approximately 75,200–98,400 tonnes/year of coarse particles are generated in

Germany, where 66-76% (57,300–65,400 tonnes/year) were transported to roadside soils and 12-20% were discharged into the aquatic environment. The fate and transport of the TRWPs in the river was not considered due to the lack of data (Baensch-Baltruschat *et al*., 2021).

1.8 Effects of TRWP on biota in the aquatic environment

The predominant focus of studies investigating the effects of TRWPs on aquatic organisms has primarily revolved around the toxic compounds released from the particles (leachates) (Table 1.8), often neglecting the consideration of various environmental compartments such as the water column, sediment, and soil (Wagner *et al*., 2018). The toxicity of TWP leachate has been attributed to the presence of polyaromatic hydrocarbons (PAHs), trace metals (Pb and Cd), benzothiazole derivatives, phthalates, phenolic derivatives, aromatic amines and resin acids, with a notable emphasis on Zinc (Wagner *et al*., 2018; Wik *et al*., 2009). In addition, the leaching potential of the toxic compounds of the rubber material will be associated with the size and shape of the tyre particle (dos Santos *et al*., 2019).

In a recent study conducted by Tian *et al*. (2022), the objective was to analyse leachate from tyre wear particles (TWP) and examine its toxic constituents, aiming to identify the main factor responsible for the significant mortality observed among Pacific Northwest coho salmon (*Oncorhynchus kisutch*). Through assessing peak area abundances and exposure to juvenile coho, the researchers effectively prioritized and detected potential toxic substances. These included plasticizers, antioxidants, emulsifiers, and various transformation products, some of which are recognized environmental pollutants. The study conclusively identified 6PPD-quinone as the principal causal toxicant underlying decades of stormwater-linked acute mortality among coho salmon (LC50 ≈ 0.8 µg/L). This concentration corresponds to levels found in actual freshwater environments, such as the Seattle region, where 6PPD-quinone concentrations ranging from 0.8 to 19 µg/L have been observed during storm events, thus validating the findings of this research (Tian *et al*., 2022).

Table 1.8. Toxicity of leachates of tread wear particles to aquatic organisms. Source: table taken from (Wik and Dave, 2009).

Test species	Effect concentration (EC/LC_{50} in mg/L)	Comment	Reference
Green algae	470; 1,640	72-h EC_{50}	Gualtieri *et al.,* (2005)
(*Pseudokirchneriella subcapitata*)	50-2,800	72-h EC_{50}	Wik *et al.,* (in press)
Water flea (*Daphnia magna*)	26,750; 53,300	48-h EC_{50}	Gualtieri *et al*., (2005)
	300-32,000	24-h EC_{50}	Wik and Dave (2005)
	100-2,400	48-h EC_{50}	
	60-400	48-h + 2h UV light EC_{50}	
	1,200->10,000	24-h EC_{50}	Wik and Dave (2006)
	300->10,000	48-h EC_{50}	
	370-7,500	48-h EC_{50}	Wik *et al.,* (in press)
Water flea (*Ceriodaphnia dubia*)	550-5,000	48-h EC_{50}	
	50-3,600	9d survival EC_{50}	
	10-1,800	9d young/female EC_{50}	
Zebrafish eggs (*Danio rerio*)	550->10,000	48-h EC_{50}	
Frog embryo (*Xenopus laevis*)	50,000-100,000	27-80% mortality 120-h exposure	Gualtieri *et al*., (2005)

In addition, Khan *et al*. (2019) assessed both acute and long-term toxicity by introducing dispersed tyre wear particles to *Hyalella azteca* in a freshwater environment. They observed that *H. azteca* consumed the tyre particles, retaining them within their digestive system for 24-48 hours (Fig. 1.7). Following a 21-day exposure period, the freshwater organism demonstrated significant sensitivity, particularly at the highest concentrations (500-2000 particles/mL), resulting in a substantial mortality rate of 93%. Although the highest TWP concentrations employed in this study do not reflect actual environmental conditions, the findings contribute to our understanding of TWP toxicity, emphasizing the need for ecotoxicological studies to encompass an examination of the effects posed by the tyre particles themselves, extending beyond the scope of merely assessing leachate compounds (Khan *et al*., 2019).

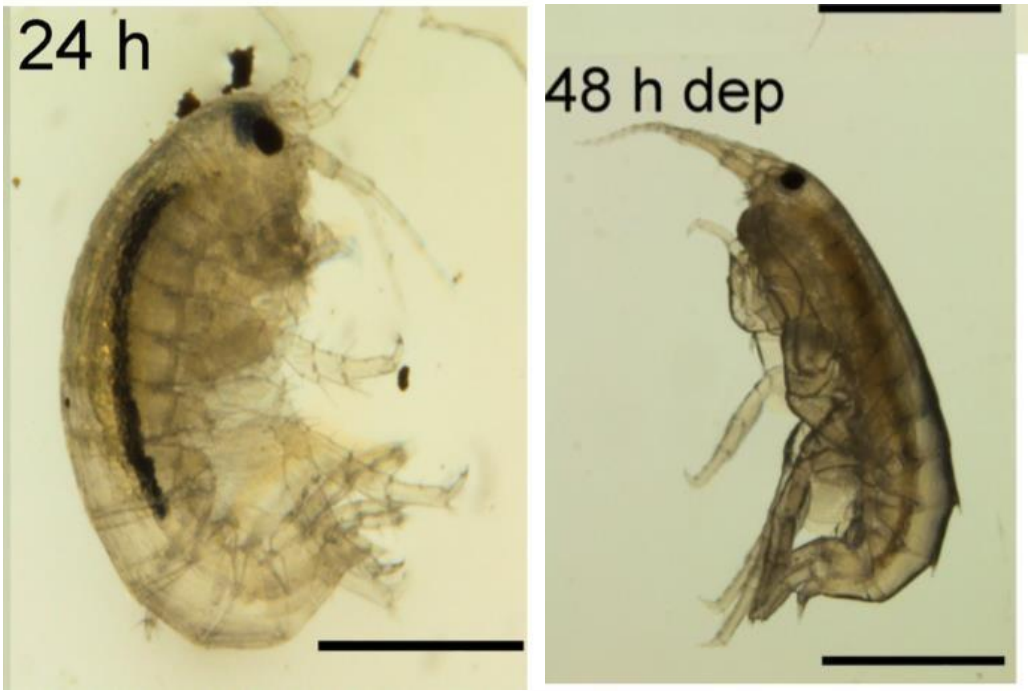

Figure 1.7. Hyalella Azteca ingesting TWP over 24h followed by 48h depuration. Source: taken from (Khan et al., 2019).

The primary concern for human health stems from the inhalation of airborne TRWPs (<PM 10). Particularly noteworthy are studies that have subjected human lung cell cultures to these particles, revealing evidence of DNA damage and provoking inflammatory reactions (Baensch-Baltruschat *et al*., 2020). Currently, a notable gap in information exists concerning potential health risks linked to the integration of TRWPs into the food chain. Nonetheless, the possibility of risk could emerge from consuming ungutted fish or bivalves, given the widely reported presence of microplastics in these organisms (Baensch-Baltruschat *et al*., 2020).

While the documentation of toxic effects has been limited to a few select species, the presence of TRWPs or their leachates in the environment continues to raise concerns, especially in anticipation of the increasing emissions every year. This underscores the rationale for extensive research on TRWPs within the environmental context.

1.9 Conclusion

This chapter has reviewed a wide range of aspects related to the characterization of TRWPs – from their generation on road surfaces to their dispersion into the environment. Additionally, the existing modelling approaches to estimate TRWP emissions and predict their fate in the environment, as well as the methodologies commonly employed to detect TRWPs in environmental matrices have been reviewed. This comprehensive review has identified important knowledge gaps that have driven the motivation behind this thesis.

Firstly, among these gaps is the need of reliable data on the physicochemical properties of TRWPs, including their size distributions, density characteristics, and interactions with other particles across various environmental compartments, with a notable dearth of such information in river sediments. These insights are critical in refining the precision of our predictions regarding the transport and fate of TRWPs within the environment.

Secondly, there is a need for enhancements in analytical techniques to accurately quantify TRWP concentrations in diverse environmental settings. Furthermore, real-world measurements of TRWP concentrations in freshwater systems are notably lacking, underscoring the necessity for more comprehensive field studies, particularly considering the significant role of river sediments as “sinks” for TRWPs.

Lastly, the absence of local emission and fate models for TRWPs at high spatial and temporal resolutions, coupled with the necessity for their validation using real-world monitoring data, highlights another knowledge gap.

These identified gaps not only emphasize the need for further research but also serve as the guiding objectives of this thesis, aiming to address these knowledge deficiencies and contribute to a more comprehensive understanding of TRWPs in our environment.

1.10 Aims and objectives

The overall aim of this thesis was to determine the emissions and exposure of urban aquatic systems to Tyre Wear Particles at high spatial and temporal resolutions. This was addressed using the following specific objectives:

(1) To develop a model that estimates tyre and road wear particles emissions into various environmental compartments at high temporal and spatial resolution, and implement the model to a specific case study city (York) (Chapter 2).

(2) To develop a methodology for the separation and analysis of tyre and road wear particles from sediment samples by Pyrolysis-GC/MS (Chapter 3).

(3) To conduct a year-long monitoring study in the York freshwater system to determine tyre and road wear particle concentrations in sediment samples and their characterization by microscopy analysis (Chapter 4).

(4) To evaluate the accuracy of the emission model in relation to TRWP concentrations in sediment samples (Chapter 4).

The work on these objectives is described in three experimental chapters:

Chapter 2 introduces a localized TRWP emissions model parameterized specifically for the city of York in the United Kingdom. This includes the development of a traffic model designed to calculate the average annual daily traffic flow for various vehicle types on each road within the study area. Through the integration of traffic data and pertinent TRWP generation and release processes, this model forecasts the spatial and temporal distribution of TRWP exposure across the city. As a result, it identifies and highlights emission hotspots of particular concern within the urban context of York.

Chapter 3 presents the development of an analytical methodology for quantifying TRWP concentrations in sediment samples. It describes a systematic approach including sample collection, pre-treatment, and preparation, along with the intricate

process of internal standard preparation and calibration curve generation for Py-GC-MS analysis. The efficacy of this method was tested through its application to samples sourced from high-traffic areas, and the results regarding TRWP concentrations are presented.

Chapter 4 presents the implementation of the Py-GC-MS protocol to analyse the concentrations of TRWP in sediments from the river system in York. The results of the spatial (11 locations across the rivers Ouse and Foss) and temporal (across five time points within a year) variations of the monitoring study are presented and discussed. The chapter also evaluates the accuracy of the emission model by comparing its results with TRWP concentrations in sediment samples. In addition, the outcomes from a microscopy analysis for the detection, characterization and quantification of TRWP and other microplastics are delivered. Multiple statistical analysis are conducted, and the resulting findings are discussed.

A final Chapter **(Chapter 5)** provides a summary of the results in alignment with the initial aims and objectives. Furthermore, this chapter presents recommendations for the reduction of TRWP emissions and provides guidance for future research.

Chapter 2. Estimation of emissions of tyre and road wear particles to urban aquatic systems

2.1 Introduction

Traffic related emissions are classified into exhaust and non-exhaust. Non-exhaust emissions, which include road, tyre and brake wear, have gained increasing attention in the scientific community in recent years (Baensch-Baltruschat *et al*., 2020; Panko *et al*., 2018; Amato *et al*., 2014a). This can be attributed to the contribution of PM10 from non-exhaust emissions to the atmosphere, which has been estimated to be as high as exhaust emissions in urban areas (Bukowiecki *et al*., 2010). Tyre wear particles originate from the contact between the tyre tread and the road. These particles will be generated mainly in the coarse fraction and deposited on road surfaces whereas less than 5% will be airborne emissions (Liu *et al*., 2021; Pohrt, 2019). Kreider *et al*., (2010) described the morphology of tyre wear particles and established that they not only consist of tyre tread material, but also include mineral incrustations from the road and fine dust from other traffic emission sources. These agglomerations of particles are collectively referred to as tyre and road wear particles (TRWP) (Gehrke *et al*., 2020). According to Rødland *et al*., (2022) the proportion of mineral encrustation within TRWP collected from road dust varies from 6% to 53%, a range influenced by factors such as driving patterns and traffic flow. For their research, they considered varying levels of mineral encrustation: a minimum (6%), an average (30%), and a maximum (53%) encrustment. These levels were employed in the calculation of TRWP mass using Pyrolysis GC-MS (Rødland *et al*., 2022). Furthermore, Sommer *et al*., (2018) investigated the characteristics of super-coarse (> 10 µm) airborne particles mobilized by wind. Their findings highlighted a notable contrast in particle encrustation between tyre particles collected from a motorway and those from an urban road, revealing proportions of approximately 10% and exceeding 50% by volume respectively. This distinction primarily stems from variations in driving speeds. In urban settings, the tyre tread particles undergo repetitive cycles of gradual roll-over processes due to frequent instances of stopping and acceleration. Conversely, on motorways, the air turbulence generated by vehicles travelling at high

speeds limits the availability of road surface material for accumulation on the tyre particles (Sommer *et al*., 2018).

Tyre and road wear particles have recently been considered a type of microplastic due to their polymer content (i.e., styrene-butadiene rubber and vulcanized natural rubber), solid state, and particle size range (1–1000 µm) (Baensch-Baltruschat *et al*., 2021; Hartmann *et al*. 2019). Several studies have identified tyre and road wear particles as a major source of microplastics in freshwater systems and marine environments (Bondelind *et al*., 2020; Siegfried *et al*., 2017; Magnusson *et al*., 2016). For example, Sundt *et al*. (2014) assessed primary and secondary microplastic emissions for Norway and reported that tyre dust was the largest contributor to microplastic concentrations in the Baltic Sea. Similarly, Lassen *et al*. (2015) conducted an evaluation of microplastic releases into Denmark's aquatic environment. They found that primary microplastics accounted for 0.9% (equivalent to a total emission of 460 – 1,670 t/year) of the overall emissions, with personal care products contributing 0.1%. In contrast, secondary microplastics constituted the majority, making up 98% of the emissions. Among these, tyre particles were identified as the leading contributor at 60% (resulting in a total emission of 4,200 – 6,600 t/year) (Lassen *et al*., 2015).

Conversely, when conducting a model analysis aimed at estimating the worldwide riverine transfer of microplastics to marine ecosystems, the primary contributor to microplastics export from rivers was identified as the fragmentation of macroplastics (i.e., mismanaged plastic waste). Nonetheless, emissions of tyre wear particles emerged as the secondary source in this context (van Wijnen *et al*., 2019).

Once tyre and road wear particles have been generated on roads they will be distributed into different environmental compartments. The main emission pathways for TRWP are soils, air, sewerage system and directly into surface water (Verschoor *et al*., 2016). According to Wagner *et al*. (2018) roadside soils are expected to be heavily contaminated with runoff emissions of tyre and road wear particles, mainly in rural roads and highways where sewerage systems are lacking. The presence of TRWP in soils will depend on the traffic volume and is directly linked to the distance

from the road. As this distance increases, TRWP concentrations gradually decline (Sieber *et al*., 2020). Notably, approximately 80% of tyre wear particles are detected within a 5-meter range from the road along highways, while other roads exhibit concentrations within the range of 1 to 3 meters (Baensch-Baltruschat *et al*., 2020). In addition, sewage sludge from waste water treatment plants (WWTP) has been employed as a fertiliser in agricultural practices in many European countries (Baensch-Baltruschat *et al*., 2021). This has resulted in the reintroduction of finer and smaller TRWP and other contaminants into the soil, further increasing the ecological risk, particularly if these particles are subsequently washed into aquatic environments (Li *et al*., 2022; Baensch-Baltruschat *et al*., 2020).

In comparison, TRWP runoff emissions in urban areas will mainly enter the sewage system and be transported to a waste water treatment plant by combined sewers or discharged directly into surface waters (Sieber *et al*., 2020). During heavy rain events, the carrying capacity of the combined sewers is exceeded. This means that the wastewater collected from households as well as the storm water from roads will be released into rivers without any treatment (Baensch-Baltruschat *et al*., 2021).

TRWP that reach surface waters become available for ingestion by aquatic organisms due to their small size, potentially affecting their digestive system (Sieber *et al*., 2020). Furthermore, tyres are composed of a combination of natural and synthetic rubber, carbon black, vulcanisation activators, and other additives (Lee *et al*., 2020). This composition raises concerns about the potentially high toxicity of TRWP, which could also act as a carrier of heavy metals (Pant and Harrison, 2013). For example, Wik and Dave (2009) observed acute toxicity in aquatic organisms, such as *Daphnia magna,* when exposed to leachates from tread particles.

Estimates of annual TRWP emissions have been calculated for multiple countries (particularly in Europe) using either the method that considers annual vehicle mileage and emission factors (EF), or the approach based on the yearly weight loss from overall tyre usage due to abrasion (Kole *et al*., 2017). However, according to Baensch-Baltruschat *et al*. (2020) a significant portion of the research has primarily centred on the total generation of TRWP on roads, often without meticulously

considering their subsequent dispersion into various environmental compartments. In addition, these studies have typically explored emissions at the regional level where spatial and temporal variations are overlooked (e.g., Sieber *et al*., 2020; Wagner *et al*., 2018; Lassen *et al*., 2015; Sundt *et al*., 2014).

This study aims to assess exposure to tyre and road wear particles in urban aquatic environments at high spatial and temporal resolution by analysing their generation, accumulation, and transport processes using an integrative modelling approach for the city of York in the UK. These findings can help identify locations and times of high emissions (hot spots) enabling more accurate exposure and risk assessment and the targeting of future management approaches, such as improved road runoff treatment.

2.2 Methodology

The modelling framework proposed by Domercq *et al*. (2018) for estimating exposure to engineered nanoparticles (ENPs) in urban environments was modified to estimate TRWP emissions in the city of York, UK. The proposed framework uses a bottom-up approach (from the source to the receptor) where factors such as local weather patterns, land cover composition, wastewater treatment plants, sewerage systems etc. are considered at a high spatial and temporal resolution. The steps in the modelling included: 1) a city analysis – urban zoning and river reach delimitation, 2) collection of traffic flow data of the city of York (vehicle kilometres travelled) and 3) modelling of emissions – where processes such as tyre and road wear particle generation, accumulation on the roadway, and wash-off during rainfall events, were calculated to obtain the TRWP emission rates across the city over time.

2.2.1 Case study

The city of York is in the northeast of England (latitude of 53°96'N and longitude of 1°09'W) (Fig. 2.1). It contains approximately 654 km of roadways and had a population of 208,163 in 2017 (https://www.york.gov.uk). This study area was selected because of the availability of temporally and spatially resolved urban information, such as traffic volumes, sewage and drainage networks and local meteorological data. Moreover, York has two main rivers, the Ouse and the Foss,

which flow through the city and converge downstream of the city centre, making them accessible for monitoring studies (Domercq, 2019).

Within the simulated area, the city is served by three WWTPs. The treatment plant called Walbutts, located northeast of the city, releases treated effluent into the river Foss. Meanwhile, the river Ouse receives discharges from two other WWTPs: Rawcliffe, situated northwest of the city, and Naburn, which presents the highest capacity and is located to the south of the city. These three facilities collectively serve a population of 20105, 28022 and 168594 respectively (Burns, 2018).

York is surrounded by an outer ring road, approximately three miles from the city centre. While this boundary was initially considered the limit of the modelled area, additional municipalities such as Strensall, Poppleton, Haxby, Bishopthorpe, and Naburn were also incorporated in the model. These municipalities are also served by the aforementioned WWTPs, as mentioned in the study by Domercq (2019).

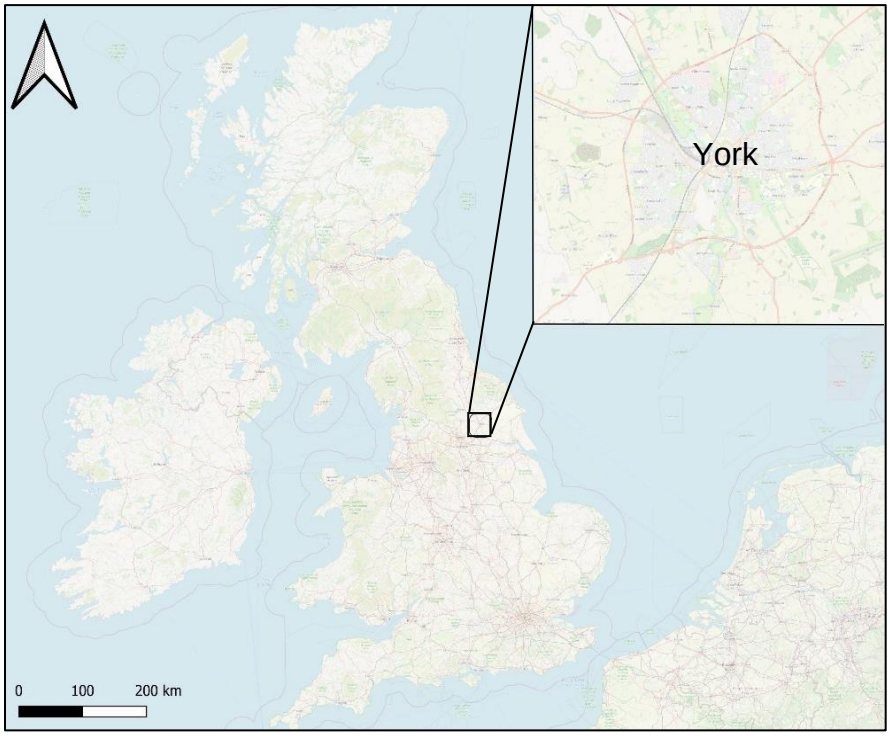

Figure 2.1. Map of the United Kingdom showing the location of the city of York in northeast England.

2.2.2 Model overview

2.2.2.1 City analysis: urban zoning and river reach delimitation

A high spatial resolution was achieved by the manual subdivision of the city of York into 12 sub-catchment areas, considered here as hydrological zones (HZs) and the delimitation of the city's freshwater systems (i.e., rivers Ouse and Foss) into 10 river sections (RS), by using the Open Source Geographic Information System - QGIS 2.18.13 with GRASS 7.2.1 software (Fig. 2.2).

The location of the WWTPs and their discharge points along with the junction of the rivers Ouse and Foss in the city centre were the main factors influencing the selection of the river reaches. On the other hand, the delimitation of the HZs was guided by the analysis of the study area's digital elevation map (DEM) (obtained from the online map and data delivery service Digimap) and the complete city drainage network maps. The network maps include the foul, surface and combined sewer networks, as well as the combined sewer overflow (CSO) and storm water outlet (SWO) locations (obtained from Yorkshire Water Services Limited). See Domercq *et al*. (2018) for an extensive explanation of the creation of the hydrological zones and river sections.

It was assumed that TRWPs emitted in each hydrological zone would be discharged into their corresponding river section (Table 2.1), enabling the identification of particle emission hot spots within the studied urban area.

Table 2.1. Connections between Hydrological zones, river sections and WWTPs serving the city (Domercq et al., 2019).

River Section	HZ connection	WWTP connection (population served)
OUSE 1	HZ 1	-
OUSE 2	HZ 2	Rawcliffe (28,022)
OUSE 3	HZ 3	-
OUSE 4	HZ 4	-
OUSE 5	HZ 5 + HZ 6	-
OUSE 6	HZ 11 + HZ 12	Naburn (168,594)
FOSS 1	HZ 10	Walbutts (20,105)
FOSS 2	HZ 9	
FOSS 3	HZ 8	
FOSS 4	HZ 7	

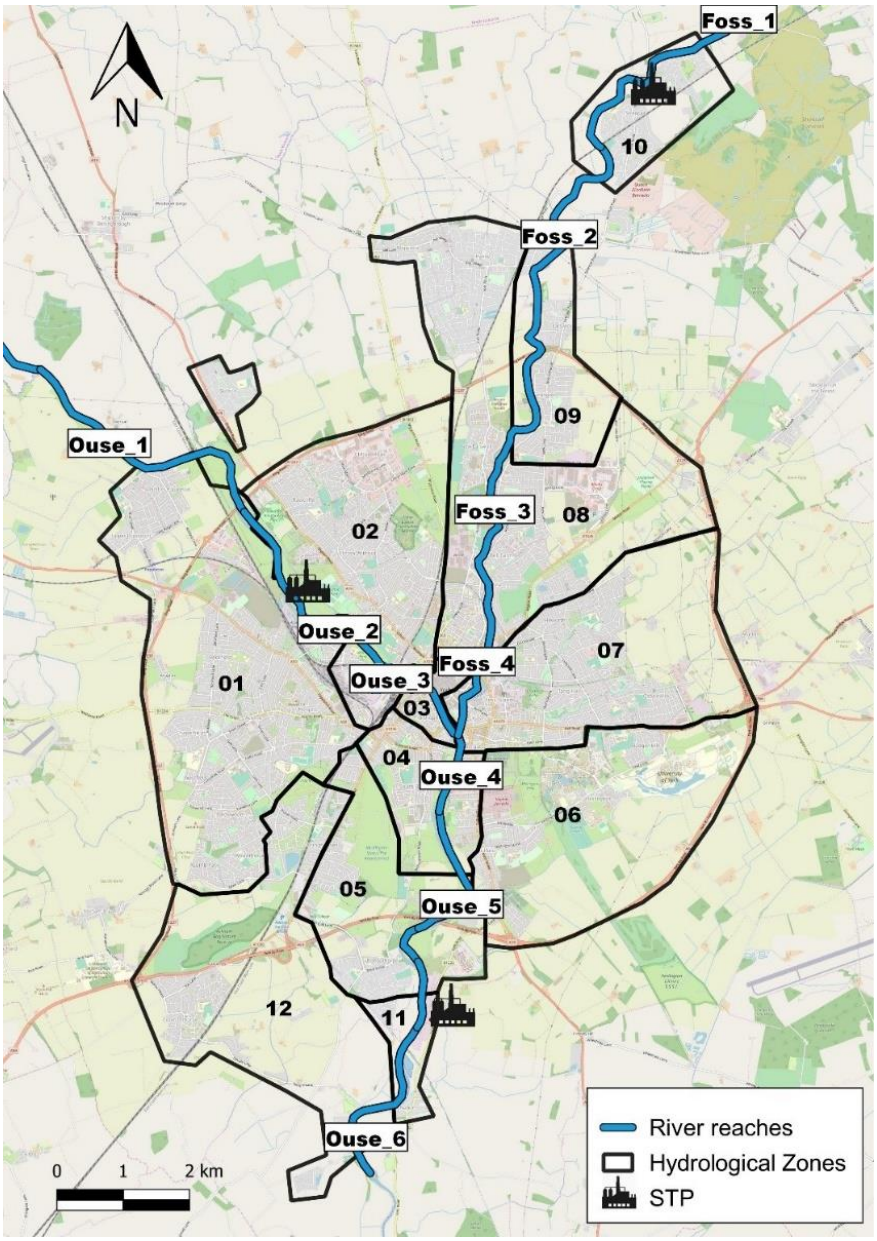

Figure 2.2. Map of the study area showing the hydrological zones and river sections as well as the location of the sewerage treatment plants.

2.2.2.2 Traffic data

Tyre and road wear emissions generated on roads were calculated based on mileage of vehicles and emission factors (EFs) reported in the literature (Baensch-Baltruschat *et al*., 2021). For the city of York, traffic data was available from the Department of Transport (https://roadtraffic.dft.gov.uk/local-authorities/202). This database consists

of the average annual daily traffic flow (i.e., number of vehicles that travel past a count point on an average day of the year) for various types of vehicles (i.e., cars, buses, light good vehicles and heavy good vehicles) at 72 count points located on some major and minor roads. As traffic information for most roads in the city was unavailable, a model was developed to estimate traffic flows based on the data collected from these 72 count points.

To achieve the developed model, a map of vector lines and a map of vector points (nodes) for Yorkshire and the Humber area were downloaded from Ordnance Survey (https://www.ordnancesurvey.co.uk/) and were used to create a vector network of the area for further analysis (Fig. 2.3A). This was possible using the function v.net in GRASS GIS 7.6.0. Secondly, the function v.net.centrality was used to compute 'closeness and betweenness centrality' for each node of the vector network. This is a measure of how often a node is a bridge between other nodes. The map of vector lines and the new map containing the betweenness centrality value, were then exported as a shape file to be further analysed in the Open Source Geographic Information System QGIS 2.18.13 with GRASS 7.2.1 software (Fig. 2.3B).

In QGIS the count points from the traffic database were projected as a delimited text file and then the function v.net.distance was used to find the shortest distance between the count points and the nodes in the network. As the final step, the attribute table of the output map was joined with the attribute table of the count point data and the attribute table of the betweenness map.

The resulting table was exported as a .csv file and opened in R (v2.12.0; http://cran.r-project.org), where a linear regression model was performed between the traffic data (cars, buses, light good vehicles and heavy good vehicles) and the betweenness value. The resulting linear equation was then applied to the rest of the nodes in the network to estimate the average annual daily traffic flow (AADF) of all the roads in the modelled area (Fig. 2.3C).

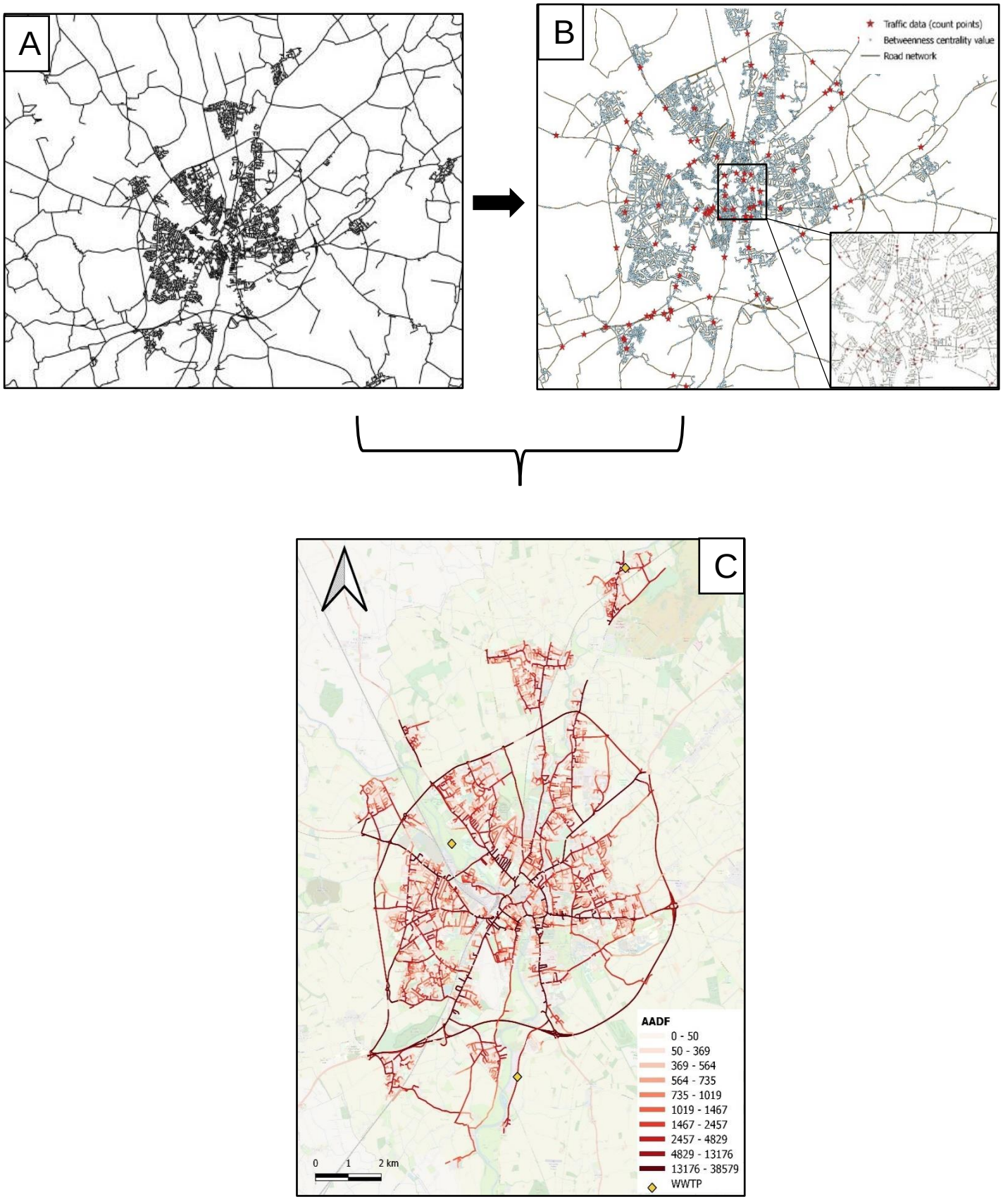

Figure 2.3. Methodology for the traffic estimation in the city of York. A) Vector network for the Yorkshire and the Humber area; B) Incorporation of the count points into the node network and C) average annual daily traffic flow for all roads in the city.

The TRWP emissions model was developed in Matlab software (MATLAB ver. R2018a) and consists of a script that integrates the spatial and temporal information of the area of study and the processes involving tyre and road wear particles generation and release in York. These input parameters were stored in Excel spreadsheets and loaded into the model by performing emission calculations per hydrological zone and river sections for 365 days of the year for 2017. The flow diagram presented in Figure 2.4 shows the pathways and environmental compartments considered in the model simulation. However, the focus of the present study was TRWP emissions into surface waters. A detailed description of the emission pathways, the emission estimation equations and the required parameters is provided in the following subsections.

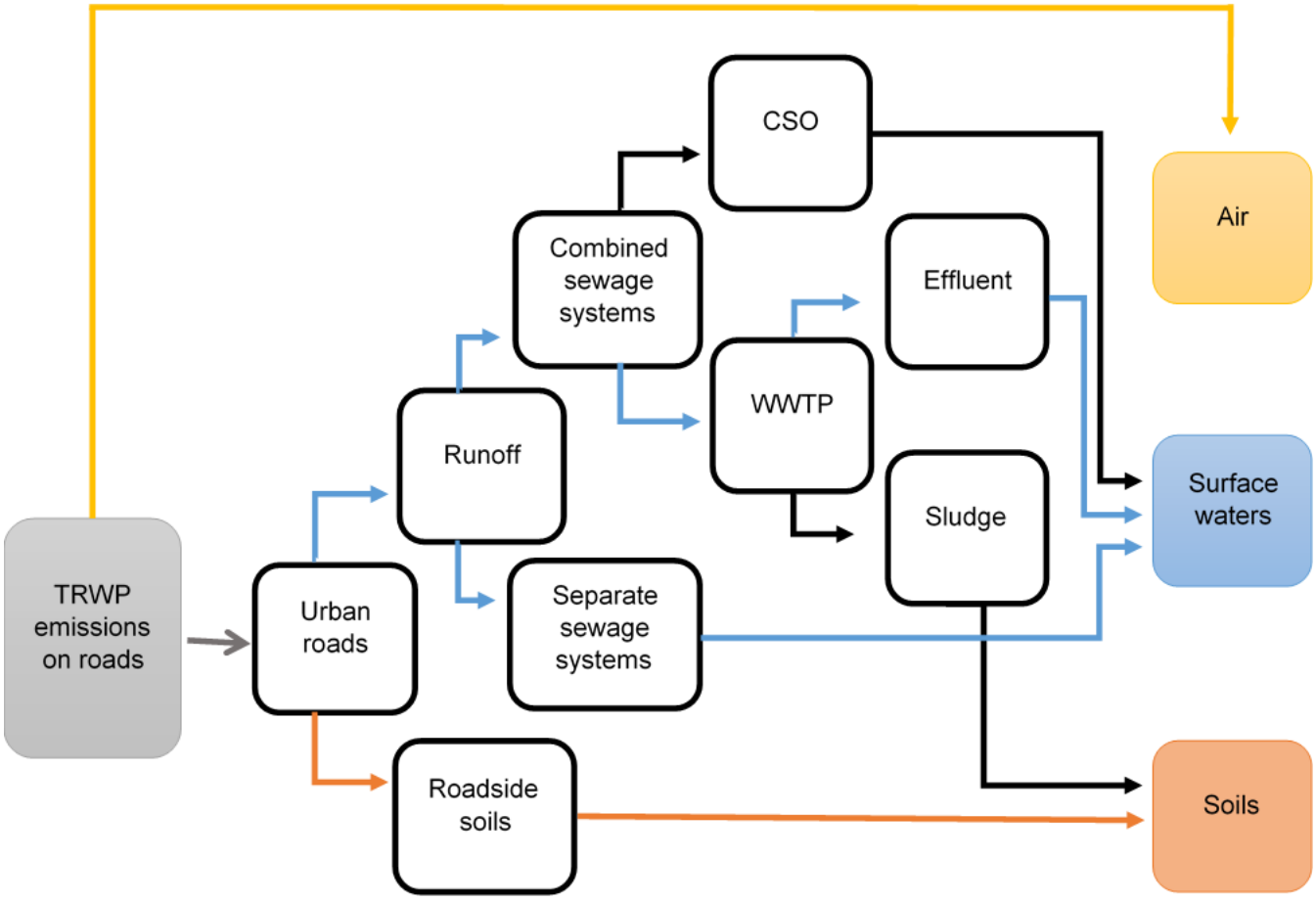

Figure 2.4. Flow diagram showing the sources of TRWP, pathways and environmental receptors included in the model estimations (black arrows indicate pathways lacking available data). Source: adapted from (Baensch-Baltruschat et al., 2021).

2.2.3 Model parametrization and assumptions

Parameters estimates were assigned based on published literature, local weather information and traffic volumes, as well as unpublished data from Yorkshire water on road runoff treatment specific to the area of study. Table 2.2 shows the assumptions on which the input values of the model were based and a complete description of the criteria followed for their selection is presented in the next subsections.

Table 2.2. Model parameter estimates for calculating TRWP emissions in the city of York.

Parameter	Unit	Data applied				Reference
Vehicle-km travelled	vehicle-km travelled yr^{-1}	Cars	940,544,517			Traffic data for the city of York for different vehicle types (Traffic model, see section 2.2.2)
		Buses	5,424,469			
		LGV	141,582,149			
		HGV	29,507,818			
		Total	1,117,058,955			
Tyre wear rate (coarse particles)	mg vehicle-km^{-1}		MIN	AVE	MAX	Emission factors for urban roads and various vehicles types (Lee *et al*., 2020; Gebbe *et al*., 1997; DELTARES and TNO, 2016; Kole *et al*., 2015; Hillenbrand *et al*., 2005)
		Cars	51	132	200	
		Buses	344	415	799	
		LGV	107	159	224	
		HGV	600	850	1200	
Fraction of tyre tread particulates emitted into the air (PM10)	%	2				Based on (Unice *et al*., 2019) TRWP fate and transport model in the Seine watershed
Street wash-off	%	Rainfall intensity < 2 mm/day = 0 > 5 mm/day = 100				Based on a linear approximation of an empirical exponential relationship used in stormwater quality models to determine the capacity of

			one rainfall event to carry a pollutant (Egodawatta *et al*., 2007; Unice *et al*., 2019)
Fraction to direct runoff (coarse particles)	%	60	Estimates for urban areas according to Verschoor *et al*. (2016)
Fraction to soil (coarse particles)	%	40	
Fraction of stormwater collected in combined sewers	%	10	Based on a study by Domercq (2019) where it was established that the combined network mainly exists in old parts of York's city centre
Fraction of stormwater collected in separate wastewater systems	%	90	
WWTP removal efficiency	%	95	Value reported in literature for MP removal in waste water treatment plants (Unice *et al*., 2019; Kawecki and Nowack, 2019; Sieber *et al*., 2020; Horton *et al*., 2017)

2.2.3.1 Emission factors

Four vehicle categories were considered in this study: passenger cars, buses, LGVs and HGVs. Emission factors provided by Lee *et al*. (2020), Gebbe *et al*. (1997), DELTARES and TNO, (2016), Kole *et al*. (2015) and Hillenbrand *et al*. (2005) were used to create a minimum, maximum and average emission scenario (MIN, MAX and AVE, respectively) to calculate the annual TRWP generation in the city of York. In the literature, EFs have been reported for each vehicle category, however, a distinction between urban areas, rural roads and highways should also be considered when determining the specific tyre wear rate by vehicle type (Klein *et al*., 2018). Emissions per vehicle - kilometre in urban roads are expected to be higher due to driving dynamics such as, constant acceleration and braking, and cold starts associated with traffic lights (Klein *et al*., 2018).

DELTARES and TNO, (2016) is the only study that has carried out a road differentiation in its emission factor calculations. For this reason, the AVE emissions scenario of this study includes the EFs proposed by DELTARES and TNO, (2016) for

cars, buses, LGVs and HGVs on urban roads. For the MIN and MAX scenarios, different data sets were combined.

2.2.3.2 Release pathways

TRWP mass is generated in the fine and coarse fraction (Panko *et al*., 2013). Several studies agree that approximately 0.1 to 5% will be airborne emissions, while the rest will be deposited onto the road surface as coarse particles (Baensch-Baltruschat *et al*., 2020; Wik and Dave, 2009). In this study, it was assumed that only 2% of the total emissions were released into the atmosphere as particles less than 10 µm in size. This value was based on the parameters presented in the mass balance model for TRWP emissions in the Seine river basin carried out by Unice *et al*. (2019). Additionally, insights from the study conducted by Charbouillot *et al*. (2023), which measured a 2.20% emission factor for PM_{10}, further supported this estimation.

The remainder of the TRWP emissions (i.e., coarse particles) will be distributed between roadside soil and runoff. The fractions in which tyre and road wear particles are released into the different environmental compartments will vary depending on the road type (i.e., urban, rural or highways) (Baensch-Baltruschat *et al*., 2020). For example, Kaufmann *et al*. (2007) estimated that approximately 50–60% of particles larger than 10 µm would be transported into the sewage system in urban areas. Conversely, in rural roads and highways, approximately 20-30% and 10% of such particles would be directly released into surface waters or other stormwater treatment facilities, respectively (Kaufmann *et al*., 2007).

In the study by Unice *et al*. (2019), the assumed proportion for the transport of non-airborne particles was 50% for runoff and 50% for soil. However, the authors overlooked the differentiation between types of roads in their modelling work for the Seine watershed. On the other hand, Verschoor *et al*. (2016) and Ten Broeke *et al*. (2008) considered a 40% and 90% retention rate in roadside soil for urban areas and outside urban areas, respectively.

In the present study, a runoff rate of 60% was employed, with a corresponding 40% retention in soils.

While $PM_{2.5}$ and PM_{10} are commonly used as standard measures for assessing air pollution due to their extensive data availability and direct implications for human health, it is worth noting that larger particles exceeding 10 μm in diameter may also be present in the atmosphere (AQEG, 2019). These larger particles typically have a short atmospheric residence time, often recirculating within street canyons rather than being transported over long distances (AQEG, 2019). Furthermore, the resuspension of TRWPs introduces another source of non-exhaust particles into the air. However, research on resuspension emissions remains limited, and thus was not considered in this study (AQEG, 2019).

2.2.3.3 Wash-off Fraction

Diffuse emissions, such as those from tyre and road wear particles, are triggered by rainfall events. A study conducted by Egodawatta *et al*. (2007) concluded that not all storm events have the capacity to mobilize pollutants accumulated on road surfaces and recommended the use of wash-off coefficients to estimate runoff emissions on urban roads. Unice *et al*. (2019) presented a simplified version of a stormwater quality model with a linear relationship that assumes that no emissions will happen with less than 2 mm/day precipitation and 100% of the particles will be washed off with a rainfall intensity of 5 mm/day or higher. The wash-off percentage in this study was estimated with the following equation:

$$x = \frac{y - 2}{0.03} \quad (1)$$

Where *x* is the percentage of particles that will be mobilized into the sewer system and *y* is the precipitation intensity (mm/day) (Hagström, 2021)**.**

2.2.3.4 Transport in the sewerage system

The drainage system in the city of York consists of three main sewage networks: foul water, surface water, and combined (Domercq, 2019). The foul water network

transports contaminated water from households to sewage treatment plants for processing. Meanwhile, the surface water network releases runoff water into surface waters such as rivers and local streams, without any prior treatment, through stormwater outlets. In contrast, the combined network collects both, wastewater from households and stormwater from streets, directing the combined flow to WWTPs for appropriate treatment. However, during periods of heavy rainfall, the combined sewage system could overflow, leading to the discharge of raw polluted water directly into rivers (Sieber *et al*., 2020; Brombach *et al*., 2005).

In the present study, it was assumed that 90% of runoff water was directed to surface water sewers and the remaining 10% was transported to WWTPs through combined sewers. This was based on the description of the combined network by Domercq (2019) where it was established that it exists mainly in the old parts of York's city centre. In addition, due to lack of information, combined sewer overflows were not considered.

2.2.3.5 Wastewater treatment efficiency

Wastewater treatment plants employ various physical, chemical, and biological processes to remove contaminants from wastewater before it is discharged back into the environment (Liu *et al.*, 2021). One common method used is known as primary settling treatment, where gravity is utilized to separate solids from liquid. In this process, wastewater is allowed to settle in large sedimentation tanks, allowing heavier particles to gradually sink to the bottom forming a mass of solids called sludge, while clearer water is discharged or further treated (Liu *et al.*, 2021).

The effectiveness of WWTPs in removing tyre and road wear particles remains uncertain. Nevertheless, several studies have attempted to estimate this efficiency by incorporating microplastics removal data, and tyre and road wear particles characteristics such as size and density. For instance, Horton *et al*. (2017) reported high removal rates of up to 99% for microplastic retention in different WWTPs. Thus, it is reasonable to infer that TRWPs will also predominantly be captured, largely within the sludge due to their higher density compared to other microplastics (Baensch-Baltruschat *et al*., 2021). However, given the scarcity of data regarding TRWPs in

WWTPs, this study relies on the assumptions made by Unice *et al.* (2019) and Baensch-Baltruschat *et al.* (2021) to establish a conservative estimate of 95% WWTP removal efficiency.

2.2.4 Runoff emission equation

To estimate runoff emissions of TRWPs, the following equation was developed as a function of time:

$$RO_{Emiss}(t) = \left(P_{Emiss}(t) \cdot T_{lag}(t) + E_{Residual}\right) \cdot WF \quad (2)$$

Where P_{Emiss} represents the rate of tyre and road wear particles emitted at the frictional interface of the tyre and road surface for the time step simulated (mg/day). T_{lag} is a factor that considers the delay in the TRWP emissions between the generation of the particles and their actual discharge into surface waters and is measured in the same units as the time scale chosen for P_{Emiss} (e.g., days). $E_{Residual}$ is the number of pollutants left over from the last precipitation (mg/day), and WF is the fraction of pollutants that a rainfall event has the capacity to wash-off (%).

Runoff emissions are dependent on rainfall events. This means that during a dry day TRWPs would still be generated and deposited (accumulated) on urban roads but no emission to surface waters would happen until the next rain event. T_{lag} was therefore set as 0 on the dry day to indicate no discharge into the rivers, and on rainy days a value of 1 + *the number of preceding dry days* to account for the TRWPs built up. $EResidual$ will depend on the value of the WF, even if T_{lag} has a value of 1, rainfall events have the capacity to wash-off only a fraction of pollutants available, and the rest of the pollutants would remain on the road surface. These residual TRWPs on each rainy day will be added to the next day. When WF is equal to 1 all TRWPs available for runoff will be transported to the sewage system and $EResidual$ would become zero.

TRWP emissions were calculated based on the approach that uses mileage of vehicles and emission factors (EF). Therefore, the following formula was created:

$$P_{Emiss}(t) = DT(t) \cdot \mathrm{EF} \cdot R_{Release} \quad (3)$$

Where $DT(t)$ (Daily Traffic) is the vehicle-km travelled for cars, buses, light good vehicles and heavy good vehicles (vehicle-km/day), EF (Emission Factor) is the mass of tyres released from the wear process per unit time over distance travelled expressed in milligrams per kilometre, and $R_{Release}$ is the fraction of tyre and road wear particles that will enter the sewage system. Therefore, the value of $R_{Release}$ is the fraction to direct runoff minus the fraction of tyre tread particulates emitted into the air (Table 1).

Daily traffic in the study area was calculated by multiplying AADF (See section 2.2.2) by the corresponding length of road per hydrological zone. The following formula was applied:

$$DT_{,HZ} = \sum_{j=0}^{n} N_{j,HZ} \times L_{,HZ} \quad (4)$$

Where $N_{j,HZ}$ is the number of vehicles of each type travelling in the HZ per day (AADF), and $L_{,HZ}$ is the length of the road in the selected HZ (in km).

Once TRWP runoff emissions have been calculated, they will follow two pathways: the surface water sewage system (E_{SW}) or the combined sewers (E_{WWTP}). The first, will discharged TRWPs emissions directly into the rivers and the second will transport them to the WWTPs. The following equations were applied:

$$E_{SW} = RO_{Emiss} \times f_{SW} \quad (5)$$

$$E_{WWTP} = RO_{Emiss} \times f_{WWTP} \quad (6)$$

Where RO_{Emiss} is the runoff emissions of TRWPs, f_{SW} is the fraction of runoff emissions entering the surface water sewage system, and f_{WWTP} is the fraction of runoff emissions entering the combined sewage system and therefore, the WWTPs. WWTPs have a retention efficiency of 95%. This means that the remaining 5% will be discharged into surface waters *via* WWTP effluent. The following equation was established:

$$E_{Effluent} = E_{WWTP} \cdot (1 - C_{Ret}) \quad (7)$$

Where E_{WWTP} is the runoff emissions that ended up in the WWTP, and C_{Ret} (Retention coefficient) is the TRWP retention coefficient or removal fraction in a WWTP.

The total emission of tyre and road wear particles to the rivers was calculated as the sum of the direct emission to surface water and the indirect emission through treated sewage. The river sections without WWTP outlets will only receive direct emissions from surface water sewers. For this purpose, the following formula was established:

$$E_{River} = E_{SW} + E_{Effluent} \quad (8)$$

Where E_{SW} is the runoff emissions directly discharged into the rivers through surface water sewers, and $E_{Effluent}$ is the treated sewage from WWTPs.

The model generated TRWP emission data in milligrams per day per hydrological zone and river section for the year 2017, which were utilized to construct the various graphs presented in the results section.

2.3 Results

The following TRWP emission results are expressed on a tread basis, meaning that road mineral encrustations were not taken into account in the calculations.

The total predicted annual emissions of TRWPs generated on the city of York's roads, as well as their distribution in the different environmental compartments are presented in Table 2.3. For the minimum (MIN) scenario, a total TRWP emission of 82.6 tonnes/year was estimated, corresponding to a per capita emission of 0.40 kg/year. In contrast, a total value of 259.5 tonnes/year and a per capita value of 1.25 kg/year was calculated for the maximum (MAX) scenario. The considerable difference between both scenarios is mainly due to the significantly higher emission factors applied in the MAX scenario, especially for passenger cars (four times greater) and HGVs (two times greater).

Emissions for the average (AVE) scenario were based on the EFs provided by DELTARES and TNO (2016). As a result, TRWP emissions of 173.9 tonnes/year and per capita of 0.84 kg/year were estimated. The results shown below will mainly focus on the TRWP emissions calculated in the average scenario since the use of the EFs proposed by DELTARES and TNO (2016) have been recommended by many authors. This is due to the differentiation between types of vehicles and tyre wear emissions generated on urban areas, rural roads and highways (Baensch-Baltruschat *et al*., 2021; Unice *et al*., 2019; Vogelsang *et al*., 2019).

Table 2.3. Emission of TRWPs into different environmental compartments.

Environmental compartment	Percent of release	Annual TRWPs emissions (tonnes /year) MIN scenario	Annual TRWPs emissions (tonnes/year) AVE scenario	Annual TRWPs emissions (tonnes/year) MAX scenario
Generation on roads	100%	82.6	173.9	259.5
PM10	2%	1.6	3.4	5.1
Coarse particles				
Roadside soil	40%	32.4	68.2	101.7
Runoff (pre-treatment)	60%	48.6	102.3	152.6

2.3.1 Emission ranges of TRWPs in York

The estimation of the total amount of TRWPs discharged into York's surface waters, for the different vehicle types considered in this study (cars, buses, LGVs and HGVs), over the simulated year and for the three simulated scenarios minimum (MIN), average (AVE) and maximum (MAX), is presented in Figure 2.5.

The total TRWPs emitted into rivers in the city of York and summed across vehicle types for the minimum scenario was 41 tonnes/year (4.10×10^{10} mg/year), for the average scenario was 86.30 tonnes/year (8.6×10^{10} mg/year), and for the maximum scenario was 128.75 tonnes/year (12.8×10^{10} mg/year). The emissions for the AVE scenario were twice as high as the emissions for the MIN scenario. The MAX scenario however is almost twice as much again and an order of magnitude higher than the MIN scenario. Over the three scenarios, cars had the highest emission values of the four vehicle types studied, whereas buses had the lowest emission values.

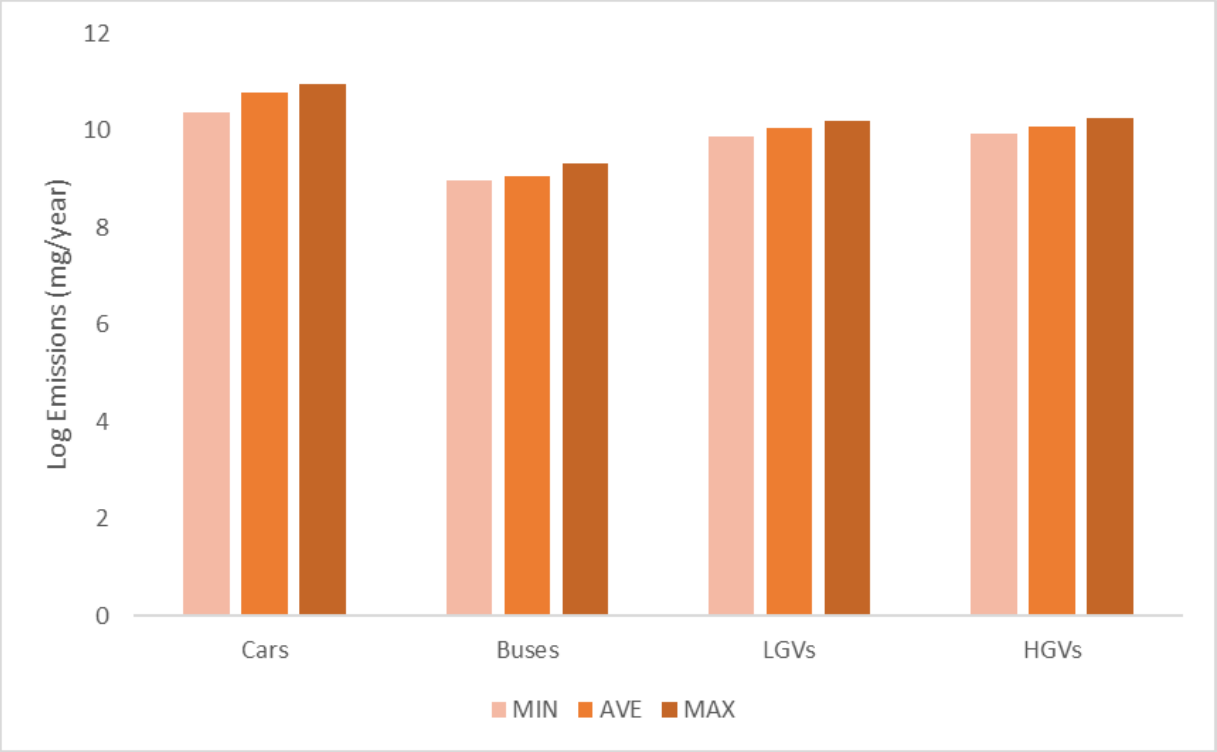

Figure 2.5. Estimated total emissions of TRWP to York's river system during the year 2017 for Cars, Buses, LGVs and HGVs and the minimum (MIN), average (AVE) and maximum (MAX) emitting scenarios.

The total emission of TRWPs generated per vehicle type (cars, buses, LGVs and HGVs) during the year 2017 and for all RSs and HZs for the simulated average scenario is presented in Figures 2.6 and 2.7.

In all river sections and hydrological zones, cars contributed the most to TRWP emissions, followed by HGVs, LGVs and buses. The exceptions were in river sections FOSS1 and FOSS2, and hydrological zones HZ9, HZ10 and HZ11 where LGVs emissions were higher than HGVs. These results can be expected as the annual vehicle-kilometres travelled for cars in 2017 for the city of York was 940,544,517 vehicle-km/year; 5,424,469 vehicle-km/year for buses, 141,582,149 vehicle-km/year for LGVs and 29,507,818 vehicle-km/year for HGVs. Cars annual driving distance is one order of magnitude and two orders of magnitude higher than HGVs and buses, respectively. Although LVGs annual mileage is one order of magnitude higher than

HGVs, they exhibited lower emissions. This was due to the tyre wear rate (EF) attributed to HGVs, which is five times higher (in all scenarios) than that of LGVs.

The river section with the highest TRWP emissions was OUSE5 where cars contributed with 12,872.36 kg/year, buses with 222.49 kg/year, LGVs with 2,360.27 kg/year, and HGVs with 2,836.72 kg/year. In contrast, the river section FOSS1 received the lowest amount of TRWPs where cars emitted 1,429.08 kg/year, buses 28.03 kg/year, LGVs 254.35 kg/year, and HGVs 243.08 kg/year. Regarding hydrological zones, it is evident that HZ1 exhibited the highest TRWP emissions with 10,805.31 kg/year attributed to cars, 201.56 kg/year to buses, 1,945.74 kg/year to LGVs and 2,045.86 kg/year to HGVs. In comparison, HZ11 recorded the lowest emissions, with 284.74 kg/year, 5.92 kg/year, 49.74 kg/year and 40.90 kg/year originating from cars, buses, LGVs and HGVs, respectively.

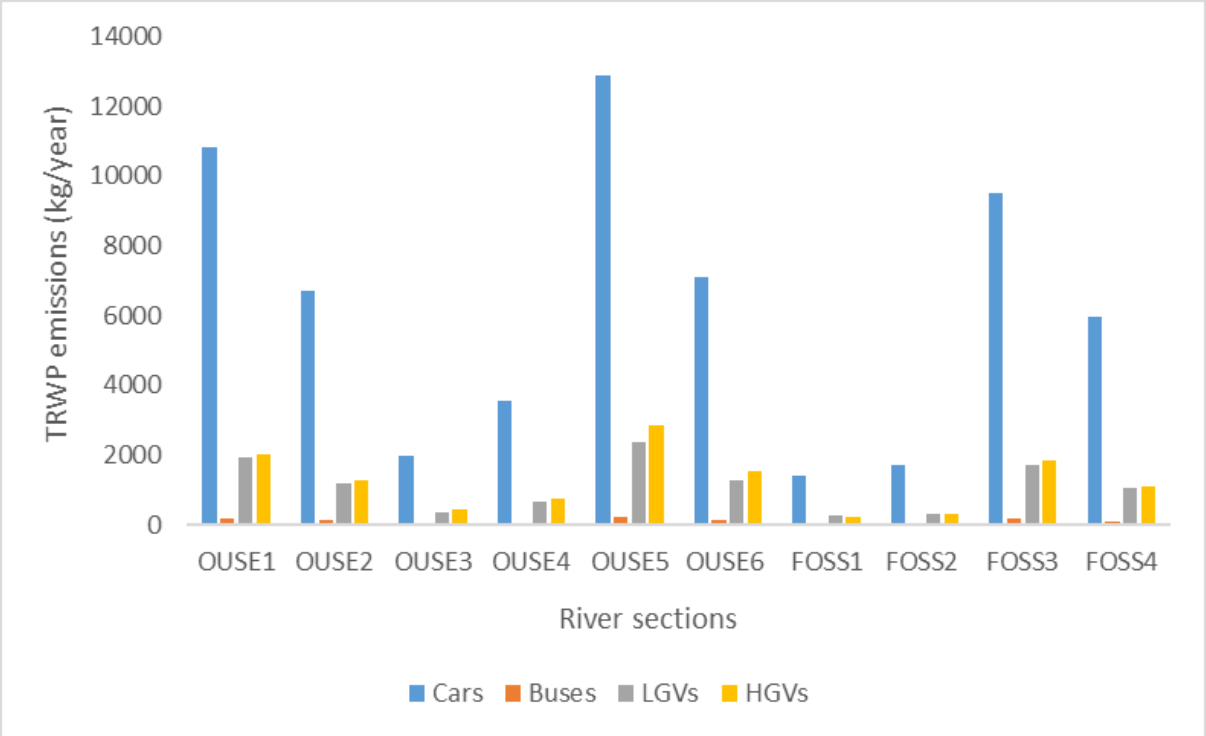

Figure 2.6. Total estimated emissions in kg to York's river sections (OUSE1, OUSE2, OUSE3, OUSE4, OUSE5, OUSE6, FOSS1, FOSS2, FOSS3 and FOSS4) during the year 2017 per vehicle type (Cars, Buses, Light good vehicles and Heavy good vehicles) and for the average scenario.

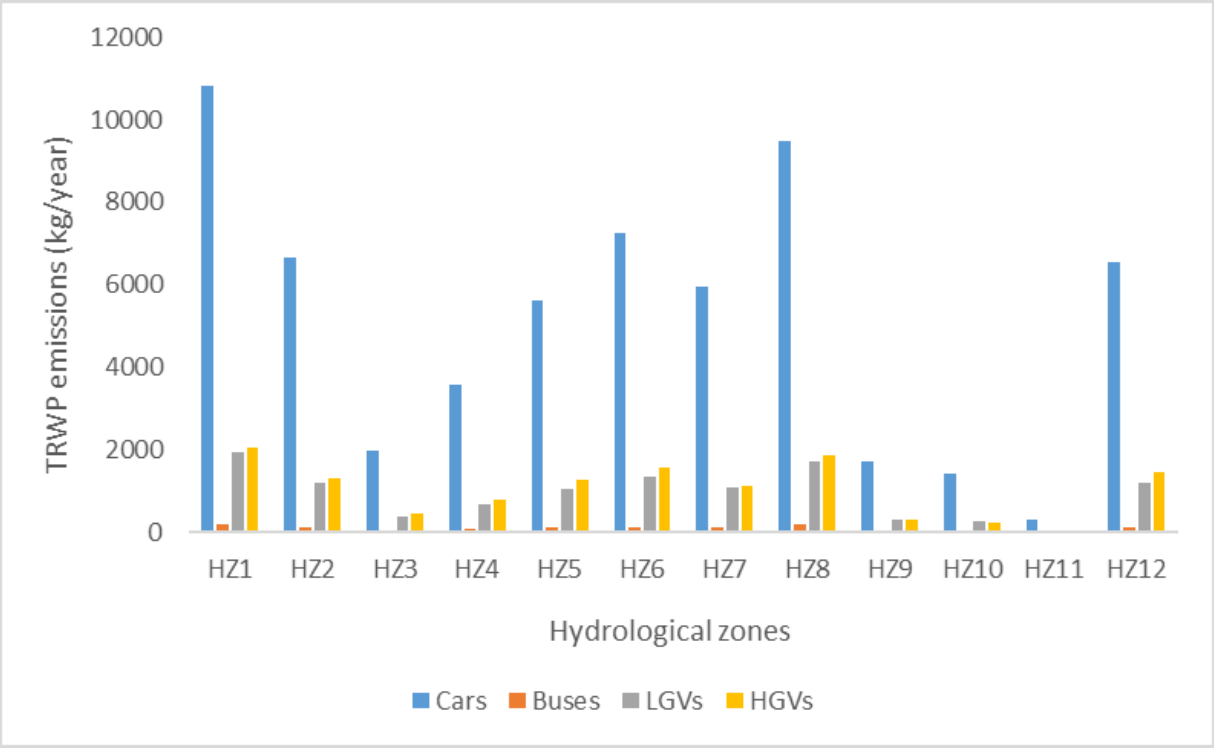

Figure 2.7. Total estimated emissions in kg to York's hydrological zones during the year 2017 per vehicle type (Cars, Buses, Light good vehicles and Heavy good vehicles) and for the average scenario.

2.3.2 Spatial variation of emissions

The spatial variability of the mass of TRWPs emitted in the different hydrological zones and discharged in all the river sections per day for the average scenario is presented on the map in Figure 2.8. Additionally, the average daily emissions for the three simulated scenarios (MIN, AVE and MAX) per RS and HZ are plotted next to the map presented in this figure.

The highest TRWP emissions were found in the northeast and northwest of the city, specifically hydrological zones HZ8 and HZ1, respectively. Additionally, significant contributions come from the east in HZ6. These areas discharge TRWP runoff emissions to the three river sections, FOSS3, OUSE1 and OUSE5, respectively. Notably, these river sections also exhibit the highest emission rates.

In contrast, the hydrological zone HZ11, located in the south of the city, stands out as the lowest runoff emitting area. HZ11 releases its runoff to the river section OUSE6, which not only receives TRWP emissions from HZ12 but also wastewater effluent from WWTP Naburn. Consequently, OUSE6 is anticipated to display a higher level of TRWP emissions. On the other hand, the river sections FOSS1 and FOSS2 receive the lowest runoff emissions.

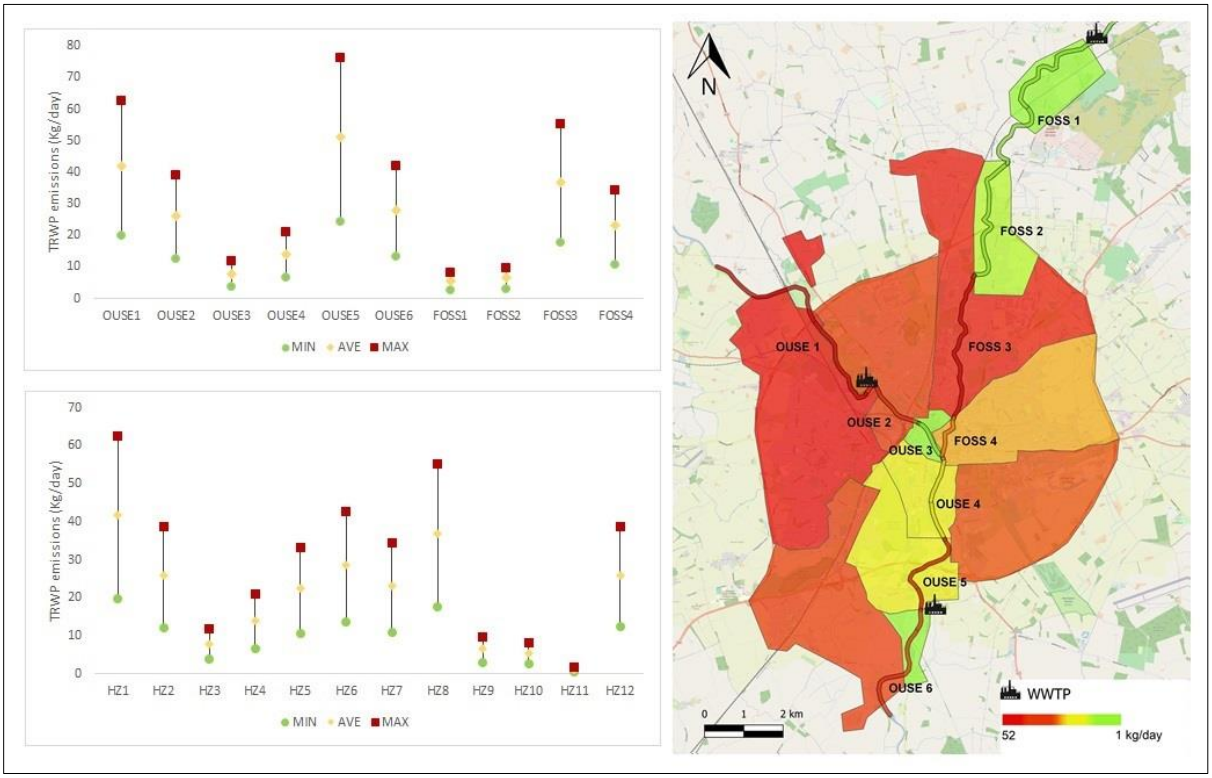

Figure 2.8. Mean daily emissions of TRWP to York's river sections (OUSE1, OUSE2, OUSE3, OUSE4, OUSE5, OUSE6, FOSS1, FOSS2, FOSS3 and FOSS4) and hydrological zones for the three simulated scenarios minimum (MIN), average (AVE) and maximum (MAX) including a map of mean emission values per day with the HZs and RSs for the average scenario.

2.3.3 Temporal variation of emissions

The temporal variability of the total TRWP emissions for the average scenario through 2017 for the river Ouse and the river Foss is presented in Figures 2.9 and 2.10, respectively.

The river Ouse was divided into six sections, two of which receive treated effluent from WWTPs. These are, OUSE2 (WWTP Rawcliffe) and OUSE6 (WWTP Naburn). The order of highest to lowest emissions of tyre and road wear particles in the river sections are as follows: OUSE5, OUSE1, OUSE6, OUSE2, OUSE4 and OUSE3.

The amount of TRWPs emitted into rivers on any given day depended on rainfall intensity, but more importantly, in the number of preceding dry days (TRWP that have been accumulating on the road due to no rain activity). For example, the day with the highest rainfall intensity in 2017 was the 23/08/17 with a value of 25.81 mm/day, however, the TRWP that reached the river Ouse that day were 1.18 $\times 10^9$ mg (1.18 tonnes). In contrast, the day of the year that exhibited the highest emissions of 5 $\times 10^9$ mg (5 tonnes) was the 01/02/17 with a rainfall intensity of only 4.71 mm/day. This can

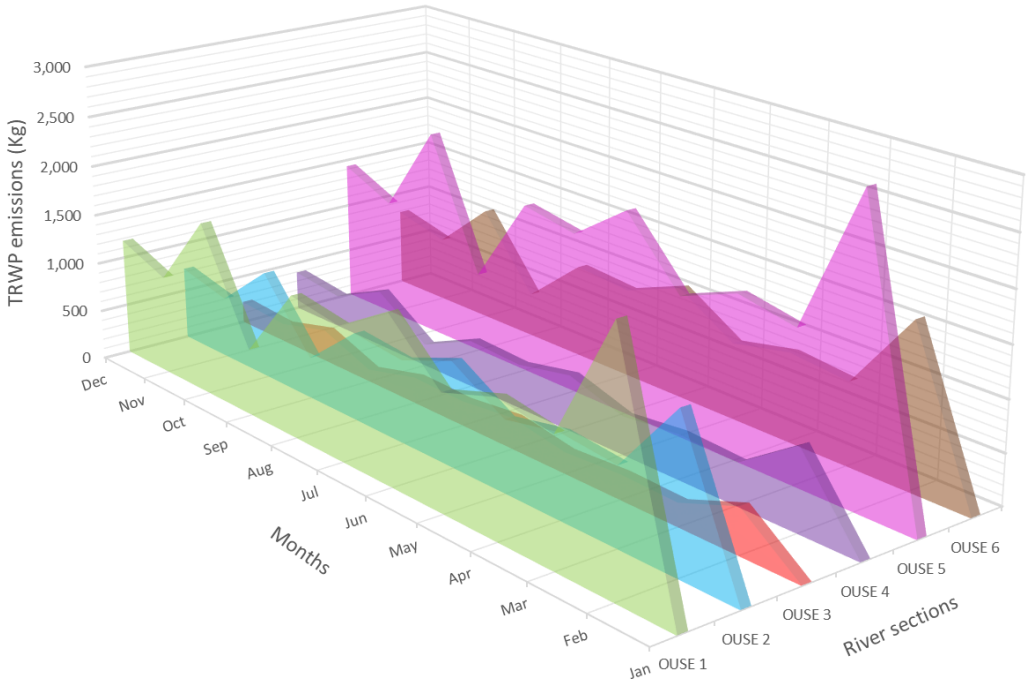

Figure 2.9. Daily TRWP emissions in Kg to the delimited river sections of the river Ouse over the year 2017 (AVE scenario).

be attributed to the 30 dry days (from the 02/01/17 to the 31/01/17) where TRWPs were being generated on roads but no discharge to the rivers was happening.

The river Foss was divided into four sections, with only RS FOSS1 receiving treated effluent from a WWTP named Walbutts. The river section with the highest discharge of runoff emissions is FOSS3, followed by FOSS4, FOSS2 and FOSS1.

On the day with the highest TRWP emissions (01/02/17), a total amount of 2.13 $\times 10^9$ mg (equivalent to 2.13 tonnes) entered the river Foss.

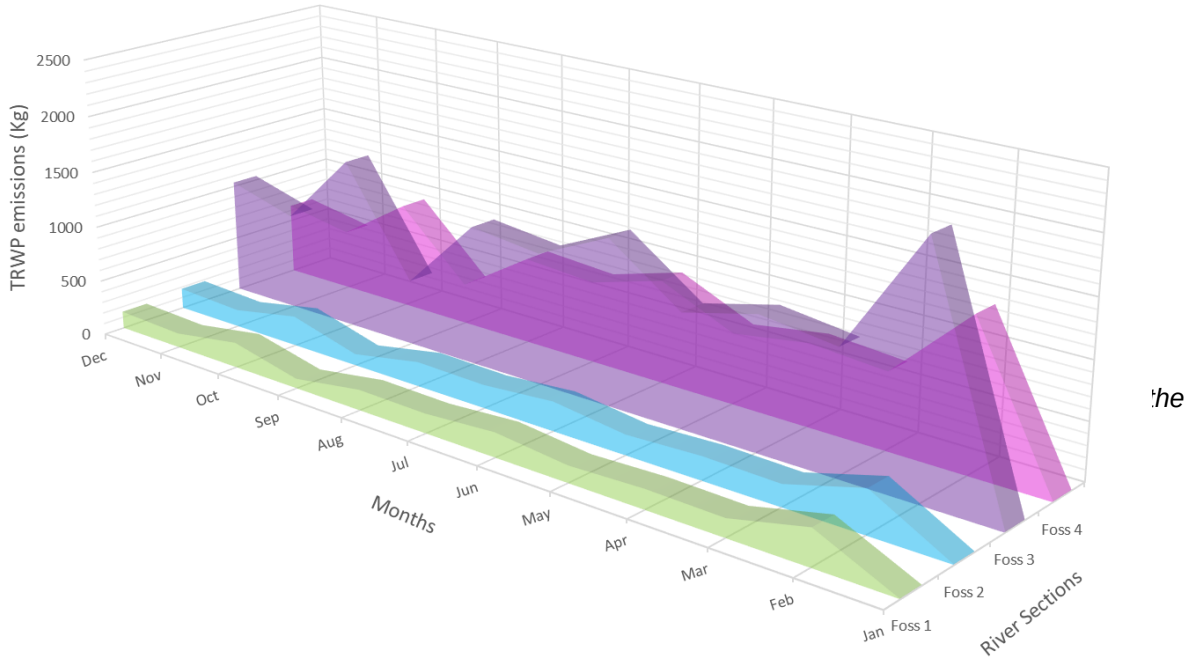

Figure 2.10. Daily TRWP emissions in Kg to the delimited river sections of the river Foss over the year 2017 (AVE scenario).

The temporal variations of two river sections (OUSE6 and FOSS1) that receive treated effluents from the WWTP, as well as the 2017 rainfall pattern, are presented in figures 2.11 and 2.12.

The total calculated TRWP emissions for the river section OUSE6 amounted to 1.03×10^{10} mg (equivalent to 10.3 tonnes), while for FOSS1, the value was 1.95×10^{9} mg (1.95 tonnes). This notable difference between the two river sections can be in part attributed to the population served by each WWTP they are connected to. Specifically, RS OUSE6, which receives drainage from Naburn WWTP, serves a significantly larger population of 168,594. In contrast, FOSS1 is connected to the Walbutts WWTP, catering to a population of 20,105 inhabitants. This significant variation in population served by the respective WWTPs contributes to the order of magnitude difference in TRWP emissions between the two river sections.

According to my calculations, out of the 365 days of the year, only 68 days showed runoff emissions to surface waters meaning that rainfall events on those days were able to mobilize particles from the road to the rivers.

The months in 2017 expected to have the highest TRWP emissions (according to the model set up) are February and October with a value for OUSE6 of 1.61×10^{9} mg (1.61 tonnes) and 1.14×10^{9} mg (1.14 tonnes) respectively, and for FOSS1 of 3.14×10^{8} mg (0.31 tonnes) and 2.22×10^{8} mg (0.22 tonnes) respectively. Comparatively, the month with the lowest emissions is January with a value of 9.61×10^{6} mg (0.009 tonnes) for the OUSE6 and 1.87×10^{6} mg (0.001 tonnes) for the FOSS1.

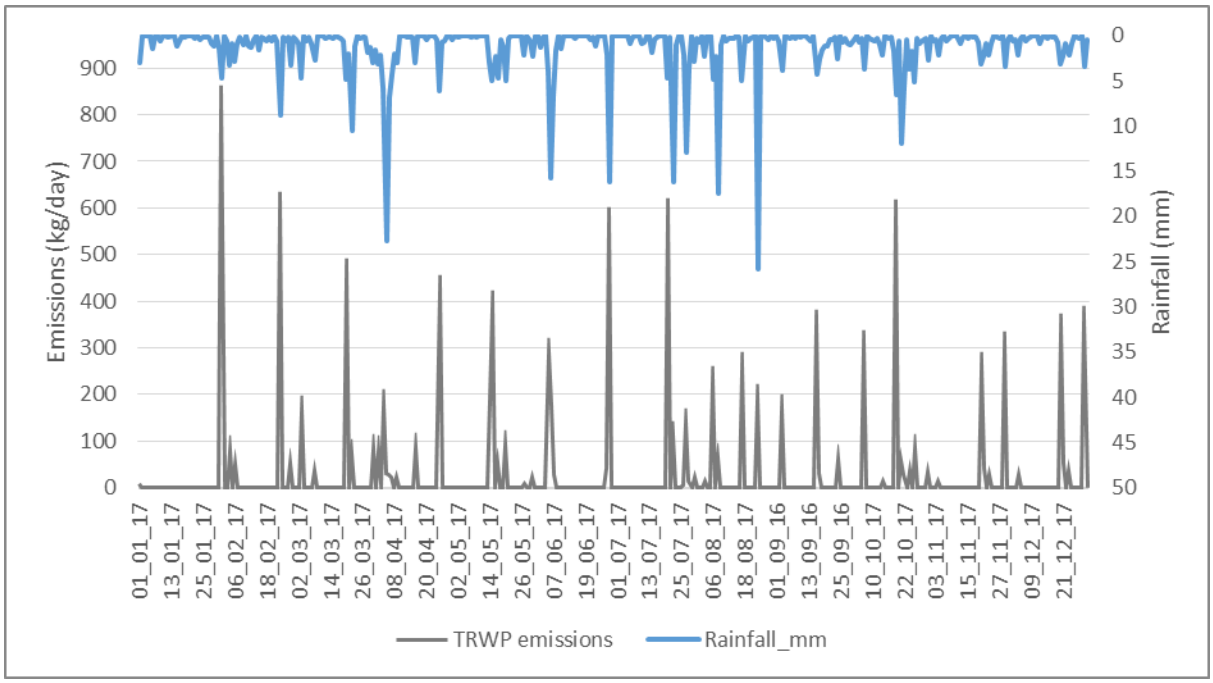

Figure 2.11. Estimated daily TRWP emissions for the RS OUSE6 during 2017 for the average scenario (in grey) and the rainfall pattern for the same year (plotted in blue on the secondary axis).

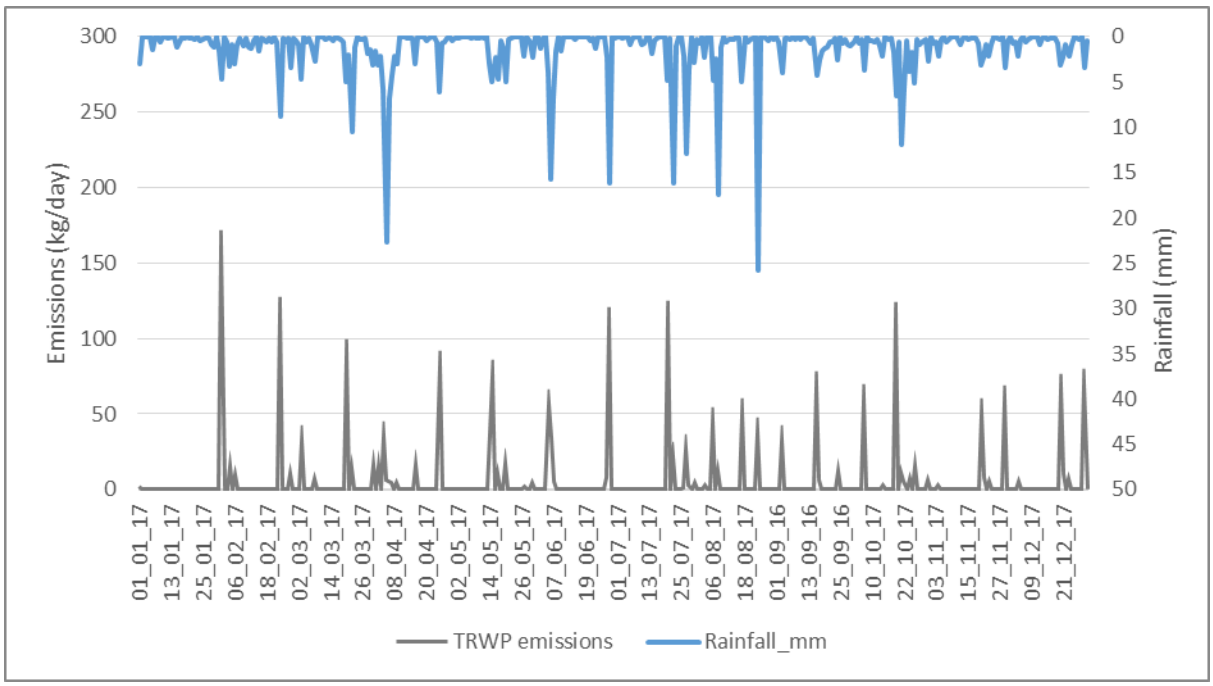

Figure 2.12. Estimated daily TRWP emissions for the RS FOSS1 during 2017 for the average scenario (in grey) and the rainfall pattern for the same year (plotted in blue on the secondary axis).

2.4 Discussion

This Chapter describes the implementation of a spatially and temporally resolved TRWP emissions model within the city of York. This approach integrates outcomes from a traffic model and the processes governing TRWP generation and transportation. The results not only reveal TRWP emission estimates across various scenarios within the city but also pinpoint zones with elevated runoff emissions and identify the vehicles predominantly responsible for such emissions. In addition, the parameters employed in this research are derived from available data, resulting in the omission of certain influential factors affecting tyre wear emissions due to their lack in the literature. However, these factors are thoroughly discussed in subsequent sections.

2.4.1 Emission ranges of TRWP in York

The only study to have estimated the amount of tyre wear and tear in the UK dates back to 1996 and was conducted by the Environment Agency (Environment Agency News, 1999). Their approach involved measuring the collective weight of the 37 million car and truck tyres discarded that year, amounting to around 380,000 tonnes. They then inferred that 10-20% of a tyre's weight is gradually lost during its lifespan. Consequently, by adopting this methodology, the cumulative tyre wear for 1996 is estimated to range between 38,000 and 76,000 tonnes per year (Kole *et al*., 2017). Furthermore, Kole *et al*. (2017) built upon the Environmental Agency's initial estimation of tyre wear, recalculating the contemporary figures by considering the change in the UK population from 1996 to 2016. With the UK population reaching 64 million in 2016, the projected emissions would have increased to a range of approximately 42,000 to 84,000 tonnes per year, with an average of around 63,000 tonnes annually. It's worth noting that this analysis does not factor in the advancements in tyre technology over the two decades nor does it assume an increase in mileage per capita since 1996 (Kole *et al*., 2017). Nevertheless, it provides a reasonably estimate of tyre wear emissions in the UK.

To facilitate a comparison between this study and the UK's tyre wear estimates, the average projected tyre wear emissions for 2016 (63,000 tonnes per year) were

adopted and adjusted according to York's population for the year 2017 (208,163 inhabitants). This calculation resulted in a total tyre wear emission of 204.91 tonnes/year, corresponding to a per capita value of 0.98 kg/year. Interestingly, this outcome closely resembles my own estimate of 173.9 tonnes per year, with a corresponding per capita emission of 0.84 kg/year (for the average scenario).

When considering the upper range of emissions (84,000 tonnes per year), the calculated figure rises to 273.21 tonnes per year, translating to a per capita value of 1.31 kg/year for York. Once more, this aligns with the MAX scenario of the model, which predicts 259.5 tonnes per year and a per capita emission of 1.25 kg per/year. This suggests that the overall methodology and underlying assumptions used in developing the traffic model for this study are likely robust.

The model estimates also fall within the same range as the per capita emission rates reported for European countries, which exhibited values ranging from 0.5 to 1.5 kg/year (Kole *et al*., 2017). Additionally, Unice *et al*. (2019) reported a slight regional variation in per capita emissions within France. Specifically, they calculated a higher per capita value for the Seine watershed (1.8 kg/year) compared to the national average (1.2 kg/year) (Unice *et al*., 2019). This observation leads me to consider the potential for similar regional variations within the United Kingdom, with York potentially exhibiting lower tyre wear emissions than the national estimate due to its lower population density and road network.

In this study, it was observed that 49.61% of the total TRWPs emitted in York reached the city's surface waters during the simulated year. This value is influenced by local factors such as road type (i.e., urban, rural, or highways) and sewage systems (i.e., the proportion of stormwater that enters combined sewers) (Kole *et al*., 2017). For this analysis, a stormwater fraction of 10% directed to combined sewers was assumed based on Domercq's study (2019), which identified the presence of combined sewers in the historic parts of York's city center. Similarly, Bondelind *et al*. (2020) reported that just 8% of runoff volume in Sweden undergoes treatment, either at a sewage treatment plant or local facilities. This results in a significant portion of TRWPs within stormwater being directly released into aquatic systems without any

form of processing (Bondelind *et al*., 2020). According to Jekel (2019), in cases where treatment is unavailable, coarser TRWPs in stormwater could potentially settle within the sewer system. However, this potential loss pathway was not included in the current study due to the lack of available data and the likelihood of it being of minor significance (Jekel, 2019).

In contrast, numerous studies have documented a smaller proportion of tyre and road wear particles being released into surface water (e.g., Wagner *et al*., 2018; Lassen *et al*., 2015). For instance, Sieber *et al*. (2020) calculated that approximately 22% of the TRWP emitted into the environment end up in Swiss waters, while a significant 74% is deposited within a proximity of 5 meters from the road, and the remaining 4% is introduced into soils. However, their assessment considered the significant factor that approximately 70% of Switzerland's entire sewer system consists of combined sewers designed to channel stormwater toward wastewater treatment facilities. In addition, Unice *et al*. (2019) estimated that 18% of the TRWP transported by runoff (50% of TRWP generated on roads), ultimately reach freshwater bodies. This outcome was in part attributed to the high fraction of urban runoff being directed to combined sewers and wastewater treatment plants (75%). The large differences in the proportion of TRWP released into surface waters, as reported in the literature, arises from the fact that TRWP emissions and pathways are location dependent. The treatment of road runoff stands out as a main factor in determining the amount of rubber particles that ultimately enter surface water. Additionally, the consideration of distinct environmental compartments varies across each study, further contributing to the complexity of making meaningful comparisons between them.

In this study, the consideration of erosion from roadside soils as a pathway into surface waters was omitted, following the assessment by Unice *et al*. (2019) that deemed it as a negligible contributor to surface water contamination in the Seine River. Consequently, the soil compartment is regarded as a predominant sink, accounting for approximately 40% to 90% of the total TRWP produced on the roadways.

2.4.2 Spatial variation of emissions

Significant spatial variability in TRWP emissions was observed within the city, along with a corresponding spatial variation in the receiving emissions along the rivers Ouse and Foss. This can be attributed to both the positioning of the WWTP outlets and the model set up, where the emitting areas (HZ) are linked to their respective river segment (RS).

The detected spatial distribution of TRWP emissions in York primarily arises from variations in traffic density, distance travelled, and the prevalence of specific vehicle types across the different HZs. For instance, the HZ with the highest emissions (HZ1, situated in the northwest of the city) corresponds to the area experiencing the highest traffic volume. Likewise, it is evident that the river sections receiving the lowest TRWP runoff emissions (Foss1 and Foss2) are those collecting runoff from smaller areas with lower traffic loads, exemplified by HZ9 and HZ10.

The impact of vehicle weight on TRWP emissions has been highlighted in prior research (e.g., Yan *et al*., 2021; Kim and Lee, 2018; Aatmeeyata *et al*., 2009), revealing a correlation between TRWP emissions and load. This suggests that an increase in load leads to a corresponding rise in the amount of tyre wear particles released (Kim and Lee, 2018). Furthermore, Youn *et al*. (2021) conducted a quantitative analysis of TRWP in road dust samples collected from both industrial and residential areas. They found that the concentration of TRWP in industrial road dust (ranging from 9,804 to 39,738 µg/g) was notably greater than that in residential areas (ranging from 6,400 to 14,876 µg/g). These findings indicate a higher emission factor for TRWP in industrial areas when compared to residential areas, likely due to the increased traffic volume of trucks commonly found in industrial zones (Youn *et al*., 2021). In the present study, the distribution of vehicle types within each HZ contributed to the spatial variation in emissions. For instance, heavy goods vehicles (HGVs), which exhibit the highest tyre wear emission factor, are less common in the city centre compared to buses and cars. Conversely, a higher frequency of HGVs would be anticipated on the outer ring road of the city.

2.4.3 Temporal variation of emissions

The source of tyre and road wear particles entering the aquatic environment is diffuse emissions, making it dependent on factors such as rainfall events, rainfall intensity, and dry periods. Consequently, the year-round temporal variation of TRWP emissions in York is entirely influenced by the prevailing weather conditions. Specifically, the assumption was made that even on days without rainfall events (dry days), TRWP continue to be generated on the road surface, although there is no direct runoff emission into the river. Thus, dry days were considered as accumulation days because, in cases of rainfall events, the TRWP emission to the river section was scaled by a factor proportional to the number of preceding TRWP accumulation days. Moreover, rainfall intensity also influenced TRWP emissions, as not all storm events have the potential to mobilize the TRWP that have accumulated on road surfaces. Consequently, on days characterized by precipitation intensities lower than 2 mm/day, no TRWP emissions into the river section would occur, and these days were considered as additional accumulation days. Hence, the days characterized by both a high rainfall intensity and the most consecutive preceding dry days exhibited the highest TRWP emissions.

The assumptions made in this study are in good agreement with the results reported by Kang *et al*. (2022), who identified a correlation between the concentration of microplastics (including tyre wear, road-marking paint, and bitumen) in road dust and the duration of drying periods. Notably, their research revealed that a longer drying period corresponded to a higher microplastic concentration. For example, on day 0, the microplastic concentration was 552 MPs/g, whereas on day +3 of the drying period the concentration increased by a factor of 2.7 resulting in a count of 1530 MPs/g. In addition, their findings also validated that for accumulated MPs on roads to be effectively washed away by runoff, a higher intensity of rainfall is required (Kang *et al*., 2022).

2.4.4 Uncertainties

In the current locally-scaled model, the input data related to TRWP generation, subsequent runoff transport and treatment, as well as weather information, exhibits a significantly higher level of detail compared to numerous other national mass balance studies. Nevertheless, despite this comprehensive approach, uncertainties persist and need to be addressed. Firstly, the different emission scenarios developed in the present analysis were based on emission factors collected from the literature. However, it has been argued that certain studies are outdated and may not accurately reflect the behaviour or characteristics of contemporary tyres (e.g., Williams and Cadle, 1978). Furthermore, only a limited number of investigations have conducted experiments with passenger car tyres under real-world driving conditions (e.g., Gebbe *et al*., 1997). However, it is worth noting that some studies have exhibited a lack of transparency regarding the methodologies and technical instruments employed (Mennekes and Nowack, 2022). Considering the factors mentioned above, there is a clear need for new studies that incorporate variations in vehicle properties (such as weight), road surface conditions, tyre tread composition, and ambient temperature to ensure accurate estimations of TRWP emissions. These studies should aim for a global applicability perspective, allowing for meaningful comparisons among studies and across different countries.

Secondly, the potential contribution of TRWP deposited on sidewalks, house walls, and front gardens through drift on urban roads, as well as the impact of street cleaning, were not factored into the calculations due to the lack of available data in the literature. Additionally, my assessment took into account that the roads in York are constructed with hot-rolled asphalt rather than porous asphalt, a determination made in consultation with the City of York Council. Porous asphalt is believed to retain approximately 40% of tyre wear particles, as indicated by expert-based assessments (Mian *et al*., 2022). The Netherlands is well-known for having approximately 95% of its motorways constructed using porous asphalt, contributing to their comparatively lower per capita annual emissions (Kole *et al*., 2017). Consequently, this study did not account for any retention of tyre wear particles within the asphalt.

Furthermore, the phenomenon known as the 'first flush', observed in urban stormwater runoff, occurs when the initial stages of a rainfall event carry significantly higher concentrations of pollutants, up to 85% of particles accumulated on road surfaces, compared to the later stages of the event (Do *et al*., 2023; Maniquiz-redillas *et al*., 2022). This effect is influenced by several factors, including antecedent dry days, storm intensity and particle size (Sun *et al.,* 2023; Morgan *et al.,* 2017). For example, in a study conducted by Morgan *et al.* (2017) the 'first flush effect' was investigated concerning suspended solids discharged from a residential drainage system outlet in Kimmage, Ireland. The study analysed 14 storm events and found that 11 of them demonstrated a moderate first flush effect. However, a notable first flush effect was observed in a minority of events, especially for finer solids, such as those in the <10 μm fraction.

In the present study, the ‘first flush effect’ was not accounted for when estimating the runoff emissions of TRWPs on urban roads. Consequently, while the linear equation provides a simplified estimate of wash-off percentage based on precipitation intensity, it may not fully capture the dynamics of the 'first flush effect’. Studies examining the presence of emerging pollutants, such as microplastics and tyre and road wear particles, during the 'first flush' are limited (Maniquiz-redillas *et al.,* 2022). Therefore, future research is necessary to understand their behaviour in stormwater runoff.

Lastly, combined sewer overflow events (CSOs) are triggered by heavy rainfall and result in the discharge of partially diluted raw sewage into surface waters. Previous research has sought to quantify the impact of CSOs. For instance, Unice *et al*. (2019) determined that within the Seine River basin, approximately 5% of the total TRWP mass is released to CSOs annually. Similarly, Sieber *et al*. (2020) estimated a loss rate of 3.2% for combined sewer overflows in Switzerland. In the case of York, the absence of available CSO data led to their exclusion from the model. However, it highlights the significance for wastewater operators to gain insights into the proportion of CSOs in their annual wastewater flows and to ensure transparency in sharing this information. This practice is essential to improve the accuracy of exposure assessments in the environment.

2.5 Conclusion

In this chapter, a TRWP emissions model was developed and implemented in a case study involving a small urban area. The model approach involved a thorough assessment of several components, such as traffic flow, emission factors, sewerage systems, and precipitation data. The outcome of this analysis resulted in the determination of emission ranges for the different environmental compartments studied (air, soil, surface waters). Furthermore, the areas within the city that make the most significant contributions to these emissions, as well as the temporal patterns that characterize these emissions were identified.

Regarding TRWP emissions, this study has highlighted several knowledge gaps that need to be addressed. Specifically, there is a need for additional research to establish more accurate and up-to-date emission factors, investigate the behaviour of TRWP within WWTPs, validate the pathways of TRWP distribution to soil, sewerage systems, and air, and assess the impact of street cleaning on TRWP concentrations. In addition, it is also necessary to consider the implementation of certain mitigation measures. These include the installation of road runoff treatment systems in areas lacking combined sewers, adopting appropriate methods for sewage sludge disposal instead of spreading it on agricultural land, enforcing speed limits, conducting regular pavement cleaning, and optimizing the sewerage system to reduce overflows and prevent untreated sewage discharge.

The shift from conventional motorized vehicles to electric ones will certainly result in a notable decrease in exhaust emissions; however, it will not have a corresponding impact on reducing tyre wear emissions. As the amount of TRWP is anticipated to continue to increase each year, the growing concern over consequential environmental issues remains. Thus, the development of localized and spatially resolved models, utilizing available local data within a city, holds the potential to enhance the reliability of risk assessment outcomes.

Chapter 3. Method development for the separation and analysis of tyre and road wear particles from sediment samples by Pyrolysis-GC/MS

3.1 Introduction

As demonstrated in the previous Chapter, the prediction of emissions, and distribution of TRWPs in the natural environment is a complex problem and relies on the availability of model input parameters, such as particle properties, many of which remain uncertain. There is also a significant shortage of concentration data on TRWPs in the environment that is necessary for model calibration and evaluation (Klöckner *et al*., 2020). Therefore, many researchers have highlighted the urgent need for the development of reliable and standardized analytical methodologies to quantify and characterize TRWPs in the environment. This would ultimately enhance the comparability and shareability of data on a global scale (Mattonai *et al*., 2022; Thomas *et al*., 2022; Kovochich *et al*., 2021; Yakovenko *et al*., 2020) and also allow for the generation of TRWP occurrence data that can be used for the evaluation of emission and fate models for these materials.

Recently, pyrolysis-gas chromatography–mass spectrometry (Py-GC-MS) has emerged as a robust method for quantifying TRWPs in environmental samples (Cho *et al*., 2023; Mattonai *et al*., 2022). This technique uses thermal energy to efficiently break down large molecules into simpler fragments, including monomers, dimers and trimers (Yakovenko *et al*., 2020). These fragments are subsequently separated *via* gas chromatography and identified through mass spectrometry (Pico and Barcelo, 2020; Yakovenko *et al*., 2020), allowing for their use as markers to determine the concentrations of TRWPs in environmental matrices (Pico and Barcelo, 2020) (Fig. 3.1). This thermo-analytical method offers several advantages over alternative approaches such as Fourier-transform infrared spectroscopy (FT-IR), Raman spectroscopy, SEM/EDX and ICP-MS. Advantages of Py-GC-MS include it allows the detection of particles at the nano scale, it has heightened sensitivity and compatibility

with various purification and extraction processes (Pico and Barcelo, 2020). The outcome of this technique provides mass concentration data, complementing the information derived from microscopic analysis such as size, morphology, and number of particles (More *et al*., 2023).

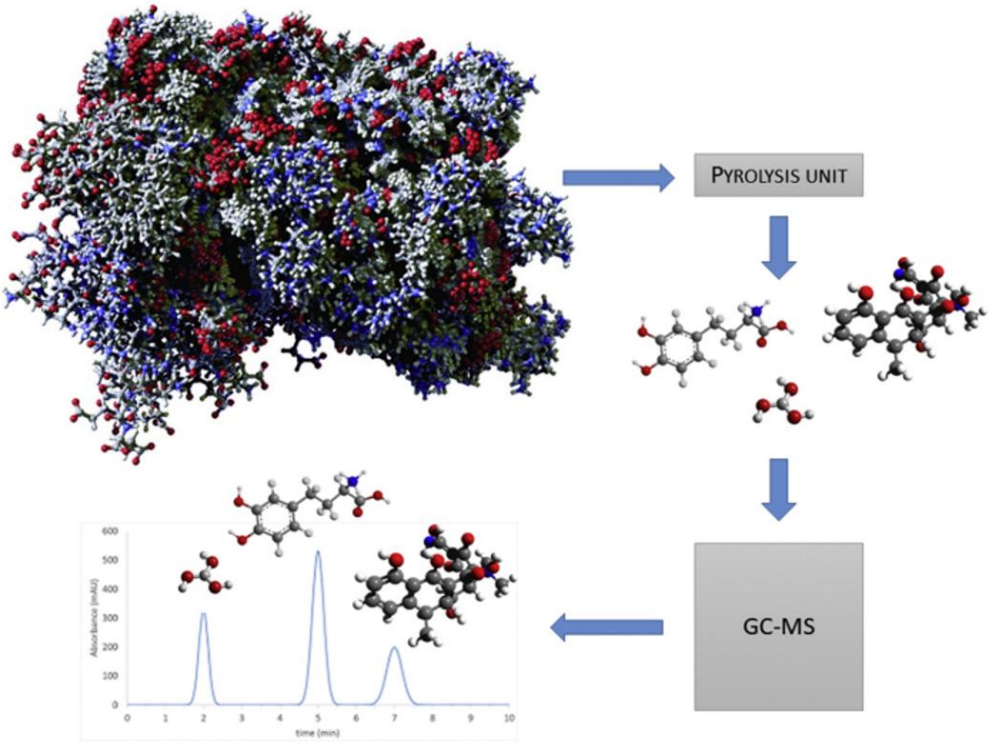

Figure 3.1. Representation of the Py-GC-MS process. Source: taken from (Pico and Barcelo, 2020).

Numerous markers have been employed for the analysis of TRWPs in diverse environmental contexts (e.g., Kumata *et al*., 2002; Reddy and Quinn, 1997; Kumata *et al*., 1996; Kim *et al*., 1990; Spies *et al*., 1987). These markers include benzothiazole (BT), 24MoBT (2-(4-morpholinyl) benzothiazole), HOBT (2-hydroxybenzothiazole), and NCBA (Ncyclohexyl-2-benzothiazolamine), which are types of benzothiazoles commonly used as vulcanization accelerators in rubber production (Federico *et al*., 2023; Unice *et al*., 2013; Wik and Dave, 2009). Nevertheless, none of these markers have proven to be reliable indicators of the presence of tyre particles, as they lack specificity to rubber polymers and are not retained within tyre treads in the

environment (Unice *et al*., 2013). For example, NCBA is also present in antifreeze leakages from automobile radiators, so its use as a maker potentially leads to an overestimation of TRWPs in the environment. Conversely, benzothiazoles are susceptible to leaching in aquatic environments, possibly resulting in an underestimation of TRWPs (Mengistu, 2023; Unice *et al*., 2013). Consequently, recent studies have proposed the use of elastomers as markers, given their prevalence as a major component of tyre wear particles (Federico *et al*., 2023; Mattonai *et al*., 2022).

Specifically, styrene butadiene rubber (SBR), the primary constituent in passenger car tyres, has been advocated as a marker due to its high specificity to tyre tread, ensuring there are no other major sources of SBR in the environment (Eisentraut *et al*., 2018, Wik and Göran, 2009). Additionally, SBR aligns with the marker criteria established by Wagner *et al*. (2018), including its presence in all tyres regardless of the manufacturer, resistance to leaching when in contact with surface water or sediment and a significant high concentration in tyre and road wear particles (Unice *et al*., 2013).

Unice *et al*., (2012), conducted one notable study that employed polymer markers for quantifying TRWPs in environmental media. In their research, they introduced a Py-GC-MS methodology where the pyrolysis product 4-vinylcyclohexene was used to estimate the cumulative SBR/BR content (assuming a composition of 15% styrene and 85% butadiene within the SBR+BR total mass) and the pyrolysis product dipentene was used to quantify NR. The method also featured the integration of a deuterated polymer internal standard to correct for the marker's influence on decomposition product generation and mitigate matrix effects in the sample (Unice *et al*., 2013). This method was subsequently incorporated into two ISO technical specifications for the quantification of SBR/BR and NR in soil/sediment and ambient air samples (ISO/TS 20593:2017 and ISO/TS 21396:2017) (More *et al*., 2023; Mattonai *et al*., 2022).

While ISO methods and the majority of TRWP studies employing pyrolysis-gas chromatography-mass spectrometry traditionally analyse samples as a whole without

prior preparation, pre-treatment techniques have been utilized in previous microplastics research involving Py-GC-MS (Bouzid *et al*., 2022, Pico and Barcelo, 2020). It is important to recognize that TRWP exhibit distinct compositional and morphological differences compared to common thermoplastics (More *et al*., 2023).

The pre-treatment of samples involves the digestion of organic matter and the concentration of plastic particles through density separation. Several chemicals have been utilized to digest organic matter from samples, including 10% potassium hydroxide (KOH), Fenton reagent, hydrochloric acid (HCl), sodium hydroxide (NaOH), nitric acid (HNO_3), and hydrogen peroxide (H_2O_2). In some cases, specific combinations of these chemicals are employed at particular temperatures and durations (Wagner and Lambert, 2018; Hanvey *et al*., 2017). Notably, hydrogen peroxide (30%) stands out as the most frequently used method for digestion in microplastics studies, with reported high removal rates achieved after a few hours at 70 °C (Kang *et al*., 2022; Monira *et al*., 2022; Wiggin and Holland, 2019; Klein *et al*., 2015).

After digestion of the samples, the subsequent step involves isolating the TRWPs from the environmental matrix, and this is achieved using density separation solutions. Commonly used solutions for this method include sodium chloride (NaCl), sodium iodide (NaI), calcium chloride ($CaCl_2$), zinc chloride ($ZnCl_2$) and oil-based media such as canola and castor oil (Thomas *et al*., 2022; Mattonai *et al*., 2022). This step becomes particularly crucial due to the limited sample size allowed for Py-GC-MS analysis, where the precise separation of target particles from the environmental matrix significantly influences the analytical accuracy and reliability (Mattonai *et al*., 2022, Yakovenko *et al*., 2020). Consequently, numerous studies have recommended the inclusion of pre-treatment procedures in the Py-GC-MS analysis of TRWPs, especially for samples characterized by low traffic influence and complex matrices, such as river sediments (Mattonai *et al*., 2022; Rødland *et al*., 2020).

The objective of this chapter was to introduce pre-treatment procedures for TRWP analysis, aimed at minimizing interference and matrix effects caused by organic and inorganic constituents within the samples, while ensuring the sample's

representativeness. Subsequently, Pyrolysis-GC-MS analysis was conducted, following the ISO/TS 21396:2017 method with certain adjustments. This proposed methodology was then applied to sediment samples collected from regions characterized by significant traffic influence to test the method.

This methodology holds the potential for application across various environmental matrices, however, the present study predominantly centred on the analysis of river sediments. This focus aligns with existing literature, which underscores that TRWPs, once introduced into the aquatic environment *via* road runoff, exhibit a propensity for sedimentation owing to their high density and size distribution. Consequently, river sediments are recognized as reservoirs for TRWPs, effectively capturing and retaining between 70% and 90% of these particles. It is worth noting that these percentages, along with further percentages mentioned in the chapter regarding TRWPs in sediments, are derived from within the 60% estimated to reach the river.

3.2 Materials and methods

3.2.1 Tyre samples

In order to assess the methodology for extracting TRWPs from sediment matrices, two-year-old used tyres were obtained from a local garage. Specifically, tyre particles (TP) samples were then generated by employing an electric file to abrade the treads of both a passenger car tyre (Continental 205/55 R16) and a van tyre (Laufenn 235/65R16). To ensure proper storage and preservation, the resulting tyre particles from each tyre type were collected and placed in individual glass jars.

3.2.2 Validation of the extraction method

The efficacy of the density separation extraction method was evaluated through recovery tests, employing soil collected from a remote hill area on the University of York campus east (53°57'03.9"N 1°01'46.8"W). Although the chosen soil diverges from typical river sediment samples, its selection stemmed from its lack of TRWP presence and minimal vegetation interference, providing a clean baseline for testing.

In order to simulate diverse scenarios, the soil was spiked with a combination of car and van tyre particles varying in sizes and concentrations. Equal amounts of car and van TP were used to ensure representation of the different vehicles typically found in urban environments. While cars may be more prevalent, incorporating van tyre particles accounts for the presence of other vehicle types. The selection of TP sizes was based on TRWP size ranges reported in the literature, spanning from 10 to 500 µm (Parker-jurd *et al*., 2021; Klöckner *et al*., 2020; Bondelind *et al*., 2020). The generation of distinct TP sizes was achieved by using stainless steel sieves with openings measuring 90, 250, and 500 µm (Fig. 3.2). The level of spiking was adjusted to replicate TP concentrations observed in river sediment, ranging from 0.2 to 42 mg/g as reported by Arias *et al*. (2022). Furthermore, higher concentrations of 80 mg TP/g were taken into account to address scenarios significantly influenced by traffic, as observed in road dust and roadside soil samples (Klöckner *et al*., 2019).

A total of 10 comprehensive spiking combinations (as detailed in Table 3.1) were applied to approximately 1g of oven-dried soil. These spiked samples, including a blank for comparison, were subjected to thorough mixing and underwent the same processing steps as the actual field samples (refer to sections 2.4, 2.5 and 2.6). Recovery efficiencies were calculated using the following equation (Quinn *et al*., 2017):

$$\%\, recovery = (weight\ of\ TP\ extracted / weight\ of\ TP\ spiked)\ X\ 100 \qquad (1)$$

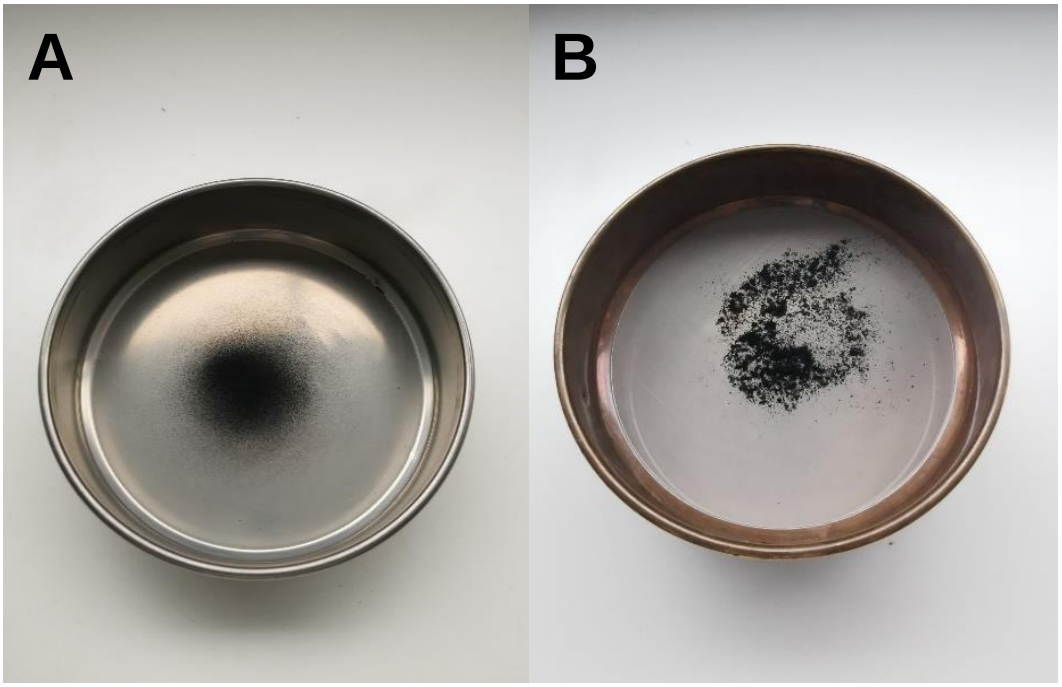

Figure 3.2. Tyre particle sizes generated using sieves: (A) 90 µm and (B) 250 µm.

Table 3.1. Combinations of the spiking experiment, delineating the TP sizes and concentrations within each sample.

Sample	Size of tyre particle (TP) [µm]	Spiking level (mg TP/g)
Blank	---	---
C1	500	5
C2	500	20
C3	500	80
C4	250	5
C5	250	20
C6	250	80
C7	90	5
C8	90	20
C9	90	80
C10 (Mix)	500/250/90	30

3.2.3 Environmental sediment sampling

The selection of sampling locations was guided by the study conducted by Maltby *et al*. (1995), which identified streams significantly contaminated by motorway runoff discharges in the UK. For the sites 'Pigeon Bridge Brook' and 'Butterthwaite Ditch', a total of three sampling locations were designated for each site. These included an upstream point before the entry of stormwater runoff into the stream, a location directly downstream from this point of entry, and a subsequent downstream location. The annual average daily traffic flows for these locations are 142,653 vehicles for Pigeon Bridge Brook and 116,168 vehicles for Butterthwaite Ditch (https://roadtraffic.dft.gov.uk). Conversely, at the 'Rockley Dike' site, only two sampling points were considered, consisting of one upstream and one downstream of the motorway runoff discharge (Fig. 3.3). After sampling, it was discovered that the grid coordinates for the location 'Rockley Dike' were incorrect in Maltby *et al*.'s paper. Although the actual sampled location is still influenced by a nearby highway, its traffic impact is significantly lower. While it was not the originally intended location, it does offer data on a river affected by a smaller road with an annual average daily traffic flow of 15,000 vehicles. Consequently, the decision was made to include this location in the study, adding valuable data to the results.

The sampling was conducted in June 2021, with sediment samples collected from the middle of the stream using a stainless steel spade. At each sampling location, approximately 600 g of sediment, ranging from 5 to 10 cm in depth, was collected in triplicate and placed into individual 1 L glass jars. These samples were then stored at -5°C until analysis.

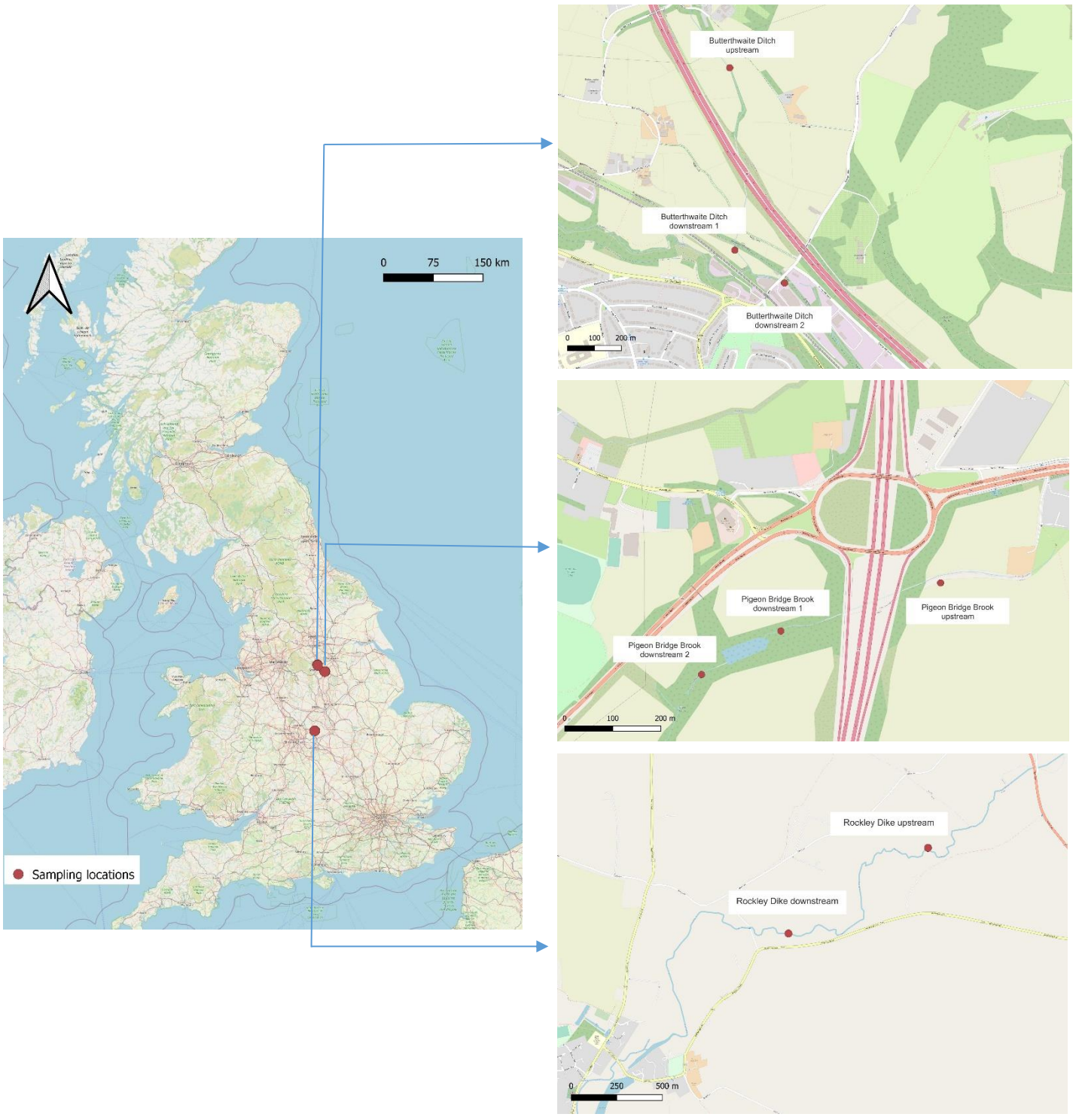

Figure 3.3. Maps of the sampling locations: Butterthwaite Ditch (BD), Pigeon Bridge Brook (PBB) and Rockley Dike (RD). Rockley Dike sampled locations were as follows: upstream (52°37'14.52" N, 1°29'27.41" W) and downstream (52°36'59.51" N, 1°30'8.38" W).

3.2.4 Drying and sieving

Sediment samples (approximately 200g in aluminium trays) were dried in an oven at 105 °C for 24 - 48 hours until the water content was fully evaporated (Unice *et al*., 2013). Following this, the dried sediment was homogenized using a pestle and mortar. As previously discussed, the size ranges of TRWP vary across the literature. For instance, tyre wear particles derived from road simulators are notably smaller (<200 µm) (Wagner *et al*., 2018), in contrast to TRWPs found in real-world environmental samples, such as sediment collected from an open settling pond system treating highway runoff, which exhibited a size range from 11 to 1,500 µm (Kovochich *et al*., 2021b). As a result, this study established a maximum size threshold of 2 mm, which was applied when oven-dried sediment samples were sifted through a 2 mm stainless steel sieve.

3.2.5 Sample digestion

The presence of organic matter in sediments interferes with the analysis of TRWP and therefore, should be removed prior to the extraction of TRWP using density separation methods (Thomas *et al*., 2022). The digestion method most frequently employed in microplastic studies is 30% hydrogen peroxide (H_2O_2) (More *et al*., 2023; Kang *et al*., 2022; Mattonai *et al*., 2022; Chico-Ortiz *et al*., 2020; Leads and Weinstein, 2019). As noted by Hanvey *et al*., (2017) H_2O_2 was identified as the optimal solution for digesting samples with a high content of organic matter due to its ability to effectively maintain the integrity of polymer size, shape, and resulting spectra, outperforming alternative solutions.

Here, subsamples of approximately 30g of dried sediment (three replicates per sampling point) were introduced into a 500 ml glass beaker. Deionised water (50 ml) and 10 ml of 30% hydrogen peroxide (Fisher Chemical) were added to each beaker, and the contents were gently stirred to achieve a homogeneous suspension (Ziajahromi *et al*., 2020). The resulting mixture was subsequently heated at 50°C for two hours. Afterward, the hotplate was turned off, and the sample was left overnight. This process of adding 10 ml of hydrogen peroxide and undergoing a two-hour heating cycle was repeated until no observable bubbles remained in the beaker

(Monira *et al*., 2022; Leads and Weinstein, 2019). It is worth noting that no deionised water was added to the 1g spiked samples during the method validation, as 5 - 10 ml of the 30% hydrogen peroxide was sufficient to cover the sediment without any issues.

Once digestion was finalized, the samples were carefully transferred into 50 ml centrifuge tubes, aided by a gentle spray of deionized water along the beaker's inner surface to remove any particles adhering to the walls. Subsequently, the samples underwent three rounds of centrifugation (Hettich Rotanta 460) at 3500 rpm for 10 minutes each, ensuring thorough cleansing to remove any chemical residues.

3.2.6 Density separation of TRWP from sediment samples

In a recent investigation, Jung and Choi (2022) developed a classification method of TRWPs in road dust using a density separation technique. The outcomes of this analysis revealed the absence of TRWPs with densities below 1.20 g/cm³ or exceeding 1.70 g/cm³. Additionally, other studies have reported an estimated TRWP density of 1.8 g/cm³ (Unice *et al*., 2019; Klöckner *et al*., 2019). As a result, the potential exists to enrich TRWPs within sediment samples using density separation solutions (ranging from 1.2−1.9 g/cm³), as TRWPs exhibit greater buoyancy compared to the sediment mineral fraction (2.5 g/cm³) (Thomas *et al*., 2022).

Previous studies have employed a range of solutions for microplastic and TRWP extraction, including sodium chloride (NaCl), sodium iodide (NaI), calcium chloride ($CaCl_2$), and zinc chloride ($ZnCl_2$) (Mattonai *et al*., 2022). However, certain drawbacks have been reported. For instance, $ZnCl_2$ with a final density of 1.7 g/cm³ can prove to be costly, corrosive, toxic, and environmentally harmful, potentially even causing polymer degradation. On the contrary, sodium chloride (NaCl) at 1.2 g/cm³, while being economical, safe for the environment, and readily accessible, is suited only for low-density polymers. It’s use may therefore lead to an underestimation of TRWP concentrations due to their higher densities in comparison to other types of microplastics (Thomas *et al*., 2022).

Due to these limitations of these different solutions, recent research has recommended the use of polytungstate salts which have elevated densities (2.2 g/cm³) and thus ensure precise TRWP extraction, while preserving the particle characteristics intact (Mattonai *et al*., 2022). In this study, I employed LST Fastfloat, a solution consisting of sodium heteropolytungstates with low toxicity, dissolved in water (Polytungstates Europe). This liquid of high density (2.80 g/cm³) is characterized for having a remarkably low viscosity, enabling float-sink separations that are twice as fast as those achieved with sodium or lithium polytungstate and facilitating a quicker filtration process (www.polytungstate.co.uk/heavyliquids).

To extract TRWP from the sediment samples, the separation solution was prepared by gradually adding deionised water to the LST Fastfloat liquid until it reached the targeted density of 1.95 g/cm³. Subsequently, this solution was mixed in a beaker using a magnetic stir bar, allowing for complete dissolution. Approximately 15 ml of this mixture was added to each of the digested samples in the centrifuge tubes. The tubes were agitated with a vortex mixer for two min and then centrifuged at 3500 rpm for 15 min (Ziajahromi *et al*., 2020). These steps were repeated two times for each sample to increase the recovery rate of TRWPs in the sediment (Ziajahromi *et al*., 2020; Besley *et al*., 2017).

The resulting supernatant was carefully filtered through glass fibre filters (Whatman GF/F, pore size 0.7 µm) using a vacuum pump system. To eliminate any excess Fastfloat, the filters were rinsed with deionized water during filtration and subsequently placed in individual glass petri dishes (Blair *et al*., 2019). Following filtration, the environmental samples were stored at room temperature for further Pyrolysis-GC-MS analysis. Meanwhile, the spiked samples underwent a drying process at room temperature over the course of a week before being weighed to calculate recovery percentages (Bye and Johnsen, 2019).

3.2.7 Loss on ignition analysis

The determination of organic matter content in each sediment sample involved placing approximately 5g of pre-dried sediment into a Carbolite muffle furnace. These

samples were subjected to a temperature of 550°C for a duration of four hours, followed by cooling in a desiccator at room temperature over the course of a day.

The loss on ignition (LOI) was subsequently calculated through the application of the following formula:

$$\mathrm{LOI}_{550} = ((\mathrm{DW}_{105} - \mathrm{DW}_{550}) \,/\, \mathrm{DW}_{105}) \,\mathrm{X}\, 100 \qquad (2)$$

Where DW_{105} represents the initial weight of the sample which was oven-dried at 105°C prior to combustion, and DW_{550} reflects the dry weight of the sample after exposure to 550°C heat (Chico-ortiz *et al*., 2020).

3.2.8 Sediment grain size analysis

To conduct particle size analysis, 10g of each sediment sample was placed in a 250 ml tall beaker and treated with 10 ml of 30% hydrogen peroxide to eliminate organic material. The beakers were left overnight in a fume cupboard to start the digestion process. Subsequently, an additional 10 ml of 30% H_2O_2 was added, and the beakers were placed on a hot plate at 75°C until no further reaction was observed. Upon cooling, the samples were transferred to 50 ml centrifuge tubes, topped up with deionized water, and centrifuged at 3500 rpm for 10 min. This step was repeated twice more to ensure complete removal of any remaining H_2O_2. The laser granulometer Malvern Mastersizer 2000 (pump speed = 1500) was used for the particle size analysis. The results were recorded in triplicate, reporting particle volume percentages within 100 size intervals ranging from 0.02 to 2000 µm (Chico-ortiz *et al*., 2020).

3.2.9 Pyrolysis GC-MS analysis

Pyrolysis-Gas Chromatography-Mass Spectrometry (Py-GC-MS) was carried out using a CDS Pyroprobe 5000 series pyrolysis instrument attached to an Agilent 7890B GC system and Agilent 5977A MSD. CDS 5250T and Agilent MassHunter

software was used to control the instruments. Mass spectrometer tuning was performed using the Masshunter autotune function before each run sequence to verify instrument performance. Detailed Pyrolysis GC-MS conditions are presented in Table 3.2.

Table 3.2. Instrumental conditions for Pyrolysis-GC-MS measurements.

Parameter	**Settings**
Pyrolyzer	
Pyroprobe conditions	Initial: Ambient, 0.00s; Heating rate: 20.00°C/mS; Final temperature: 670°C, 5.00s hold
Valve oven	300°C
Transfer line	310°C
Mode	No trap
Purge time	0.20 min
Equilibrate time	0.20 min
Post-pyrolysis time	4.00 min
Gas Chromatogram - Mass Spectrometer	
GC inlet	300°C, split injection (250:1)
Injection source	Manual
Carrier gas	Helium
Column	Agilent HP-5MS UI 30m x 0.250mm x 0.25µm
Column flow rate	1ml/min constant flow
Oven (gradient)	Initial 50°C for 5 min; 25°C/min to 300°C, hold for 10 min
Run time	25 min
MSD transfer line	300°C
Mass Spectrometer	Single quad positive electron ionization mode at 70 eV
Scan Mode	m/z = 35 to 550 (1.5 scans/sec)

3.2.9.1 Method optimization for sample analysis

To improve the repeatability and signal sensitivity of the analysis, an evaluation of sample presentation approaches was conducted. Specifically, pre-treated samples were compared with an untreated sample, followed by a comparison between the two pre-treated sample variations. The test samples were spiked with a TP concentration

of 5 mg/g, a concentration previously reported for sediment samples (Unice *et al*., 2013). The spiking process involved the following steps: a) 1g of reference soil was spiked with 5 mg of TP material (passenger car TP) without any pre-treatment.
b) For the second sample, 30g of soil was spiked with 150 mg of TP. These samples followed the same treatment protocol as the field samples, including the removal of organic matter using 30% hydrogen peroxide and the extraction of TWPs through density separation. After filtration, the filter was placed in a glass petri dish, and the sample intended for pyrolysis was directly obtained from the filter (referred to as GF filter).

c) Finally, 30g of soil was spiked with 150 mg of TP and subjected to identical processing steps as the field samples. Post-filtration, the filtered material was carefully scraped from the filter using a stainless steel spatula and transferred into a small glass vial (referred to as glass vial samples). Both the filters and glass vials were weighed before and after the analysis.

Additionally, an evaluation of potential interferences from background media was conducted, including the analysis of an unspiked sediment sample, an unspiked sample after pre-treatment, a piece of unused glass fibre filter, and a piece of wool. For the Py-GC-MS analysis, approximately 4 mg of each sample was loaded into a quartz tube and subjected to the instrument's predefined conditions. The peak area of the pyrolysis product 4-vinylcyclohexene (VCH) was identified and compared among the samples.

3.2.9.2 Standard stock solutions

In accordance with the ISO method (ISO/TS 21396:2017), TRWP mass concentration in environmental samples was determined by identifying and quantifying polymer pyrolysis byproducts. The polymers used were NR and SBR/BR, along with their associated markers dipentene and 4-vinylcyclohexene, respectively. However, it has been noted that NR can potentially yield false positive results due to the detection of its decomposition products, such as dimers and higher oligomers of isoprene, in organic matter (Eisentraut *et al*., 2018). To address this concern, this study

exclusively utilized SBR, with its decomposition product, 4-vinylcyclohexene, serving as the specific marker compound for the elastomer. In addition, a deuterated internal standard was used to increase GC/MS efficiency and correct for matrix effects influencing polymer pyrolysis and fragment recovery (Rauert *et al*., 2021; Unice *et al*., 2012).

The standard polymers were obtained from Polymer Source, Inc. (Dorval, QC, Canada) (Table 3.3) and were used to prepare stock solutions. Random Copolymer Poly(styrene-co-butadiene) equivalent to SBR-1500 (P42084-SBdran) was the calibration polymer for SBR standard and deuterated Poly(1,4-butadiene-d6) (P41833-dBd) was used as internal standard.

To prepare the stock internal standard solution, 57.4 mg of deuterated Poly(1,4-butadiene-d6) (d-PB) was carefully weighed and introduced into a graduated flask. Two-thirds of 10 ml of chloroform (Acros Organics) were added, and the mixture was left to dissolve overnight. Subsequently, the remaining volume of solvent was added, and the solution was left for an additional 24 hours to ensure complete polymer dissolution (More *et al*., 2023). Similarly, two stock calibration solutions were prepared by introducing approximately 10 mg and 1g of SBR standard into separate graduated flasks, each having a target volume of 100 ml of chloroform. These calibration solutions followed the same dissolution process as the internal standard solution (More *et al*., 2023; Unice *et al*., 2012).

Table 3.3. Standard polymer materials.

Polymer	**Use**	**Pyrolysis product**	**Indicator ions (m/z)[a]**	**Molecular ion (m/z)**	**Retention time (min)**
Styrene butadiene rubber (SBR)	Calibration polymer	4-vinylcyclohexene (VCH) (CAS 100-40-3)	39, **54**, 79, 108	108	5.2
Poly(1,4-butadiene-d6) (d-PB)	SBR Internal standard	Deuterated butadiene dimer (d-BdD)	**60**, 120, 42, 86	120	5.03

[a] Bold values used for calibration and quantification based on ISO/TS 21396:2017 and Rødland *et al*., (2020).

3.2.9.3 Calibration curves

Calibration curves were prepared at the beginning of each pyrolysis run. This was achieved by precisely pipetting the chloroform solutions (as detailed in Table 3.4) into the sample holder, which consisted of a quartz tube containing a rod and a wool plug. Subsequently, the solvent was allowed to evaporate naturally at room temperature for 30 minutes (Bye and Johnsen, 2019). Moreover, internal standard calibration curves were constructed using a least-squares regression with a quadratic fit, aiming for a coefficient of determination (R^2) greater than 0.99. The response ratio (Y) was calculated as the peak area of the SBR standard pyrolysis marker (4-vinylcyclohexene) divided by the peak area response for the deuterated internal standard. The amount ratio (X) was determined as the mass of SBR standard divided by the mass of deuterated internal standard (with identical mass amounts used in calibration curve preparation) (More *et al*., 2023; Unice *et al*., 2012; ISO/TS 21396:2017). Additionally, blank samples were included in each calibration curve analysis and periodically throughout the study (More *et al*., 2023).

The quality and stability of the internal standard stock solution, which was employed throughout the entire analysis, was assessed by ensuring that the peak areas never deviated by more than 25% compared to the peak area obtained on the initial calibration with a freshly prepared solution (Unice *et al*., 2012).

Table 3.4. Calibration points for SBR

Calibration point	SBR stock solutions[a]	SBR volume added to sample holder (µL)	d-PB volume added to sample holder (µL)	Mass of SBR (µg)	Mass of d-PB (µg)
SBR-1	S-1	10	10	1.01	57.4
SBR-2	S-2	1	10	10.1	57.4
SBR-3	S-2	2.5	10	25.25	57.4
SBR-4	S-2	5	10	50.5	57.4
SBR-5	S-2	10	10	101	57.4

[a] Stock calibration solution S1 contains 10 mg of SBR in 100 ml of chloroform, while S2 comprises 1g of SBR in 100 ml of chloroform (based on ISO/TS 21396:2017).

3.2.9.4 Sample preparation and measurement

The pyrolysis analysis was carried out by inserting approximately 10 mg of the environmental field samples into a pre-weighed quartz tube. After sealing these sample tubes with quartz wool, they were spiked with 10 µL of the internal standard solution and allowed to evaporate at room temperature for 30 minutes (Rauert *et al*., 2021; Bye and Johnsen, 2019).

The chromatogram peaks corresponding to the marker compound and the deuterated internal standard were identified and quantified utilizing the Agilent MassHunter Qualitative and Quantitative software, in conjunction with the National Institute of Standards and Technology (NIST) mass spectrometry search library. Furthermore, 4-vinylcyclohexene peak areas underwent manual inspection for quality control and were subsequently normalized based on both the sample weight and the peak area of the deuterated butadiene dimer prior to the calculation of the tyre tread mass (Rosso *et al*., 2023; Unice *et al*., 2012)

The limits of detection (LOD) and quantification (LOQ) for SBR, determined by analysing the decomposition product 4-vinylcyclohexene, were calculated as three times the instrument signal-to-noise ratio (S/N) and five times the S/N, respectively (ISO/TS 21396:2017).

3.2.9.5 Tyre polymer quantification

To determine the concentration of TRWP in the sediment samples, the initial step involved calculating the polymer mass within the sample, specifically SBR/BR. This calculation was then followed by considering the rubber fraction in the tyre tread, the percentage of mineral encrustment in TRWP, and the total sediment mass in the sample (ISO/TS 21396:2017).

The quantification of SBR/BR mass in the samples was achieved by using the calibration curves and applying a correction factor for the SBR standard (Random Copolymer Poly(styrene-co-butadiene). This correction is advised to account for the variance in styrene content between the polymer standard employed in the calibration curve preparation and the styrene content found in SBR/BR used for tyre tread

manufacturing (More *et al*., 2023; Rauert *et al*., 2021). Therefore, the adjustment was made using the following formula:

$$\mathrm{M_{SBR}} = \mathrm{M_{STD}\,x}\,\frac{(1-\mathrm{Sc})}{(1-St)} = \mathrm{M_{STD}\,x}\,\frac{(1-0.235)}{(1-0.150)} = \mathrm{M_{STD}\,x}\,0.9 \qquad (3)$$

Where M_{SBR} represents the corrected mass of SBR/BR in the sample (µg), M_{STD} is the calculated mass of SBR in the analysis based on the 4-vinylcyclohexene marker and calibration curves developed using the polymer standard (µg), Sc represents the percentage of styrene content in the SBR calibration standard used in the study (23.5%), and St is the average styrene content in tyre tread (15%).

According to the ISO method, the polymer content in tyre tread, including SBR/BR and NR, is approximately 50% (with individual fractions assumed to be 44% for SBR and 45% for NR). However, a study conducted by Eisentraut *et al*. (2018) estimated that SBR makes up only 11.3% of the total polymer content in tyre material. This estimation was based on a comprehensive literature review that considered global production volumes of major elastomer tyre compounds and the specific fractions used in tyre production across all types of tyres. Furthermore, a similar finding was reported by Rauert *et al*. (2021). In their study, they employed pyrolysis GC-MS along with the marker compound 4-vinylcyclohexene to assess the synthetic rubber content in 39 commercially available tyres. Their analysis revealed a mass percentage range spanning from <0.05% to 28%, with an average value of 9.3% (Rauert *et al*., 2021).

To calculate the final concentration of TRWP, the ISO method makes an assumption of a 50% mass contribution from tread polymer and a 50% mass contribution from mineral encrustations in TRWP. However, given the uncertainties surrounding the level of encrustation in TRWP, which has been observed to vary between 6% and 53% (Rødland *et al*., 2022; Sommer *et al*., 2018), it is advisable to report monitoring study results as tyre tread. This approach helps mitigate the risk of either

underestimating or overestimating concentrations, depending on the chosen percentage of encrustation (Baensch-Baltruschat *et al*., 2020).

In this study, an 11.3% SBR content in the tyre material was considered when converting the measured polymer concentration to tread polymer concentration. In addition, TRWP results are expressed on a tread basis, and all values are referenced to the total dry mass of the sample. This led to the application of the following formula:

$$M_T = \frac{(M_{SBR})}{F_r \, X \, W} \qquad (4)$$

Where M_T is the mass concentration of TRWP as tread in the sediment samples (µg/g), M_{SBR} represents the adjusted mass of SBR/BR in the sample (µg), F_r is the synthetic rubber fraction in tyre tread and, W is the total weight of the sediment sample (g).

3.2.10 Quality assurance and quality control

Multiple precautions were implemented to prevent the occurrence of microplastic contamination both in the field and within the laboratory setting. During the sample collection process, certain steps were taken to ensure the prevention of cross contamination between samples. For example, after each sampling location, the stainless steel spade was thoroughly rinsed with deionized water and then cleaned with blue roll. Alongside this, nitrile gloves were consistently worn while handling the sediment. Furthermore, the glass jars containing the sediment samples were covered with aluminium foil prior to the placement of their respective lids. This measure was implemented to ensure an added layer of protection against any external factors that could potentially introduce contamination.

In the laboratory, strict adherence to safety protocols was maintained, including wearing a white cotton laboratory coat and blue nitrile gloves throughout all procedures. The pre-treatment method of sample digestion was performed under a

decontaminated steel fume hood to minimize possible airborne contamination. The subsequent processes of density separation and filtration were carried out in a clean space where all surfaces were sanitized after processing each sample. Additionally, whenever possible, stainless steel and glass equipment were used, and meticulous care was taken to wash them with detergent and rinse them with deionized water before each use. As a measure to assess the potential presence of airborne particles within the laboratory, a glass beaker containing deionized water was deliberately left exposed during the course of laboratory activities. Subsequent microscopic examination of the deionized water revealed no evidence of contamination from airborne microplastics.

3.2.11 Statistical analysis

The data underwent log transformation to achieve normality and homogeneity of variances. Subsequently, a two-way analysis of variance (ANOVA) was conducted, followed by the Tukey multiple comparison test, to determine if there were significant differences in the response variable TRWP mass concentration across sampling locations and between upstream and downstream sites. Furthermore, a separate two-way ANOVA, followed by the Tukey multiple comparison test, was carried out to assess potential variations in organic matter concentrations among different sampling locations.

3.3 Results and discussion

In this study, the focus of sample pre-treatment was to reduce potential interferences and matrix effects originating from organic matter and inorganic constituents during the Pyrolysis-GC-MS analysis. Figure 3.4 provides an overview of the sampling and analysis procedures detailed in this chapter.

1. River sediment collection with a stainless steel spade or grab sampler
2. Pre-treatment of the samples
Sediment characterization (organic matter content and particle size analysis)
Oven drying at 105 °C (24 - 48 hours)
Homogenization of the sample by mortar and pestle
Size separation using a 2 mm stainless steel sieve
3. Extraction of TRWP
Organic matter digestion with 30% hydrogen peroxide (48 - 72 hours)
Density separation with LST Fastfloat (1.95 g/cm^3)
Sample filtration under vacuum onto glass fibre filters (Whatman GF/F, pore size 0.7 µm)
4. Pyrolysis GC-MS analysis
Preparation of the deuterated internal standard and calibration curve
Sample Preparation (placing the weighed sample into a quartz tube)
Pyrolysis of the sample and subsequent dimer measurement using GC-MS

Figure 3.4. Generalized sampling and analysis procedures for TRWPs in sediment.

3.3.1 Validation of the TRWP extraction method

To evaluate the efficacy of the solutions employed for sample digestion (30% hydrogen peroxide) and the separation of tyre particles from sediments (Fastfloat), an extraction method assessment was conducted by spiking an environmental background soil sample with reference tyre particles of varying sizes (ranging from 90 to 500 µm) and concentrations (5 to 80 mg TP/g). Recovery rate efficiencies of the different spiking combinations are presented in Figure 3.5.

The mass recovery for concentrations of 5 and 20 mg TP/g consistently exceeded 110% across all size categories. However, at a concentration of 80 mg TP/g, the average recovery rate dropped to 90%, with the lowest recovery observed for the 250

µm size TPs (86%). Additionally, the mixed sample, containing all TP sizes at a concentration of 30 mg TP/g, demonstrated a 92% recovery rate. Similar results were obtained by Klöckner *et al*. (2019), with the highest recovery efficiency of tyre cryogrind from sediment samples (123%) observed at a concentration of 2 mg/g, while a higher concentration (200 mg/g) resulted in a recovery of 85%. In general, their study, which employed sodium polytungstate (SPT) with a density of 1.9 g/cm³, showed an average recovery of 95 ± 17%, closely aligning with the average recovery rate observed in this study, at 96 ± 7.5%.

As previously mentioned, these elevated concentrations of tyre particles (>80 mg TP/g) are anticipated primarily in samples with high traffic influence, such as road dust (Klöckner *et al*., 2019). In contrast, lower concentrations (ranging from 5 to 20 mg TP/g) have been documented in river sediments and stormwater management systems (Mengistu *et al*., 2022; Unice *et al*., 2013).

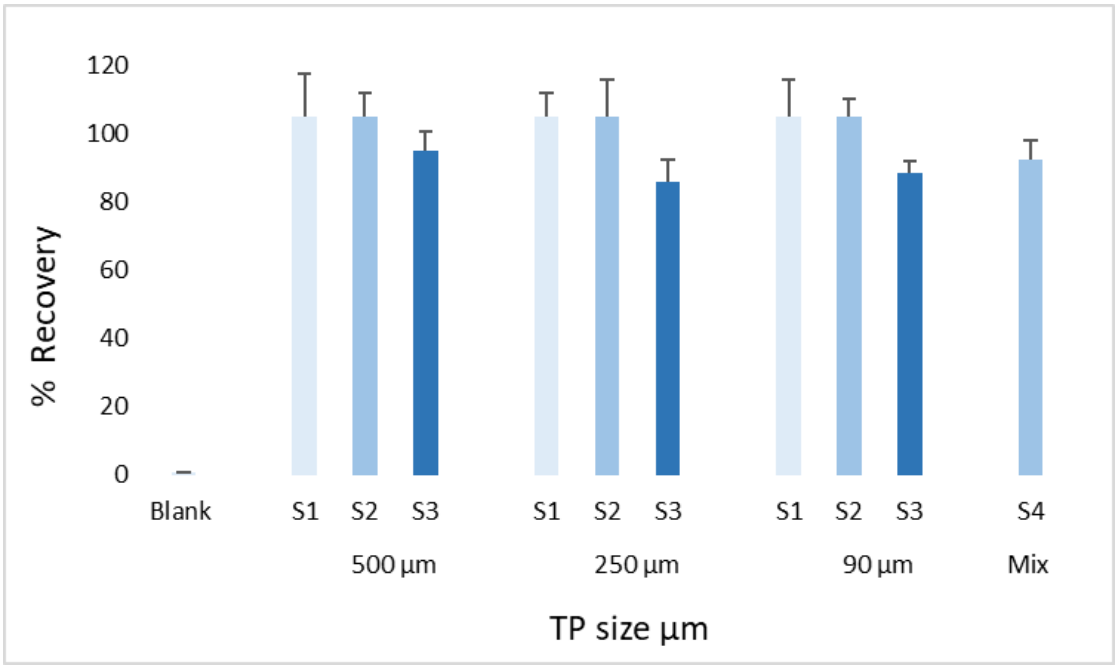

Figure 3.5. Recovery rate efficiencies for the different spiking combinations of the extraction method validation. TP spiking levels are as follows: S1) 5 mg/g, S2) 20 mg/g, S3) 80 mg/g and S4) 30 mg/g. Error bars represent standard deviations and n=3.

Laboratory-generated tyre particles were used in this study to conduct method validation experiments, as a reference material for TRWPs was not available. However, it is worth noting that these particles may exhibit a different composition than real-world TRWPs since they lack mineral encrustations that typically originate from the road or the surrounding environment, potentially affecting their density (Jung and Choi, 2022). Nevertheless, the use of cryogenic milling of tyre treads and similar methods for artificially generating tyre particles has been widely accepted in the scientific community as an appropriate substitute for TRWPs. This is primarily because TRWP predominantly consists of tyre tread compounds such as polymers, vulcanizing agents, accelerating agents, antioxidants, and fillers (Klöckner *et al*., 2021). As a result, tyre cryogrinds have been employed in previous studies for comparing and characterizing TRWPs (More *et al*., 2023; Thomas *et al*., 2022; Klöckner *et al*., 2019). Furthermore, the density separation procedure employed in this research took into account the density values reported in the literature for TRWP, which typically falls below 1.8 g/cm^3 (Kang and Kim, 2023; Jung and Choi, 2022; Klöckner *et al*., 2021). Therefore, the results obtained from these laboratory-generated particles are expected to be applicable for the study of TRWPs in the environment.

While 30% hydrogen peroxide is a favoured method for digestion in microplastics research due to its documented high removal rates at 70 °C (Kang *et al*., 2022), it is important to consider the potential for polymer loss at elevated temperatures (Thomas *et al*., 2022). In this study, precautions were taken to preserve the integrity of tyre particles, including maintaining temperatures below 70 °C during heating on the hot plate and allowing samples to react for the majority of the time (up to a maximum of 72 hours) at room temperature (Wagner and Lambert, 2018; Forrest *et al*., 2017). Additionally, TP recovery exceeded 100% in the majority of samples, indicating successful recovery after pre-treatment with 30% hydrogen peroxide.

Therefore, both 30% hydrogen peroxide and Fastfloat solutions were employed consistently in all subsequent testing, and in the analysis of environmental samples.

3.3.2 Optimizing sample presentation for enhanced Py-GC-MS analysis

The assessment of sample presentations for Py-GC-MS analysis encompassed a comparison between pre-treated samples and an untreated sample, as well as an examination of potential interferences from background media (Fig. 3.6). Inspection of the chromatographs of spiked samples revealed that pre-treatment significantly enhanced the signal and response for the SBR marker, identified as 4-vinylcyclohexene (Figure A1.1 in the Appendix). Consequently, the mean peak area of the GF filter sample surpassed that of the glass vial sample by one order of magnitude and exceeded that of the untreated sample by three orders of magnitude. Following the confirmation that pre-treated samples outperformed untreated ones (Figure A1.2 in the Appendix) and that the background media samples lacked any polymer pyrolysis products, a second test was conducted for the two pre-treated sample variations (Fig. 3.7).

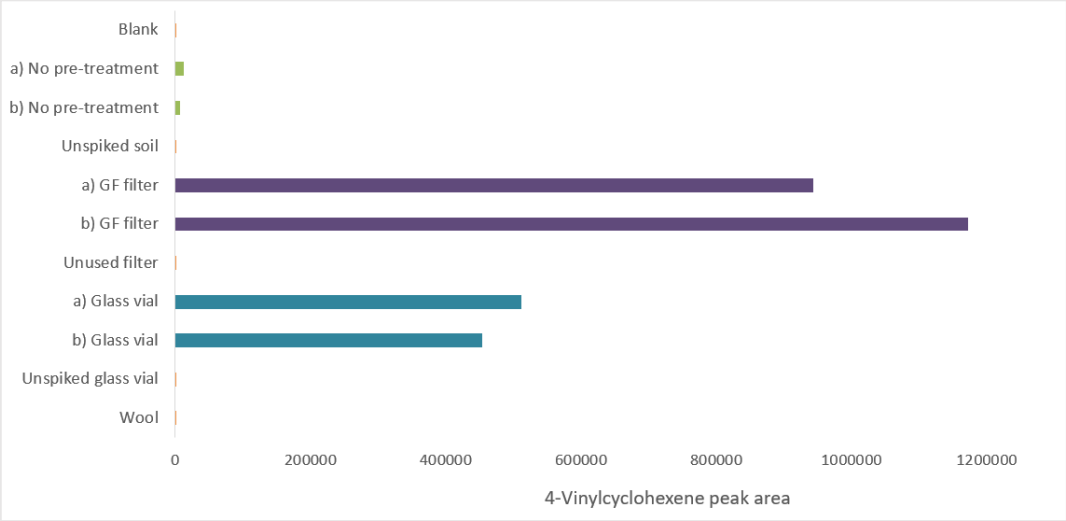

Figure 3.6. Peak areas of the marker compound 4-vinylcyclohexene in different sample presentations as part of the method optimization for sample analysis.

According to More *et al*. (2023), the target Relative Standard Deviation (% RSD), calculated as the standard deviation divided by the mean and multiplied by 100%, for replicate sample analyses should not exceed 20%. In the case of the triplicate pre-treated samples, the RSD for the glass vial samples was found to be 2.52%, while for

the GF filter samples, it was higher at 21.81%. As a result, despite the GF filter sample generating a stronger signal during pyrolysis, the glass vial sample presentation was selected for the analysis of environmental samples due to its consistent repeatability and ease of handling. The glass vials were weighed before and after the filtered sample transfer, and the resulting weight difference was used to calculate the SBR content in the samples.

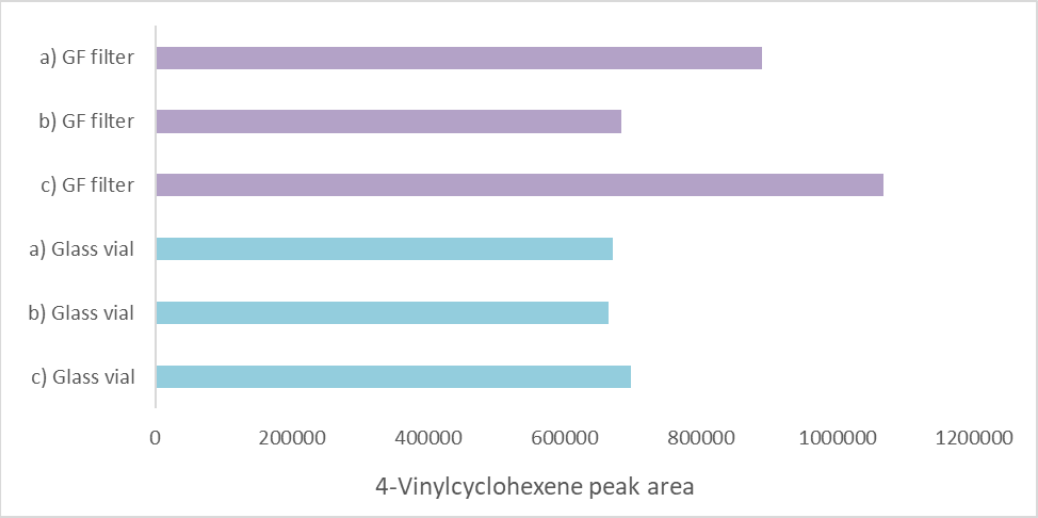

Figure 3.7. Peak areas of the marker compound 4-vinylcyclohexene for the comparison of the two pre-treated sample variations.

3.3.3 SBR calibration standard marker and internal standard

The implementation of an internal standard calibration aimed to enhance the precision of quantitative pyrolisis-GC/MS analysis by compensating for variables that influence fragment generation rates, such as differences in pyrolysis conditions, sample size, and matrix compounds (Unice *et al*., 2012). An example of a calibration curve used in this study for the quantification of SBR/BR mass in the samples is presented in Figure 3.8. All generated calibration curves exhibited a coefficient of determination of 0.999 or greater. Additionally, the pyrogram and mass spectra for the midpoint (SBR-5) calibration standard marker alongside the internal standard marker is depicted in Figure 3.9. The chromatogram peak corresponding to the pyrolysis marker of SBR was cross-referenced and identified in the NIST database as 4-vinylcyclohexene.

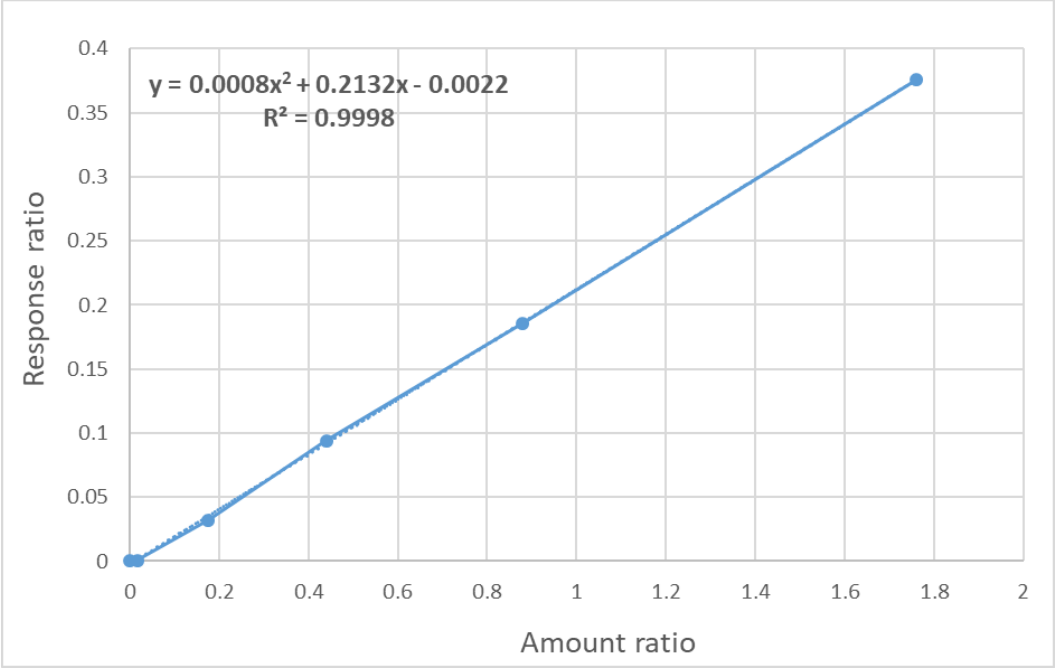

Figure 3.8. Calibration curve for SBR used in the analysis of field samples.

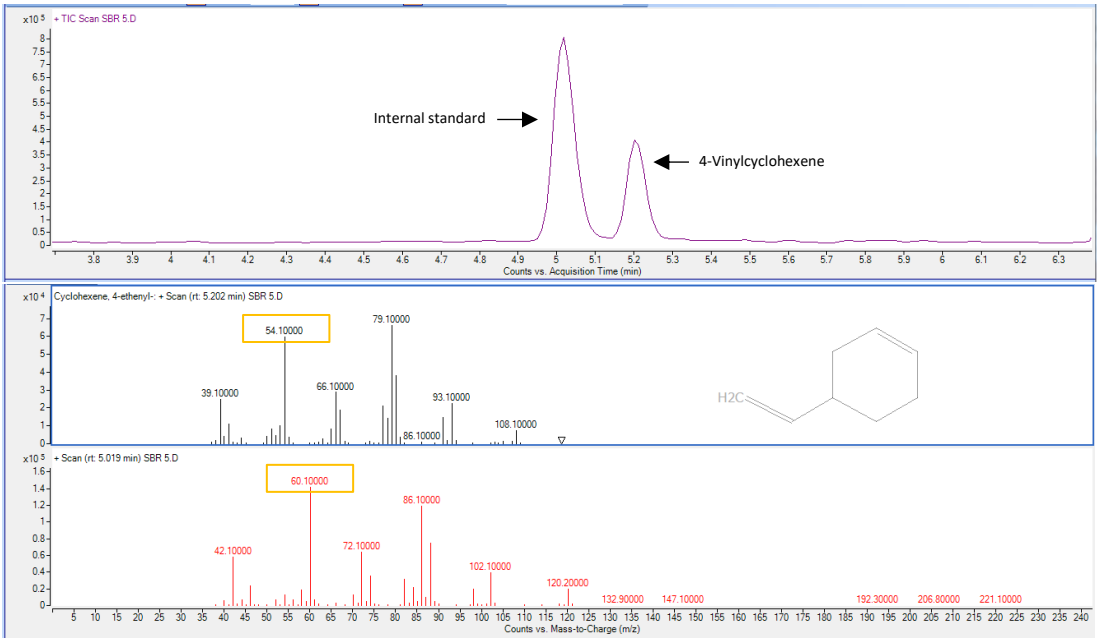

Figure 3.9. Pyrogram and mass spectra for SBR calibration curve midpoint (SBR-5). Highlighted yellow boxes indicate the target ions for quantification: m/z 54 for VCH and m/z 60 for the internal standard.

A study conducted by Youn *et al*. (2021) explored two calibration curve methods for quantifying microplastics originating from tyre and road wear in road dust. These methods included a liquid stock solution and a solid particle-based calibration. In the liquid stock calibration, they followed the ISO/TS 20593:2017 method, dissolving SBR (SBR 1502) standard in chloroform and injecting it into the pyrolysis sample cup at varying volumes (5, 10, 25, and 50 µL). In contrast, the solid calibration involved cryomilled SBR (SBR 1502) standard used at different concentrations (0.1, 0.3, and 0.6 mg). As a result, the two methods produced distinct calibration curves. While both exhibited strong linearity ($R^2 > 0.994$), the authors concluded that the use of the SBR standard in a chloroform solution could potentially result in inaccurate concentrations due to difficulties in dissolving SBR in chloroform (Youn *et al*., 2021). Hence, in this study, great emphasis was placed on ensuring the complete dissolution of both the SBR standard and the internal standard before commencing the analysis. Visual inspection was consistently conducted to confirm their dissolution. Notably, the study by Youn *et al*. (2021) did not incorporate the use of an internal standard.

3.3.4 LOD/LOQ

Throughout the pyrolysis analysis, each run included the analysis of one blank (an empty pyrolysis cup). A total of 8 blank samples were analysed, and in all cases, no SBR/BR was detected. The limit of detection (LOD), calculated as 3 times the signal-to-noise ratio (S/N), for the pyrolysis marker 4-vinylcyclohexene, was determined to be 0.32 µg, while the limit of quantification (LOQ), calculated as 5 times S/N, was established at 0.38 µg.

3.3.5 Sediment grain size and organic material analysis

The results of the two-way ANOVA analysis indicated a statistically significant interaction between the three sampling locations and upstream and downstream points on organic matter concentrations ($F_{(3,16)}$=6.12 and P<0.001). Additionally, simple main effects analysis revealed significant differences in organic matter content among the three sampling locations and between upstream and downstream points (P<0.001). According to the Tukey Post-hoc test, all pairs of groups exhibited

significant differences (P<0.05). The sampling site with the highest overall organic matter content was Pigeon Bridge Brook, specifically observed in sample PBB-DO1, which registered a concentration of 17 wt% per gram. In contrast, Rockley Dike exhibited the lowest organic matter content, with sample RD-UP recording 1.53 wt% per gram. Notably, locations situated immediately downstream of the stormwater outlet consistently displayed the highest organic matter levels across all sampling points (Fig. 3.10).

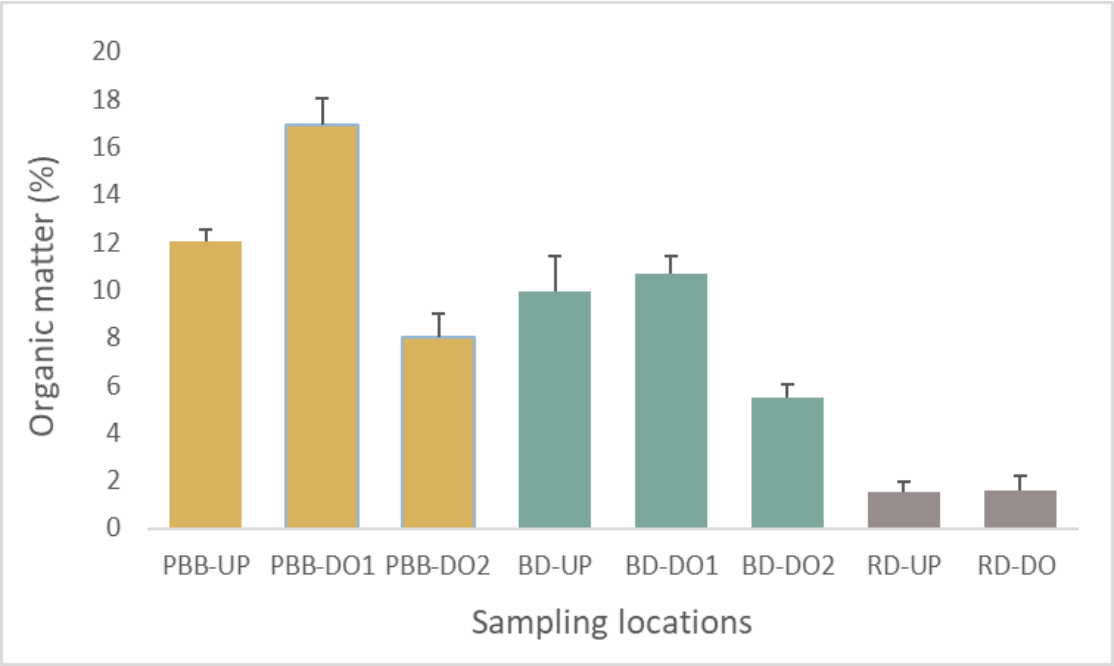

Figure 3.10. Percentage of organic matter in the sediment samples collected at Butterthwaite Ditch (BD), Pigeon Bridge Brook (PBB) and Rockley Dike (RD), with UP denoting upstream locations and DO representing downstream locations. Error bars represent standard deviations; n=3 per sampling location.

Particle size analysis revealed that in most locations, such as PBB-UP, PBB-DO1, PBB-DO2, BD-UP, and BD-DO2, the sediment was primarily composed of silt (particles ranging from 4 µm to 62.9 µm), constituting over 60% of the total composition. In contrast, samples from RD-UP and RD-DO were characterized by a higher proportion of sand particles (ranging from 63 µm to 2000 µm). Specifically, RD-UP had a composition

of 94% sand, 4.5% silt, and 1% clay (particles ≤3.9 µm), while RD-DO exhibited a sediment composition of 69% sand, 24.5% silt, and 6.52% clay (Fig. 3.11).

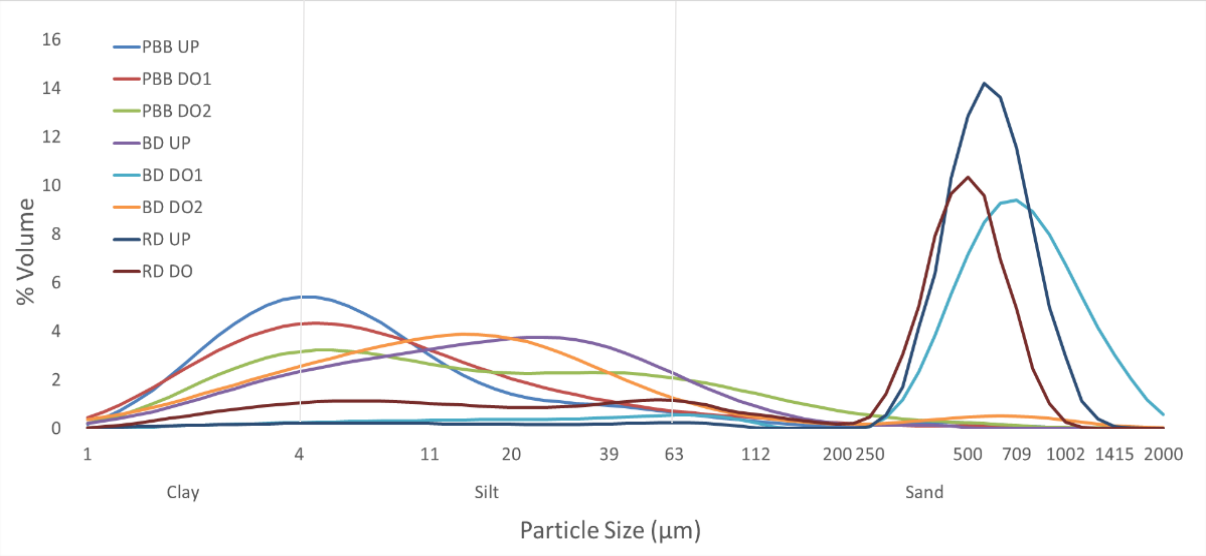

Figure 3.11. Particle size distribution of the collected sediment samples, classified according the Udden–Wentworth grain-size scale (Wentworth, 1922).

3.3.6 TRWP concentrations in environmental samples

The sediment sample processing method and subsequent Py-GC-MS analysis were further tested using environmental samples with a high traffic influence. The presence of SBR/BR, and consequently TRWPs, in the sediment samples was confirmed by the identification of 4-vinylcyclohexene with matches exceeding 95% (according to the NIST search library) and the detection of diagnostic ions for peak area qualification (see Fig. 3.12).

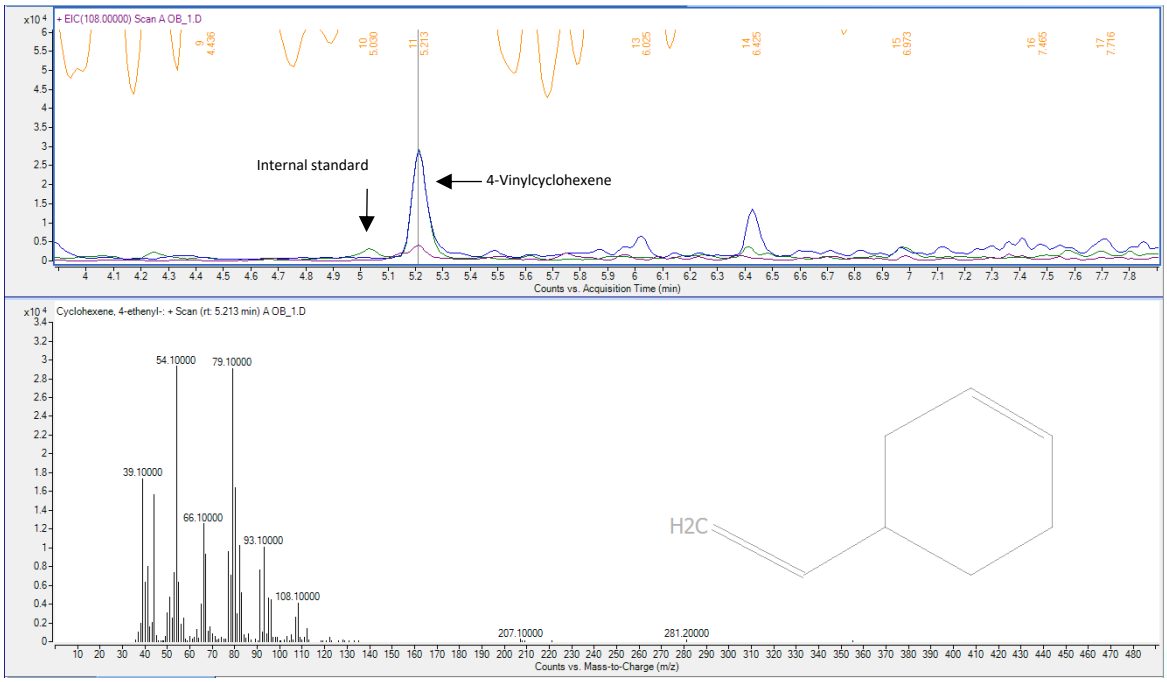

Figure 3.12. Pyrogram and mass spectra for the field sample Butterthwaite Ditch (downstream 1).

The TRWP concentrations in sediment for the different sampling locations are presented in Figure 3.13. TRWPs were detected by the pyrolysis marker in all sampled areas. The results of the two-way ANOVA analysis indicated a statistically significant interaction between sampling locations and upstream and downstream points on TRWP sediment concentrations ($F_{(3,16)}$=9.64 and P<0.001). Simple main effects analysis further demonstrated significant differences in TRWP concentrations across the three sampling locations and between upstream and downstream points (P<0.001). Furthermore, post-hoc analysis using the Tukey test revealed significant distinctions among all pairs of groups (P<0.05). Notably, the highest measured concentrations were observed immediately downstream of the storm drain outlet, followed by the second downstream location, while the upstream locations consistently exhibited the lowest concentrations across all three studied regions. Among the downstream locations, Pigeon Bridge Brook exhibited the highest TRWP concentration at 16,281 µg/g, followed by Butterthwaite Ditch at 4,148 µg/g, and Rockley Dike at 620 µg/g. Despite the limited sample mass of approximately 10 mg utilized in the pyrolysis analysis, the results from laboratory replicates have

demonstrated satisfactory repeatability, with relative standard deviations (RSD) consistently below 20%. These RSD values ranged from 5.12% in the PBB-DO1 sample to a maximum of 18.2% in RD-UP sample.

Figure 3.13. Sediment concentrations of tyre and road wear particles presented on a tread basis. Error bars indicate standard deviations; n=3 per sampling location.

The findings reported here align with those of Maltby *et al*. (1995), who observed that the downstream location of Pigeon Bridge Brook was the most significantly affected by motorway runoff discharges. This impact was evident through notable increases in sediment concentrations of total hydrocarbons, aromatic hydrocarbons, and heavy metals. These effects were attributed, in part, to the relatively small size of the stream compared to the other sampled locations, the length of road that drained into it (1,500 m) and the higher traffic volume.

Several studies focusing on TRWP concentrations in rivers have highlighted sedimentation as a crucial process for TRWP removal from surface waters, owing to

their significantly higher density compared to water (Wagner *et al*., 2018). As mentioned by Vercauteren *et al*. (2023) highways are recognized as prominent TRWP emission hotspots, particularly those situated near densely populated urban areas, attributed to their high traffic volume. However, studies examining TRWP concentrations originating from highway runoff in river sediments remain notably limited, making direct comparisons challenging. Therefore, the findings of this study can be compared with data obtained from highway settling ponds and highway runoff detention systems. For instance, Klöckner *et al*. (2019) documented a concentration range of 0.3 to 11 mg/g (TRWP expressed as tread) based on existing literature, which closely aligns with the results presented in this study, falling within the range of 0.10 to 16.2 mg/g. Similarly, Jarlskog *et al*. (2022) employed automated Scanning Electron Microscopy/Energy Dispersive X-ray spectroscopy (SEM/EDX) single particle analysis to examine sediment samples from a roadside gully pot and a stormwater well in a rural highway. Their approach involved the classification of TWPs using a machine learning algorithm. Their findings revealed a TWP concentration (in the size fraction >20 µm) of 3.5 mg/g in the roadside gully pot sediment and 14.5 mg/g in the stormwater sediment (Jarlskog *et al*., 2022). Despite variations in analytical methods and sampling techniques between Jarlskog *et al*.'s study and the present study, their results are in good agreement with those obtained here. On the other hand, Rødland *et al*. (2022) introduced an innovative methodology for TRWP analysis using pyrolysis-GC-MS. In their approach, they used a combination of pyrolysis markers derived from styrene butadiene rubber (SBR) and styrene butadiene styrene (SBS) standard polymers to estimate TRWP and polymer-modified bitumen concentrations. When applying this method to sediments extracted from roadside gully-pots situated within a tunnel, TRWP (as tread) concentrations were measured within the range of 4.75 to 53 mg/g. Notably, these results fall within the same order of magnitude as the TRWP concentrations identified in the sediments examined in the present study.

In all three sampling areas, the station immediately downstream from the discharges exhibited higher TRWP concentrations compared to the station further downstream

from the outlet. These variations in TRWP concentrations can be attributed to the natural sinking and entrapment of denser TRWP in the sediment once discharged into the river. Conversely, smaller and less dense particles, typically with fewer mineral encrustations, travel further downstream. A similar trend was observed in a case study involving bioretention cells, where TWP concentrations were significantly higher (30.9 mg/g) in close proximity to the bioretention cell inlet compared to a point 5 meters away (19.8 mg/g) (Mengistu *et al*., 2022). The authors of the study suggested that the absence of the size fraction <50 µm in the system could be attributed to a reduction in the retention efficiency of finer tyre wear particles, which would be transported out of the system with stormwater (Mengistu *et al*., 2022).

In addition, various studies have documented the dispersion of airborne TRWP, which can travel considerable distances from their source of origin (Mizuguchi *et al*., 2023; Forrest *et al*., 2017). For instance, Jarlskog *et al*. (2022) conducted an investigation into the atmospheric deposition of airborne particles at varying distances from the road, specifically at distances of 3.1 m, 4.8 m, 27.1 m, and 100 m. Their findings revealed the presence of TWP at all distances, (13 g/m^2, 5.6 g/m^2, 6.4 g/m^2, and 2 g/m^2, respectively), showcasing a general trend of decreasing concentrations with increasing distance from the road. The authors of this study concluded that the finer fraction of TWP, ranging from 2 to 20 µm in size, and representing the predominant composition of road dust particles in their samples, is particularly susceptible to being transported over long distances through both air and water pathways (Jarlskog *et al*., 2022). Thus, the presence of TRWP at the upstream stations in the current study may be attributed to the atmospheric transport of tyre particles originating from the nearby highways. Additionally, the rural landscape surrounding the sampling sites, characterized by agricultural activities, could contribute to the potential wash-off of TRWPs deposited onto agricultural fields through the application of sewage sludge (Baensch-Baltruschat *et al*., 2021).

3.3.7 Limitations of the methodology

The homogenization of dried sediment using a pestle and mortar in the pre-treatment stage may lead to particle fragmentation, potentially altering their physical characteristics (Lusher *et al.,* 2020). Nevertheless, this method was selected for its simplicity and effectiveness in achieving sample homogeneity. Measures were taken to mitigate fragmentation during the grinding process, including the application of gentle pressure and limiting grinding durations. This precaution is particularly crucial when microscopy analysis and particle quantification are involved, as further fragmentation could skew TRWP abundance estimates. It is worth noting that Pyrolysis-GC-MS, in contrast, offers detection at the nano scale and provides mass concentration data, mitigating concerns related to particle fragmentation. Furthermore, in the post-filtration processing step, it should be noted that the action of scraping the filtered material from the filter using a stainless steel spatula and transferring it into a small glass vial may potentially result in sample loss or the unintentional transfer of filter particles to the glass vial. To address this concern, the weights of both the filter and the glass vials were measured before and after filtration, and both weights were factored into the determination of the final sample weight.

The composition of tyres varies based on multiple factors such as vehicle type (e.g., car or truck), seasonal conditions (e.g., summer or winter tyres), and brand (Mattonai *et al*., 2022). Traditionally, it was believed that passenger car tyres primarily consist of synthetic rubber (SBR), while truck tyres are primarily made of natural rubber, containing minimal to no SBR (Mattonai *et al*., 2022; Youn *et al*., 2021; Eisentraut *et al*., 2018). Consequently, when this study employed an approach that relied solely on SBR to estimate tyre wear particles in a sample, there was a potential risk of underestimating TRWP originating from heavy-duty vehicles. However, a study by Rauert *et al*. (2021) investigated the composition of 14 truck tyres using Py-GC-MS with 4-vinylcyclohexene as the SBR marker compound. Their findings contradicted the previous notion, indicating that 9 of these truck tyres contained substantial SBR/BR compositions (up to 28%), surpassing that typically found in passenger car

tyres. This high SBR/BR content suggested that truck tyres could indeed have measurable concentrations of SBR/BR as a significant component of their formulation (Rauert *et al*., 2021). As a result, the method proposed in this study allows for the calculation of TRWP from both car and truck tyres in the sampled materials.

In addition, determining tyre concentrations from the samples requires understanding the relative proportions of SBR, BR, and NR present in the tyre tread. As previously mentioned, the ISO method utilized an assumed 50% polymer content in the tread, based on surveys of various tyre manufacturing companies (Unice *et al*., 2012). However, recent research, such as studies by Rødland *et al*. (2022) and Rauert *et al*. (2021), has shown variations in SBR/BR concentration calculated using the pyrolysis product 4-vinylcyclohexene across different tyre brands and models. According to Rauert *et al*. (2021), these variations were found to be significantly lower than the assumed SBR/BR mass of 44% in passenger car tyres. Consequently, by employing the estimated 11.3% SBR content in tyres within this study, a proactive step has been taken to prevent potential underestimation of TRWP concentrations associated with the ISO assumption. However, it is important to acknowledge that tyre compositions can evolve over time, and given the lack of transparency from tyre manufacturers regarding their formulations, it is advisable to analyse the SBR/BR concentration in a wide array of commercially available tyres relevant to the study area. This is especially relevant because tyre formulations and production practices can differ between countries, such as the use of studded tyres in certain regions (Mattonai *et al*., 2022). Such a comprehensive approach will aid in reducing uncertainties associated with calculating the polymer fraction of TRWP based on rubber concentrations.

Considerable uncertainty also applies to the determination of tyre-derived and road-derived fractions within TRWP calculations. Previous studies (Kreider *et al*., 2010) and the ISO method have employed a 50% attribution to both tyre and road mineral components in TRWPs. However, recent investigations focusing on characterizing TRWPs collected from road surfaces have revealed a wide-ranging mineral encrustment, spanning from 6% to 53% (Sommer *et al*., 2018). This variation depends

on factors such as road type, vehicle speed, and driving patterns (Klöckner *et al*., 2021; Kovochich *et al*., 2021; Sommer *et al*., 2018). For example, highways have been associated with lower encrustment levels (<10%) compared to urban roads, primarily due to differences in vehicle velocities and the constant braking and accelerating actions typical of urban environments. Consequently, assuming a uniform 50% mineral encrustation for all particles in this study would have led to an overestimation of TRWP concentrations (Rodland *et al*., 2022; Sommer *et al*., 2018). However, comprehensive studies addressing mineral encrustation on TRWP remain scarce, underscoring the critical need for further research characterizing TRWP across various environmental compartments. This will significantly contribute to advancing our understanding of their composition, ultimately providing more reliable values for their quantification (Mattonai *et al*., 2022).

Lastly, there may be uncertainties linked to the possible presence of 4-vinylcyclohexene from non-tyre sources in the environment. However, it is worth noting that there is currently a lack of available information on this matter, and any potential positive bias resulting from any other source is anticipated to be minimal (Rosso *et al*., 2023; Unice *et al*., 2013).

3.4 Conclusion

This study presents a comprehensive methodology for analysing TRWP in sediment samples, encompassing key steps such as sampling, digestion, extraction, and Pyrolysis-GC-MS analysis. The pre-treatment of the samples before Py-GC-MS analysis yielded significant improvements, such as an enhancement in the response and resolution for the SBR marker compound by effectively mitigating interference from matrix components. Additionally, this pre-treatment contributed to heightened repeatability in laboratory replicates, with relative standard deviations consistently below 20%. Notably, the analysis of environmental samples revealed the presence of the marker compound 4-vinylcyclohexene and the deuterated internal standard, thus, confirming the presence of tyre polymer in the samples.

The concentration of TRWPs varied across the three sampling locations, ranging from 0.10 to 16.2 mg/g. These variations were predominantly attributed to the traffic volume at each location and the dimensions of the receiving stream. Furthermore, these concentration levels align with earlier assessments of highway runoff detention systems, confirming the role that stormwater runoff plays as a significant pathway for TRWP transport into the environment. This is particularly concerning considering that the majority of road runoff from highways is discharged into freshwater systems without undergoing any treatment, emphasizing the need for comprehensive mitigation strategies.

To increase the precision of TRWP quantification in environmental samples utilizing polymer pyrolysis markers, it is necessary to undertake extensive assessments of SBR/BR content in commonly available tyres within the specific study area. Additionally, characterizing TRWP from diverse environmental matrices is essential to improve our understanding of the road and mineral fraction of TRWP. Lastly, there exists a notable knowledge gap concerning the impact of aging and degradation processes on tyre particles in the environment, specifically in terms of their polymer content and the formation of pyrolysis markers during Py-GC-MS analysis. Hence, future research should focus on investigating these aspects to deepen our comprehension of TRWPs in the environment.

The work outlined in this Chapter describes the development and evaluation of a methodology for the measurement of TRWPs in aquatic sediments. The method exhibits good recoveries, low variability, and is able to detect TRWPs at concentrations relevant to the environment. In the next Chapter, the method is applied in a year-long monitoring study in rivers in York.

Chapter 4. Spatial and temporal variations of tyre and road wear particle concentrations in the river sediments of York

4.1 Introduction

The previous Chapter described the development and evaluation of a Py-GC–MS method for the quantitation of TRWPs in environmental samples. In this chapter, the method is used to explore the spatio-temporal distribution of TRWP concentrations in the sediments of York's rivers. This investigation follows the methodology outlined in Chapter 3 and aligns with the river section delimitations presented in Chapter 2, which guided the selection of sampling locations.

Several Py-GC-MS-based monitoring studies have been conducted on TRWPs in various environmental compartments, including road dust, gully pots, snow, soil, air, and surface runoff (Rødland *et al*., 2023; Rødland *et al*., 2022; Rødland *et al*., 2022b; Parker-Jurd *et al*., 2021; Goßmann *et al*., 2021; Youn *et al*., 2021; Unice *et al*., 2013; Panko *et al.,* 2013). In comparison, studies analysing TRWP concentrations in river sediments are relatively scarce. Previous research has reported concentrations spanning a wide range, from 800 to 300,000 µg/g d.w. This significant variation in concentration values, exceeding two orders of magnitude, has been attributed to the absence of appropriate markers specific to rubber polymers and the lack of an internal standard (Unice *et al*., 2013).

In addition, despite TRWPs being recognized as the primary source of microplastics in the environment (Stojanovic *et al.,* 2022), their identification and characterization in microplastic studies remains limited (Knight *et al*., 2020; Wagner *et al.,* 2018). This can be attributed to the small size of TRWPs, their complex chemical composition, the incorporation of road-derived materials and the incompatibility with conventional microplastic analysis techniques like FTIR and Raman spectroscopy (Rosso *et al*., 2023). Nevertheless, it is important to recognize that the environmental fate of TRWPs is influenced by both their mass concentration and the distinctive characteristics of the particles, including size and density (Kovochich *et al.,* 2021).

Therefore, understanding the size distributions of TRWPs in different environmental matrices holds significant potential to improve strategies related to road runoff mitigation, predict their transport in surface waters, and evaluate their impact on aquatic organisms (Klöckner *et al.,* 2020).

While microplastics have been documented in surface waters and sediments on a global scale, the majority of microplastic surveys involve one-time sampling events, often overlooking the crucial aspect of temporal variability (e.g., Keene and Turner, 2023; Shu *et al.,* 2023; Chaisanguansuk *et al.,* 2023; Eibes and Gabel, 2022; Choudhary *et al.,* 2022; Klein *et al.,* 2015). This oversight can introduce significant challenges when interpreting data results, potentially leading to an incomplete understanding of the true extent of microplastic contamination in the environment (Leads *et al*., 2023). Accurately quantifying the microplastic load in riverbeds over time and space is of utmost importance as many organisms live, feed and reproduce in benthic habitats and their productivity plays a pivotal role in supporting the entire riverine ecosystem (Woodward *et al.*, 2021).

To the best of my knowledge, no previous study has investigated the temporal variations in TRWP concentrations in urban river sediments. Therefore, the primary aim of this study was to quantify TRWP concentrations in the sediments of the river Ouse and Foss in the city of York over the course of a year. Furthermore, the analytical methodologies employed in this study provided an opportunity to explore “traditional” microplastic levels. Consequently, the following objectives were incorporated into the study: (1) to determine the relative abundance of the most prevalent thermoplastics in the environment using Py-GC-MS; (2) to identify and quantify the abundance of both TRWPs and “traditional” microplastics through microscopy analysis; and (3) to characterize the physical properties of TRWPs, including density, size and aspect ratio, in river sediments.

4.2 Materials and methods

4.2.1 Sampling locations

The sampling locations were selected to ensure accessibility from bridges or floating jetties and to align with the river sections used in the emissions model detailed in Chapter 2. In total, sediment samples were obtained from 11 sites along the rivers Ouse and Foss in the city of York, UK (Fig. 5.1). Samples were taken quarterly, aligning with the changing seasons (February, May, August, and November). To minimize potential variability, the sampling was consistently conducted in the same order, approximately on the same day, and at the same time each month, covering the period from May 2021 to May 2022. At each site, sediment samples were extracted from the upper 10 cm of the sediment bed, utilizing a stainless steel Van Veen sediment grab sampler. For most locations, samples were collected from the midpoints of bridges, with the exception of sites Ouse SP1, Ouse SP2 and Ouse SP6, where sampling was conducted directly from the riverbank. In every location, approximately 600 g of sediment was collected in triplicate and placed into individual 1 L glass jars. Following collection, the samples were promptly transported to the laboratory and stored at -5°C until analysis.

4.2.2 Sample preparation

The sediment samples underwent the same processing steps as outlined in Chapter 3 for Py-GC-MS analysis. Briefly, the procedure involved drying the sediment samples in an oven at 105 °C for 24 to 48 hours. Once dry, the sediment was homogenized using a pestle and mortar and then sieved through a 2 mm stainless steel sieve. Subsequently, triplicate subsamples, each comprising approximately 30 g of dried sediment, were treated with 30% hydrogen peroxide to eliminate organic matter. The treated samples were then centrifuged with deionized water at 3500 rpm for 10 minutes to remove any residual chemicals.

To extract TRWPs from the sediments, roughly 15 ml of LST Fastfloat, with a density of 1.95 g/cm^3, was added into each of the digested samples in the centrifuge tubes. The tubes were then subjected to two minutes of agitation with a vortex mixer and then centrifuged at 3500 rpm for 15 minutes. These extraction steps were repeated

twice for each sample to enhance the recovery rate of TRWPs in the sediment. The resulting buoyant fraction was then filtered through glass fibre filters (Whatman GF/F, pore size 0.7 µm) using a vacuum pump system and rinsed with deionized water to eliminate any excess Fastfloat. After filtration, the material retained on the filter was carefully scraped using a stainless steel spatula and transferred into labelled small glass vials. These vials were then stored at room temperature, awaiting further analysis *via* Pyrolysis GC-MS.

The same procedures were repeated for microscopic analysis, with variations starting from the density separation step. For these samples, a multistep density separation procedure was performed using sodium chloride (Sigma-Aldrich) and LST Fastfloat to assess the density of TRWPs and to enhance the visibility of low-density microplastics within the filters (Thomas *et al*., 2022). The sodium chloride solution (NaCl) was prepared by dissolving the salt in deionized water to achieve a final density of 1.2 g/cm^3, while the Fastfloat solution maintained its previous density of 1.95 g/cm^3. Triplicate subsamples, each containing approximately 30 g of digested sediment in 50 ml centrifuge tubes, were subjected to a two-step process. First, 15 ml of NaCl solution was added and centrifuged at 3500 rpm for 15 minutes, after which the supernatant was transferred to a clean centrifuge tube. Subsequently, 15 ml of LST Fastfloat was added to the same tube and centrifuged again at 3500 rpm for 15 minutes. After extraction, the supernatants from both solutions were separately filtered using a vacuum pump system with glass fibre filters (Whatman GF/F, pore size 0.7 µm) and then placed in labelled glass petri dishes to dry at room temperature for subsequent microscopic analysis.

In addition, loss on ignition and particle size analysis were carried out for all sediment samples, following the steps presented in Chapter 3.

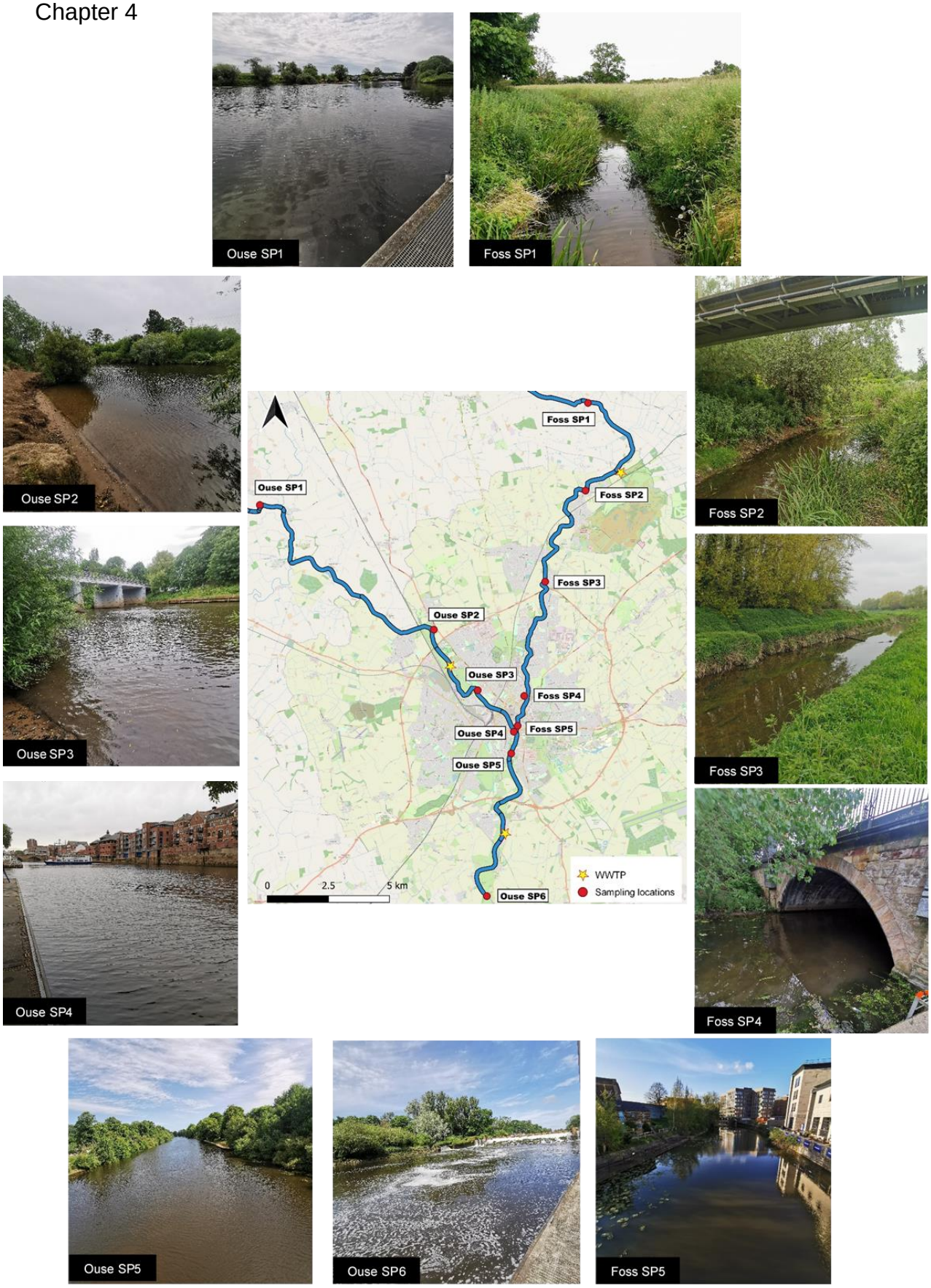

Figure 4.1. Sampling locations across the river Ouse and Foss in the city of York, UK.

4.2.3 Pyrolysis GC-MS analysis

The mass concentration of TRWP in the sediment samples was determined using the procedure outlined in Chapter 3. The standard polymers were obtained from Polymer Source, Inc. (Dorval, QC, Canada). Random Copolymer Poly(styrene-co-butadiene) served as the calibration polymer for the SBR standard, while deuterated Poly(1,4-butadiene-d6) (P41833-dBd) was used as the internal standard.

Other types of plastics were also monitored within the samples. While calibration curves were not specifically prepared for their analysis, polymer identification relied on the detection of indicator compounds obtained from the pyrolysis of pure polymer standards (Table 4.1) (Rosso *et al*., 2023; Bouzid *et al*., 2022). The subsequent confirmation of peak identities was achieved by comparing their mass spectra with those included in the NIST search library (Rosso *et al*., 2023). The determination of microplastic relative abundance in the samples was based on the peak areas of the marker compounds, which were subject to manual inspection for quality control. The identified microplastic polymers included Polypropylene (PP: Sigma-Aldrich), Poly-(methyl methacrylate) (PMMA: Sigma-Aldrich), Polyethylene terephthalate (PET: Sigma-Aldrich), Polycarbonate (PC: Goodfellow), Polyethylene (PE: Biorenewable development centre, York, UK), Polyvinyl chloride (PVC: Sigma-Aldrich), and Nylon (N66: Biorenewable development centre, York, UK). These particular polymers were selected due to their widespread production and prevalence in the environment (Bouzid *et al*., 2022; Hendrickson *et al*., 2018).

The pyrolysis analysis involved placing approximately 10 mg of the field samples into pre-weighed quartz tubes. These tubes were then sealed with quartz wool, spiked with 10 µL of the internal standard solution, and left to evaporate at room temperature for 30 minutes (Rauert *et al.,* 2021; Bye and Johnsen, 2019).

Table 4.1. Selected indicator compounds for the polymer standards.

Polymer	Pyrolysis product	Indicator ions (m/z)[a]	Molecular ion (m/z)	Retention time (min)
Polypropylene (PP)	2,4-Dimethyl-1-heptene	70, 83, **126**	126	5.40
Poly-(methyl methacrylate) (PMMA)	Methyl methacrylate	41, 69, 89, **100**	100	2.79
Polyethylene terephthalate (PET)	Benzoic acid	51, 77, **105,** 122	122	9.49
Polycarbonate (PC)	Bisphenol A (BA)	91, 119, 165, **213**, 228	228	14.33
Polyethylene (PE)	1-Decene (C10)	**83**, 97, 111, 140	140	7.80
Polyvinyl chloride (PVC)	Benzene	52, 74, **78**	78	2.25
Nylon (N66)	Cyclopentanone	39, **55**, 84	55	4.10
Styrene butadiene rubber (SBR)	4-vinylcyclohexene (VCH)	39, **54**, 79, 108	108	5.2
Poly(1,4-butadiene-d6) (d-PB)	Deuterated butadiene dimer (d-BdD)	42, **60**, 86 120	120	5.03

[a] Bold values used for identification and quantification based on ISO/TS 21396:2017 and *Rødland et al.,* (2020).

4.2.4 Microscopic analysis

The identification and quantification of microplastics was performed manually by visual examination of the filters using a Zeiss Axio Zoom V16 stereomicroscope equipped with an integrated camera, employing magnifications ranging from x20 to x50. TRWPs were identified based on morphological characteristics as described in the literature, including being black particles with a rugged surface, elongated or cylindrical in shape, and potentially covered with mineral encrustations from the road (Ostini *et al*., 2022; Leads and Weinstein, 2019; Sommer *et al*., 2018; Kreider *et al*., 2010). Furthermore, tyre particles underwent a tactile assessment in which their rubbery consistency was evaluated by manipulating them with forceps. Particles that returned to their original shape without breaking or separating upon compression were considered as tyre particles and included in the analysis, while those not

meeting these criteria were excluded (Ostini *et al*., 2022; Knight *et al*., 2020). The aspect ratio of TRWPs was determined by measuring both their longest length and their widest width (Jung and Choi, 2022).

Thermoplastic particles were categorized by their type, including fragments, fibres, spheres, films, glitter, and paint (Hidalgo-Ruz *et al.,* 2012). To distinguish plastic particles from non-plastic materials, the hot needle test was employed following the procedure described by De Witte *et al.* (2014). This test involved heating a standard sewing needle to a red-hot tip using an open flame and then promptly bringing it in contact with the particle under examination. Previous studies have shown that when exposed to a hot needle, plastic tends to melt or curl, while non-plastic or biological materials disintegrate or remain unchanged (Leads and Weinstein, 2019; Hendrickson *et al*., 2018). Furthermore, all microplastics were categorized by size (ranging from 50-149 µm, 150-249 µm, 250-499 µm, 500-1000 µm, and >1000 µm) and colour. In this study, the upper size limit was set at 2 mm, determined by the sieve opening, while the lower limit was defined as 50 µm due to the constraints of visual identification below this size (Knight *et al*., 2020). Microplastic abundance was calculated by enumerating the microplastics in the samples and expressed as the total number of microplastics per kilogram of dry sediment (Ostini *et al*., 2022; Blair *et al*., 2019).

Airborne contamination of samples was avoided by wearing cotton clothes, laboratory coats and nitrile gloves. Additionally, the classification of plastic particles was performed within a controlled cleanroom environment, where all surfaces and equipment were meticulously cleaned with distilled water prior to any analysis (Santana *et al*., 2016).

4.2.5 Fourier-Transform Infrared Spectrometry (FT-IR) analysis

TRWPs were initially identified based on the specified physical criteria listed above. However, a select group of black particles (≥400 µm; n=10) underwent further analysis using a Spotlight 400 FT-IR spectrometer equipped with a diamond Attenuated Total Reflectance accessory by Perkin Elmer. The analysis encompassed the full wavelength range of FT-IR (600 - 4000 cm^{-1}) at a resolution of 4 cm^{-1}. To

maintain accuracy, a background run was performed at the beginning of each analysis, and the crystal was meticulously cleaned with ethanol between samples. Additionally, a tyre particle standard derived from a passenger car tyre (Continental 205/55 R16) was also analysed, and its spectrum was compared with those obtained from the suspected TRWPs found in the sediment samples.

4.2.6 Statistical analysis

The data underwent normality testing through visual inspection of QQ plots and the Shapiro-Wilks test. Additionally, homoscedasticity was evaluated utilizing the Fligner-Killeen test to confirm the assumption of homogenous variance across the dataset. Subsequently, a two-way analysis of variance (ANOVA) was performed, followed by the Tukey multiple comparison test, to determine if there were significant differences in the response variable TRWP mass concentration between sampling locations and months.

The non-parametric Kruskal-Wallis test, followed by Dunn's Multiple Comparison test, was applied to assess potential statistical differences in microplastics abundance as a function of sampling locations and months. Furthermore, the chi-square independence test was employed to explore associations between sampling locations and microplastics size, colour, and morphology (Ross *et al.,* 2023). Pearson correlation analysis was also conducted to investigate relationships between TRWP mass concentrations with sediment size composition, organic matter, and TRWP abundance in the samples. All statistical analyses were conducted using RStudio (v4.3.1), and significance for all statistical tests was set at $P < 0.05$. Lastly, all maps were created using QGIS 3.32.2.

4.3 Results

4.3.1 TRWP concentrations in sediment samples by Pyrolysis GC-MS

The concentrations of TRWPs in sediment across the various sampling locations and months are depicted in Figure 4.2. The presence of TRWPs was confirmed through the detection of the pyrolysis marker 4-vinylcyclohexene in all the samples analysed.

An illustration of a pyrogram and the mass spectra of a sediment sample from the river Foss in York is presented in Figure A2.1 of the Appendix.

The response variable “TRWP mass concentration” was not normally distributed (*Shapiro–Wilks* test for normality, W=0.7373 and P<0.001). To address this, a log transformation ($\log_e$) was applied, resulting in data that conformed to normality (*Shapiro–Wilks* test for normality, W=0.9661 and P=0.123) and met the assumption of homogeneity of variance (*Fligner-Killeen* test of homogeneity of variances, X^2=31.088, df=54 and P=0.994).

The results of the two-way ANOVA analysis indicate a statistically significant interaction between sampling locations and months ($F_{(40,109)}$= 22.75 and P<0.001). Simple main effects analysis further reveals significant differences in TRWP sediment concentrations among the sampling locations (P<0.001). According to the Tukey Post-hoc test, these differences are particularly pronounced between Foss SP5—Ouse SP1, Foss SP4—Ouse SP1, Ouse SP4—Ouse SP1, Ouse SP6—Foss SP5, and Ouse SP6—Ouse SP4, all with *p*-values of P<0.0001. The highest TRWP concentration among locations was recorded at Foss SP5, with a mean value of 1,455.7 µg/g averaged across the five time points, while the lowest concentration was observed at Ouse SP6, with a mean value of 23.07 µg/g over the same time span.

Additionally, the simple main effects analysis reveals significant differences in TRWP sediment concentrations between the sampling months (P<0.001). As indicated by the Tukey Post-hoc test, all group pairs were significantly different (P<0.05), with the exception of the months May 2021—May 2022, where the *p*-value was P=1. August exhibited the highest mean TRWP concentrations across all sampling locations, while May 2021 showed the lowest.

Among the sampling locations and the months, Foss SP5 in August recorded the highest concentration, with a detected value of 2,975.73 ± 563.75 µg/g, followed by Ouse SP4 in February with a concentration of 2,615.06 ± 514.9 µg/g. In contrast, the lowest concentration was observed at Ouse SP2 in August, measuring 5.88 ± 0.93 µg/g, followed by Ouse SP6 in February with a value of 10.86 ± 2.11 µg/g.

Figure 4.2. Sediment concentrations of tyre and road wear particles across the different sampling locations and months, along with a map displaying the mean TRWP mass over the five months sampled, reported on a tread basis. Error bars represent standard deviations; n=3 per sampling location and month.

4.3.2 Identification of thermoplastics with Pyrolysis GC–MS

The presence of PVC, Nylon 6/6, PP, PMMA, PE, PET and PC in the sediment samples was confirmed using Pyrolysis GC-MS. It is worth noting that calibration curves were not prepared for the analysis of thermoplastics; therefore, there is no quantification data for them, and the results are presented as relative abundance. Additionally, no polymer peaks were detected in the blanks.

Detailed pyrograms and mass spectra of the pyrolysis marker, corresponding to polymer standards and matching pyrolysis markers detected in the sediment samples are available for reference in figures A2.3 to A2.9 of the Appendix.

As illustrated in Figure 4.3, the relative abundance of polymers within the samples exhibited significant variability across the different sampling locations and months. Notably, polyethylene displayed a consistently high relative abundance across most sampling locations and months. In contrast, both polyvinyl chloride (PVC) and Nylon 6/6 demonstrated lower abundances, though they were still detectable in every location, with both showing a peak of abundance in the sample Ouse SP4 collected in May 2022. Polypropylene exhibited relatively low abundance in the sampling locations of the river Ouse compared to the locations in the Foss, with the latter showing significantly higher levels. Particularly noteworthy were Foss SP3 and Foss SP5, both collected in May 2022, and Foss SP5 collected in November, where PP displayed elevated relative abundances.

The relative abundances of polymethyl methacrylate (PMMA) and polyethylene terephthalate (PET) were consistently lower than those of the other polymers. PMMA was primarily present in the locations Foss SP5, Foss SP3, and Ouse SP4, with the highest abundance detected in Ouse SP3 collected in August. Similarly, PET showed relatively low levels across most locations, with Foss SP5 and Ouse SP4 registering the highest abundances. Polycarbonate was the least frequently detected polymer across all sampling locations and months, with Ouse SP3, Ouse SP4, and Ouse SP5 showing the highest relative abundances in November, August, and May 2021, respectively.

Figure 4.3. Relative abundance of thermoplastics in sediment samples across various sampling locations and months.

4.3.3 Sediment grain size and organic material analysis

Statistical analyses involved data transformations to ensure normality. To achieve this, the variables percentage of clay, silt, and sand underwent square root transformations, all demonstrating normality in subsequent assessments by the Shapiro-Wilk test (W=0.933 - 0.983 and P=0.160 - 0.644). Additionally, organic matter data was $\log_e$ transformed, successfully achieving normality (*Shapiro-Wilk test*, W=0.95584, P=0.071).

The results of particle size analysis for each of the sampling months can be found in Figures A2.10 to A2.14 within the Appendix. In general, sediment in the river Ouse exhibited a coarser grain size in comparison to that of the Foss. Ouse sediment samples were primarily composed of sand, accounting for an average of over 65% of the volume across all locations and months. Ouse SP6 stood out with the highest proportion of sand particles, presenting an average composition of 98% sand, 1.39% silt, and 0.27% clay. In contrast, sediment samples from the Foss were characterized by a higher composition of silt, with an average percent of volume exceeding 48% across all samples. Foss SP5 displayed the highest proportion of clay and silt particles, exhibiting an average composition of 15% sand, 58.3% silt, and 26.7% clay. Pearson analysis revealed a significant correlation (P<0.001) between TRWP mass concentration and sediment texture classification (clay, silt, or sand). This correlation was positive (R=0.6) between TRWP concentration and the percentage of clay/silt particles, while it was negative (R= -0.58) between TRWP concentration and the percentage of sand (Fig. 4.4 A-C).

The loss on ignition analysis revealed variations in organic matter content between the Ouse and Foss locations. Ouse samples showed a lower mean organic matter concentration, ranging from 1.2 to 3.7 wt% per gram, while Foss locations exhibited higher organic matter content, ranging from 4.7 to 16 wt% per gram across all samples. The highest recorded organic matter content was in Foss SP2 collected in November, with a value of 34.5 wt% per gram, whereas the lowest was in Ouse SP6 collected in February, with a value of 0.94 wt% per gram (see Figure A2.15 in the Appendix). Pearson analysis indicated a significant positive correlation (P<0.001,

R=0.8) between the percentage of organic matter and TRWP concentration in all analysed samples (Fig. 4.4 D).

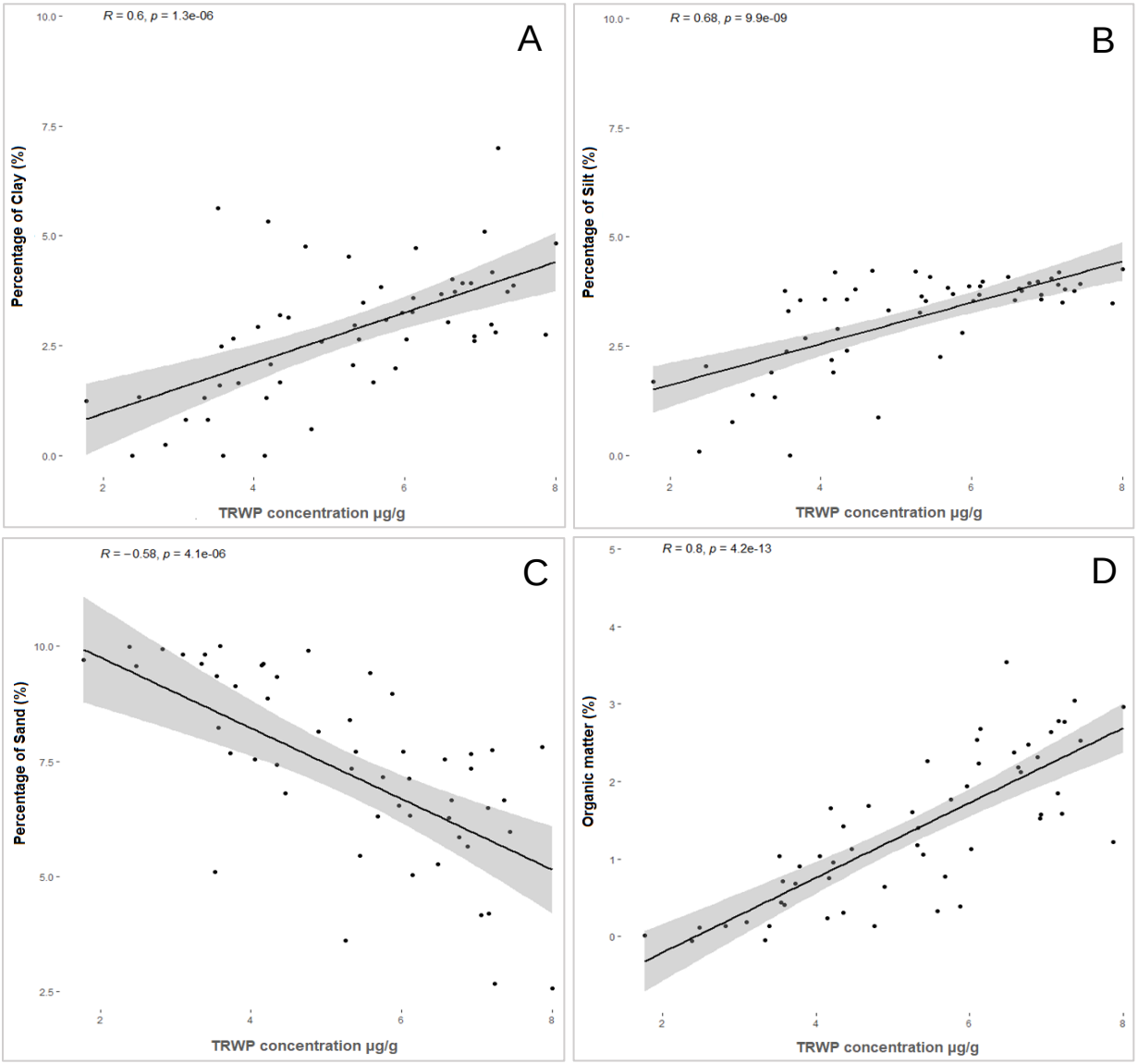

Figure 4.4. Pearson correlation results between TRWP concentrations, sediment grain size classified into percentage of clay, silt and sand (A – C), and organic matter (D) for all sample locations and months.

4.3.4 Microscopic analysis

Microplastics (>50 µm) were detected in all samples analysed. Figures 4.5 and 4.6 showcase a diverse array of identified microplastics, including tyre and road wear particles, fragments, fibres, spheres, films, glitter, and paint. Unless specified otherwise, microplastics found in the different density solutions (NaCl and Fastfloat) were combined to calculate the final microplastic abundance results.

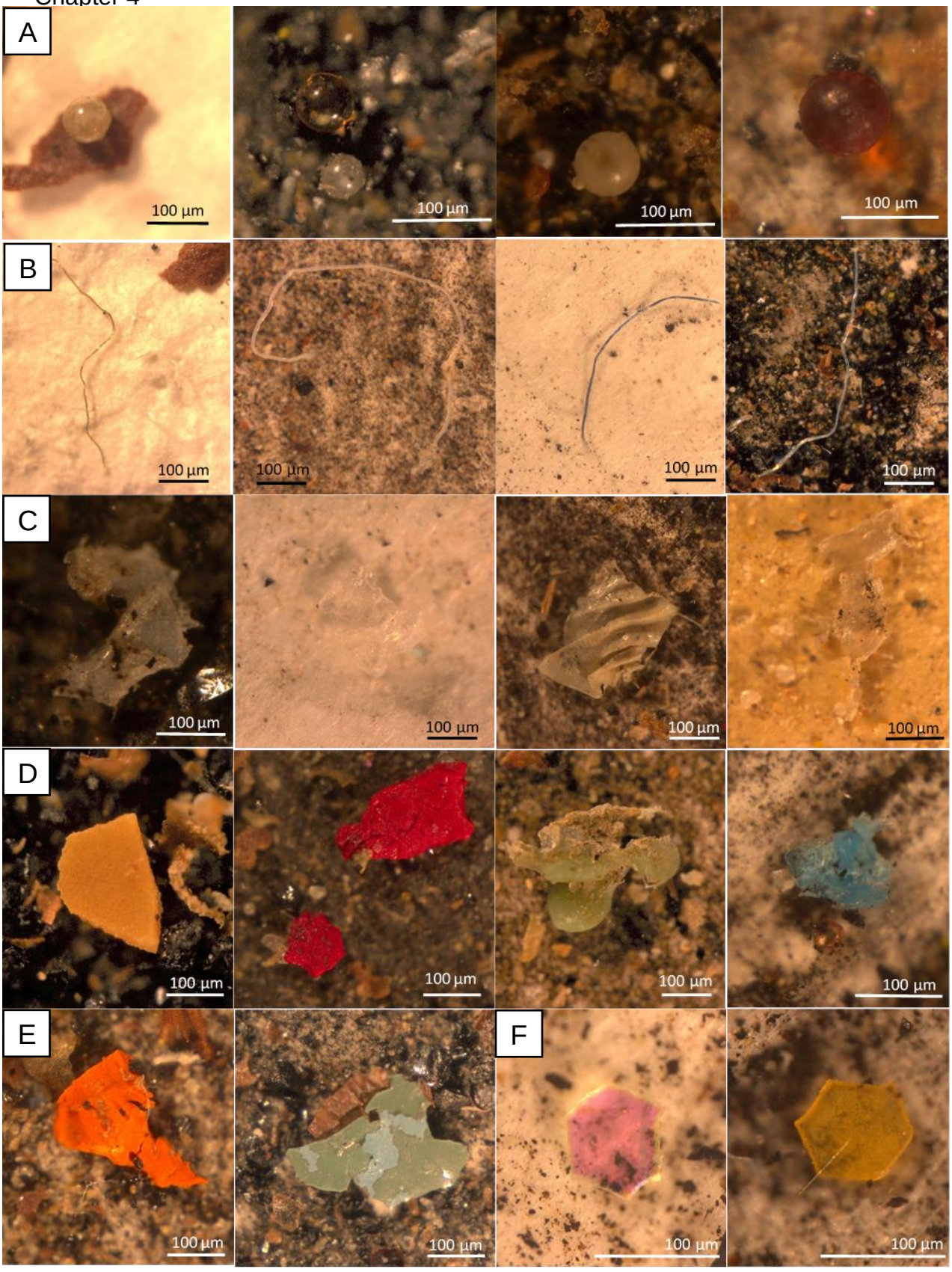

Figure 4.5. Representative morphologies of the microplastics identified in the sediment samples. (A) spheres, (B) fibres, (C) films, (D) fragments, (E) paint and (F) glitter.

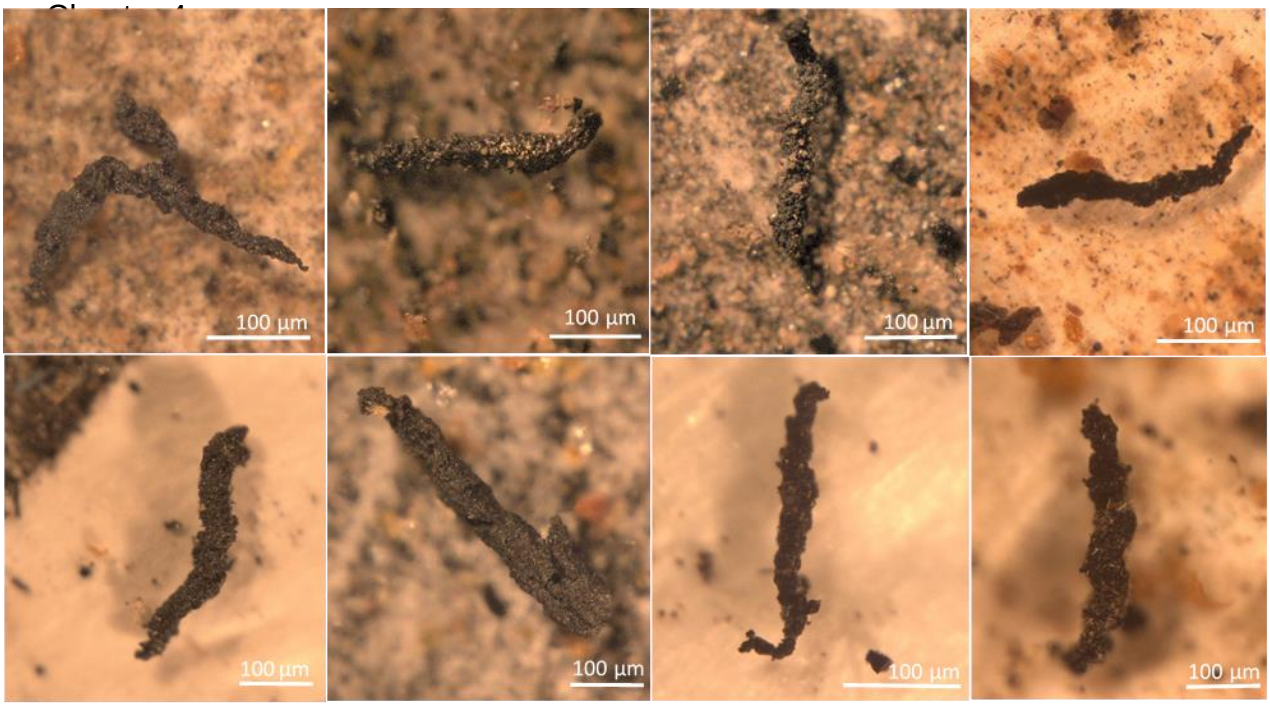

Figure 4.6. Examples of the tyre and road wear particles identified in the sediment samples.

The variable "microplastics abundance" initially exhibited non-normality across all groups (*Shapiro–Wilks* test for normality, W=0.8073 and P<0.001). Despite undergoing multiple transformations, the data still did not conform to normality (*Shapiro–Wilks* test for normality, W=0.7448 and P<0.001). However, it did meet the assumption of homogeneity (*Fligner-Killeen* test of homogeneity of variances, X^2=16.776, df=10, and P=0.079).

Microplastic abundance displayed variability between sampling locations, ranging from a mean value of 320 microplastics/kg in the river Ouse to 4,653.33 microplastics/kg in the river Foss, averaged across all months. The Kruskal-Wallis analysis revealed a significant difference in microplastic abundance among the different locations (H=39.20, df=10, P<0.001). Subsequent Dunn tests confirmed that microplastic abundance was significantly higher at Foss SP4 and Foss SP5, as indicated by p-values <0.001, while showing significantly lower abundance at locations Ouse SP1, Ouse SP2, and Ouse SP6 (P=0.001). The variability in microplastic abundance between the months was evident, with May 2021 showing the lowest levels (mean value 1,272.72 microplastics/kg) and November displaying the highest concentrations (mean value of 2,363.64 microplastics/kg) across all

sampling locations. Nevertheless, the Kruskal-Wallis analysis did not indicate a significant difference in microplastic abundance concerning the sampling months (*H*=4.24, df=4, *P*=0.374).

A total of 3,093 microplastics were collected from the Ouse sampling locations. The mean microplastic abundance per sample (30 g of dried sediment), averaged across all months, was as follows: 12.2 ± 6.97 for Ouse SP1, 9.6 ± 6.58 for Ouse SP2, 14 ± 10.70 for Ouse SP3, 101.8 ± 81 for Ouse SP4, 55.8 ± 55.97 for Ouse SP5 and 12.8 ± 6.72 for Ouse SP6. Notably, Ouse SP4 exhibited the highest microplastic count, with the most substantial abundance observed in the sample collected in February, reaching 7,966.6 ± 1,047.7 microplastics/kg. In contrast, Ouse SP2 had the lowest microplastic abundance, with the least amount recorded in the sample collected in August, measuring 133.33 ± 33.3 microplastics/kg (Fig. 4.7).

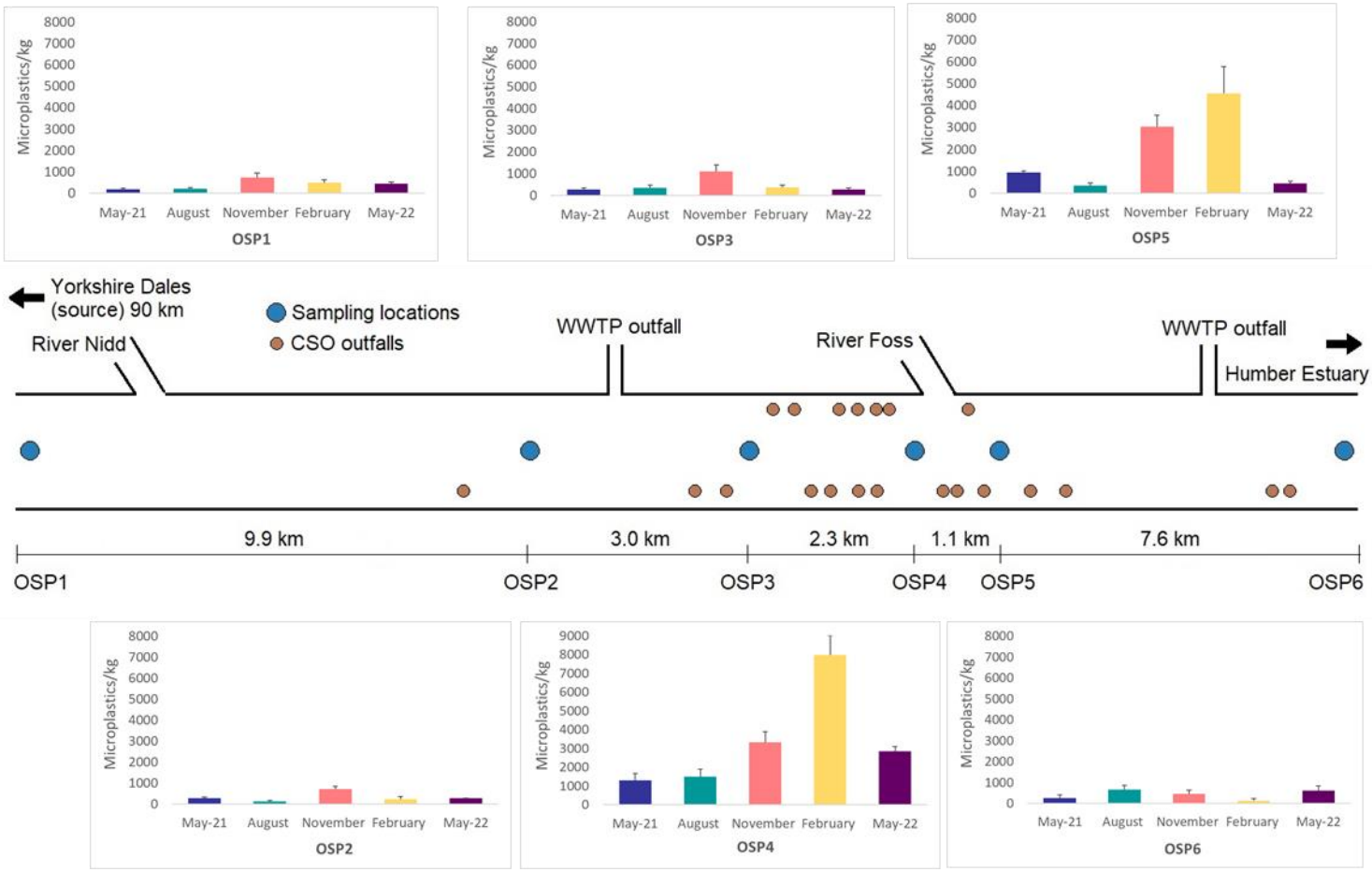

Figure 4.7. Microplastic abundances expressed as the total number of items per kilogram of dry weight of sediment for the river Ouse sampling sites. Error bars represent standard deviations; n=3 per sampling location and month.

A total of 5,625 microplastics were collected from the Foss sampling locations. The mean abundance of microplastics per sample (30 g of dried sediment), averaged across all months, revealed the following figures: 25.2 ± 9.83 for Foss SP1, 28.8 ± 16.54 for Foss SP2, 63 ± 36.15 for Foss SP3, 118.4 ± 35.16 for Foss SP4, and 139.6 ± 32.26 for Foss SP5. In general, the location exhibiting the highest microplastic count was Foss SP5, with the highest abundance recorded in the sample collected in August, amounting to 6,266.66 ± 693.62 microplastics/kg. In comparison, the location with the lowest microplastic abundance was Foss SP1, with the least amount recorded in the sample collected in February, measuring 366.66 ± 66.6 microplastics/kg (Fig. 4.8).

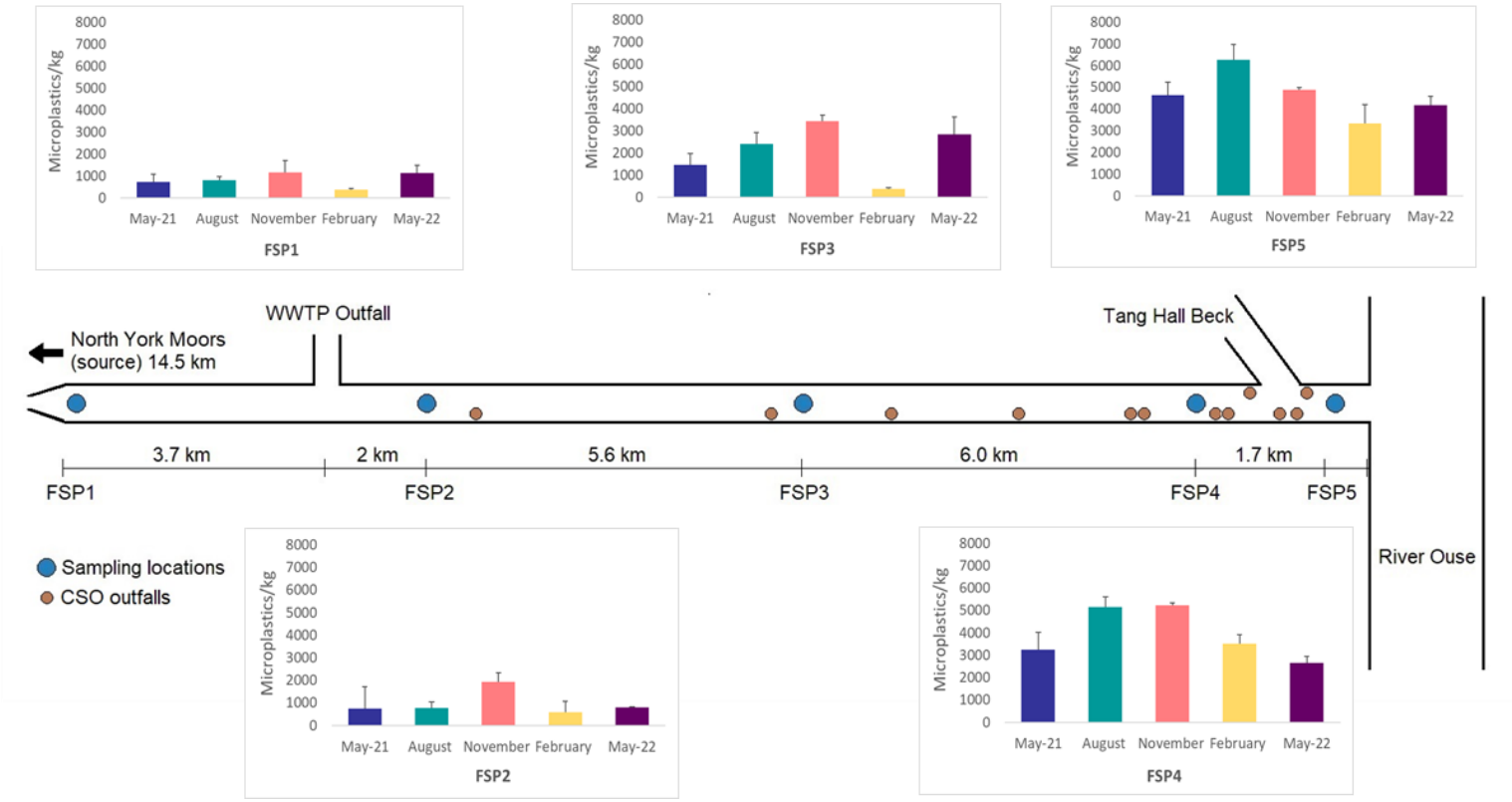

Figure 4.8. Microplastic abundances expressed as the total number of items per kilogram of dry weight of sediment for the river Foss sampling sites. Error bars represent standard deviations; n=3 per sampling location and month.

In the sediment samples from the river Foss, TRWPs emerged as the predominant microplastic type, making up 33.7% of the total. Fragments followed closely behind, constituting 29.7%. Fibres, films, and spheres came next, each contributing 21.9%, 7.5%, and 5.72%, respectively. Microplastics with the smallest contribution to the overall total were glitter and paint, both accounting for less than 1.5% (Fig. 4.9).

A dependence between sampling location and the type of microplastic was found (X^2=619.14, df=60 and P<0.001), with Foss SP1, Foss SP2 and Foss SP3 associated with higher levels of fragments and films, but lower levels of spheres and tyre and road wear particles. On the other hand, Foss SP4 was associated with lower levels of fibres and films and higher levels of fragments and spheres, whereas Foss SP5 was strongly associated to high levels of paints and fibres and lower levels of films and fragments.

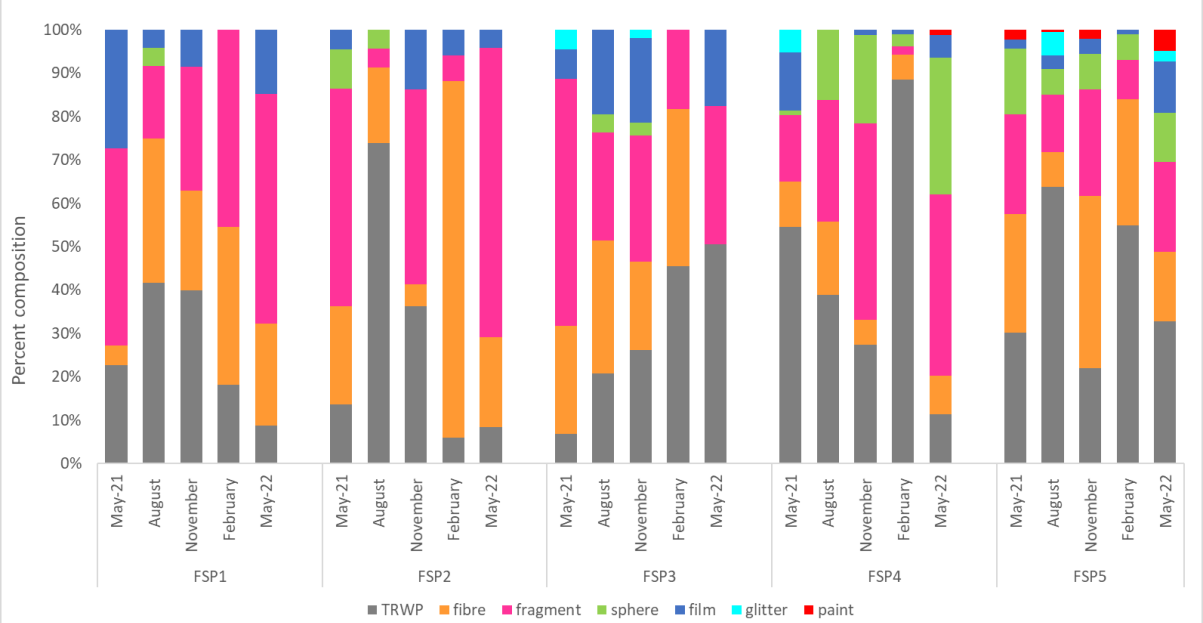

Figure 4.9. Percent composition of microplastic types found in sediment samples from the river Foss, n=3 per sampling location and month.

Fibres dominated the microplastic composition in sediment samples from the river Ouse, comprising 32.5% of the total microplastics, and coming in second place were TRWPs at 27.8%. Following these were fragments and films, accounting for 24.24%

and 9.5%, respectively. Spheres, glitter, and paint collectively made up less than 6% of the total microplastics content (Fig. 4.10).

In the context of the river Ouse, the sampling sites that presented an association with higher levels of fibres and fragments and lower levels of tyre and road wear particles were Ouse SP1 and Ouse SP2. Interestingly, Ouse SP4 was associated with extremely high levels of spheres, high levels of glitter and lower levels of fibres and fragments, while Ouse SP5 was associated with high levels of tyre and road wear particles and low levels of spheres and fragments. In addition, Ouse SP6 was associated with higher levels of fibres and lower levels of spheres and tyre and road wear particles (Chi-squared residuals provided in Table A2.1 of the Appendix).

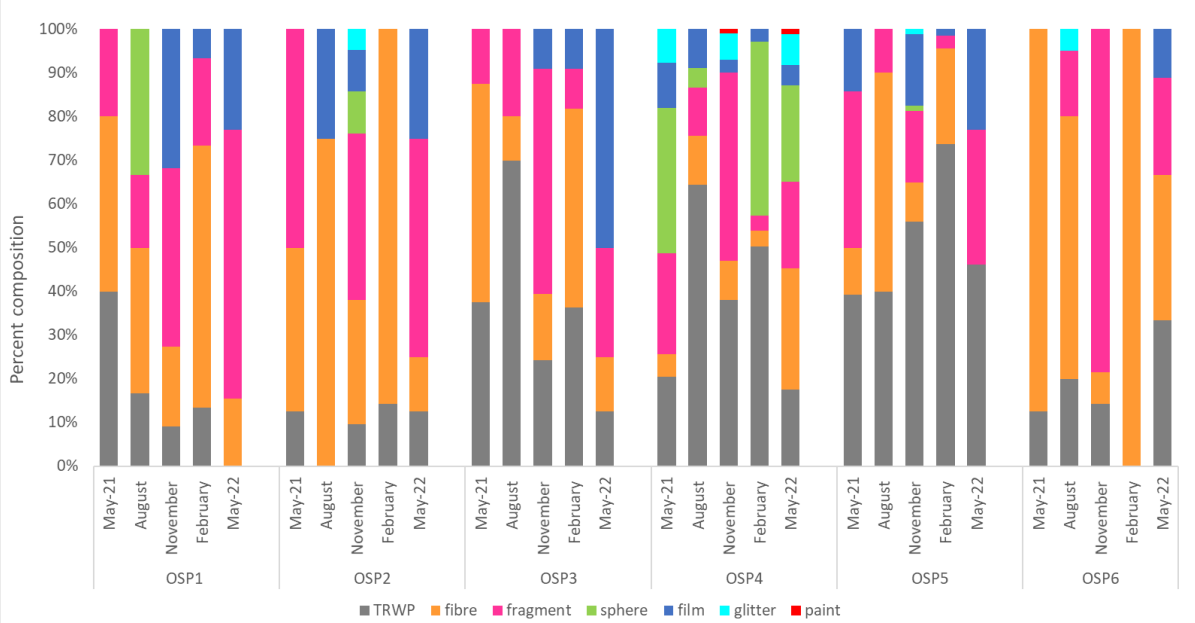

Figure 4.10. Percent composition of microplastic types found in sediment samples from the river Ouse, n=3 per sampling location and month.

In the sediment samples from the river Foss, transparent microplastics were the most prevalent (40%), followed by black (35%) and blue (11%). On the other hand, white, orange, and red were less common, accounting for 6.4%, 2%, and 1.8%, respectively. All other colours together contributed less than 3.5% to the total. The majority of the black particles were identified as tyre and road wear particles, while the majority of

the white particles were categorized as spheres. Additionally, all holographic particles were identified as glitter (Fig. 4.11).

A dependence between sampling location and microplastics colour was found (X^2=512.93, df=120, and P<0.001) with Foss SP1, Foss SP2, Foss SP3 associated with lower levels of black and white microplastics, but higher values of transparent and blue particles. In addition, Foss SP3 presented a positive association with yellow microplastics, which was not seen for any of the other locations. Foss SP4 was associated with fewer blue microplastics, while Foss SP5 showed a higher concentration of green and orange microplastics in comparison.

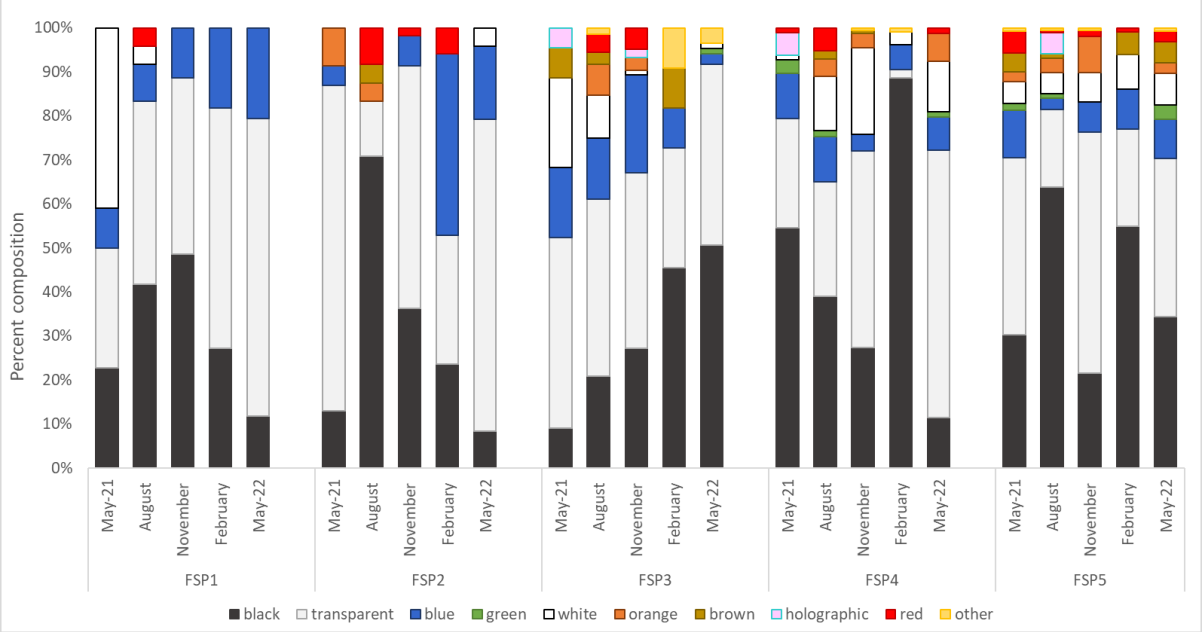

Figure 4.11. Percent composition of microplastic colours found in sediment samples from the river Foss, n=3 per sampling location and month.

Black was the most abundant microplastic colour identified in the sediment samples from the river Ouse, comprising 34.4% of the total microplastics. Following closely were transparent particles, constituting 32.2%. Blue, white and red particles contributed 23%, 5.5% and 2.7% respectively to the overall microplastic count. The remaining microplastics collectively constituted less than 4% of the total (Fig. 4.12).

The river section Ouse SP1 was associated with a lower presence of black microplastics but a higher presence of blue and red particles. In comparison, Ouse SP2 exhibited a positive association with blue, pink and transparent microplastics, and a negative association with black particles. Furthermore, Ouse SP3 was associated with more microplastics of blue colour and fewer white microplastics, whereas Ouse SP4 presented a positive association with holographic and white microplastics and a negative relationship with blue, orange and transparent microplastics. Lastly, Ouse SP5 was associated with fewer orange, transparent and white particles, but higher black, blue and brown particles, while Ouse SP6 was associated with higher blue, green and pink microplastics and fewer black, and white microplastics (Chi-squared residuals provided in Table A2.2 of the Appendix).

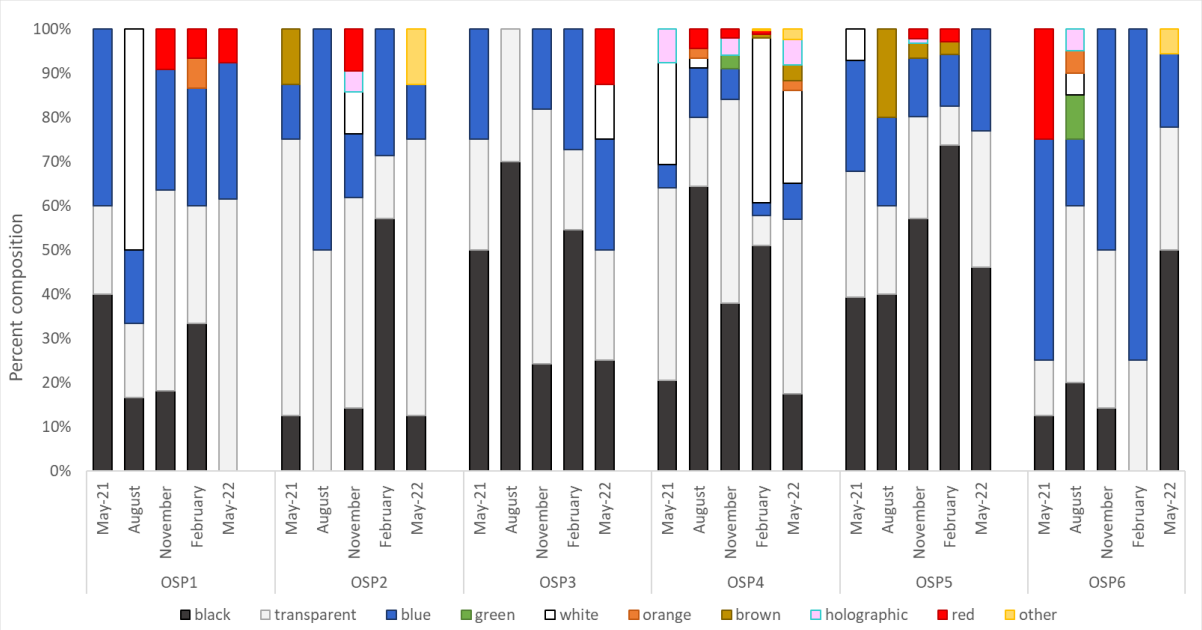

Figure 4.12. Percent composition of microplastic colours found in sediment samples from the river Ouse, n=3 per sampling location and month.

The size analysis of the microplastic particles in the sediment samples from the river Foss revealed that the most prevalent size category was 50-149 µm, accounting for 50.8% of the total microplastics. Secondly, the 150-249 µm category accounted for 21.4% of the total count, while sizes within the range of 250-499 µm and 500–1,000

µm constituted 17.6% and 8.5%, respectively. Notably, the >1,000 µm category was the least abundant, comprising only 1.5%. Additionally, all spheres and glitter particles fell within the 50-149 µm category, while the only particles larger than 1,000 µm were fibres (Fig. 4.13).

A relationship between sampling location and particle size was also established (X^2=194.93, df=40, and P<0.001), with Foss SP2 and Foss SP5 associated with fewer microplastics larger than 1000 µm, but more microplastics between 250 and 499 µm. Foss SP3 was associated with more microplastics greater than 1000 µm, but fewer microplastics within the 50-149 µm category, whereas Foss SP4 was associated with smaller particle sizes between 50 and 149 µm.

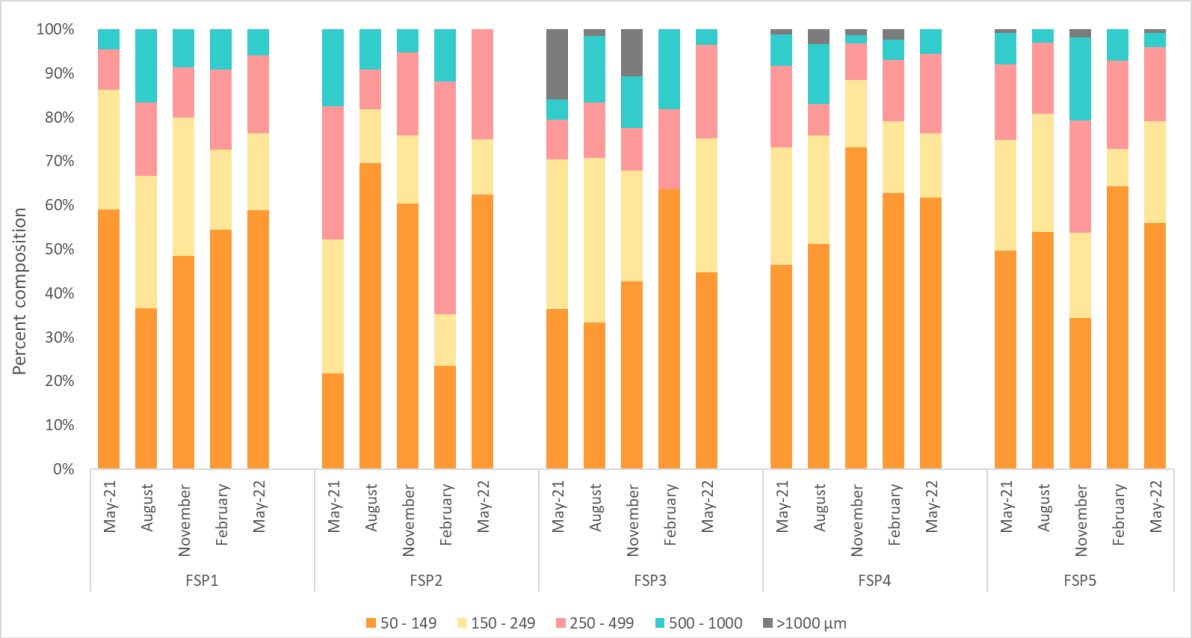

Figure 4.13. Percent composition of microplastic sizes found in sediment samples from the river Foss, n=3 per sampling location and month.

The most abundant size category in the river Ouse samples was 50-149 µm comprising 52%, of the total, followed by 150-249 µm (19.7%), 250-499 µm (18.8%) and 500 – 1,000 µm (10%). The least abundant size category was >1,000 µm, constituting less than 1% (Fig. 4.14).

The river section Ouse SP4 was associated with more microplastics within the 50-149 µm category and fewer microplastics between 150 and 1000 µm. Moreover, Ouse SP5 was associated with fewer microplastics within the 250-499 µm size range and more microplastics between 500 and 1000 µm. Lastly, Ouse SP6 presented a positive association with particles between 500 and 1000 µm, but a negative one with particles within the 150-249 µm category (Chi-squared residuals provided in Table A2.3 of the Appendix).

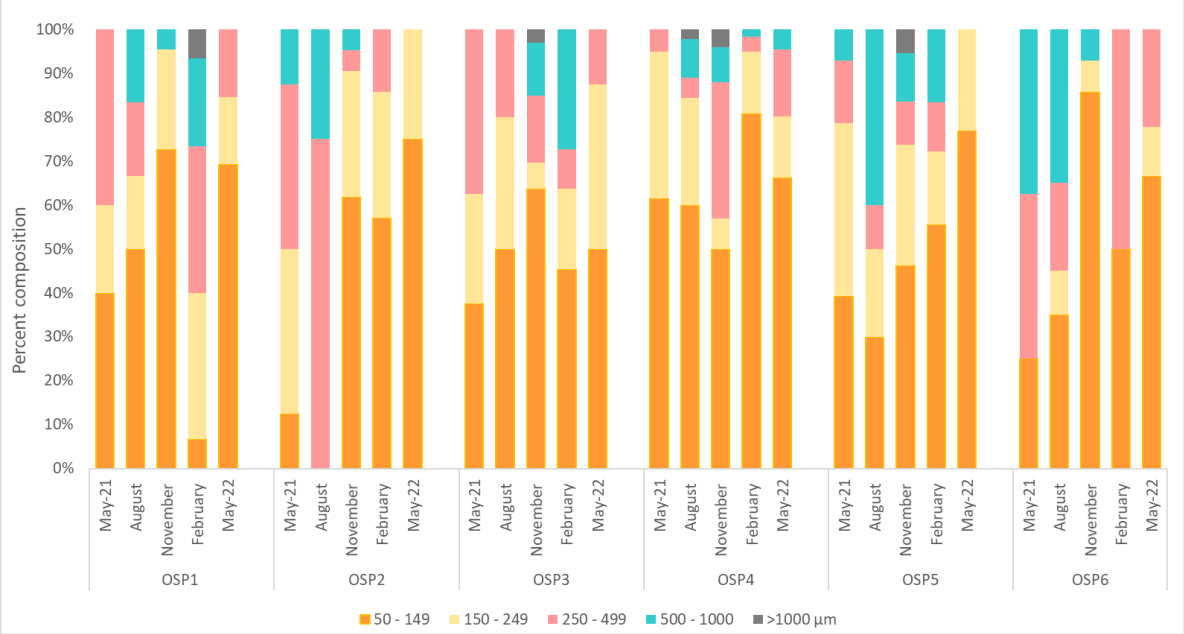

Figure 4.14. Percent composition of microplastic sizes found in sediment samples from the river Ouse, n=3 per sampling location and month.

4.3.4.1 Characterization of TRWPs

TRWPs were detected in all samples except for those collected from Ouse SP1 in May 2022, Ouse SP2 in August, and Ouse SP6 in February. To evaluate the TRWP density in sediment samples, two extraction solutions with different densities, NaCl (1.2 g/cm^3) and Fastfloat (1.95 g/cm^3), were employed. As depicted in Figure 4.15, the extraction with NaCl yielded a limited amount of TRWP in only a few locations, with fewer than four particles per sample. In contrast, the Fastfloat solution appeared to be more effective, resulting in the extraction of a higher number of particles. The

sampling site registering the highest TRWP abundance was Foss SP5, recording an average of 1,933.33 particles/kg across all months, peaking at 4,000 particles/kg in August. In contrast, Ouse SP2 exhibited the lowest TRWP abundance, averaging 33.3 particles/kg across all months, with August showing no recorded particles.

Pearson analysis revealed a significant positive correlation ($P<0.001$, $R=0.85$) between the TRWP concentrations (µg/g) determined by Py-GC-MS and the TRWP abundance (particles/kg) identified through microscope analysis in the sediment samples (Figure A2.16 in the Appendix).

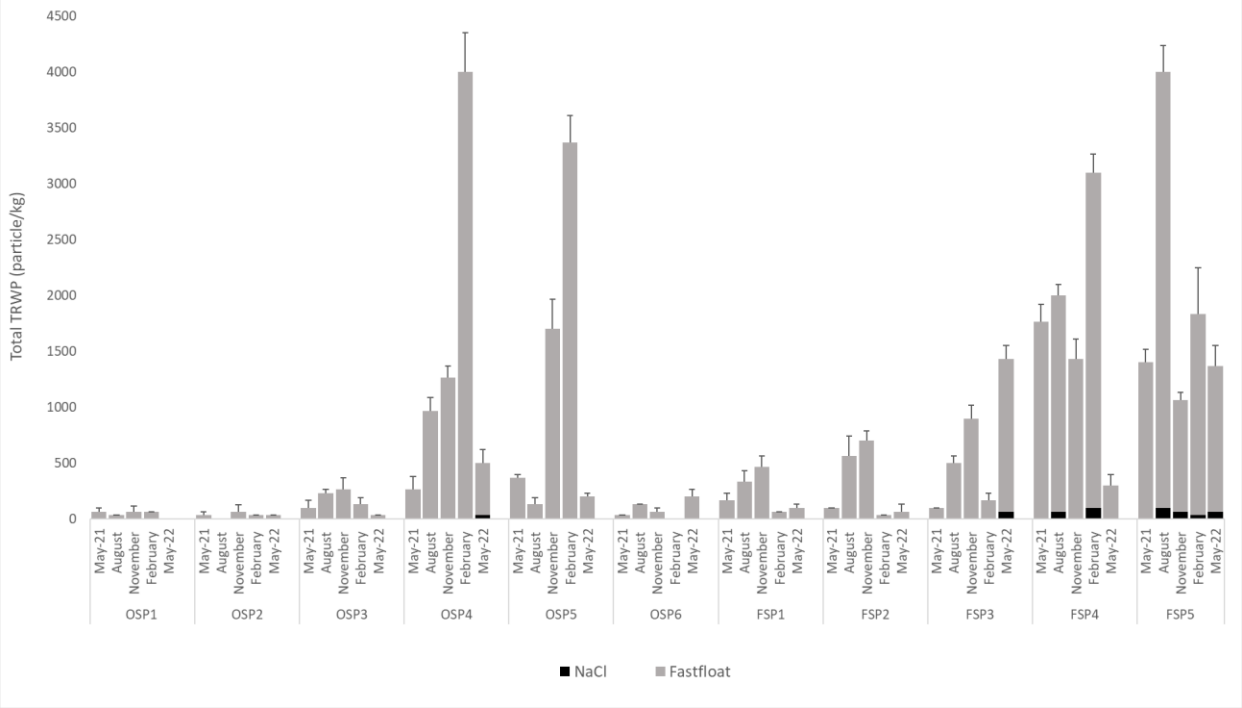

Figure 4.15. TRWP abundance in the sediment samples from all sampling locations and months. Error bars represent standard deviations; n=3 per sampling location and month.

The length of the TRWPs, measured along their longest axis, exhibited a range from 50 µm to 570 µm across all samples. Notably, 31% of the TRWPs fell within the 50-100 µm size category, 32.6% measured in the range of 100-150 µm, 28.5% ranged from 150-250 µm, and 7.8% measured between 250-580 µm. The median length was 122 µm, while the mode was recorded at 102 µm (Fig. 4.16).

The recorded aspect ratios spanned from a minimum of 1.5 to a maximum of 11.2 across all samples, with approximately 46% of all particles falling within the range of 4.5 to 5.5 (see Fig. 4.17).

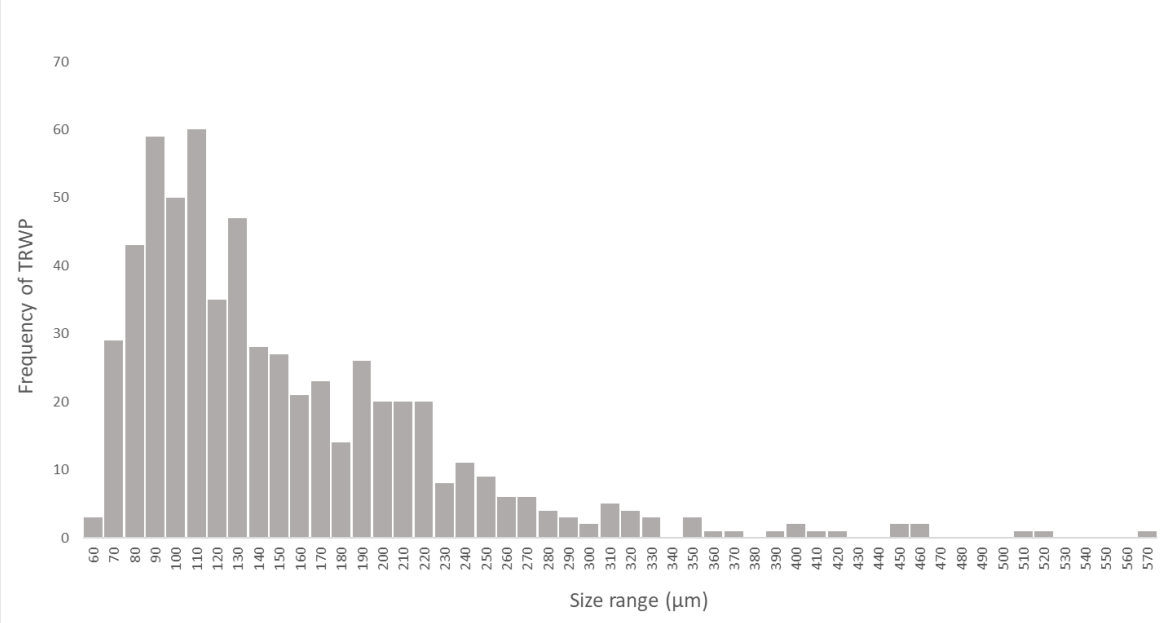

Figure 4.16. Size distribution of TRWP from the sediment samples, n=55.

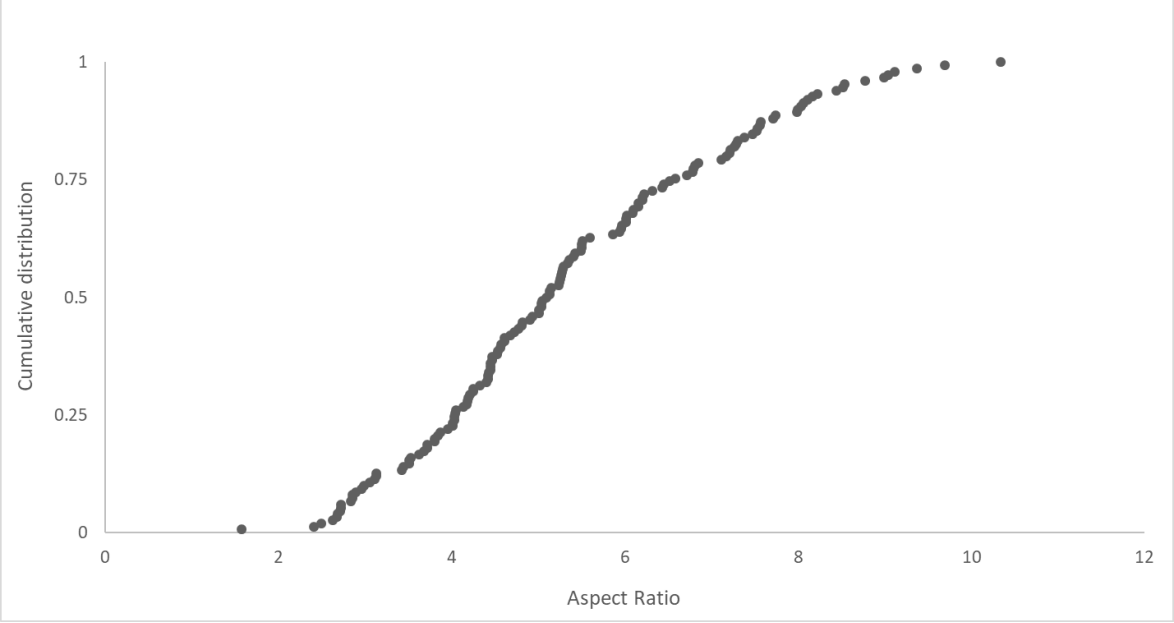

Figure 4.17. Aspect ratio of TRWP from sediment samples, n=55

4.3.5 FT-IR analysis

The TRWPs collected from the sediment samples could not be matched to a specific synthetic polymer in the FTIR library. Nevertheless, their FTIR spectra closely resemble the spectrum of the standard tyre particle. This resemblance is evident in characteristic features such as the downward sloping spectra and the presence of common peaks, including prominent intensities at 2,913 and 2,847 cm^{-1}, as well as peaks around 2,096 cm^{-1} (Fig. 4.18). These significant similarities in spectral patterns between the reference tyre particle and the field-collected TRWPs suggest a potential origin of the analysed particles from tyre degradation.

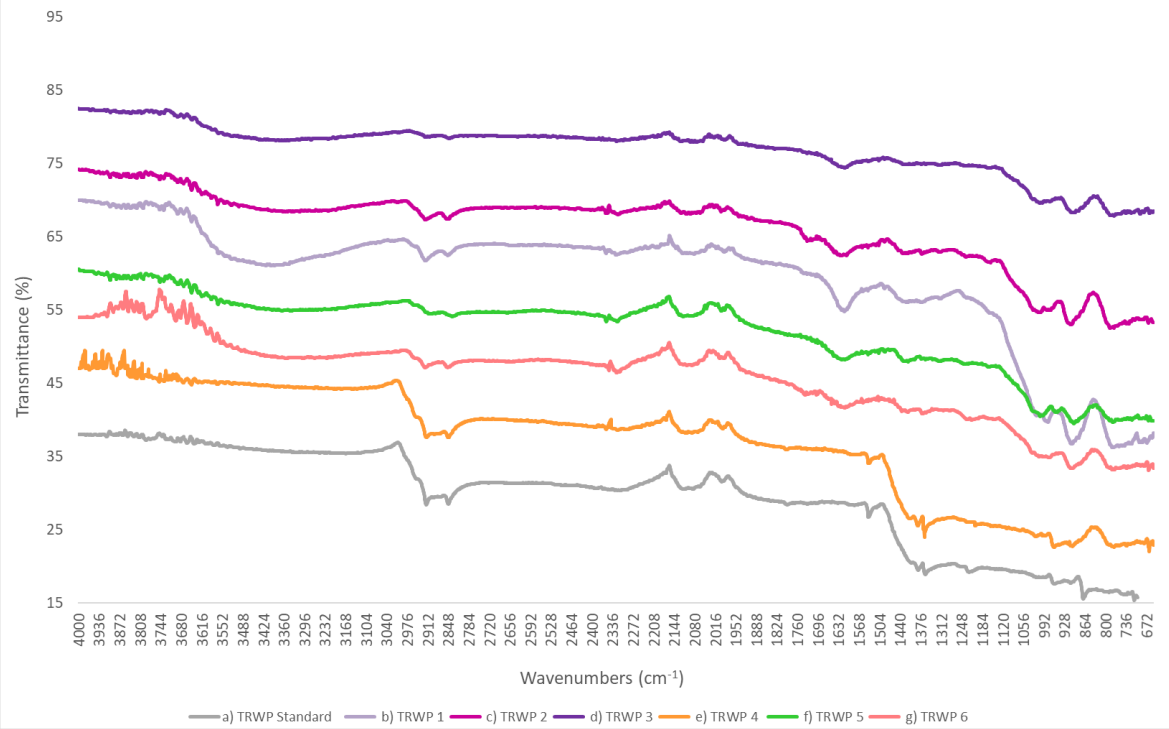

Figure 4.18. Representative FT-IR spectra of suspected TRWPs detected in the sediment samples and the spectrum of a tyre particle standard produced from a passenger car tyre (grey).

4.4 Discussion

4.4.1 TRWP concentrations in sediment samples

This study provides compelling evidence of the inherent variability of TRWP concentrations in river sediments across different sampling locations within an urban

environment throughout the year. It underscores the significance of conducting long-term studies to ensure data reliability and minimize the uncertainties associated with single-time sampling due to temporal variations (Baensch-Baltruschat *et al*., 2020).

Studies examining TRWP concentrations in river sediments are relatively scarce. For instance, Kumata *et al*. (2000) analysed sediment samples collected from two Japanese rivers, the Sumidagawa and Tamagawa, and estimated TRWP concentrations by GC-MS- Flame photometric detector (FPD) using the markers NCBA and 24MoBT. Their findings revealed tyre tread concentrations within the range of 800–3,900 µg/g dw for the Sumidagawa River and 400–2,300 µg/g dw for the Tamagawa River. Similarly, Zakaria *et al*. (2002) conducted an analysis using GC/FPD and the marker NCBA to investigate TRWP concentrations in riverine and estuarine sediments in Malaysia, specifically the Pinang and Klang estuaries as well as the Malacca River. Their study reported tyre tread concentrations spanning from 92–590 µg/g (as detailed in Baensch-Baltruschat *et al*., 2020). These results are in good agreement with the concentrations observed in the present study, which ranged from 5.88 to 2,975.7 µg/g dw across all sampled locations and months. However, it is worth noting that the use of benzothiazoles as markers may introduce some uncertainty, as they lack specificity for tyre wear and can potentially leach into aquatic environments (Federico *et al*., 2023; Baensch-Baltruschat *et al*., 2020).

In a more recent study conducted by Unice *et al*. (2013), TRWP concentrations were analysed in surficial sediments from three river basins located in France (Seine), USA (Chesapeake) and Japan (Yodo). They employed pyrolysis GC-MS and used dipentene and 4-vinylcyclohexene as markers for NR and SBR/BR, respectively. The average TRWP concentration as tread across all sampled sites was 998.94 µg/g dw, with a range of 18 to 3,700 µg/g. These results closely align with the TRWP concentrations found in the sediments of the present study.

As discussed in Chapter 3, this study reports TRWP concentrations in terms of tyre tread, primarily due to the challenges in accurately quantifying the mass contribution of the mineral content within TRWP. However, to demonstrate the variability of TRWP concentrations influenced by the presence of mineral encrustations, a range of

encrustment levels was considered, including a minimum (6%), an average (30%), and a maximum (53%), as outlined by Rødland *et al*. (2022) and illustrated in Figure A2.2 in the Appendix. For example, under the MIN encrustment level, the sampling point with the highest concentration, Foss SP5 in August, would exhibit a concentration of 3,165.67 µg/g. However, under the AVE and MAX levels, this concentration would rise to 4,251.05 µg/g and 6,331.35 µg/g, respectively. These significant differences between encrustment level values highlights the necessity for further studies to examine the impact on TRWPs' mineral content considering variables such as driving conditions, road surface types, and vehicle speeds (Rødland *et al*., 2022).

In general, TRWP concentrations were higher in the river Foss when compared to the river Ouse. These variations can be attributed to differences in river size and depositional characteristics. The river Foss, with an approximate average width of 9.2 m, is smaller than the Ouse, which has a width of 35.7 m, resulting in the river Ouse experiencing higher levels of dilution. In addition, the sediment in the river Foss primarily comprises silt and clay and contains a higher organic matter content, in contrast to the predominantly sandy composition and lower organic matter content characterizing the sediment in the river Ouse. Notably, a positive correlation between observed TRWP concentrations, the percentage of silt and clay, and the organic matter content in the sediment was consistently evident across all samples collected in this study. These findings align with the conclusions drawn in Unice *et al*.'s study, where they emphasized that finer grain sizes (silt/clay) and higher organic carbon content in sediment significantly contribute to elevated TRWP concentrations in all the areas they investigated.

Similar findings have also been reported in microplastics research, where positive relationships have been identified between the abundance of microplastics and the silt/clay content within sediments. This emphasises that sediments characterized by finer grain size and elevated organic matter content effectively serve as "traps" for microplastics (Bakir *et al*., 2023, Leads *et al*., 2023; Mendes *et al*., 2021).

Furthermore, several studies have documented an association between increased TRWP abundances and higher occurrences of braking and acceleration, particularly related to traffic lights and cornering events in urban areas (Venghaus *et al*., 2023; Mengistu *et al*., 2021; Knight *et al*. 2020). In the current study, the highest TRWP concentrations were observed in Ouse SP4, Foss SP4 and Foss SP5, all located in the city centre of York. Therefore, while it is true that the city's ring road experiences higher traffic volumes, the heightened TRWP concentrations observed in these central locations may be attributed to specific driving patterns observed in the city centre. These patterns are characterized by more intense and frequent instances of braking and acceleration, which, in turn, generate a greater abundance of TRWPs.

The variability in the mass concentration of TRWPs across the sampling months is likely influenced by monthly variations in precipitation levels (Vercauteren *et al*., 2023). In a related study, Mahjoub *et al*. (2023) investigated the occurrence of tyre wear particles during four rainfall events and three baseflow measurements in an urban catchment within Tehran metropolis. Their results showed the highest abundance of TRWPs during rainfall events ranging from 3.3–60.5 particles/L, compared to baseflow measurements ranging from 0.5–3 particles/L. This highlights the role of urban stormwater runoff as the main terrestrial source of TRWPs in aquatic environments (Mahjoub *et al*., 2023).

Moreover, amid the Covid-19 pandemic in 2020, the city of York experienced a reduction in traffic volume by approximately 22.50%. This decrease was a consequence of the three national lockdowns implemented in the UK, which restricted travel for non-essential workers (Department for Transport: roadtraffic.dft.gov.uk/local-authorities/202). In a study conducted by Devereux *et al*. (2023b) an analysis of microplastics in water samples from five sites along the river Thames was carried out from May 2019 to May 2021. The researchers detected Acrylonitrile butadiene styrene (ABS) in their samples, which is commonly associated with tyre wear particles. Interestingly, they observed a decrease in ABS levels from pre-Covid-19 abundances during the first lockdown at each sampling location. However, following the easing of lockdown measures and a return to more typical

routines, ABS concentrations increased to levels surpassing those observed pre-Covid-19. The authors attributed this ABS increase to people choosing individual car travel over carpooling or using public transport due to concerns about Covid-19 transmission (Devereux *et al*., 2023b). In the present study, TRWP concentrations in May 2021 were generally lower than those in May 2022. However, these differences were not statistically significant.

4.4.2 FT-IR analysis of the TRWPs

As discussed before, FTIR is not the optimal choice for TRWP analysis due to the interference of IR light absorption caused by the presence of carbon black, a component added to tyres for UV protection (Ziajahromi *et al*., 2020). Nevertheless, some studies have employed this method for the purpose of cross-validation and successfully identified components of tyres, such as acrylonitrile, butadiene/styrene and carbon black (Mahjoub *et al*., 2023; Ziajahromi *et al*., 2023; Ziajahromi *et al*., 2020; Leads and Weinstein, 2019).

The obtained spectra of the field TRWPs analysed in this study closely align with those reported in the scientific literature (Rosso *et al*., 2023; Thomas *et al*., 2022; Kovochich *et al*., 2021; Ziajahromi *et al*., 2020). For example, all of them presented characteristic bands, including prominent intensities at 2,913 and 2,847 cm^{-1}, which confirm the presence of symmetrical and asymmetric stretching vibrations of methylene groups (Kovochich *et al*., 2021b). Additionally, a comparative analysis of the spectral characteristics of the suspected TRWPs from sediment samples with a reference tyre particle revealed shared features, including the downward sloping spectra typical of carbon-black-filled particles and the presence of common peaks (Thomas *et al*., 2022). The differences observed between the field TRWPs' spectra and the spectrum of the laboratory-generated tyre particle may be attributed to the mineral fraction of TRWPs acquired from contact with the road, which may influence their chemical composition (Kovochich *et al*., 2021b; Kreider *et al*., 2010).

Furthermore, TRWPs in the environment may undergo several processes, including oxidation, mechanical aging, biodegradation, and leaching, all of which can affect

their properties (Wagner *et al*., 2022). A study conducted by Klun *et al*. (2023) revealed the presence of additional peaks in the FTIR spectra of 12-week-aged TWPs compared to the spectra of pristine tyre particles. This provides further support for the idea that environmental weathering may have altered the chemical composition of the field-collected TRWPs in the present study, particularly considering their unknown residence time in the river sediments (Klun *et al*., 2023). Nonetheless, despite the limitations associated with FTIR spectra analysis, the results obtained from this method, in conjunction with visual analysis (distinct morphology and rubbery texture) were used as evidence to confirm that the field-collected particles in this study were TRWPs.

4.4.3 Microplastic abundances in sediment samples

Microplastics abundances in this study exhibited a range from 133.33 to 7,966.66 particles/kg across all sampling locations and months. These results fall within the range of microplastics (sized between 20 µm - 5 mm) previously reported in seafloor sediments along the UK coast, with recorded abundance ranging from 0 to 6,933 particles/kg dw and a mean value of 3,057 ± 2,299 particles/kg dw for the years 2020 and 2021 (Bakir *et al*., 2023). The authors determined that microplastic hotspots were located near rivers and harbours, with TRWPs and (macro) litter identified as the primary land-based sources of microplastics entering the marine environment (Bakir *et al*., 2023).

Similarly, a study carried out by Hurley *et al*. (2018) investigated the presence of microplastics (sized between 63 µm - <5 mm) in sediment samples from 26 locations along the river Irwell in the UK. They reported a mean abundance of 3,434.61 particles/kg (ranging from 100 to 26,800 particles/kg), with only two locations exhibiting extremely high concentrations (>15,100 particles/kg), while the remaining sites had abundances below 7,000 particles/kg. The spatial variability observed in Hurley *et al*.'s study was attributed to locations in close proximity to effluent from sewage treatment, areas with a higher density of combined sewer overflows, and the density of microplastics (Hurley *et al*., 2018). The results obtained in the present study are in good agreement with those reported by Hurley *et al*., (2018). Conversely,

microplastic abundances reported in sediment samples from the river Thames in the UK were lower, ranging from 185 to 332 particles/kg (Horton *et al*., 2017). However, this variation in microplastic abundances was probably due to the particle size range considered in Horton *et al*.'s study, which focused solely on large microplastics within the 1 to 4 mm size range. In the present study the most abundant size category for both the river Foss and Ouse was 50-149 µm, accounting for 53% of the total microplastics, whereas the size category >1,000 µm constituted less than 1.5% of the total. According to Ziajahromi *et al*. (2023), a negative relationship exists between microplastic particle size and microplastic abundance, with microplastic concentrations decreasing as particle size increases. This underscores the significance of including smaller size ranges in microplastic studies to prevent underestimation of microplastic abundance (Ziajahromi *et al*., 2023).

The distribution of microplastics in rivers is influenced by a combination of factors including river morphology, rainfall events, hydrological conditions, and particle characteristics such as shape, density and size. Additionally, these microplastics interact with suspended particulate matter and the surrounding biota (Bakir *et al*., 2023; Devereux *et al*., 2023a). In the context of this study, several factors may explain the differences in microplastic concentrations between the river Foss and the river Ouse. The greater volume of water within the river Ouse contributes to the dilution of microplastics, while the river Foss, characterized by lower flow rates, allows for an extended microplastic retention within the river. This retention time provides more opportunities for biofouling and sedimentation processes, potentially contributing to the higher microplastic concentration observed in the river Foss compared to the river Ouse. Similar findings were reported in the tributaries of the Charleston Harbour, USA, where higher concentrations of microplastics in the sediments of the Ashley river and the Wando river were attributed to an increase in sediment and microplastic deposition as a result of reduced river flow (Leads and Weinstein, 2019).

Furthermore, understanding how microplastics interact with suspended sediment and organic matter is crucial for determining their fate in aquatic environments (Leiser *et al.,* 2021). The process of flocculation involves the aggregation of fine-grained

particles and organic matter, such as organic carbon, driven by cohesive forces (Laursen *et al.,* 2022). This aggregation occurs through collisions and subsequent bonding of suspended material within the water column. Once formed, flocs exhibit distinct settling characteristics compared to individual particles. They possess larger sizes and greater mass, resulting in enhanced settling velocities and facilitating their removal from the water column (Laursen *et al.,* 2022; Darabi *et al.,* 2021). Therefore, the higher presence of finer sediment and organic matter in the river Foss, compared to the river Ouse, may contribute to more extensive floc formation due to increased particle aggregation, potentially accelerating the sedimentation of microplastics.

The variation in microplastic abundance across the sampling locations was significant. Interestingly, locations immediately downstream of a WWTP outfall, such as Foss SP2, Ouse SP3, and Ouse SP6, displayed lower microplastic concentrations compared to the city centre sites in York, where the highest microplastic abundances were observed. This difference may be due to the high number of Combined Sewer Overflow (CSO) outlets in the city centre, particularly in the river Ouse, compared to the rest of the city. As shown in Figure A2.17 of the appendix, the city centre of York experiences a significant number of CSO spills, with the highest number of spills recorded at the CSO located upstream of Ouse SP4 (referred to as Woolworths CSO), which in 2021 spilled 166 times for a total of 2,950 hours. This data further explains the association of Ouse SP4 with extremely high levels of spheres and glitter, likely originating from untreated wastewater discharges *via* CSOs. Additionally, this hypothesis is supported by the elevated microplastic abundances observed in samples collected from Ouse SP4 and Ouse SP5 in February. This coincides with the fact that CSO spills are often triggered by heavy rainfalls (Arias *et al*., 2022), and in February 2022, the UK was affected by three named storms within the space of a week, including Dudley, Eunice and Franklin (Met Office, 2022). The latter occurred approximately two weeks prior to the February sampling, potentially causing significant stress on the sewerage system and leading to the release of sewage and stormwater from CSOs upstream of Ouse SP4 and Ouse SP5. However, it is worth noting that while CSO spill data is publicly accessible

(https://theriverstrust.org/sewage-map), the exact dates of these spill events are not provided, making it challenging to correlate microplastic abundances with potential CSO discharges.

Several studies have identified combined sewage overflow events as a potentially major source of microplastics in freshwater systems (Vercauteren *et al*., 2023; Devereux *et al*., 2023b; Devereux *et al*., 2023a; Woodward *et al*., 2021). For instance, a study conducted by Forrest *et al*., (2017), measured microplastic concentrations in the Ottawa River during heavy rainfall and an active CSO event. Their results showed that during heavy rainfall microplastic concentrations doubled compared to baseline conditions (rising from 24 to 48 particles/m^3), while downstream of a CSO outlet, microplastic abundances were seven times higher compared to ambient conditions (increasing from 24 to 167 particles/m^3). Forrest *et al*.'s study highlights the importance of temporal events in influencing the abundance of microplastics in river systems.

Furthermore, the Covid-19 pandemic did not contribute to a significant difference in microplastic abundance between May 2021 and May 2022. Nevertheless, the relative abundance of polypropylene (PP) was higher in May 2022 in the river Foss locations, compared to May 2021. Similarly, some locations in both rivers exhibited increased relative abundances of polyethylene (PE) in May 2022 compared to May 2021. A study carried out by Devereux *et al*. (2023b) investigated the short-term impact of the Covid-19 pandemic on microplastic abundance in surface water of the river Thames. They found a gradual increase in PP from pre-Covid-19 abundances to post-Covid-19, with lockdown 3 (January to March 2021), exhibiting the highest PP abundances. The authors attributed this increase in PP levels to the amplified use and inadequate disposal of single-use plastics (i.e., plastic bags and food packaging containers) along with personal protective equipment (PPE) (i.e., masks and gloves). Masks, in particular, predominantly consist of polymers such as PP, PS and PE (Devereux *et al*., 2023b). It is important to recognize that the full-scale impact of the Covid-19 pandemic on plastic pollution may not become apparent for several years, as the

complete degradation of the masks and gloves that were mass-produced during this period may require an extended timeframe (Devereux *et al*., 2023b).

In addition, the polymers consistently detected in all sampling locations and months included PVC, Nylon, PP and PE. These findings align with previous research, which has reported these polymers as the most frequently detected in the environment (Bakir *et al*., 2023; Ziajahromi *et al*., 2023; Devereux *et al*., 2023a; Nantege *et al*., 2023). This outcome was expected, as these polymers are among the most widely used plastics in consumer products (i.e., packaging, carrier bags, and textiles) and various industrial applications (Nantege *et al*., 2023; Chaisanguansuk *et al*., 2023; Horton *et al*., 2017).

4.4.4 Characterization of TRWPs in sediment samples

Study-wide, TRWPs were the predominant microplastic particle type, accounting for 31% of the total microplastics. This aligns with findings from various studies in different environmental contexts, such as road dust, stormwater, wastewater, atmospheric deposition, and sediments, where the presence of TRWPs consistently exceeds that of thermoplastic particles (e.g. Vercauteren *et al*., 2023; Leads *et al*., 2023; Ostini *et al*., 2022; Kang *et al*., 2022; Worek *et al*., 2022; Parker-Jurd *et al*., 2021; Jarlskog *et al*., 2022). In contrast, Leads and Weinstein (2019) identified fibres as the main contributors to microplastic concentrations (constituting 52.5%) in the sea surface, intertidal and subtidal sediments of the Charleston Harbour estuary, USA. TRWPs occupied the second position, contributing 17.1% to the overall microplastic load in their study. However, it is worth noting that their study employed a NaCl density separation solution (1.2 g/cm^3) to extract microplastics from the different environmental matrices. This method may have contributed to an underestimation of TRWP concentrations, particularly in sediment samples, as the TRWPs prone to sedimentation tend to have a higher proportion of road-derived aggregates, resulting in increased density (Wagner *et al*., 2018). In the present study, the NaCl solution retrieved only 1.39% of the total TRWPs in the samples, whereas the Fastfloat solution (1.95 g/cm^3) appeared to offer superior TRWP recovery, accounting for 98.6% of the total TRWPs. These results underscore the importance of employing

appropriate quantification methods for TRWPs, including the use of denser solutions to ensure optimal isolation of TRWPs from sediment matrices.

TRWP abundance ranged from 33.3 to 4,000 particles/kg across all sampling locations and months. Similar results were obtained by Ziajahromi *et al*. (2023), who reported TRWP concentrations of 1,450 to 4,740 particles/kg in sediment samples collected from microlitter capture devices during rainfall events. In addition, TRWP size distributions reported in the literature exhibit variations depending on the environmental compartment (e.g., road dust and river sediments) and the protocols used for collection and analysis (Kovochich *et al*., 2021b). For example, Kovochich *et al*. (2021b) observed differences in the size ranges of TRWPs collected in sediments from an open settling pond system and road dust collected from a tunnel. The latter displayed smaller particle sizes ranging from 8−315 µm, whereas sediment particles spanned from 11−1,588 µm. The authors attributed this variation to the capture and settling of airborne particles within the tunnel's walls and aging processes in sediments that include aggregation of TRWPs with other environmental particles, such as minerals (Kovochich *et al*., 2021b). In the present study, the TRWPs exhibited a size range of 50 to 570 µm, with a mode of 102 µm. These findings are consistent with other distribution data, indicating that most TRWPs in the environment occupy smaller size fractions (<150 µm) as they are more easily transported by stormwater runoff. In contrast, larger particles (>500 µm) may settle in drainage channels, gully pots or the sewerage system (Forrest and Vermaire, 2023; Ostini *et al*., 2022; Parker-Jurd *et al*., 2021; Ziajahromi *et al*., 2020). Moreover, Jung and Choi, (2022) analysed TRWPs in road dust samples and reported aspect ratios ranging from 1.2 to 5.2. In comparison, Kovochich *et al*. (2021b) found aspect ratios of 1.5 to 10 in TRWPs from road dust and sediment samples, with the majority of particles having an aspect ratio greater than 2.5. These results are in good agreement with the aspect ratios observed in this study, ranging from 1.5 to 11.2.

It is important to acknowledge that the current study excluded TRWPs smaller than 50 µm in size due to challenges in their reliable identification using microscopy methods. As a result, it is possible that TRWP abundances could have been

underestimated. This became apparent in cases where TRWPs larger than 50 µm were absent in samples collected from Ouse SP1 in May 2022, Ouse SP2 in August, and Ouse SP6 in February. However, the use of Py-GC-MS confirmed the presence of TRWPs in all samples. This underscores the significance of employing multiple methods for TRWP analysis that complement each other, enabling cross-referencing of results and reducing uncertainties.

4.4.5 Comparison between the emissions model results and the TRWP concentrations in sediment samples

The advancement of modelling efforts aimed at understanding TRWP emissions and their dispersion across various environmental compartments (including freshwater, sediment, soil, and the sea) is of utmost significance in order to address potential concerns related to both human health and environmental impacts. Furthermore, areas chosen for case studies that have already undergone assessments of TRWP concentrations in soil and sediment offer a unique opportunity for a preliminary evaluation of the accuracy of the models, which, in turn, can significantly influence the direction of future research priorities (Unice *et al*., 2019).

In the present study, a preliminary assessment was conducted on both the TRWP emission model results and the TRWP concentrations in the sediments of the rivers Ouse and Foss (Fig. 4.19 and Fig. 4.20). To achieve this, the sampling locations were paired with their corresponding river sections, as outlined in Chapter 2, to address the imbalance in the number of sampling locations compared to river sections. It is important to note that the data used for TRWP concentrations in sediment corresponded to May 2021, rather than May 2022. Additionally, for the model emissions data, the emission data of the day of sampling was selected, and in cases where zero emissions were recorded for that day, the nearest day with emissions was chosen.

As illustrated in Figure 4.19, the spatial distribution of TRWPs in sediment samples does not precisely mirror the modelled emissions for the river Ouse. The modelled emissions identified hotspots on the city's outskirts, characterized by heavy traffic flow

and a higher number of HGVs associated with elevated tyre wear emission factors. In contrast, the sediment samples revealed hotspots in the city centre, which may be attributed to a greater incidence of braking and acceleration related to traffic lights and cornering events in the city centre. Additionally, the frequent CSO spills that occur in the city centre of York may also contribute to the elevated sediment TRWP concentrations.

These differences could be partially attributed to the delimitation of the hydrological zones detailed in Chapter 2, where larger areas were expected to exhibit higher emissions. Consequently, the relatively small zone allocated to the city centre of York may have resulted in lower emissions. Moreover, the absence of CSO data in the model, due to information limitations, may have led to underestimated emissions in York's city centre. On the other hand, it is also worth noting that the sampling method might have led to an underestimation of TRWP concentrations in sediment samples, particularly in locations where sampling was conducted directly from the riverbank and the sediment primarily consisted of sandy particles. This was particularly evident in areas such as Ouse SP1, Ouse SP2, and Ouse SP6, which exhibited the lowest TRWP concentrations. In addition, it is important to acknowledge that TRWPs, once introduced into the environment, are known for their persistence, degrade slowly, and gradually accumulate in river sediments over time (Wagner *et al*., 2018). For instance, Alves *et al.* (2023) analysed the vertical distribution of microplastics in sediment cores from the Patos-Mirim System, a large coastal lagoon in southern Brazil. The authors found that in most of the sediment cores, the upper 70 to 80 cm exhibited microplastic presence, dating back to the early 1970s. Therefore, the observed TRWP concentrations in sediment samples may reflect not only recent emissions but also historical inputs and sedimentation processes, contributing to the discrepancies between modelled emissions and observed concentrations.

In the case of the river Foss (Fig. 4.20), the spatial variation trend of TRWP concentrations in sediment samples appears to align with the modelled emissions. This alignment is evident in the gradual increase of emissions from Foss 1, situated on the outskirts of the city, to Foss 4, located in the city centre. The smaller size of

the river Foss may have played a role in facilitating more accurate and representative sediment sampling. Additionally, the delineation of hydrological zones for the areas linked to the river Foss might better capture real-world conditions.

Furthermore, the disparities in the temporal trends of TRWP emissions and sediment concentrations in both rivers may be attributed to the variability in rainfall data. As previously discussed, the fluctuation in TRWP mass concentrations across the sampling months is probably influenced by monthly variations in precipitation levels. Consequently, some differences are to be expected, given that the model incorporated rainfall data from 2017, whereas sediment sampling occurred in 2021 and 2022. Nevertheless, as illustrated in Figures 4.19 and 4.20, both sediment samples and modelled emissions consistently exhibited reduced emissions during the month of May. This could be attributed to the general decrease in precipitation during May, resulting in lower emissions, regardless of the specific year.

TRWP emissions were calculated based on the data currently available; therefore, conducting more in-depth investigations and gathering reliable data concerning CSOs, emission factors, WWTPs' removal capacity, and the TRWP fraction entering sewerage systems is necessary to enhance the precision of these estimations. Despite these data limitations, this preliminary study offers an initial estimation of the spatial and temporal emission trends of TRWPs within an urban area.

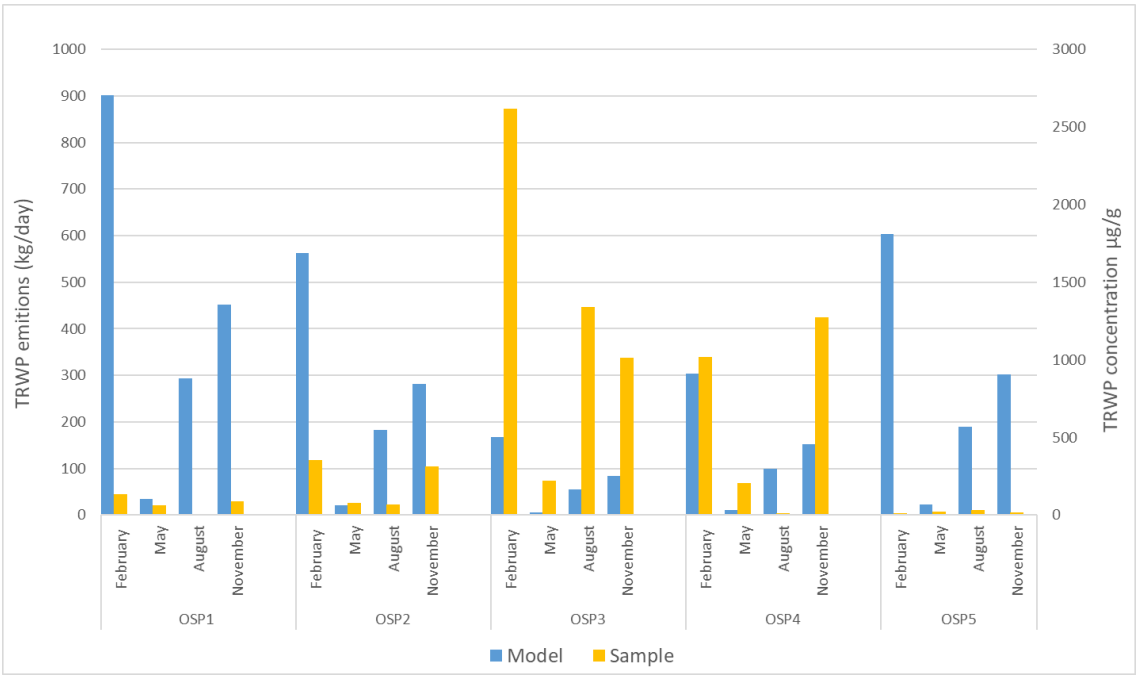

Figure 4.19. Comparison between the emissions model results and the TRWP concentrations in sediment samples for the river Ouse.

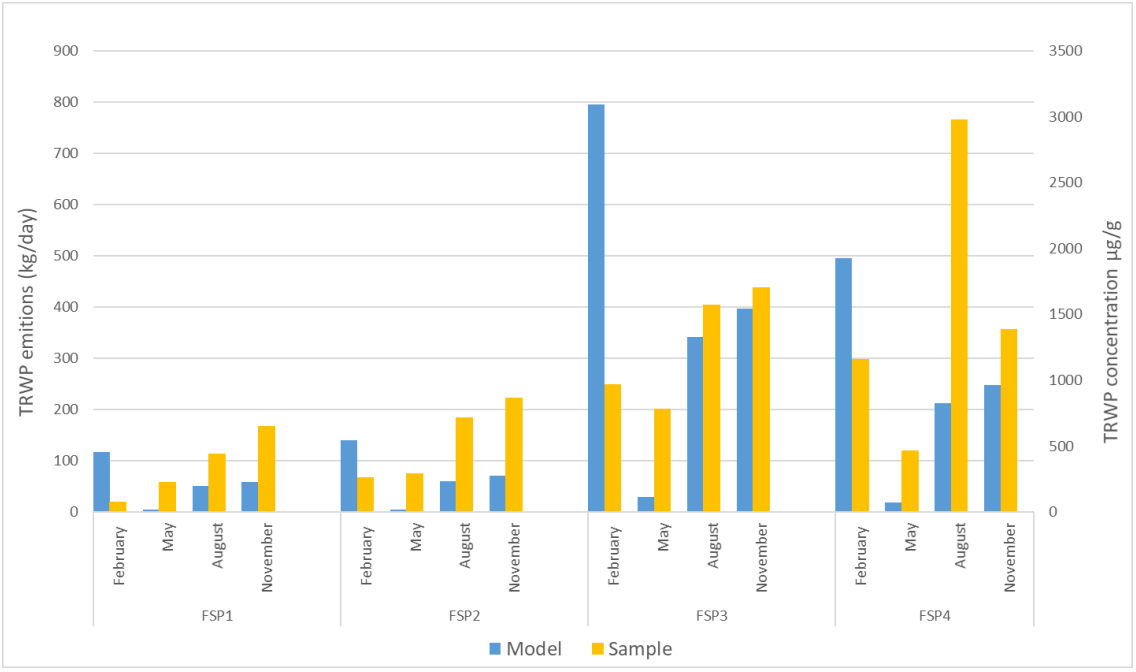

Figure 4.20. Comparison between the emissions model results and the TRWP concentrations in sediment samples for the river Foss.

4.5 Conclusion

This study is the first to report the temporal variation in TRWP concentrations in urban river sediments throughout the span of a year, highlighting the importance of long-term sampling events to accurately assess TRWP contamination levels and associated environmental risks.

Similarly, microplastics were detected at all sites and throughout all months sampled, with TRWPs emerging as the predominant microplastic type across all samples. These results suggest that the majority of microplastic abundance within the river Ouse and Foss is of secondary origin, resulting from the degradation of larger plastic debris, the wear of synthetic fibres by washing, and tyre abrasion on road surfaces.

The high presence of spheres and glitter (point source microplastics) in city centre sampling locations strongly indicates that CSOs represent a significant source of microplastics into the river. This emphasises the urgency of implementing more stringent effluent discharge regulations in the UK, alongside investment in wastewater treatment and storage capacity, microplastic capture technology, and measures to combat recurring untreated effluent discharges into rivers.

Furthermore, additional research is required to investigate the changes in the chemical properties of tyre wear particles and other microplastics as they age and degrade in the environment. This will aid in their accurate detection using spectrometry methodologies and enhance our understanding of their behaviour in natural settings.

In summary, the findings underscore that rivers serve not only as contributors of microplastics to the ocean but also as a sink for dense plastic particles, which hold the potential for significant environmental and ecological impacts due to their small size and their bioavailability to a wide range of aquatic organisms.

Chapter 5. General discussion and recommendations

5.1 Summary and key findings

In order to identify key knowledge gaps in TRWP research, an extensive literature review was conducted in Chapter 1. This comprehensive analysis encompassed various aspects of TRWPs, with a focus on the factors influencing their generation on roads, their chemical composition, and physical properties, including size, morphology and density. The review revealed significant variations in TRWP properties across existing literature, highlighting the need for further research to characterize particle size distributions and density across different environmental compartments, essential for an accurate understanding of their fate and transport in the environment.

Furthermore, the chapter explored different methods for the estimation of TRWP emissions as well as the latest modelling approaches concerning their fate in freshwater systems. It was apparent that most TRWP emission estimates had been conducted on a global and regional scale. Additionally, the only UK-specific estimate, dating back to 1996, relied on an approximation based on the weight of discarded tyres and an assumed weight loss of 10-20% during usage. This underscored the necessity for local-scale TRWP emission estimates, offering high spatial and temporal resolutions to account for the complexity of urban environments, characterized by spatial and temporal variations in activity, population density, and land cover types.

Finally, the review included different analytical techniques used for the detection and quantification of TRWPs, providing insights into the advantages and shortcomings of each method. It was found that thermo-analytical techniques, such as pyrolysis-gas chromatography–mass spectrometry, coupled with the use of polymeric markers, have been reported in the literature as a robust method for quantifying TRWPs in environmental samples. However, these techniques require further refinement, as several studies have recommended the inclusion of pre-treatment procedures before

Py-GC-MS analysis to minimize interference and matrix effects caused by organic and inorganic constituents within the samples. Furthermore, the need for real-world measurements of TRWPs in freshwater systems, particularly in river sediments, as these are considered sinks for TRWPs was also highlighted. The identified knowledge gaps formed the foundation of this thesis and were further investigated in the subsequent chapters.

In Chapter 2, the development of a modelling approach aimed to fulfil objective (1) by estimating TRWP emissions into various environmental compartments at high spatial and temporal resolution, focusing on a specific case study (York, UK). This approach involved several key steps. First, the city and its associated rivers, the Ouse and Foss, were delineated into zones and river sections, respectively. Subsequently, a comprehensive traffic model was developed to calculate the average annual daily traffic flow for various vehicle categories, including cars, buses, LGVs and HGVs, across the entire study area. Local parameters, such as daily rainfall intensity, were also collected. Finally, spatially and temporally resolved emissions were estimated per vehicle type, hydrological zone and river section over the course of a year.

The use of this approach allowed the successful identification of emission hotspots within the city of York and temporal emission trends for the period simulated. Notably, the findings revealed that cars were the primary contributors to TRWP emissions in York, This outcome was expected due to the considerably higher annual vehicle-kilometres travelled by cars compared to other vehicle categories. In addition, the areas generating the highest emissions were identified, which were characterized by substantial traffic volumes and a higher prevalence of vehicles associated with elevated tyre wear emission factors (i.e., HGVs in the outer ring road of the city). On the other hand, the days with the highest emissions correlated with increased rainfall intensity and a higher number of preceding dry days. This data underscored the presence of spatial variations between areas, which corresponded to varying emission rates in the rivers, further corroborating the spatial and temporal variability of TRWP emissions at the local scale.

Nevertheless, it is important to acknowledge that some conservative assumptions were made in this study, and further refinement will be necessary as more data becomes available. For example, the assumption that only 10% of stormwater is collected in combined sewers was based on the study by Domercq (2019), which established that the combined network mainly exists in old parts of York's city centre. A more precise assessment of the percentage of stormwater reaching WWTPs is essential to enhance the accuracy of TRWP emission estimates into surface waters.

In Chapter 3, the aim was to develop a methodology for the separation and analysis of TRWPs from sediment samples using Py-GC-MS, aligning with objective (2). This method focused on the implementation of pre-treatment procedures to mitigate potential matrix interferences. The sample preparation steps included the digestion of organic matter and the extraction of TRWPs by density separation. Firstly, a validation of the extraction method was conducted to assess the efficacy of the density separation solution (LST Fastfloat with a density of 1.95 g/cm^3) through recovery tests. The results indicated favourable mass recoveries for concentrations of 5 and 20 mg TP/g, consistently exceeding 110% across all size categories. However, higher concentrations of 80 mg TP/g exhibited slightly lower recovery rates, averaging 90%. This outcome aligned with findings from Klöckner *et al.* (2019), who observed a similar trend in recovery efficiency of tyre cryogrind from sediment samples. Consequently, the Fastfloat solution was considered a suitable choice for the density separation method and was consistently used throughout the study.

Secondly, an evaluation of sample presentation approaches was conducted to improve the repeatability and signal sensitivity of the Py-GC-MS analysis. Two pre-treated sample variations were compared: 1) samples intended for pyrolysis were directly obtained from the filter (referred to as GF filter), and 2) the filtered material was carefully scraped from the filter using a stainless steel spatula and transferred into a small glass vial (referred to as glass vial samples). The results revealed higher relative standard deviations (RSD) for the GF filter samples (21.81%) compared to the glass vial samples (2.52%). As a result, despite the stronger signal generated by the GF filter sample during pyrolysis, the glass vial sample presentation was selected

for the analysis of environmental samples due to its consistent repeatability and ease of handling.

Finally, the proposed method was tested by analysing sediment samples collected from regions characterize by significant traffic influence. The results demonstrated the detection of TRWPs by the pyrolysis marker in all sampled areas, and the laboratory replicates consistently showed satisfactory repeatability, with RSD consistently below 20%. The concentration of TRWPs exhibited variation across the three sampling locations, ranging from 0.10 to 16.2 mg/g, which was consisted with earlier assessments of highway runoff detention systems (e.g., Jarlskog *et al.*, 2022; Rødland *et al.,* 2022; Klöckner *et al*., 2019). The methodology proposed in this chapter revealed that pre-treatment of samples before Py-GC-MS analysis led to significant improvements, including enhanced response and resolution for the SBR marker compound by effectively mitigating interference from matrix components. Nevertheless, uncertainties regarding the challenge of mathematically correlating the experimental response provided by the analytical method with the amount of analyte in the sample were identified and discussed, alongside the need for further studies.

Chapter 4, aimed to fulfil objective (3) by employing the methodology introduced in Chapter 3 to determine the concentrations of TRWPs in sediment samples of the rivers in York and characterize them using microscopy analysis.

The analysis of sediment samples revealed a wide range of TRWP concentrations, spanning from 5.88 to 2,975.7 µg/g dw across all sampled locations and months. These results aligned with findings from previous studies (e.g., Unice *et al*., 2013; Zakaria *et al*., 2002; Kumata *et al*., 2000). The results of the two-way ANOVA analysis indicated significant differences in TRWP sediment concentrations among sampling locations and months. These variations were mainly attributed to differences in river size between the river Ouse and Foss, depositional characteristics, higher occurrences of braking and acceleration, and monthly fluctuations in precipitation levels.

In addition to TRWPs, the study identified and quantified “traditional” microplastics using microscopy analysis. It was found that microplastic abundance displayed

variability among sampling locations, with mean values ranging from 320 microplastics/kg in the river Ouse to 4,653.33 microplastics/kg in the river Foss, averaged across all months. These results fell within the range of microplastic levels previously reported in sediments across the UK (e.g., Bakir *et al*., 2023; Hurley *et al*., 2018). The Kruskal-Wallis analysis identified significant differences in microplastic abundance among the sampling locations, although the differences in microplastic abundance across sampling months were not statistically significant. The observed spatial variability was attributed to increased sediment and microplastic deposition due to reduced river flow rates in the river Foss compared to the river Ouse, as well as areas with a higher density of combined sewer overflows.

Study-wide, TRWPs dominated the microplastic composition in the sediment samples. The most prevalent microplastic colours were black, blue, and transparent, and the most common size category was 50-149 µm. The abundance of TRWP ranged from 33.3 to 4,000 particles/kg across all sampling locations and months, in line with findings by Ziajahromi *et al*. (2023). TRWP density in sediment samples aligned with the value previously reported in the literature of 1.8 g/cm^3 (Unice *et al*., 2019; Klöckner *et al*., 2019). Furthermore, their size distribution ranged from 50 to 570 µm, with a mode of 102 µm. These findings are consistent with other distribution data suggesting that smaller TRWPs (<150 µm) are more readily transported by stormwater runoff, while larger particles (>500 µm) tend to settle in drainage channels, gully pots or the sewerage system (Forrest and Vermaire, 2023; Ostini *et al*., 2022; Parker-Jurd *et al*., 2021; Ziajahromi *et al*., 2020).

This study underscores the significance of extended sampling periods for a comprehensive assessment of TRWP and microplastic contamination in the environment, as well as the value of employing multiple methods for the analysis of TRWPs (i.e., microscopy and Py-GC-MS) to cross-reference results and reduce uncertainties. Additionally, the final objective (4) was effectively addressed in this chapter by evaluating the accuracy of the emission model regarding TRWP concentrations in sediment samples. This was achieved by aligning sampling locations with their respective river sections. The findings revealed discrepancies

between the spatial distribution of modelled emissions and observed TRWP concentrations for the river Ouse, potentially influenced by traffic patterns, model limitations and sampling methods. Conversely, for the river Foss, TRWP concentrations closely mirrored modelled emissions, suggesting more accurate sediment sampling and delimitation of hydrological zones. This underscores the importance of further investigation and reliable data collection to refine estimations in urban areas.

5.2 Recommendations for the reduction of TRWP emissions

A comprehensive understanding of the primary factors contributing to tyre wear generation is pivotal for identifying potential hotspots and devising effective solutions. These influential factors include driving style, road curvature, road surface composition, vehicle specifications, tyre design, and weather conditions (Venghaus *et al.,* 2023; Verschoor *et al.,* 2016). The following sections delve into these factors and explore some of the solutions proposed by the scientific community.

5.2.1 Tyre material

The tyre industry places a strong emphasis on advancing tyre materials to optimize various tyre attributes. These attributes encompass a wide range of factors, including the need for sufficient friction and therefore safety of drivers, minimizing noise levels, reducing rolling resistance, and enhancing tyre durability to minimise wear. An increase in rubber durability can help reduce wear and rolling resistance. However, this can lead to decreased friction compromising driver safety and creating additional noise while in use (Fussell *et al*., 2022). Finding the balance between tyre wear, grip and rolling resistance is a complex challenge, as these three factors are interconnected and optimising one often leads to compromises that affect the other two (Gehrke *et al*., 2023).

One common approach to address this challenge involves replacing carbon black with silica as a filler material in tyres. Silica (specifically “highly dispersible” (HD) silica) offers higher abrasion resistance than carbon black without sacrificing the rolling resistance or grip of the tyre. However, the abrasion of the tyre decreases with the addition of silica resulting in the emission of finer micro particles (Gehrke *et al*., 2023).

The development of “Green Silica” offers an environmentally friendly alternative in this process. Additionally, materials like nanoprene and nanosilica have shown potential for further abrasion reduction. However, their adoption comes with trade-offs, including the costs associated with nanotechnology, unreliable production methods and potential unobserved environmental impacts (Gehrke *et al*., 2023).

The pursuit of “Green tyres” has been driven by these requirements, aiming to meet the aforementioned criteria through cure optimisation, process efficiency and by moving away from the use of toxic, carcinogenic materials in the manufacturing process (Bijina *et al.*, 2023).

5.2.2 Tyre pressure

The air pressure in tyres significantly influences tyre wear rates by affecting the contact area between the tyre and the road as well as the contour of this contact area. Lower inflation pressure results in a larger contact area and places a greater load on the tyre’s shoulders, leading to increased wear on these areas. On the other hand, over-inflated tyres cause excessive wear at the centre of the tyre (Gehrke *et al.*, 2023).

To address this issue, tyre monitoring systems can be used to notify the driver when the pressure drops below a specific threshold, allowing drivers to take corrective action (Johannesson and Lithner, 2022). It is advisable to check tyre pressure every 14 days or before a long travel. This practice not only contributes to a reduction in tyre wear emissions but also extends the overall lifespan of the tyres (Stojanovic *et al.*, 2022).

5.2.3 Weight of vehicles

The weight of vehicles has a direct impact on the emission of TRWPs, with heavier vehicles contributing to higher emissions. The introduction of electric cars, while promising in reducing PM10 pollution through the elimination of exhaust emissions and reduced brake wear, poses a challenge due to the added weight of their battery packs. It was estimated that electric cars are approximately 20% heavier than Internal Combustion Engine (ICE) cars, therefore, this weight difference is expected to contribute to a 20% increase in TRWP emissions when assuming a linear correlation

between vehicle weight and tyre wear emission (Kole *et al*., 2017). To fully maximize the environmental benefits of electric cars, it is necessary to explore options for reducing their mass. This can be achieved through design modifications, size reduction, the use of denser Li-ion batteries, or downsizing the battery packs. These strategies are essential to ensure that electric vehicles continue to represent a sustainable choice for the future (Fussell *et al.,* 2022; Kole *et al*., 2017).

5.2.4 Driving behaviour

There is a direct correlation between driving speed and the production of TRWPs. Higher speeds result in increased generation of TRWPs, which are also characterized by smaller particle size compared to those produced at slower speeds. This effect is further exacerbated when driving at high speeds on curved road sections (Gehrke *et al.,* 2023; Fussell *et al.,* 2022).

Similarly, heavy acceleration and breaking during driving result in elevated TRWP emissions (Gehrke *et al.,* 2023; Fussell *et al.,* 2022). Traffic calming measures such as traffic lights, speed bumps and give way signs contribute to additional acceleration and breaking, further increasing TWRP generation (Fussell *et al*., 2022).

One approach to control driving behaviour is the introduction of speed and acceleration limiters designed to reduce the forces transmitted across the contact points between the tyre and the road. However, it is important to note that deceleration limitation is not considered due to safety concerns. Promoting the adoption of acceleration limiters can be challenging because vehicle acceleration is a key selling point in the automotive industry (Gehrke *et al.*, 2023). Conversely, the use of self-driving cars offers a potential solution to reduce tyre wear by programing vehicles to exhibit gradual acceleration, slow turning, and predictive traffic behaviour, reducing the need for intensive braking (Stojanovic *et al.*, 2022). Furthermore, the introduction of roundabouts instead of traffic lights is suggested to not only minimize tyre wear emissions but also reduce brake wear and fuel consumption (Stojanovic *et al.*, 2022).

5.2.5 Road Surface

The condition of the road surface plays a significant role in determining the extent of tyre emissions into the environment. Tyre wear particles accumulate within the surface pockets of the road, and are subsequently removed from these pockets during rainfall events, making their way into the aquatic environment. To mitigate these emissions, a proactive approach involves more frequent road cleaning, complemented by effective washing and filtration techniques to prevent the TRWPs from entering the water system (Stojanovic *et al.*, 2022). Furthermore, road surface composition should also be taken into consideration. For example, the use of open asphalt concrete not only reduces emissions but also promotes the retention of coarser tyre wear particles (Kole *et al*., 2017).

5.2.6 Reduction in road traffic

A more direct approach to lower TRWP emissions can be achieved through the reduction of road traffic. There is a clear cause-and-effect relationship between the number of kilometres travelled and the amount of TRWPs generated. Reducing road traffic is feasible for most commuters by opting to travel by foot or by bike. Additionally, the use of public transportation also contributes to a reduction in TRWPs generated. In the case of industrial sectors, the transportation of goods can be shifted to non-road methods, such as water or rail transport (Fussell *et al.*, 2022).

Control over traffic usage can be enforced through policy instruments. By making car usage less convenient and alternative transportation methods more appealing, policy initiatives can encourage a change in transport choices (Fussell *et al.,* 2022).

Another method to influence transportation preference is to restrict access to certain areas. This can be achieved by establishing environmental zones, implementing car bans on specific roads during designated times, reducing the availability of parking spaces or imposing financial measures such as taxes and charges (Fussell *et al*., 2022).

5.2.7 WWTPs and sewage system

Management of sewage systems and wastewater treatment plants (WWTPs) plays a critical role in controlling the contamination of surface waters. To address this issue, two primary strategies are considered. The first involves enhancing WWTP treatment efficiency to reduce the load of tyre wear particles (TRWPs) entering surface waters. Surprisingly, there is a lack of systematic studies analysing the processes responsible for removing TRWPs within WWTPs.

The second approach aims to limit the use of separated sewer systems, which directly discharge road runoff into surface waters without any treatment. However, implementing this strategy would require a significant increase in WWTP capacity, making it a costly solution. A more feasible alternative involves the development of efficient TRWP trapping devices. These devices can be deployed either in road gutters before runoff enters the sewer system or just before its discharge into surface waters. One effective method is to collect runoff and temporarily store it in a sedimentation basin, which can significantly reduce the TRWP load, especially for larger particles (Kole *et al*., 2017).

5.3 Recommendations for future research

The research presented in this PhD thesis has provided new insights into TRWP emissions and their presence in urban aquatic systems with a high level of spatial and temporal detail. Nevertheless, this study has identified areas of research that need to be addressed in the future, including:

1. Enhanced emission factors (EF): Future studies should focus on establishing more precise and up-to-date emission factors, accounting for various vehicle characteristics (e.g., weight), road types (urban, rural, highways), road surfaces (asphalt or concrete), and ambient temperatures. These efforts should aim for a global perspective, enabling meaningful cross-study comparisons and international applicability.

2. Runoff emissions: Further research is essential to validate the proportion of TRWPs that are transported into aquatic environments *via* runoff versus those retained within road surfaces and subsequently distributed to soils, with the distinction made between highways, urban and rural areas. Additionally, studies should assess the removal efficiency of TRWP in WWTPs, as existing research has predominantly focused on other types of microplastics.

3. Combined Sewer Overflows (CSOs): Addressing the lack of available information on CSOs is crucial. Research should delve into the causes of CSOs and methods for their prevention. Transparency and data sharing by wastewater operators are pivotal to achieving accurate exposure assessments in the environment.

4. Py-GC-MS analysis: Further studies employing Py-GC-MS and polymeric markers should include in their investigations the analysis of the SBR/BR and NR concentration in a wide range of commercially available tyres relevant to their study area. This comprehensive approach is especially relevant due to variations in tyre formulations and production practices across different regions, such as the use of studded tyres.

5. Mineral encrustations in TRWP: Research should be directed towards characterizing the fractions within TRWPs originating from tyres and road surfaces across diverse environmental compartments. Factors such as road type, vehicle speed, and driving patterns should be considered. This approach will significantly contribute to our understanding of TRWP composition and enhance the accuracy of quantification.

6. Aging and degradation studies: Investigating the changes in the chemical properties of tyre wear particles as they age and degrade in the environment, specifically in terms of their polymer content, is crucial. This research will aid in their accurate detection using Py-GC-MS and spectrometry methodologies, providing insights into their behaviour in natural settings.

7. Modelling work: Future research should consider coupling the emissions model with a sediment dynamics model. This integration would significantly enhance the accuracy and reliability of forecasting outcomes.

8. Raising Awareness: The need to increase awareness of TRWP contamination among stakeholders, consumers, industry, and the scientific community cannot be overstated. Such awareness will pave the way for collaborative solutions aimed at reducing tyre wear emissions and their environmental impact.

Appendices

APPENDIX 1

A1. Supplementary information Chapter 3

A1.1 Pyrolysis-GC-MS: Method optimization for sample analysis

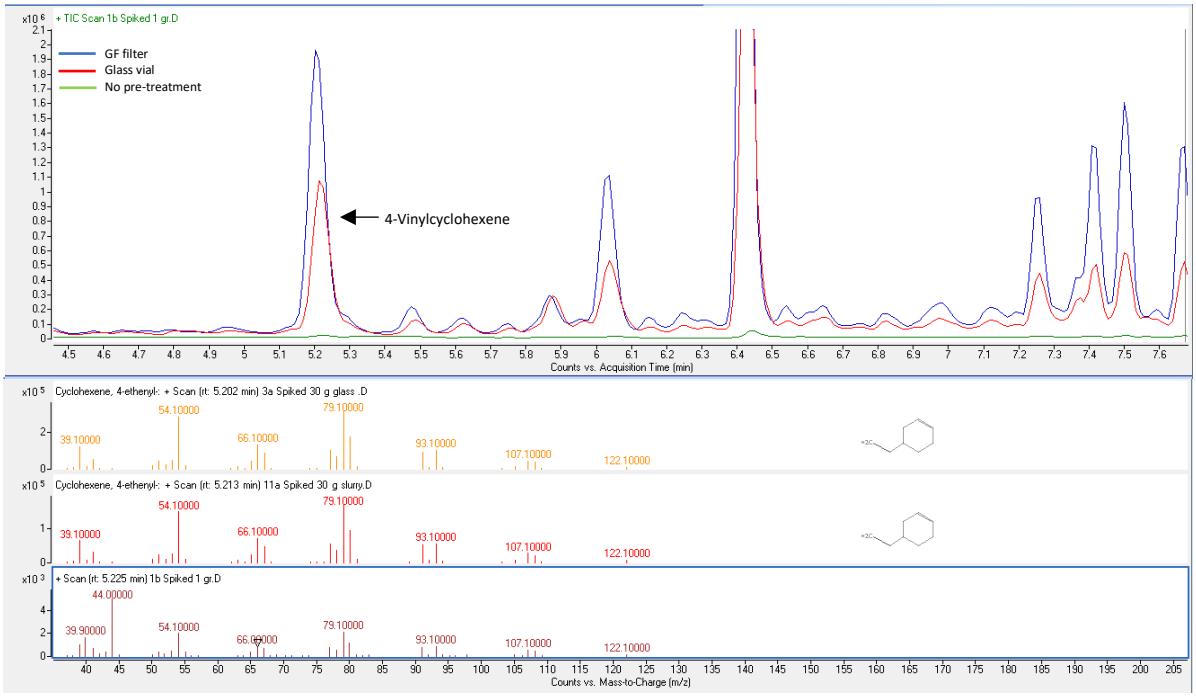

Figure A1.1. Pyrogram and mass spectra for the two pre-treated sample variations (GF filter and glass vial) and the untreated sample.

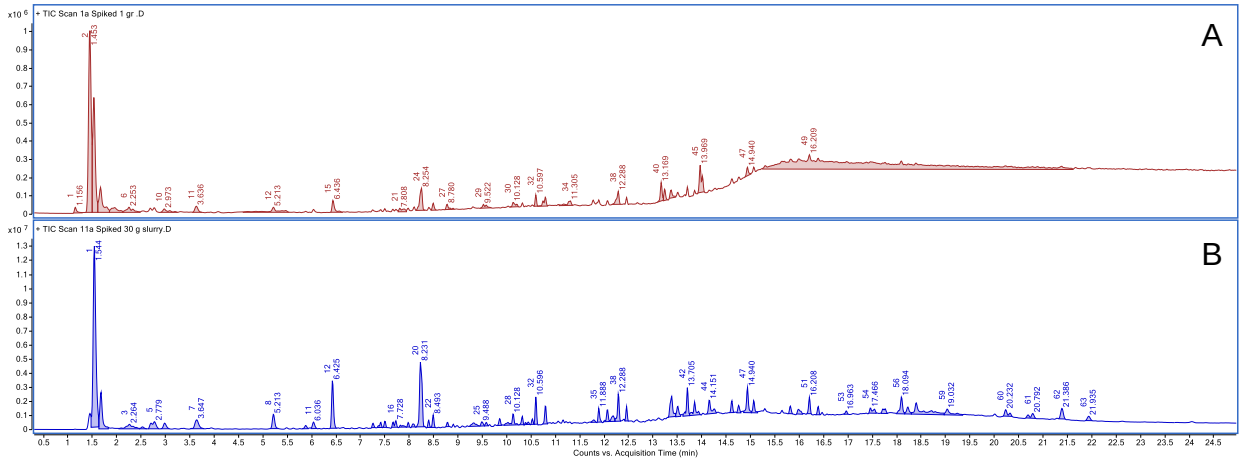

Figure A1.2. Total ion chromatograms (TIC) for the untreated sample (A) and the pre-treated glass vial sample (B). A detailed examination of these chromatograms reveals an improvement in response and peak resolution within the pre-treated sample.

APPENDIX 2

A2. Supplementary information Chapter 4

A2.1 Pyrolysis-GC-MS analysis

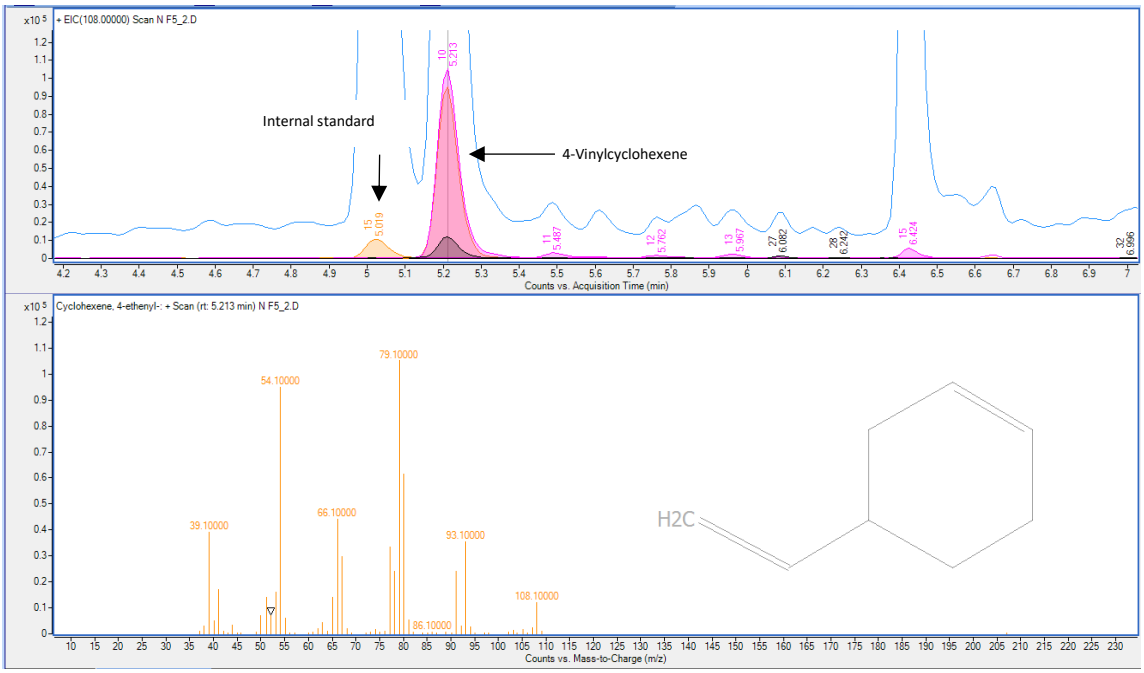

Figure A2.1. Pyrogram and mass spectra obtained from the sediment sample Foss SP5 collected in the month of November.

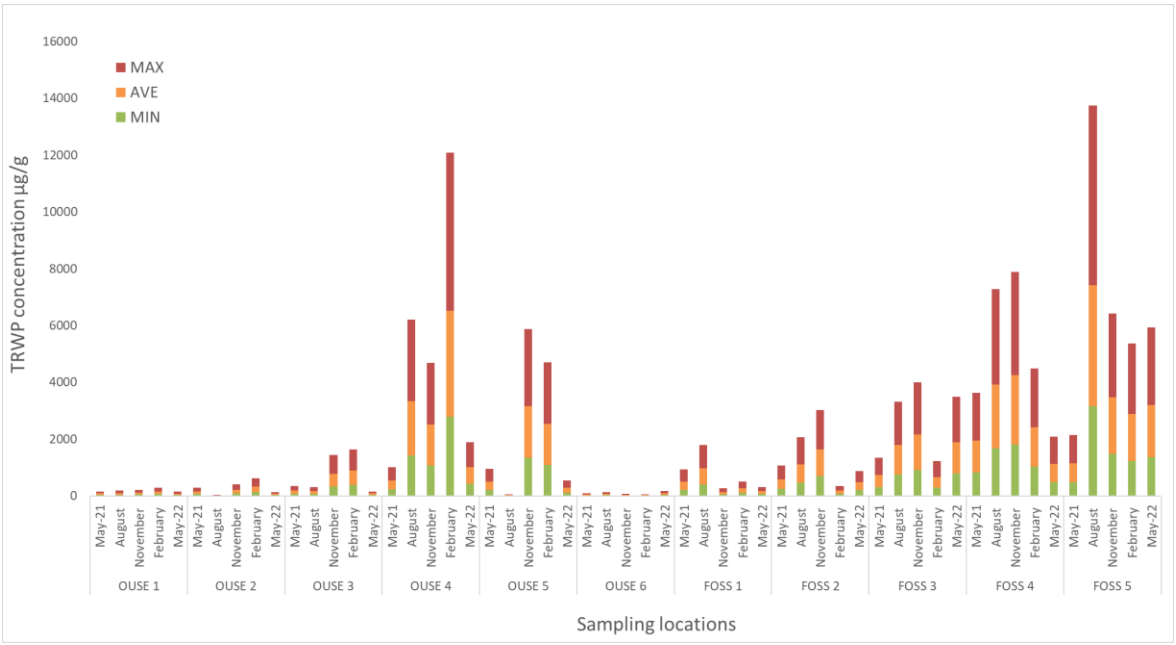

Figure A2.2. Sediment concentrations of tyre and road wear particles with a minimum (6%), an average (30%), and a maximum (53%) level of encrustment.

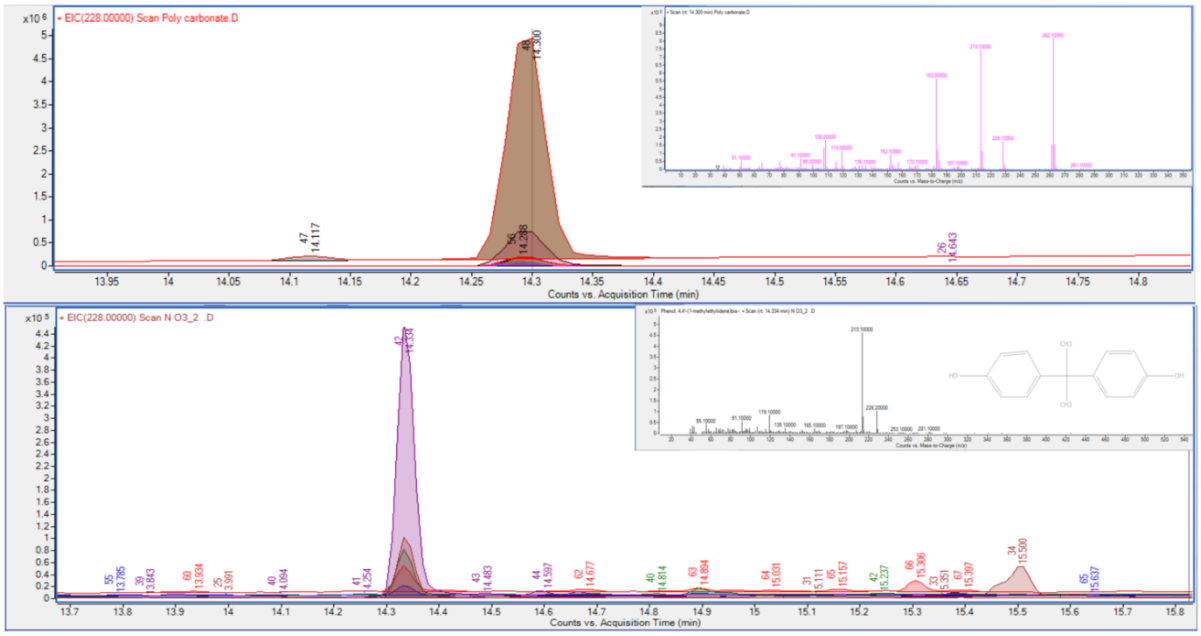

Figure A2.3. Pyrogram and mass spectra of the pyrolysis marker (Bisphenol A) for the polycarbonate polymer standard (top), alongside the corresponding marker detected in the sediment sample Ouse SP3 collected in November (bottom).

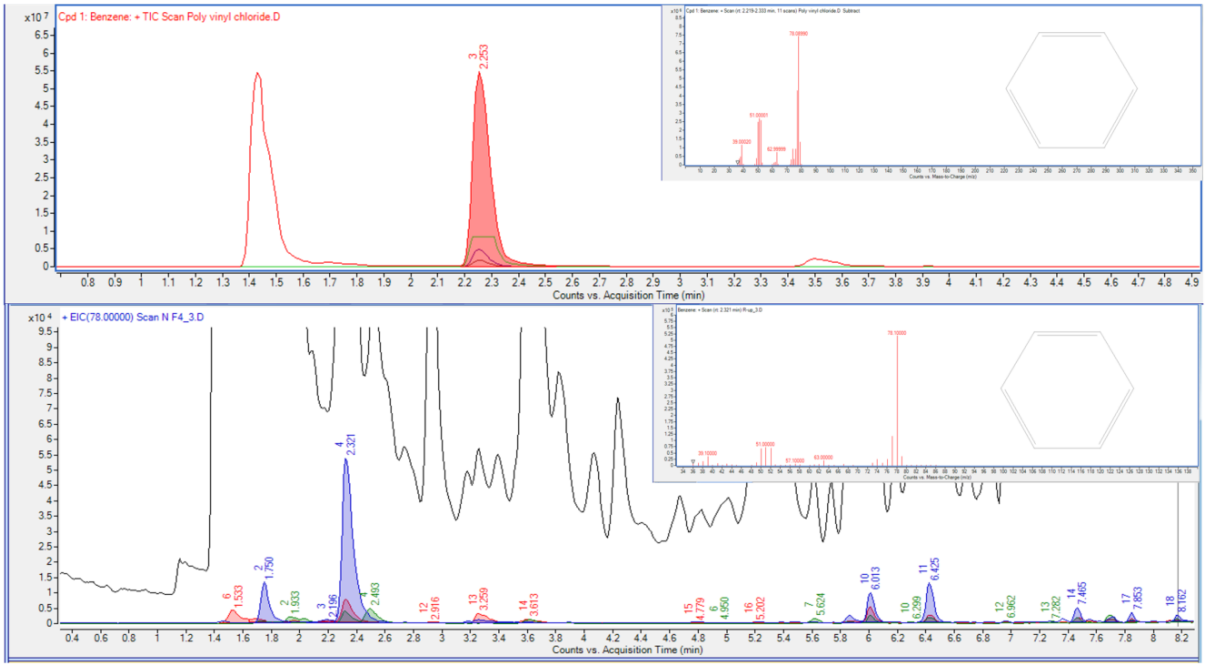

Figure A2.4. Pyrogram and mass spectra of the pyrolysis marker (Benzene) for the Polyvinyl chloride polymer standard (top), alongside the corresponding marker detected in the sediment sample Foss SP4 collected in November (bottom).

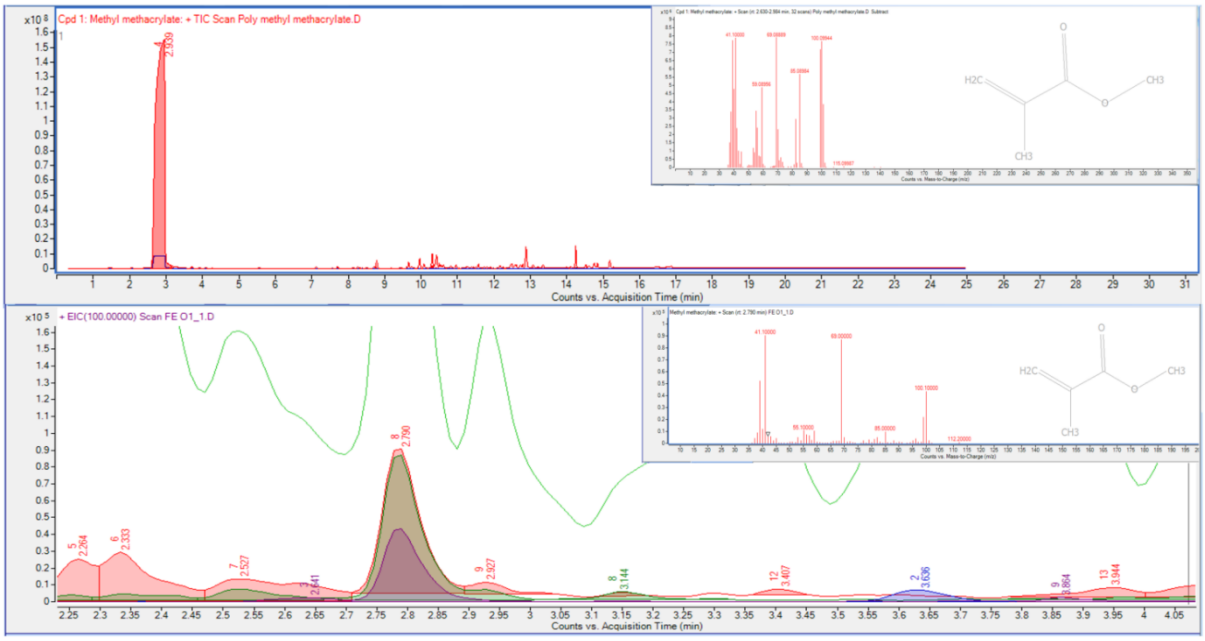

Figure A2.5. Pyrogram and mass spectra of the pyrolysis marker (Methyl methacrylate) for the Poly-(methyl methacrylate) polymer standard (top), alongside the corresponding marker detected in the sediment sample Ouse SP1 collected in February (bottom).

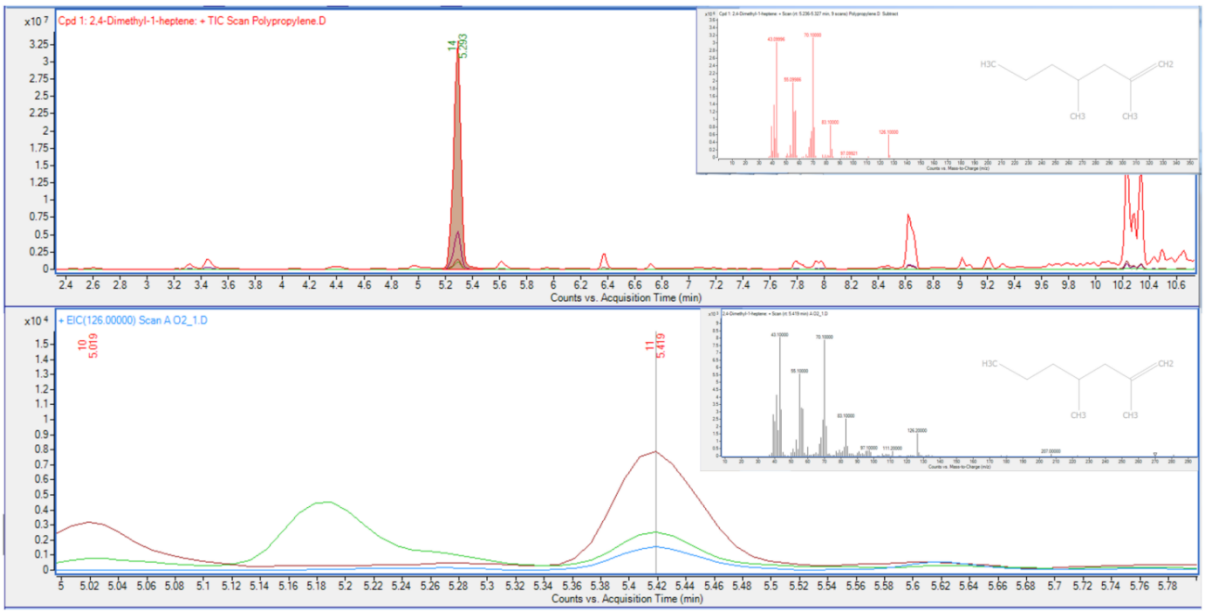

Figure A2.6. Pyrogram and mass spectra of the pyrolysis marker (2,4-Dimethyl-1-heptene) for the Polypropylene polymer standard (top), alongside the corresponding marker detected in the sediment sample Ouse SP2 collected in August (bottom).

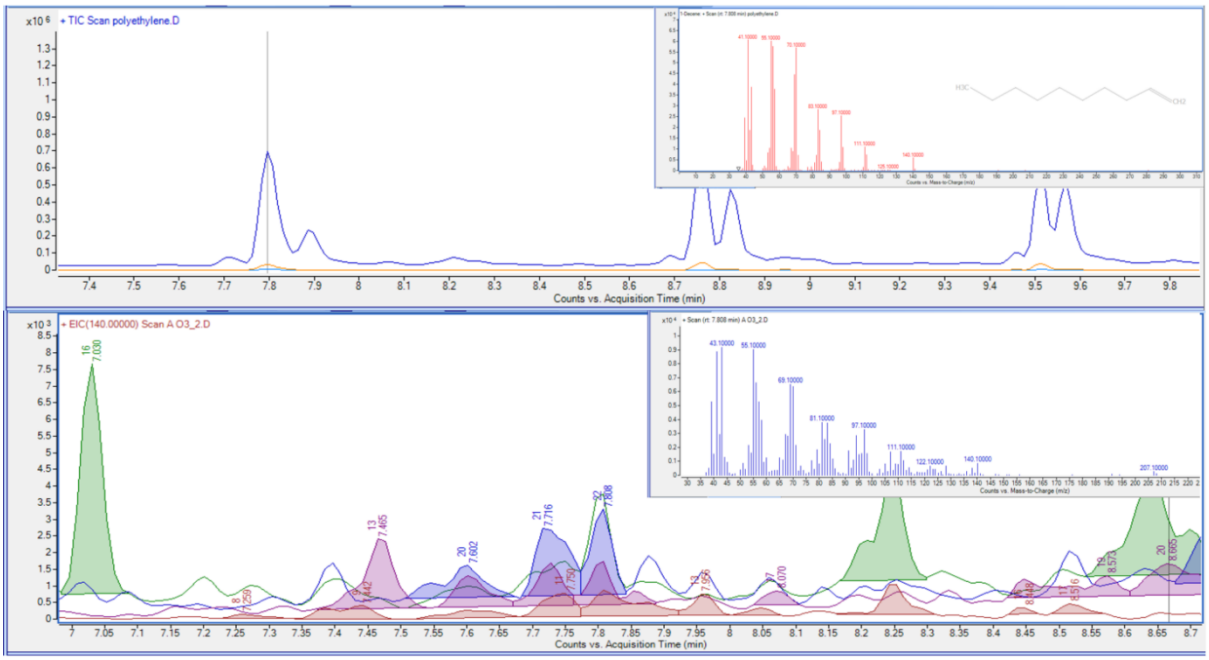

Figure A2.7. Pyrogram and mass spectra of the pyrolysis marker (1-Decene) for the Polyethylene polymer standard (top), alongside the corresponding marker detected in the sediment sample Ouse SP3 collected in August (bottom).

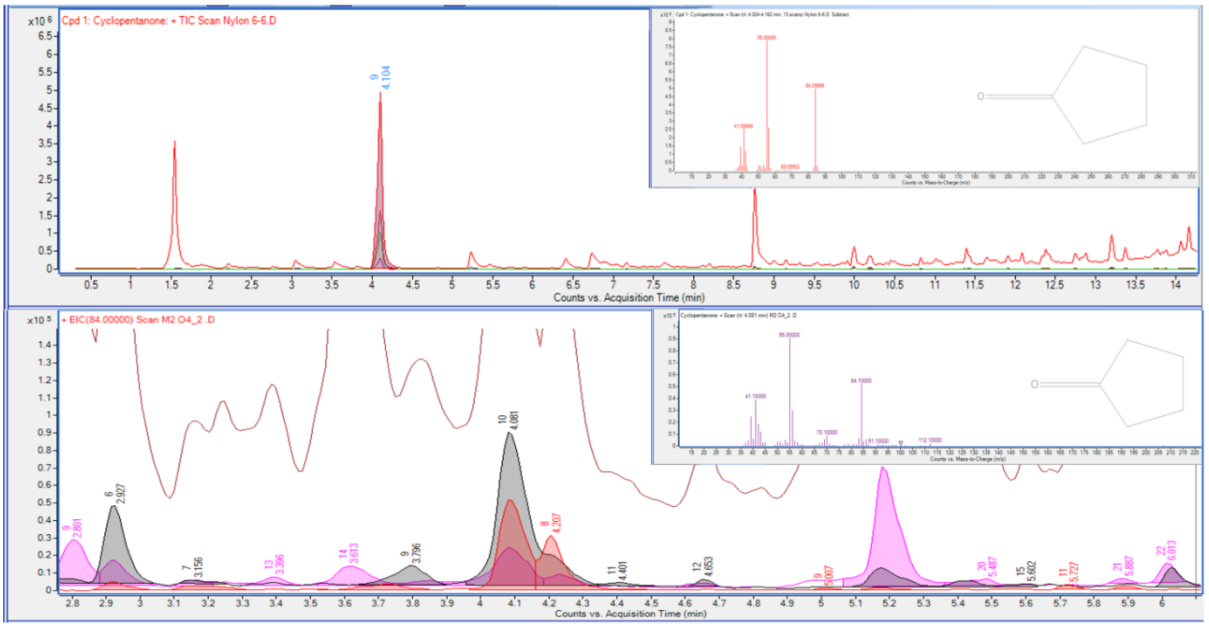

Figure A2.8. Pyrogram and mass spectra of the pyrolysis marker (Cyclopentanone) for the Nylon (N66) polymer standard (top), alongside the corresponding marker detected in the sediment sample Ouse SP4 collected in May 2022 (bottom).

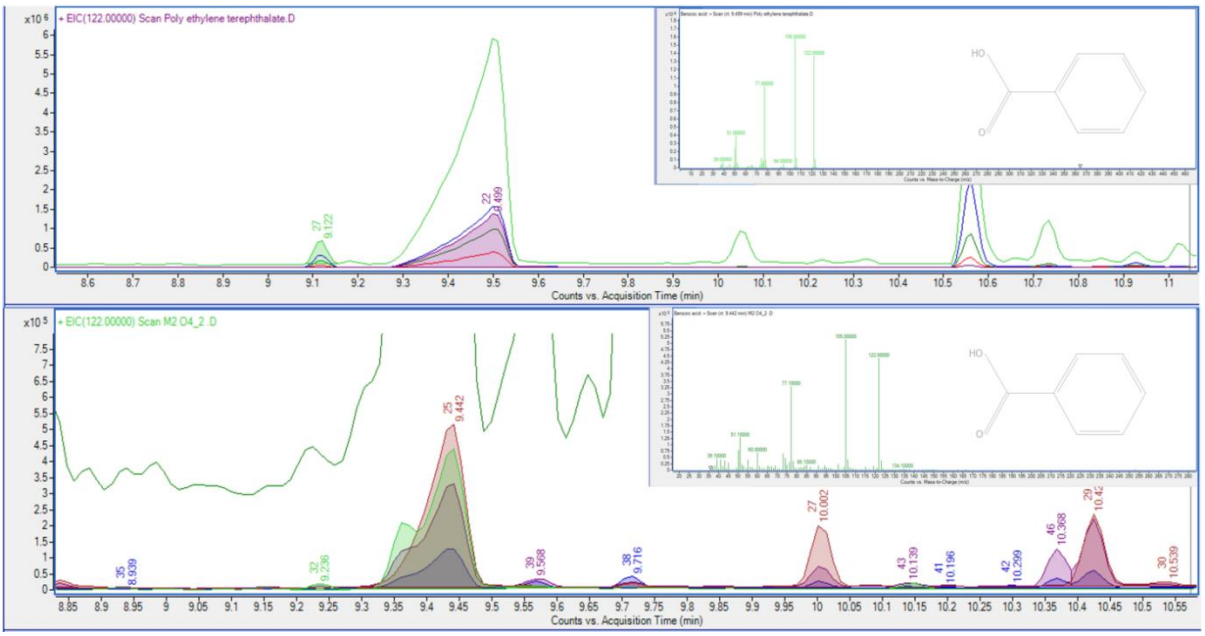

Figure A2.9. Pyrogram and mass spectra of the pyrolysis marker (Benzoic acid) for the Polyethylene terephthalate polymer standard (top), alongside the corresponding marker detected in the sediment sample Ouse SP4 collected in May 2022 (bottom).

A2.2 Grain size and organic material analysis

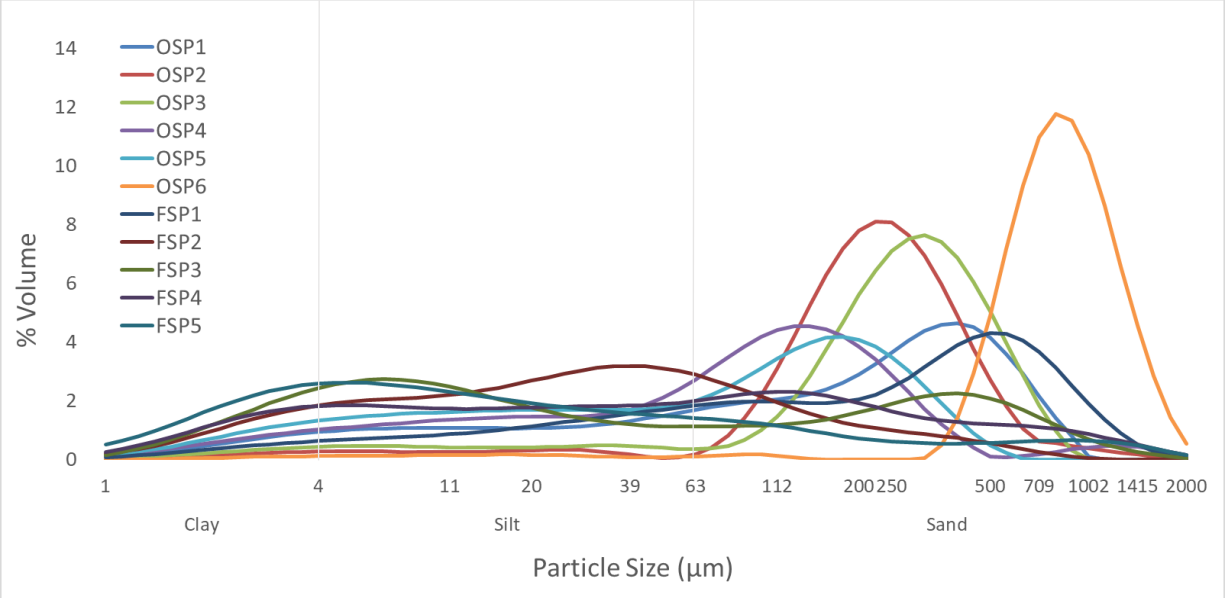

Figure A2.10. Particle size distribution of the sediment samples collected in May 2021, classified according to the Udden-Wentworth grain-size scale (Wentworth, 1922).

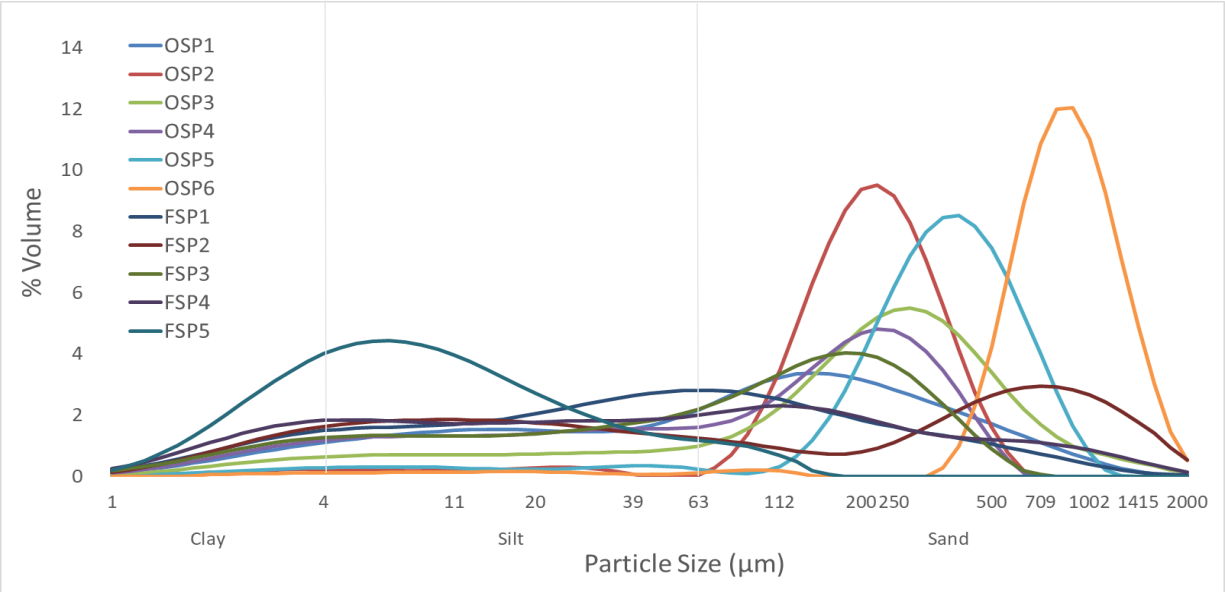

Figure A2.11. Particle size distribution of the sediment samples collected in August 2021, classified according to the Udden-Wentworth grain-size scale (Wentworth, 1922).

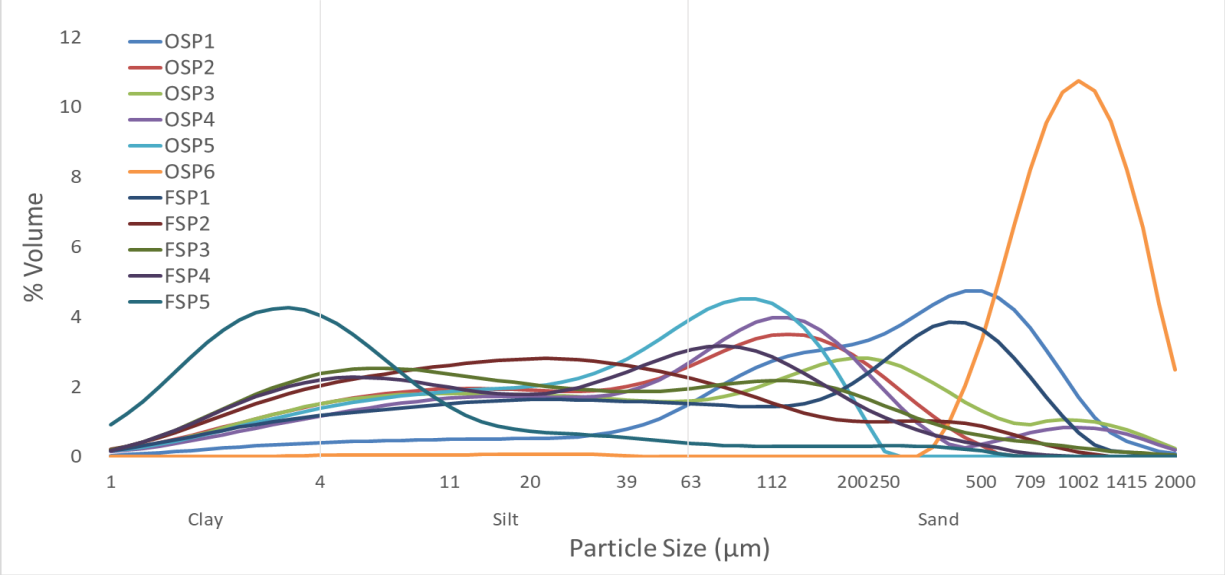

Figure A2.12. Particle size distribution of the sediment samples collected in November 2021, classified according to the Udden-Wentworth grain-size scale (Wentworth, 1922).

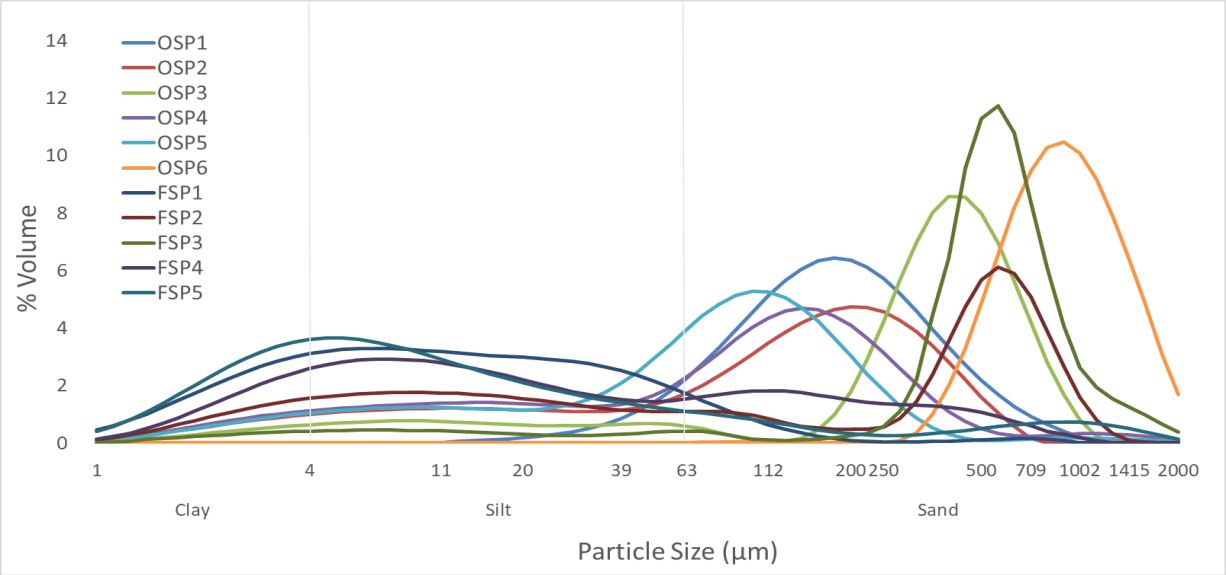

Figure A2.13. Particle size distribution of the sediment samples collected in February 2022, classified according to the Udden-Wentworth grain-size scale (Wentworth, 1922).

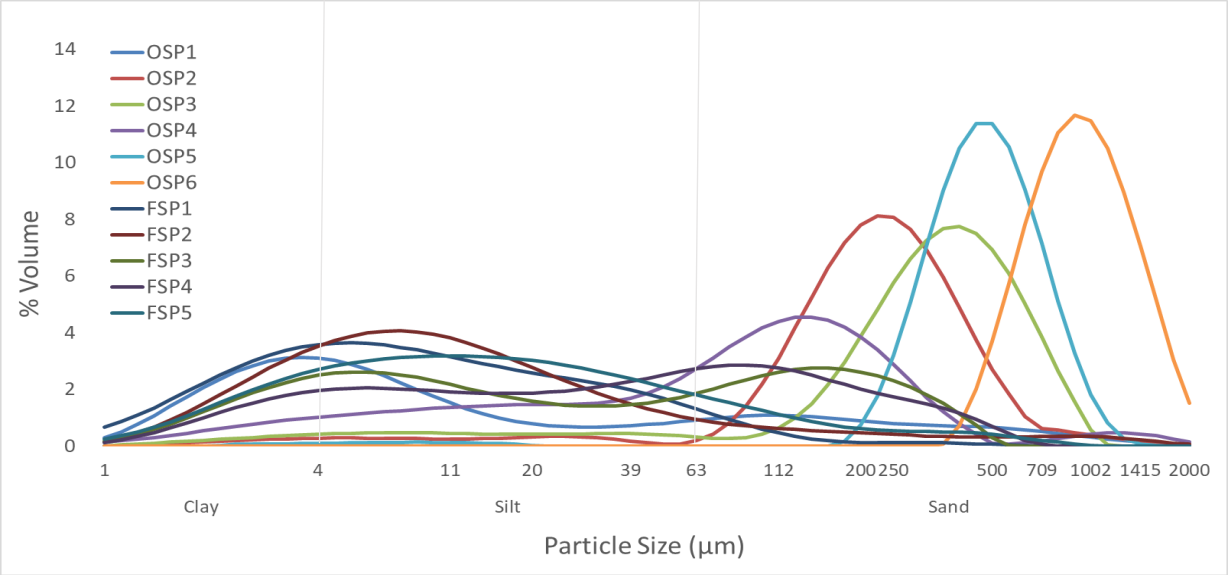

Figure A2.14. Particle size distribution of the sediment samples collected in May 2022, classified according to the Udden-Wentworth grain-size scale (Wentworth, 1922).

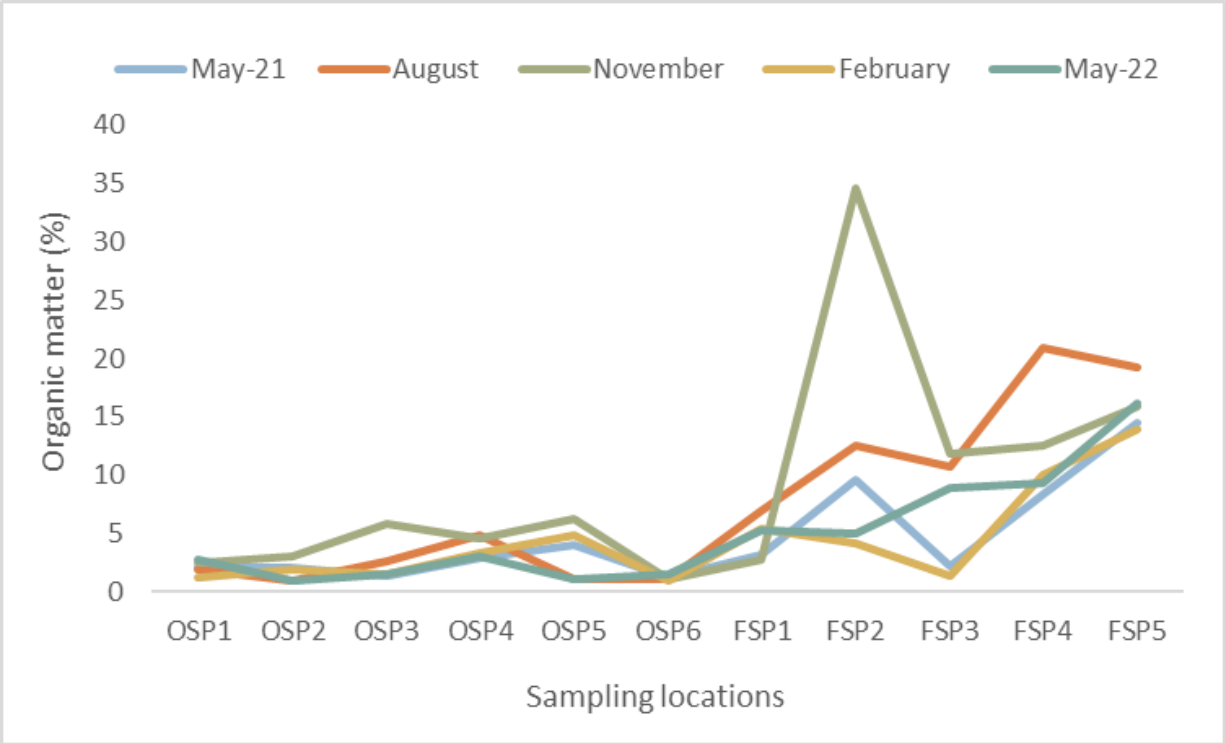

Figure A2.15. Organic matter percentage in sediment samples from various sampling locations and months.

A2.3 Chi-squared test

Standardized cell residuals for the chi-square independence tests between sampling locations and microplastic characteristics (morphology, colour and size). Residuals with absolute values greater than 1.96 indicate a significant deviation from independence. Positive residuals, highlighted in green, signify an observation of more microplastics in that category than expected under independence of variables. Conversely, negative residuals showing the opposite trend are highlighted in red (Ross *et al.,* 2023).

Table A2.1. Chi Squared Residuals between sampling locations and microplastic types.

Chi Squared Residuals Morphology							
	Fibre	Film	Fragment	Glitter	Paint	Sphere	TWP
Foss1	1.393	2.159	3.12	-1.315	-0.832	-3.292	-2.242
Foss2	1.381	0.308	3.45	-1.416	-0.896	-3.065	-1.808
Foss3	0.265	6.531	3.141	-0.156	-1.315	-4.586	-2.829
Foss4	-4.537	-3.254	2.011	-1.105	-1.253	3.332	1.507
Foss5	3.166	-2.613	-2.986	1.088	4.663	-0.711	0.887
Ouse1	2.475	3.329	1.973	-0.915	-0.579	-1.681	-3.486
Ouse2	3.582	0.939	1.361	0.42	-0.513	-1.298	-3.209
Ouse3	1.007	1.457	1.562	-0.98	-0.62	-2.663	-0.89
Ouse4	-4.363	-2.19	-3.539	3.03	-0.476	10.788	0.614
Ouse5	-0.513	1.107	-3.965	-1.446	-1.238	-5.127	5.966
Ouse6	5.519	-1.142	0.717	0.129	-0.593	-2.546	-2.447

Table A2.2. Chi Squared Residuals between sampling locations and microplastic colours.

Chi Squared Residuals Colour													
	Black	Blue	Brown	Green	Grey	Holographic	Orange	Pink	Purple	Red	Transparent	White	Yellow
Foss1	-1.802	1.316	-1.299	-0.975	-0.208	-1.195	-1.542	-0.55	-0.294	-0.894	2.876	-0.444	-0.465
Foss2	-1.706	0.176	-0.683	-1.05	-0.224	-1.286	0.147	-0.592	-0.317	0.749	4.063	-3.377	-0.501
Foss3	-2.805	1.811	0.868	-0.894	-0.329	0.228	0.842	1.429	-0.465	0.842	2.415	-2.007	3.345
Foss4	0.888	-2.53	-1.402	1.187	-0.452	-1.052	1.429	-1.195	-0.639	-0.363	0.384	0.375	-0.019
Foss5	0.632	-2.631	1.506	1.611	1.548	0.376	2.684	0.243	0.748	-0.34	0.385	-1.626	-1.097
Ouse1	-2.625	4.499	-0.904	-0.679	-0.145	-0.831	-0.141	-0.383	-0.205	2.654	0.973	-1.089	-0.324
Ouse2	-1.979	1.514	0.446	-0.602	-0.128	0.619	-0.952	2.605	-0.182	1.149	1.654	-1.138	-0.287
Ouse3	0.022	1.956	-0.968	-0.727	-0.155	-0.891	-1.15	-0.41	-0.219	-0.28	0.928	-2.133	-0.347
Ouse4	0.136	-2.825	-0.695	-0.431	-0.418	3.012	-2.132	-0.202	1.1	-1.487	-3.843	10.784	0.135
Ouse5	5.767	2.409	2.207	-1.452	-0.309	-1.215	-2.295	-0.819	-0.438	0.319	-4.746	-4.651	-0.692
Ouse6	-1.636	5.472	-0.926	2.181	-0.148	0.323	-0.19	2.158	-0.21	0.72	-0.584	-2.004	-0.331

Table A2.3. Chi Squared Residuals between sampling locations and microplastic sizes.

	Chi Squared Residuals Size (µm)				
	50 - 149	150 - 249	250 - 499	500 - 1000	>1000
Foss1	-0.887	0.982	0.508	0.733	-1.364
Foss2	-1.082	-0.748	3.479	0.243	-1.468
Foss3	-3.721	3.26	0.111	1.691	6.655
Foss4	2.502	-0.962	-2.77	-1.488	-0.259
Foss5	-1.895	1.252	3.083	-0.156	-1.973
Ouse1	-0.614	0.27	0.633	0.352	0.105
Ouse2	-0.429	0.547	0.613	-0.197	-0.842
Ouse3	0.044	-0.504	0.197	0.496	-0.033
Ouse4	3.893	-2.56	-2.338	-2.956	-0.917
Ouse5	-0.025	0.314	-2.034	2.14	0.434
Ouse6	-0.219	-2.344	1.504	3.079	-0.972

A2.4 Characterization of TRWP

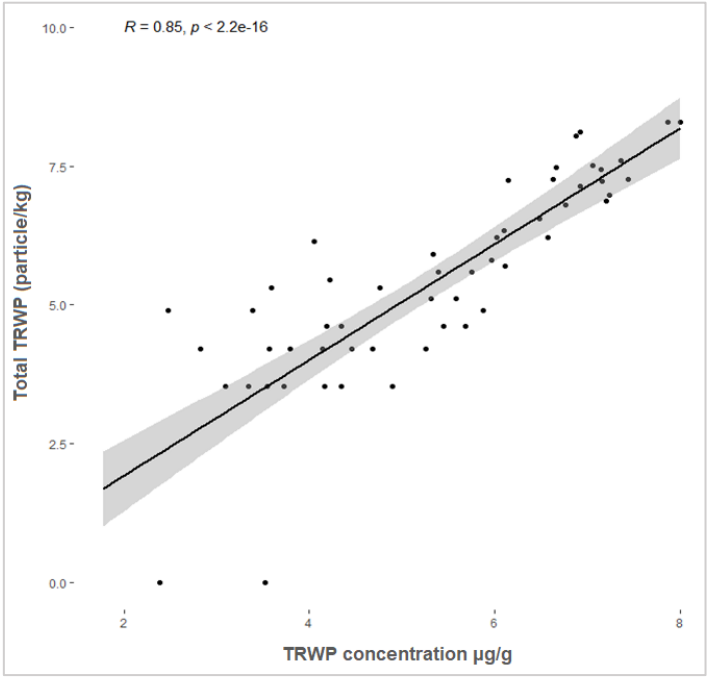

Figure A2.16. Pearson correlation between TRWP mass concentrations and TRWP abundance in the sediment samples. The variable TRWP abundance underwent a log(x+1) transformation, while the variable TRWP concentration was log_e transformed to achieve a normal distribution.

A2.5 Combined sewer overflows (CSOs) in the city of York

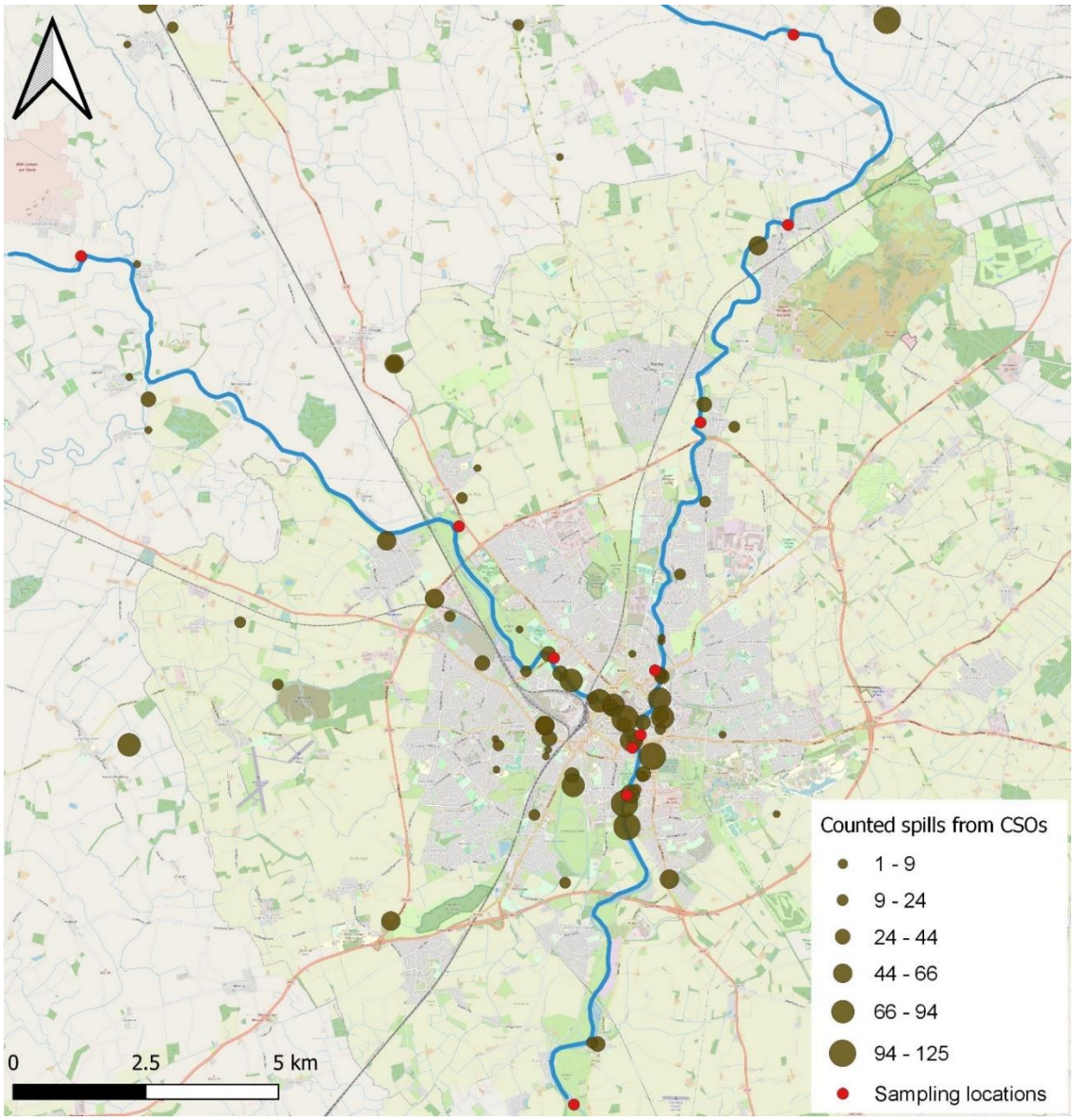

Figure A2.17. CSO events per year in the city of York (averaged over the years 2021 and 2022). Source: https://theriverstrust.org/sewage-map.

Abbreviations

24MoBT = 2-(4-Morpholinyl) Benzothiazole

AADF = Average Annual Daily traffic Flow

ANOVA = Analysis of Variance

ATR = Attenuated Total Reflectance

BD-UP/DO = Butterthwaite Ditch – Upstream/Downstream

BR = Butadiene Rubber (Poly-Butadiene)

BT = Benzothiazole

CAS = Chemical Abstracts Service

CSO = Combined Sewer Overflow

DDT = Dichloro-Diphenyl-Trichloroethane

DEM = Digital Elevation Map

DO = Dissolved Oxygen

DT = Daily Traffic

EC = Electric Conductivity

EF = Emission Factors

ENP = Engineered Nanoparticles

FTIR = Fourier-Transform Infrared Spectrometry

GF = Glass Fibre

GIS = Geographical Information System

HGV = Heavy Goods Vehicle

HOBT = 2- Hydroxybenzothiazole

HZ = Hydrological Zones

ICP-MS = Inductively Coupled Plasma–Mass Spectrometry

ISO = International Organization for Standardization

LC50 = 50% Lethal Concentration

LGV = Light Goods Vehicle

LOD = Limits of Detection

LOI = Loss on Ignition

LOQ = Limit of Quantification

Abbreviations

MP = Microplastics

NCBA = N-Cyclohexyl-2-Benzothiazolamine

NIST = National Institute of Standards and Technology

NR = Natural Rubber

PA = Polyamide

PAHs = Polycyclic Aromatic Hydrocarbons

PBB-UP/DO = Pigeon Bridge Brook-Upstream/Downstream

PBD = Polybutadiene

PC = Polycarbonate

PCB = Polychlorinated Biphenyl

PE = Polyethylene

PET = Polyethylene Terephthalate

POP = Persistent Organic Pollutant

PM = Particulate Matter

PMMA = Poly-(methyl methacrylate)

PP = Polypropylene

PS = Polystyrene or Styrofoam

PVC = Polyvinyl chloride

Py-GC-MS = Pyrolysis-Gas Chromatography-Mass Spectrometry

RD-UP/DO = Rockley Dike-Upstream/Downstream

RS = River Section

RSD = Relative Standard Deviation

S/N = Signal-to-Noise ratio

SBR/BR = Styrene-Butadiene Rubber

SBS = Styrene Butadiene Styrene

SEM/EDX = Scanning Electron Microscopy/Energy Dispersive X-ray spectroscopy

SPA = Single Particle Analysis

SPM = Suspended Particle Matter

SPT = Sodium Polytungstate

SWO = Storm Water Outlet

T = Temperature

Abbreviations

TED−GC−MS = Thermal Extraction Desorption Gas Chromatography−Mass Spectrometry

TIC = Total Ion Chromatogram

ToF-SIMS = Time-of-Flight Secondary Ion Mass Spectrometry

TP = Tyre Particle

TRWP = Tyre and Road Wear Particles

TSS = Total Suspended Solids

TWP = Tyre Wear Particles

UK = United Kingdom

VCH = 4-vinylcyclohexene

WWTP = Wastewater Treatment Plant

References

Aatmeeyata, Kaul, D. S. and Sharma, M. (2009). Traffic generated non-exhaust particulate emissions from concrete pavement: A mass and particle size study for two-wheelers and small cars. *Atmospheric Environment*, 43 (35), Elsevier Ltd., pp.5691–5697. [Online]. Available at: doi:10.1016/j.atmosenv.2009.07.032.

Alves, F. L., Pinheiro, L. M., Bueno, C., Agostini, V. O., Perez, L., Fernandes, E. H. L. and Weschenfelder, J. (2023). The use of microplastics as a reliable chronological marker of the Anthropocene onset in Southeastern South America. Science of the Total Environment 857, pp.1–12.

Amato, F., Alastuey, A., de la Rosa, J., Verdona, A.M., Pandolfi, and Lozano García, M. (2014b). Trends of road dust emissions contributions on ambient PM levels at rural, urban and industrial sites in Southern Spain. Atmos. Chem. Phys. 14, 3533–3544.

AQEG, 2019. Non-exhaust Emissions from Road Traffic. Air Quality Expert Group, Department for Environment Food and Rural Affairs, London. https://uk-air.defra.gov.uk/assets/documents/reports/cat09/1907101151_20190709_Non_Exhaust_Emissions_typeset_Final.pdf. (Accessed 03 April 2024) [Last accessed).

Arias, A. H., Alfonso, M. B., Girones, L., Piccolo, M. C. and Marcovecchio, J. E. (2022). Synthetic microfibers and tyre wear particles pollution in aquatic systems: Relevance and mitigation strategies. Environmental Pollution, 295 [Online]. Available at: doi:10.1016/j.envpol.2021.118607.

Atmospheric Environment, 244 (June 2020), Elsevier Ltd., p.118018. [Online]. Available at: doi:10.1016/j.atmosenv.2020.118018.

Baensch-Baltruschat, B., Kocher, B., Kochleus, C., Stock, F. and Reifferscheid, G. (2021). Tyre and road wear particles - A calculation of generation, transport and release to water and soil with special regard to German roads. *Science of the Total Environment*, 752, The Authors., p.141939.

Baensch-Baltruschat, B., Kocher, B., Stock, F. and Reifferscheid, G. (2020). Tyre and road wear particles (TRWP) - A review of generation, properties, emissions, human health risk, ecotoxicity, and fate in the environment. *Science of the Total Environment*, 733, The Authors., p.137823.

References

Bakir, A., Doran, D., Silburn, B., Russell, J., Archer-Rand, S., Barry, J., Maes, T., Limpenny, C., Mason, C., Barber, J. and Nicolaus, E. (2023). A spatial and temporal assessment of microplastics in seafloor sediments: A case study for the UK. Front. Mar. Sci. 9:1093815. doi: 10.3389/fmars.2022.1093815.

Ballent, A., Purser, A., de Jesus Mendes, P., Pando, S. and Thomsen, L. (2012). Physical transport properties of marine microplastic pollution. Biogeosciences Discussions, 9 (12), pp.18755–18798.

Baumann, W. and Ismeier, M. (1998). Rubber: Facts and Figures on Environmental Protection; Springer: Berlin, Germany.

Bergmann, M. and Klages, M. (2012). Increase of litter at the Arctic deep-sea observatory HAUSGARTEN. *Marine Pollution Bulletin*, 64, 2734-2741.

Besley, A., Vijver, M.G., Behrens, P., Bosker, T. (2017). A standardized method for sampling and extraction methods for quantifying microplastics in beach sand. *Mar. Pollut. Bull. 114, 77–83.*

Besseling, E., Quik, J. T. K., Sun, M. and Koelmans, A. A. (2017). Fate of nano- and microplastic in freshwater systems: A modeling study. *Environmental Pollution*, 220, Elsevier Ltd., pp.540–548.

Bian, B. and Zhu, W. (2009). Particle size distribution and pollutants in roaddeposited sediments in different areas of Zhenjiang, China. *Environmental Geochemistry and Health*, 31 (4), pp.511–520.

Bijina, V., Jandas, P. J., Joseph, S., Gopu, J., Abhitha, K. and John, H. (2023). Recent trends in industrial and academic developments of green tyre technology. Polymer Bulletin, 80 (8), pp.8215–8244. [Online]. Available at: doi:10.1007/s00289-022-04445-2.

Blair, R. M., Waldron, S., Phoenix, V. and Gauchotte-Lindsay, C. (2017). Micro- and Nanoplastic Pollution of Freshwater and Wastewater Treatment Systems. Springer Science Reviews, 5 (1), *Springer International Publishing*., pp.19–30.

Blair, R. M., Waldron, S., Phoenix, V. R. and Gauchotte-Lindsay, C. (2019). Microscopy and elemental analysis characterisation of microplastics in sediment of a freshwater

urban river in Scotland, UK. *Environmental Science and Pollution Research*, Environmental Science and Pollution Research.

Bondelind, M., Sokolova, E., Nguyen, A., Karlsson, D., Karlsson, A. and Björklund, K. (2020). Hydrodynamic modelling of traffic-related microplastics discharged with stormwater into the Göta River in Sweden. *Environmental Science and Pollution Research*, 27 (19), Environmental Science and Pollution Research., pp.24218–24230. [Online]. Available at: doi:10.1007/s11356-020-08637-z.

Bouzid, N., Anquetil, C., Dris, R., Gasperi, J., Tassin, B. and Derenne, S. (2022). Quantification of Microplastics by Pyrolysis Coupled with Gas Chromatography and Mass Spectrometry in Sediments : Challenges and Implications. Microplastics, 1, 229–239.

Brombach, H., Weiss, G., and Fuchs, S. (2005). A new database on urban runoff pollution: comparison of separate and combined sewer systems. Water Sci. Technol. 51, 119–128.

Browne, M., Crump, P., Niven, S.J., Teuten, E., Tonkin, A., Galloway, T. and Thompson, R. (2011). Accumulation of microplastic on shorelines worldwide: sources and sinks. *Environ. Sci. Technol.* 45:9175–9179.

Bukowiecki, N., Lienemann, P., Hill, M., Furger, M., Richard, A., and Amato, F. (2010). PM10 emission factors for non-exhaust particles generated by road traffic in an urban street canyon and along a freeway in Switzerland. *Atmos. Environ*. 44, 2330–2340.

Burns, E. (2018). *Assessing exposure and risks of pharmaceuticals in an urban river system*. PhD thesis (February). Available at: http://etheses.whiterose.ac.uk/20448/.

Burns, E., and Boxall, A. (2018). Microplastics in the Aquatic Environment: Evidence for of against adverse impacts and major knowledge gaps. *Environmental Toxicology and Chemistry*- Vol. 37, 11 pp. 2776-2796.

Bye, N. and Johnsen, P. (2019). Assessment of tyre wear emission in a road tunnel, using benzothiazoles as tracer in tunnel wash water. Master thesis. Norwegian University of Life Sciences. 111p.

References

Camatini, M., Crosta, G., Dolukhanyan, T., Sung, C., Giuliani, G., Corbetta, G., Cencetti, S. and Regazzoni, C. (2001). Micro-characterization and identification of tyre debris in heterogeneous laboratory and environmental specimens. *Mater. Char.* 46, 271-283.

Carbery, M., O'Connor, W. and Palanisami, T. (2018). Trophic transfer of microplastics and mixed contaminants in the marine food web and implications for human health. *Environment International,* 115 (April), pp.400–409.

Chaisanguansuk, P., Phantuwongraj, S., Jirapinyakul, A. and Assawincharoenkij, T. (2023). Preliminary study on microplastic abundance in mangrove sediment cores at Mae Klong River, upper Gulf of Thailand. Front. Environ. Sci. 11:1134988.

Charbouillot, T., Cettour, J., Schaal, P., Beynier, I., Boulat, J., Grandchamp, A., and Biesse, F. (2023). Methodology for the direct measurement of tire emission factors. *Science of The Total Environment, Volume 863,160853, ISSN 0048-9697.*

Charters, F., Cochrane, T. and O'Sullivan, A. (2015). Particle size distribution variance in untreated urban runoff and its implication on treatment selection. *Water Res.* 85, 337-345.

Chico-ortiz, N., Mahu, E., Crane, R., Gordon, C. and Marchant, R. (2020). Microplastics in Ghanaian coastal lagoon sediments : Their occurrence and spatial distribution. *Regional Studies in Marine Science 40 101509.*

Cho, M., Song, Y., Rhu, C. and Go, B. (2023). Pyrolysis Process of Mixed Microplastics Using TG-FTIR and TED-GC-MS. Polymers, 15, 241. https://doi.org/10.3390/.

Choudhary, S., Neelavanan, K. and Saalim, S. (2022). Microplastics in the surface sediments of Krossfjord-Kongsfjord system, Svalbard, Arctic. Marine Pollution Bulletin 176.

Chubarenko, I., Bagaev, A., Zobkov, M. and Esiukova, E. (2016). On some physical and dynamical properties of microplastic particles in marine environment. *Marine Pollution Bulletin*, 108 (1–2), Elsevier Ltd., pp.105–112.

Clark, J. R., Cole, M., Lindeque, P. K., Fileman, E., Blackford, J., Lewis, C., Lenton, T. M. and Galloway, T. S. (2016). Marine microplastic debris: a targeted plan for understanding and quantifying interactions with marine life. *Frontiers in Ecology and the Environment*, 14 (6), pp.317–324.

Compa, M., Ventero, A., Iglesias, M. and Deudero, S. (2018). Ingestion of microplastics and natural fibres in Sardina pilchardus (Walbaum, 1792) and Engraulis encrasicolus (Linnaeus, 1758) along the Spanish Mediterranean coast. *Marine Pollution Bulletin*, 128 (October 2017), Elsevier., pp.89–96.

Councell, T. B., Duckenfield, K. U., Landa, E. R. and Callender, E. (2004). Tire-wear particles as a source of zinc to the environment. *Environmental Science and Technology*, 38 (15), pp.4206–4214.

Cózar, A., Echevarría, F., González-Gordillo, J., Irigoien, X., Úbeda, B., Hernández, S., Palma, A., Navarro, S., García-de-Lomas, J., Ruíz, A., Fernández, M. and Duarte, C. (2014). Plastic debris in the open ocean. *Proceedings of the National Academy of Sciences,* 111, 10239–10244.

Critchell, K. and Lambrechts, J. (2016). Modelling accumulation of marine plastics in the coastal zone; what are the dominant physical processes? *Estuarine, Coastal and Shelf Science*, 171, Elsevier Ltd., pp.111–122.

Dahl, A., Gharibi, A., Swietlicki, E., Gudmundsson, A., Bohgard, M., Ljungman, A., Blomqvist, G. and Gustafsson, M. (2006). Traffic-generated emissions of ultrafine particles from pavement-tyre interface. *Atmos. Environ*. 40, 1314-1323.

Dale, A. L., Casman, E. A., Lowry, G. V., Lead, J. R., Viparelli, E. and Baalousha, M. (2015). Modeling nanomaterial environmental fate in aquatic systems. *Environmental Science and Technology*, 49 (5), pp.2587–2593.

Dale, A. L., Lowry, G. V. and Casman, E. A. (2015). Stream Dynamics and Chemical Transformations Control the Environmental Fate of Silver and Zinc Oxide Nanoparticles in a Watershed-Scale Model. *Environmental Science and Technology*, 49 (12), pp.7285–7293.

Darabi, M., Majeed, H., Diehl, A., Norton, J. and Zhang, Y. (2021). A Review of Microplastics in Aquatic Sediments : Occurrence, Fate, Transport, and Ecological Impact. Current Pollution Reports pp.40–53.

De Klein, J. J. M., Quik, J. T. K., Bäuerlein, P. S. and Koelmans, A. A. (2016). Towards validation of the NanoDUFLOW nanoparticle fate model for the river Dommel, the

Netherlands. *Environmental Science: Nano*, 3 (2), Royal Society of Chemistry., pp.434–441.

De Witte, B., Devriese, L., Bekaert, K., Hoffman, S., Vandermeersch, G., Cooreman, K. and Robbens, K. (2014). Quality assessment of the blue mussel (Mytilus edulis): Comparison between commercial and wild types. Marine Pollution Bulletin, 85(1):146-155.

DELTARES, TNO, (2016). Emissieschattingen Diffuse bronnen Emissieregistratie. Bandenslijtage wegverkeer. Rijkswaterstaat – WVL.

Devereux, R., Ayati, B., Kebede, E., Jayaratne, R. and Newport, D. (2023b). Impact of the Covid-19 pandemic on microplastic abundance along the River Thames. Marine Pollution Bulletin 189, 114763.

Devereux, R., Ayati, B., Kebede, E., Jayaratne, R. and Newport, D. (2023a). “The great source” microplastic abundance and characteristics along the river Thames. Marine Pollution Bulletin 191, 114965.

Do, T., Park, Y., Lim, B., Kim, S., Chae, M. and Chun, H. (2023). Effect of the first-flush phenomenon on the quantification of microplastics in rainwater. Marine Pollution Bulletin 187, 114559.

Domercq, P. (2019). Modelling the exposure of engineered nanoparticles in urban aquatic systems Prado Domercq. PhD thesis. University of York, UK. (March).

Domercq, P., Praetorius, A. and Boxall, A. B. A. (2018). Emission and fate modelling framework for engineered nanoparticles in urban aquatic systems at high spatial and temporal resolution. *Environmental Science: Nano*, 5 (2), Royal Society of Chemistry., pp.533–543.

Dominik, T. (2015). Assessing the Biological effects of exposure to microplastics in the Three-Spined Stickleback (*Gasterosteus aculeatus) (Linnaeus 1758*). PhD thesis. University of York. UK. 255 p.

Dris, R., Imhof, H., Sanchez, W., Gasperi, J., Galgani, F., Tassin, B. and Laforsch, C. (2015). Beyond the ocean: Contamination of freshwater ecosystems with (micro) plastic particles. *Environmental Chemistry*, 12 (5), pp.539–550.

References

Duis, K. and Coors, A. (2016). Microplastics in the aquatic and terrestrial environment: sources (with a specific focus on personal care products), fate and effects. *Environmental Sciences Europe*, 28 (1), Springer Berlin Heidelberg., pp.1–25.

Eerkes-Medrano, D., Thompson, R. C. and Aldridge, D. C. (2015). Microplastics in freshwater systems: A review of the emerging threats, identification of knowledge gaps and prioritisation of research needs. *Water Research*, 75 (October), pp.63–82.

Egodawatta, P., Thomas, E., and Goonetilleke, A. (2007). Mathematical interpretation of pollutant wash-off from urban road surfaces using simulated rainfall. *Water Res*. 41 (13), 3025–3031.

Eibes, P. M. and Gabel, F. (2022). Floating microplastic debris in a rural river in Germany : Distribution, types and potential sources and sinks. Science of the Total Environment, 816, Elsevier B.V., p.151641. [Online]. Available at: doi:10.1016/j.scitotenv.2021.151641.

Eisentraut, P., Dümichen, E., Ruhl, A. S., Jekel, M., Albrecht, M., Gehde, M. and Braun, U. (2018). Two Birds with One Stone - Fast and Simultaneous Analysis of Microplastics: Microparticles Derived from Thermoplastics and Tire Wear. *Environmental Science and Technology Letters*, 5 (10), pp.608–613.

Elisabeth, S. R., Christian, O., Reid, M., Heier, L. S., Skogsberg, E., Snilsberg, B., Gryteselv, D. and Meland, S. (2022). Characterization of tire and road wear microplastic particle contamination in a road tunnel: From surface to release. *Journal of Hazardous* Materials 435 129032. Available at: doi:10.1016/j.jhazmat.2022.129032.

Emberson-Marl, H., Coppock, R., Cole, M., Godley, B., Mimpriss, N., Nelms, S. and Lindeque, K. (2023) Microplastics in the Arctic: a transect through the Barents Sea. Front. Mar. Sci. 10:1241829. doi: 10.3389/fmars.2023.1241829.

Enders, K., Lenz, R., Stedmon, C. A. and Nielsen, T. G. (2015). Abundance, size and polymer composition of marine microplastics ≥10 μm in the Atlantic Ocean and their modelled vertical distribution. *Marine Pollution Bulletin*, 100 (1), Elsevier Ltd., pp.70–81.

Environment Agency News. Tyres in the environment: Executive summary. Sci. Total Environ. 1999, 234, 243–245.

Eunomia. 2016. Plastics in the marine environment. Bristol UK. [cited 2020 Janury 10]. Available from: http://www.eunomia.co.uk/reports-tools/plastics-in-the-marineenvironment/.

Everaert, G., Van Cauwenberghe, L., De Rijcke, M., Koelmans, A. A., Mees, J., Vandegehuchte, M. and Janssen, C. R. (2018). Risk assessment of microplastics in the ocean: Modelling approach and first conclusions. *Environmental Pollution*, 242, Elsevier Ltd., pp.1930–1938.

Faure, F., Saini, C., Potter, G., Galgani, F., de Alencastro, L. F. and Hagmann, P. (2015). An evaluation of surface micro- and mesoplastic pollution in pelagic ecosystems of the Western Mediterranean Sea. *Environmental Science and Pollution Research*, 22 (16), pp.12190–12197.

Federico, L., Masseroni, A., Rizzi, C. and Villa, S. (2023). Silent Contamination: The State of the Art , Knowledge Gaps and a preliminary risk assessment of tire particles in urban parks. Toxics, 11, 445. https://doi.org/10.3390/toxics11050445.

Ferreira, G. V. B., Justino, A. K. S., Eduardo, L. N., Schmidt, N., Martins, J. R., Ménard, F., Fauvelle, V., Mincarone, M. M. and Lucena-frédou, F. (2023). Influencing factors for microplastic intake in abundant deep-sea lantern fi shes (Myctophidae). Science of the Total Environment 867.

Forrest, S. A. and Vermaire, J. C. (2023). Spatial distribution of microplastics in a large watershed: a case study of the Ottawa River watershed. pp.1–15.

Forrest, S. A., Mcmahon, D., Adams, W. A. and Vermaire, J. C. (2017). Change in microplastic concentration during various temporal events downstream of a combined sewage overflow and in an urban stormwater creek. Front. Water 4:958130. doi: 10.3389/frwa.2022.958130.

Furuseth, I. S. and Rødland, E. S. (2020). Reducing the Release of Microplastic from Tire Wear: Nordic Efforts. REPORT - Nordic Council of Ministers, p.42. [Online]. Available at: http://urn.kb.se/resolve?urn=urn:nbn:se:norden:org:diva-7159.

Fussell, J. C., Franklin, M., Green, D. C., Gustafsson, M., Harrison, R. M., Hicks, W., Kelly, F. J., Kishta, F., Miller, M. R., Mudway, I. S., et al. (2022). A Review of Road Traffic-Derived Non-Exhaust Particles: Emissions, Physicochemical Characteristics,

Health Risks, and Mitigation Measures. Environmental Science and Technology, 56 (11), pp.6813–6835. [Online]. Available at: doi:10.1021/acs.est.2c01072.

Gajšt, T., Bizjak, T., Palatinus, A., Liubartseva, S. and Kržan, A. (2016). Sea surface microplastics in Slovenian part of the Northern Adriatic. *Marine Pollution Bulletin,* 113 (1-2), pp.392–399.

Garg, B. D., Cadle, S. H., Mulawa, P. A., Groblicki, P. J., Laroo, C. and Parr, G. A. (2000). Brake wear particulate matter emissions. *Environmental Science and Technology*, 34 (21), pp.4463–4469.

Gebbe, M., Hartung, and Berthold (1997). Quantification of tire wear from motor vehicles in Berlin. Technical University Berlin. Institute for Road and Rail Transport. ISS - vehicle technology. On demand of Senate Department for Urban Development, Environmental Protection and Technology, Berlin.

Gehrke, I., Dresen, B. and Blömer, J. (2020). Modelling the distribution of tyre wear particles in Germany. *29th Aachen Colloquium Sustainable Mobility 2020*, p.10.

Gehrke, I., Schläfle, S., Bertling, R., Öz, M. and Gregory, K. (2023). Review: Mitigation measures to reduce tire and road wear particles. Science of The Total Environment, 904 (August), p.166537. [Online]. Available at: doi:10.1016/j.scitotenv.2023.166537.

Goßmann, I., Halbach, M., Scholz-Böttcher, B.M., 2021. Car and truck tire wear particles in complex environmental samples–a quantitative comparison with “traditional” microplastic polymer mass loads. Sci. Total Environ. 773, 145667.

Gottschalk, F., Ort, C., Scholz, R. W. and Nowack, B. (2011). Engineered nanomaterials in rivers - Exposure scenarios for Switzerland at high spatial and temporal resolution. *Environmental Pollution*, 159 (12), Elsevier Ltd., pp.3439–3445.

Gottschalk, F., Scholz, R. W. and Nowack, B. (2010). Probabilistic material flow modeling for assessing the environmental exposure to compounds: Methodology and an application to engineered nano-TiO2particles. *Environmental Modelling and Software*, 25 (3), Elsevier Ltd., pp.320–332.

Gottschalk, F., Sun, T. and Nowack, B. (2013). Environmental concentrations of engineered nanomaterials: Review of modeling and analytical studies. *Environmental Pollution*, 181, Elsevier Ltd., pp.287–300.

Griffin, R. L., Green, I. and Stafford, R. (2018). Accumulation of marine microplastics along a trophic gradient as determined by an agent-based model. *Ecological Informatics*, 45 (September 2017), pp.81–84.

Grigoratos, T. and Martini, G. (2015). Brake wear particle emissions: a review. *Environmental Science and Pollution Research*, 22 (4), pp.2491–2504.

Gualtieri, M., Andrioletti, M., Vismara, C., Milani, M. and Camatini, M. (2005). Toxicity of tire debris leachates. *Environment international* 31.5 pp. 723-730.

Gustafsson, M., Blomqvist, G., Gudmundsson, A., Dahl, A., Swietlicki, E., Bohgard, M., Lindbom, J. and Ljungman, A. (2008). Properties and toxicological effects of particles from the interaction between tyres, road pavement and winter traction material. *Sci. Total Environ*. 393, 226-240.

Hagström, S. (2021). Fate and Transport of Microplastic Particles in Small Highway-Adjacent Streams. *THESIS MSc*.

Hamid, F., Bhatti, M. S., Anuar, N., Anuar, N., Mohan, P. and Periathamby, A. (2018). Worldwide distribution and abundance of microplastic: How dire is the situation? *Waste Management and Research,* 36 (10), pp.873–897.

Hanvey, J. S., Lewis, P. J., Lavers, J. L., Crosbie, N. D., De, K. P., Clarke, B. O. and Pete, P. E. T. (2017). Analytical Methods A review of analytical techniques for quantifying microplastics in sediments. pp.1369–1383. [Online]. Available at: doi:10.1039/c6ay02707e.

Harrison, R. M., Jones, A. M., Gietl, J., Yin, J. and Green, D. C. (2012). Estimation of the contributions of brake dust, tire wear, and resuspension to nonexhaust traffic particles derived from atmospheric measurements. *Environmental Science and Technology*, 46 (12), pp.6523–6529.

Hartmann, N., Huffer, T., Thompson, R.C., Hassellov, M., Verschoor, A., and Daugaard, A. (2019). Are we speaking the same language? Recommendations for a definition and categorization framework for plastic debris. *Environ. Sci. Technol*. 53, 1039–1047.

Hendrickson, E., Minor, E. C. and Schreiner, K. (2018). Microplastic Abundance and Composition in Western Lake Superior As Determined *via* Microscopy, Pyr-GC/MS, and

FTIR. Environ. Sci. Technol. 2018, 52, 1787−1796 Article [Online]. Available at: doi:10.1021/acs.est.7b05829.

Heskett, M., Takada, H., Yamashita, R., Yuyama, M., Ito, M., Geok, Y., Ogata, Y., Kwan, C., Heckhausen, A., Taylor, H., Powell, T., Morishige, C., Young, D., Patterson, H., Robertson, B., Bailey, E. and Mermoz, J. (2012). Measurement of persistent organic pollutants (POPs) in plastic resin pellets from remote islands: Toward establishment of background concentrations for International Pellet Watch. *Marine Pollution Bulletin*, 64, 445-448.

Hidalgo-Ruz, V., Gutow, L., Thompson, R. C., and Thiel, M. (2012). Microplastics in the marine environment: A review of the methods used for identification and quantification. Environ. Sci. Technol., 46, 3060−3075.

Hillenbrand, T., Toussaint, D., Böhm, E., Fuchs, S., Scherer, U., Rudolphi, A., Hoffmann, M., Kreißig, J. and Kotz, C. (2005). Copper, Zinc and Lead Entries in Waters and Soils — Analysis of Emission Paths and Possible Emission Reduction Measures; Federal Environment Agency: Dessau, Germany.

Horton, A. A., Svendsen, C., Williams, R. J., Spurgeon, D. J. and Lahive, E. (2017). Large microplastic particles in sediments of tributaries of the River Thames, UK – Abundance, sources and methods for effective quantification. *Marine Pollution Bulletin*, 114 (1), Elsevier B.V., pp.218–226.

Horton, A. A., Svendsen, C., Williams, R. J., Spurgeon, D. J. and Lahive, E. (2017). Large microplastic particles in sediments of tributaries of the River Thames, UK – Abundance, sources and methods for effective quantification. Marine Pollution Bulletin, 114 (1), Elsevier B.V., pp.218–226. [Online]. Available at: doi:10.1016/j.marpolbul.2016.09.004.

Hurley, R., Woodward, J. and Rothwell, J. (2018). Microplastic contamination of river beds significantly reduced by catchment-wide flooding. Nature Geoscience, VOL 11, 251–257.

ISO/TS 20593:2017 (2017). Ambient Air-determination of the Mass Concentration of Tyre and Road Wear Particles (TRWP)-Pyrolysis-GC-MS Method. International Organization for Standardization, Genève, Switzerland.

ISO/TS 21396:2017 (2017). Rubber — Determination of Mass Concentration of Tyre and Road Wear Particles (TRWP) in Soil and Sediments — Pyrolysis-GC/MS Method. International Organization for Standardization, Genève, Switzerland.

Jahan, R., Aniruddha, R., Kirpa, S., Uddin, G., Walker, T. R., Chowdhury, T., Uddin, J., Uddin, M., Mohammed, K. and Abubakr, M. R. (2023). Microplastic Toxicity in Aquatic Organisms and Aquatic Ecosystems : a Review. Water Air Soil Pollut 234:52.

Jambeck, J., Geyer, R., Wilcox, C., Theodore, R., Perryman, M., Andrady, A., Narayan, R. and Law, K. (2015). Plastic waste inputs from land into the ocean. *Science mag.* Vol 347, issue 6223.

Jarlskog, I., Jaramillo-vogel, D., Rausch, J., Gustafsson, M. and Andersson-sk, Y. (2022). Concentrations of tyre wear microplastics and other traffic-derived non-exhaust particles in the road environment. Environment International 170, 107618.

Jekel, M. (2019). Scientific report on tyre and road wear particles, TRWP in the aquatic environment. ETRMA, Brussels. 36p.

Jessieleena, A., Rathinavelu, S., Eswari, K., Anju, V., John, A. and Nambi, I. M. (2023). Residential houses — a major point source of microplastic pollution : insights on the various sources , their transport , transformation , and toxicity behaviour. Environmental Science and Pollution Research, pp.67919–67940.

Johannesson, M. and Lithner, D. (2022). Potential policy instruments and measures against microplastics from tyre wear: mapping and prioritisation. [Online]. Available at: http://vti.diva-portal.org/smash/get/diva2:1641512/FULLTEXT01.pdf.

Jung, U. and Choi, S. (2022). Classification and Characterization of Tyre-Road Wear Particles in Road Dust by Density. Polymers 14, 1005. https://doi.org/10.3390/ polym14051005.

Kang, H., Park, S., Lee, B., Kim, I. and Kim, S. (2022). Concentration of Microplastics in Road Dust as a Function of the Drying Period — A Case Study in G City, Korea. Sustainability, 14, 3006. https://doi.org/10.3390/su14053006.

Kang, T. and Kim, H. (2023). An Experimental Study on the Component Analysis and Variation in Concentration of Tire and Road Wear Particles Collected from the Roadside. Sustainability, 15, 12815. https://doi.org/10.3390/su151712815.

Kaufmann, P., Scheiwiler, E. and Ochsenbein, U. (2007). Road wastewater. *Tec21*. vol. 133 pp. 27–30.

Kawecki D. and Nowack B. (2019). Polymer-Specific modeling of the environmental emissions of seven commodity plastics as macro- and microplastics. *Environ Sci Technol.* 20;53(16):9664-9676. PMID: 31287667.

Keene, J. and Turner, A. (2023). Microplastics in coastal urban sediments: Discrepancies in concentration and character revealed by different approaches to sample processing. Science of the Total Environment 865.

Khan, F. R., Halle, L. L. and Palmqvist, A. (2019). Acute and long-term toxicity of micronized car tire wear particles to Hyalella azteca. *Aquatic Toxicology*, 213 (May), Elsevier., p.105216.

Khan, F. R., Rødland, E. S., Kole, P. J., Van Belleghem, F. G. A. J., Jaén-Gil, A., Hansen, S. F. and Gomiero, A. (2024). An overview of the key topics related to the study of tire particles and their chemical leachates: From problems to solutions. TrAC - Trends in Analytical Chemistry, 172. [Online]. Available at: doi:10.1016/j.trac.2024.117563.

Kim, G. and Lee, S. (2018). *Characteristics of Tire Wear Particles Generated by a Tire Simulator under Various Driving Conditions*. [Online]. Available at: doi:10.1021/acs.est.8b03459.

Kim, M. G., Yagawa, K., Inoue, H., Lee, Y.K., and Shirai, T. (1990). Measurement of tire tread in urban air by pyrolysis-gas chromatography with flame photometric detection. Atmospheric Environment Vol. 24A, N.6 pp. 1417-1422.

Klein J., Hulskotte J., Ligterink N., Dellaert S., Molnár H., and Geilenkirchen G. (2018). Methods for calculating the emissions of transport in the Netherlands. Statistics Netherlands PBL Netherlands Environmental Assessment Agency. Transport and Environment (WVL).

Klein, S., Worch, E. and Knepper, T. P. (2015). Occurrence and spatial distribution of microplastics in river shore sediments of the rhine-main area in Germany. Environmental Science and Technology, 49 (10), pp.6070–6076. [Online]. Available at: doi:10.1021/acs.est.5b00492.

References

Klöckner, P., Reemtsma, T., Eisentraut, P., Braun, U., Ruhl, A. S. and Wagner, S. (2019). Tire and road wear particles in road environment – Quantification and assessment of particle dynamics by Zn determination after density separation. *Chemosphere*, 222, Elsevier Ltd., pp.714–721.

Klöckner, P., Seiwert, B., Eisentraut, P., Braun, U., Reemtsma, T. and Wagner, S. (2020). Characterization of tyre and road wear particles from road runoff indicates highly dynamic particle properties. Water Research 185 116262.

Klöckner, P., Seiwert, B., Weyrauch, S., Escher, B. I., Reemtsma, T. and Wagner, S. (2021). Comprehensive characterization of tyre and road wear particles in highway tunnel road dust by use of size and density fractionation. Chemosphere, 279. [Online]. Available at: doi:10.1016/j.chemosphere.2021.130530.

Klun, B., Rozman, U. and Kalcikova, G. (2023). Environmental aging and biodegradation of tire wear microplastics in the aquatic environment. Journal of Environmental Chemical Engineering 11, 110604.

Knight, L., Parker-Jurd, F., Al-Sid-Cheikh, M. and Thompson, R. (2020). Tyre wear particles: an abundant yet widely unreported microplastic?. Environmental Science and Pollution Research, 27:18345–18354.

Koelmans, A. A., Besseling, E., Shim, W. J., Kiessling, T., Gutow, L. and Thiel, M. (2015). *Marine Anthropogenic Litter*.

Kole, P., Löhr, A. and Ragas, A. (2015). Car tire wear: A neglected source of microplastics? *Milieu* 5, 39-41.

Kole, P., Löhr, A. J., Van Belleghem, F. G. A. J. and Ragas, A. M. J. (2017). Wear and tear of tyres: A stealthy source of microplastics in the environment. International Journal of Environmental Research and Public Health, 14 (10). [Online]. Available at: doi:10.3390/ijerph14101265.

Kovochich, M., Liong, M., Parker, J. A., Cheun, S., Lee, J. P., Xi, L., Kreider, M. L. and Unice, K. M. (2021). Chemical mapping of tire and road wear particles for single particle analysis. Science of the Total Environment 757.

Kovochich, M., Liong, M., Parker, J. A., Cheun, S., Lee, J. P., Xi, L., Kreider, M. L. and Unice, K. M. (2021a). Science of the Total Environment Chemical mapping of tire and road wear particles for single particle analysis. 757.

Kovochich, M., Parker, J. A., Oh, S. C., Lee, J. P., Wagner, S., Reemtsma, T. and Unice, K. M. (2021b). Characterization of Individual Tire and Road Wear Particles in Environmental Road Dust, Tunnel Dust, and Sediment. pp.10–17.

Kreider, M. L., Panko, J. M., McAtee, B. L., Sweet, L. I. and Finley, B. L. (2010). Physical and chemical characterization of tire-related particles: Comparison of particles generated using different methodologies. *Science of the Total Environment*, 408 (3), Elsevier B.V., pp.652–659.

Kumar, P., Ketzel, M., Vardoulakis, S., Pirjola, L. and Britter, R. (2011). Dynamics and dispersion modelling of nanoparticles from road traffic in the urban atmospheric environment-A review. *Journal of Aerosol Science*, 42 (9), Elsevier., pp.580–603.

Kumar, P., Pirjola, L., Ketzel, M. and Harrison, R.M., (2013). Nanoparticle emissions from 11 non-vehicle exhaust sources - a review. Atmos. Environ. 67, 252e277. https://doi.org/10.1016/j.atmosenv.2012.11.011.

Kumata, H., Sanada, Y., Takada, H. and Ueno, T. (2000). Historical trends of N-cyclohexyl-2- benzothiazolamine, 2-(4-morpholinyl)benzothiazole, and other anthropogenic contaminants in the urban reservoir sediment core. Environ. Sci. Technol. 34, 246–253.

Kumata, H., Takada, H., and Ogura, N. (1996). Determination of 2-(4-morpholinyl) benzothiazole in environmental samples by a gas chromatograph equipped with a flame photometric detector. Anal. Chem., 68, 1976−1981.

Kumata, H., Yamada, J., Masuda, K., Takada, H., Sato, Y., Sakurai, T., and Fujiwara, K. (2002). Benzothiazolamines as tire-derived molecular markers: Sorptive behavior in street runoff and application to soure apportioning. Environ. Sci. Technol.,36, 702−708.

Kwak, J., Kim, H., Lee, J. and Lee, S. (2013). Characterization of non-exhaust coarse and fine particles from on-road driving and laboratory measurements. *Sci. Total Environm.* 458-460, 273-282.

Lassen, C., Hansen, F., Magnusson, K., Hartmann, B., Rehne-Jensen, P., Nielsen, T.G., and Brinch, A. (2015). Microplastics: Occurrence, effects and sources of releases to the environment in Denmark. Danish Environmental Protection Agency. Available at: http://mst.dk/service/publikationer/publikationsarkiv/2015/nov/rapport-ommikroplast.

Laursen, S. N., Fruergaard, M. and Andersen, T. J. (2022). Rapid flocculation and settling of positively buoyant microplastic and fine-grained sediment in natural seawater. Marine Pollution Bulletin 178.

Leads, R. R. and Weinstein, J. E. (2019). Occurrence of tire wear particles and other microplastics within the tributaries of the Charleston Harbor Estuary, South Carolina, USA. *Marine Pollution Bulletin*, 145 (February), Elsevier., pp.569–582.

Leads, R., Weinstein, J. E., Kell, S. E., Overcash, J. M., Ertel, B. M. and Gray, A. D. (2023). Spatial and temporal variability of microplastic abundance in estuarine intertidal sediments: Implications for sampling frequency. Science of the Total Environment 859.

Lebreton, L. C. M., Greer, S. D. and Borrero, J. C. (2012). Numerical modelling of floating debris in the world's oceans. *Marine Pollution Bulletin*, 64 (3), Elsevier Ltd., pp.653–661.

Lee, H., Ju, M. and Kim, Y. (2020). Estimation of emission of tire wear particles (TWPs) in Korea. *Waste Management*, 108, Elsevier Ltd., pp.154–159.

Leiser, R., Schumann, M., Dadi, T. and Potthoff, K. W. (2021). Burial of microplastics in freshwater sediments facilitated by iron - organo flocs. Sci Rep 11, 24072.

Li, S., Wang, H., Liang, D., Li, Y., and Shen, Z. (2022). How the Yangtze River transports microplastic to the east China sea. *Chemosphere 307 136112.*

Liu, Y., Chen, H., Gao, J., Dave, K. and Chen, J. (2021). Gap Analysis and Future Needs of Tyre Wear Particles. SAE Technical Paper Series, 1 (April).

Liu, W., Zhang, J., Liu, H., Guo, X., Zhang, X. and Yao, X. (2021). A review of the removal of microplastics in global wastewater treatment plants : Characteristics and mechanisms. Environment International 146.

Luhana, L., Sokhi, R., Warner, L., Mao, H., Boulter, P., McCrae, I., Wright, J. and Osborn, D. (2004). Characterisation of Exhaust Particulate Emissions from Road Vehicles;

Measurement of Non-Exhaust Particulate Matter; European Commission—DG TrEn, 5th Framework Programme: Brussels, Belgium.

Lusher, A., Munno, K., Hermabessiere, L. and Carr, S. (2020). Isolation and Extraction of Microplastics from Environmental Samples: An Evaluation of Practical Approaches and Recommendations for Further Harmonization. Applied Spectroscopy, 74:9, 1049-1065.

Magnusson, K., Eliasson, K., Fråne, A., Haikonen, K., Hultén, J., Olshammar, M. (2016). Swedish Sources and Pathways for Microplastics to the Marine Environment. A Review of Existing Data. Report Number C 183. Swedish. Environmental Protection Agency, Stockholm, Sweden.

Mahjoub, A., Hashemi, S. H., Sadat, S. and Petroody, A. (2023). The role of baseflow and stormwater in transport of tire and bitumen particles in Tehran city: A dense urban environment. Journal of Contaminant Hydrology 256,104180256.

Maltby, L., Forrow, D., Boxall, A., Calow, P. and Betton, C. (1995). The effects of motorway runoff on freshwater ecosystems: 1. Field study. *Environmental Toxicology and Chemistry,* Val. 14, No. 6, pp 1079-1092.

Markus, A. A., Parsons, J. R., Roex, E. W. M., de Voogt, P. and Laane, R. W. P. M. (2016). Modelling the transport of engineered metallic nanoparticles in the river Rhine. *Water Research*, 91, Elsevier Ltd., pp.214–224.

Maniquiz-redillas, M., Robles, M. E., Cruz, G., Reyes, N. J. and Kim, L. (2022). First Flush Stormwater Runoff in Urban Catchments : A Bibliometric and Comprehensive Review. Hydrology 2022, 9, 63.

Mattonai, M., Nacci, T. and Modugno, F. (2022). Analytical strategies for the quali-quantitation of tire and road wear particles - A critical review. Trends in Analytical Chemistry 154- 116650.

Meesters, J. A. J., Quik, J. T. K., Koelmans, A. A., Hendriks, A. J. and Van De Meent, D. (2016). Multimedia environmental fate and speciation of engineered nanoparticles: A probabilistic modeling approach. *Environmental Science: Nano*, 3 (4), pp.715–727.

References

Meesters, J., Koelmans, A., Quik, J. (2014). Multimedia modeling of engineered nanoparticles with simpleBox4nano: model definition and evaluation. *Environ Sci Technol* 48:5726–5736.

Mendes, A.M., Golden, N., Bermejo, R. and Morrison, L. (2021). Distribution and abundance of microplastics in coastal sediments depends on grain size and distance from sources. Mar. Pollut. Bull. 172, 112802.

Mengistu, D. (2023). Microplastics in stormwater runoff: Measuring tire wear particles (TWP) concentration in the road environment and effect of treatment systems. PhD thesis. Norwegian University of Life Sciences. Faculty of Science and Technology.

Mengistu, D., Coutris, C., Aleksander, K., Paus, H. and Heistad, A. (2022). Concentrations and Retention Efficiency of Tyre Wear Particles from Road Runoff in Bioretention Cells. Water, 14, 3233. https:// doi.org/10.3390/w14203233.

Mengistu, D., Heistad, A. and Coutris, C. (2021). Tire wear particles concentrations in gully pot sediments. Science of the Total Environment 769.

Mennekes, D. and Nowack, B. (2022). Tire wear particle emissions : Measurement data where are you ?. *Science of the Total Environment* 830.

Met Office, 2022. Storms Dudley, Eunice and Franklin, February 2022. Available at [online]: Metoffice.gov.uk https://www.metoffice.gov.uk/binaries/content/assets/metofficegovuk/pdf/weather/learn-about/uk-past-events/interesting/2022/2022_02_storms_dudley_eunice_franklin.pdf (Accessed 24 September 2023).

Mian, H. R., Chhipi-shrestha, G., Mccarty, K., Hewage, K. and Sadiq, R. (2022). An estimation of tire and road wear particles emissions in surface water based on a conceptual framework. *Science of the Total Environment* 848 (April).

Milani, M., Pucillo, F., Ballerini, M., Camatini, M., Gualtieri, M. and Martino, S. (2004). First evidence of tyre debris characterization at the nanoscale by focused ion beam. *Mater. Charact*. 52, 283–288.

Mizuguchi, H., Takeda, H., Kinoshita, K., Takeuchi, M., Takayanagi, T., Teramae, N., Pipkin, W., Matsui, K., Watanabe, A. and Watanabe, C. (2023). Direct analysis of

airborne microplastics collected on quartz filters by pyrolysis-gas chromatography / mass spectrometry. Journal of Analytical and Applied Pyrolysis 171.

Monira, S., Roychand, R., Bhuiyan, M. A., Hai, F. I. and Kumar, B. (2022). Identification, classification and quantification of microplastics in road dust and stormwater. Chemosphere 299 134389.

More, S. L., Miller, J. V, Thornton, S. A., Chan, K., Barber, T. R. and Unice, K. M. (2023). Refinement of a microfurnace pyrolysis-GC – MS method for quantification of tyre and road wear particles (TRWP) in sediment and solid matrices. Science of the Total Environment, 87 The Authors., p.162305. [Online]. Available at: doi:10.1016/j.scitotenv.2023.162305.

Morgan, D., Johnston, P., Osei, K. and Gill, L. (2017). The Influence of Particle Size on the First Flush Strength of Urban Stormwater Runoff. Water Sci. Technol. 76, 2140–2149.

Nantege, D., Odong, R., Shnada, H., Unique, A., Keke, N., Ndatimana, G., Fulbert, A., Francis, A. and Arimoro, O. (2023). Microplastic pollution in riverine ecosystems: threats posed on macroinvertebrates. Environmental Science and Pollution Research 30, 76308–76350.

Nizzetto, L., Bussi, G., Futter, M. Butterfield, D. and Whitehead, P.G. (2016). A theoretical assessment of microplastic transport in river catchments and their retention by soils and river sediments. *Environ. Sci. processes Impacts* 18 (8), 10501059.

Nowack, B. (2017). Evaluation of environmental exposure models for engineered nanomaterials in a regulatory context. *NanoImpact*, 8, Elsevier B.V., pp.38–47.

Ostini, L., Braga, R., Tomazini, F., Aparecido, A., Galileu, L., Busquets, R. and Cintra, L. (2022). Relevance of tyre wear particles to the total content of microplastics transported by runoff in a high-imperviousness and intense vehicle traffic urban area. Environmental Pollution 314, 120200.

Panko, J. M., Chu, J., Kreider, M. L. and Unice, K. M. (2013). Measurement of airborne concentrations of tire and road wear particles in urban and rural areas of France, Japan, and the United States. 72, pp.192–199.

Panko, J., Kreider, M. and Unice, K. (2018). Chapter 7 - Review of Tire Wear Emissions: A Review of Tire Emission Measurement Studies: Identification of Gaps and Future Needs. In Non-Exhaust Emissions, ed. F. Amato, 147-160. Academic Press.

Pant, P. and Harrison, R. M. (2013). Estimation of the contribution of road traffic emissions to particulate matter concentrations from field measurements: A review. *Atmospheric Environment*, 77, Elsevier Ltd., pp.78–97.

Panti, C., Giannetti, M., Baini, M., Rubegni, F., Minutoli, R. and Fossi, M. C. (2015). Occurrence, relative abundance and spatial distribution of microplastics and zooplankton NW of Sardinia in the Pelagos Sanctuary Protected Area, Mediterranean Sea. *Environmental Chemistry*, 12 (5), pp.618–626.

Parker-Jurd, F. N. F., Napper, I. E., Abbott, G. D., Hann, S. and Thompson, C. (2021). Quantifying the release of tyre wear particles to the marine environment *via* multiple pathways. Marine Pollution Bulletin 172, 112897.

Pedrotti, M. L., Petit, S., Elineau, A., Bruzaud, S., Crebassa, J. C., Dumontet, B., Martí, E., Gorsky, G. and Cózar, A. (2016). Changes in the floating plastic pollution of the mediterranean sea in relation to the distance to land. PLoS ONE, 11 (8), pp.1–14.

Pellini, G., Gomiero, A., Fortibuoni, T., Ferrà, C., Grati, F., Tassetti, N., Polidori, P., Fabi, G. and Scarcella, G. (2018). Characterization of microplastic litter in the gastrointestinal tract of *Solea solea* from the Adriatic Sea. *Environmental Pollution,* 234, pp.943–952.

Pereira, R., Rodrigues, S., Silva, D., Freitas, V., Almeida, C. and Ramos, S. (2023). Microplastic contamination in large migratory fishes collected in the open Atlantic Ocean. Marine Pollution Bulletin 186.

Pico, Y. and Barcelo, D. (2020). Pyrolysis gas chromatography-mass spectrometry in environmental analysis : Focus on organic matter and microplastics. Trends in Analytical Chemistry 130, 115964.

Pogojeva, M., Korshenko, E. and Osadchiev, A. (2023). Riverine Litter Flux to the Northeastern Part of the Black Sea. J. Mar. Sci. Eng., 11, 105. https://doi.org/10.3390/jmse11010105.

References

Pohrt, R. (2019). Tire wear particle hot spots – Review of influencing factors. *Facta Universitatis, Series: Mechanical Engineering*, 17 (1), pp.17–27.

Praetorius, A., Scheringer, M., and Hungerbuhler, K. (2012). Development of Environmental fate models for engineered nanoparticles – A case study of TiO_2 nanoparticles in the Rhine river. *Environmental Science & Technology 46* (12), 6705-6713.

Quinn, B., Murphy, F. and Ewins, C. (2017). Validation of density separation for the rapid recovery of microplastics from sediment. Analytical Methods, 9 (9), pp.1491–1498. [Online]. Available at: doi:10.1039/c6ay02542k.

Rani-borges, B., Gomes, E., Maricato, G., Henrique, L., Carvalho, F. De, Henrique, P., Pereira, C., Augusto, R. and Gonçalves, L. (2023). Unveiling the hidden threat of microplastics to coral reefs in remote South Atlantic islands. Science of the Total Environment 897.

Rauert, C., Rødland, E. S., Oko, E. D., Reid, M. J., Meland, S. and Thomas, K. V. (2021). Challenges with Quantifying Tyre Road Wear Particles: Recognizing the Need for Further Refinement of the ISO Technical Specification. Environ. Sci. Technol. Lett. 8, 231−236.

Reddy, C. M., and Quinn, J. G. (1997). Environmental chemistry of benzothiazoles derived from rubber. Environ. Sci. Technol. 31, 2847−2853.

Rødland, E. S., Christian, O., Reid, M., Heier, L. S., Skogsberg, E., Snilsberg, B., Gryteselv, D. and Meland, S. (2022). Characterization of tyre and road wear microplastic particle contamination in a road tunnel : From surface to release. Journal of Hazardous Materials 435;129032.

Rødland, E. S., Okoffo, E. D., Rauert, C., Heier, L. S., Lind, O. C., Reid, M., Thomas, K. V. and Meland, S. (2020). Road de-icing salt: Assessment of a potential new source and pathway of microplastics particles from roads. Science of the Total Environment, 738. [Online]. Available at: doi:10.1016/j.scitotenv.2020.139352.

Rødland, E. S., Heier, L. S., Christian, O. and Meland, S. (2023). High levels of tire wear particles in soils along low traffic roads. Science of the Total Environment 903 (April).

Rødland, E. S., Christian, O., Reid, M. J., Heier, L. S., Okoffo, E. D., Rauert, C., Thomas, K. V and Meland, S. (2022). Occurrence of tire and road wear particles in urban and peri-urban snowbanks , and their potential environmental implications. Science of the Total Environment 824.

Rogers, E. (2018). Investigation of polycyclic aromatic hydrocarbons (PAH) absorption from seawater to model microplastic particles. Master thesis. The Norwegian University of Science and Technology. 121p.

Ross, M., Loutan, A., Groeneveld, T., Molenaar, D., Kroetch, K., Bujaczek, T., Kolter, S., Moon, S., Huynh, A., Khayam, R., Franczak, B., Camm, E., Arnold, V. and Ruecker, N. (2023). Estimated discharge of microplastics *via* urban stormwater during individual rain events. *Front. Environ. Sci. 11:1090267.* doi: 10.3389/fenvs.2023.1090267

Rosso, B., Gregoris, E., Litti, L., Zorzi, F., Fiorini, M., Bravo, B., Barbante, C., Gambaro, A. and Corami, F. (2023). Identification and quantification of tire wear particles by employing different cross-validation techniques : FTIR-ATR Micro-FTIR , Pyr-GC / MS , and SEM. Environmental Pollution 326, 121511.

Santana, M. F. M., Ascer, L. G., Custódio, M. R., Moreira, F. T. and Turra, A. (2016). Microplastic contamination in natural mussel beds from a Brazilian urbanized coastal region: Rapid evaluation through bioassessment. Marine Pollution Bulletin, 106 (1-2), Elsevier Ltd., pp.183–189.

Schauer, J., Lough, G., Shafer, M., Christensen, W., Arndt, M., DeMinter, J. and Park, J. (2006). Characterization of Metals emitted from motor vehicles. Research Report, Health Effects Institute.

Schlining, K., Von Thun, S., Kuhnz, L., Schlining, B., Lundsten, L., Jacobsen, N., Chaney, L. and Connor, J., (2013). Debris in the deep: Using a 22-year video annotation database to survey marine litter in Monterey Canyon, central California, USA. *Deep Sea Research Part I: Oceanographic Research Papers*, 79, 96-105.

Sieber, R., Kawecki, D. and Nowack, B. (2020). Dynamic probabilistic material flow analysis of rubber release from tires into the environment. *Environmental Pollution*, 258, Elsevier Ltd., p.113573.

References

Siegfried, M., Gabbert, S., Koelmans, A. (2016). River export of plastic from land to sea: a global modeling approach. In: EGU General Assembly Conference Abstract. p 11507.

Siegfried, M., Koelmans, A. A., Besseling, E. and Kroeze, C. (2017). Export of microplastics from land to sea. A modelling approach. *Water Research*, 127, Elsevier Ltd., pp.249–257.

Shu, X., Xu, L., Yang, M., Qin, Z., Zhang, Q. and Zhang, L. (2023). Spatial distribution characteristics and migration of microplastics in surface water, groundwater and sediment in karst areas : The case of Yulong River. Science of the Total Environment 868.

Sommer, F., Dietze, V., Baum, A., Sauer, J., Gilge, S., and Maschowski, C. (2018). Tire abrasion as a major source of microplastics in the environment. *Aerosol Air Qual. Res. 18, 2014–2028.*

Spies, R. B., Anderson, B. D., and Rice, D. W. (1987). Benzothiazoles in estuarine sediments as indicators of street runoff. Nature, 327,697−699.

Stojanovic, N., Abdullah, O. I. and Grujic, I. (2022). Particles formation due to the wear of tires and measures for the wear reduction : A review. 236 (14), pp.3075–3089. [Online]. Available at: doi:10.1177/09544070211067879.

Stride, B., Abolfathi, S., Bending, G. D. and Pearson, J. (2024). Quantifying microplastic dispersion due to density effects. Journal of Hazardous Materials 466, 133440.

Sun, T. Y., Conroy, G., Donner, E., Hungerbühler, K., Lombi, E. and Nowack, B. (2015). Probabilistic modelling of engineered nanomaterial emissions to the environment: A spatio-temporal approach. *Environmental Science: Nano*, 2 (4), Royal Society of Chemistry., pp.340–351.

Sun, X., Jia, Q., Ye, J., Zhu, Y., Song, Z., Guo, Y. and Chen, H. (2023). Real-time variabilities in microplastic abundance and characteristics of urban surface runoff and sewer overflow in wet weather as impacted by land use and storm factors. Science of the Total Environment 859.

Sundt, P., Schulze, P. and Syversen, F. (2014). Sources of microplastics pollution to the marine environment. Report M-321, 2015. Project 1032, Norwegian Environmental Agency, Oslo, Norway.

References

Ten Broeke, H., Hulskotte, J., and Denier van der Gon, H. (2008). Road traffic tirewear. Emission estimates for diffuse sources. Netherlands Emission Inventory. Netherlands National Water Board – Water Unit. TNO Built Environment and Geosciences.

Thomas, J., Moosavian, S. K., Cutright, T., Pugh, C. and Soucek, M. D. (2022). Method Development for Separation and Analysis of Tyre and Road Wear Particles from Roadside Soil Samples. *Environ. Sci. Technol.* 2022, 56, 11910−11921.

Tian, Z., Zhao, H., Peter, K. T., Gonzalez, M., Wetzel, J., Wu, C., Hu, X., Prat, J., Mudrock, E., Hettinger, R., et al. (2022). A ubiquitous tire rubber – derived chemical induces acute mortality in coho salmon. *Environ. Sci. Technol. Lett.* 9, 140–146.

Troost, T. A., Desclaux, T., Leslie, H. A., van Der Meulen, M. D. and Vethaak, A. D. (2018). Do microplastics affect marine ecosystem productivity? *Marine Pollution Bulletin*, 135 (July), pp.17–29.

Unice, K. M., Kreider, M. L. and Panko, J. M. (2012). Use of a Deuterated Internal Standard with Pyrolysis-GC / MS Dimeric Marker Analysis to Quantify Tire Tread Particles in the Environment. pp.4033–4055. [Online]. Available at: doi:10.3390/ijerph9114033.

Unice, K. M., Kreider, M. L. and Panko, J. M. (2013). Comparison of tire and road wear particle concentrations in sediment for watersheds in France, Japan, and the United States by quantitative pyrolysis GC/MS analysis. *Environmental Science and Technology*, 47 (15), pp.8138–8147.

Unice, K. M., Weeber, M. P., Abramson, M. M., Reid, R. C. D., Gils, J. A. G. Van, Markus, A. A., Vethaak, A. D. and Panko, J. M. (2019). Characterizing export of land-based microplastics to the estuary - Part I : Application of integrated geospatial microplastic transport models to assess tire and road wear particles in the Seine watershed. Science of the Total Environment 646, pp.1639–1649.

Unice, K. M., Weeber, M. P., Abramson, M. M., Reid, R. C. D., van Gils, J. A. G., Markus, A. A., Vethaak, A. D. and Panko, J. M. (2019). Characterizing export of land-based microplastics to the estuary - Part II: Sensitivity analysis of an integrated geospatial microplastic transport modeling assessment of tire and road wear particles. *Science of the Total Environment*, 646, Elsevier B.V., pp.1650–1659.

Van Cauwenberghe, L., Devriese, L., Galgani, F., Robbens, J. and Janssen, C. R. (2015). Microplastics in sediments: A review of techniques, occurrence and effects. *Marine Environmental Research*, 111, Elsevier Ltd., pp.5–17.

van der Hal, N., Ariel, A. and Angel, D. L. (2017). Exceptionally high abundances of microplastics in the oligotrophic Israeli Mediterranean coastal waters. *Marine Pollution Bulletin*, 116 (1-2), Elsevier Ltd., pp.151–155.

van Wezel, A., Caris, I., Kools, S. (2015). Release of primary microplastics from consumer products to wastewater in The Netherlands. *Environ Toxicol Chem* 35:1627–1631.

van Wijnen, J., Ragas, A. M. J. and Kroeze, C. (2019). Modelling global river export of microplastics to the marine environment: Sources and future trends. *Science of the Total Environment*, 673, Elsevier B.V., pp.392–401.

Vandermeersch, G., Van Cauwenberghe, L., Janssen, C. R., Marques, A., Granby, K., Fait, G., Kotterman, M. J. J., Diogène, J., Bekaert, K., Robbens, J., et al. (2015). A critical view on microplastic quantification in aquatic organisms. *Environmental Research,* 143, pp.46–55.

Venghaus, D., Neupert, J.W. and Barjenbruch, M. (2023). Tire Wear Monitoring Approach for Hotspot Identification in Road Deposited Sediments from a Metropolitan City in Germany. Sustainability, 15, 12029.

Vercauteren, M., Semmouri, I., Acker, E. Van, Pequeur, E., Esch, L. Van, Uljee, I., Asselman, J. and Janssen, C. R. (2023). Assessment of road run-off and domestic wastewater contribution to microplastic pollution in a densely populated area (Flanders, Belgium). Environmental Pollution 333;122090.

Verschoor, A. (2015). Towards a definition of microplastics – Considerations for the specification of physico-chemical properties, *National Institute for Public Health*. RIVM Letter report 0116.

Verschoor, A., De Poorter, L., Dröge, R., Kuenen, J. and De Valk, E. (2016). Emission of Microplastics and Potential Mitigation Measures. Abrasive Cleaning Agents, Paints and Tyre Wear; National Institute for Public Health and the Environment. Bilthoven, The Netherlands.

Vogelsang, C., Lusher, A., Dadkhah, M., Sundvor, I., Muhammad M., Ranneklev, B., Eidsvoll, D. and Meland, S. (2019). Microplastics in road dust – characteristics, pathways and measures. Report, p.170.

Wagner, M. and Lambert, S. (2018). *Freshwater Microplastics The Handbook of Environmental Chemistry 58 Series Editors: Damià Barceló · Andrey G. Kostianoy*.

Wagner, S., Hüffer, T., Klöckner, P., Wehrhahn, M., Hofmann, T. and Reemtsma, T. (2018). Tire wear particles in the aquatic environment - A review on generation, analysis, occurrence, fate and effects. *Water Research*, 139, pp.83–100.

Wagner, S., Klockner, P. and Reemtsma, T. (2022). Aging of tire and road wear particles in terrestrial and freshwater environments – A review on processes, testing, analysis and impact. Chemosphere 288.

Wang, Q., Zhang, Q., Wu, Y. and Wang, X., (2017). Physicochemical conditions and properties of particles in urban runoff and rivers: Implications for runoff pollution. *Chemosphere* 173, 318-325.

Wentworth, C. (1922). Scale of grade and class terms for clastic sediments. J. Geol. 30 (5), 377-392.

Wiggin, K. J. and Holland, E. B. (2019). Validation and application of cost and time effective methods for the detection of 3–500 Mm sized microplastics in the urban marine and estuarine environments surrounding Long Beach, California. Marine Pollution Bulletin, 143 Elsevier., pp.152–162. [Online]. Available at: doi:10.1016/j.marpolbul.2019.03.060.

Wik, A. (2008). *When the Rubber Meets the Road - Ecotoxicological Hazard and Risk Assessment of Tire Wear Particles*.

Wik, A. and Dave, G. (2005). Environmental labeling of car tires – toxicity to Daphnia magna can be used as a screening method. Chemosphere 58(5):645–651.

Wik, A. and Dave, G. (2009). Occurrence and effects of tire wear particles in the environment - A critical review and an initial risk assessment. *Environmental Pollution*, 157 (1), pp.1–11.

Wik, A., and Dave, G. (2006). Acute toxicity of leachates of tire wear material to Daphnia magna – variability and toxic components. Chemosphere 64(10):1777–1784.

Williams, R., and Cadle, S. (1978). Characterization of Tire Emissions Using an Indoor Test Facility. *Rubber Chemistry and Technology* 51 (1): 7–25.

Woodward, J., Li, J., Rothwell, J. and Hurley, R. (2021). Acute riverine microplastic contamination due to avoidable releases of untreated wastewater. Nat Sustain 4, 793–802.

Worek, J., Badura, X., Białas, A., Chwiej, J., Kawon, K. and Styszko, K. (2022). Pollution from Transport: Detection of Tyre Particles in Environmental Samples. Energies, 15, 2816.

Wright, S. L., Levermore, J. M. and Kelly, F. J. (2019). Raman Spectral Imaging for the Detection of Inhalable Microplastics in Ambient Particulate Matter Samples. *Environmental Science and Technology*, 53 (15), research-article, American Chemical Society., pp.8947–8956.

Yakovenko, N., Carvalho, A. and Halle, A. (2020). Emerging use thermo-analytical method coupled with mass spectrometry for the quantification of micro (nano) plastics in environmental samples. Trends in Analytical Chemistry 131, 115979.

Yamashita, M. and Yamanaka, S. (2013). Dust resulting from tire wear and the risk of health hazards. *J. Environ. Prot*. 4, 509–515.

Yan, H., Zhang, L., Liu, L. and Wen, S. (2021). Investigation of the external conditions and material compositions affecting the formation mechanism and size distribution of tire wear particles.

Youn, J. S., Kim, Y. M., Siddiqui, M. Z., Watanabe, A., Han, S., Jeong, S., Jung, Y. W. and Jeon, K. J. (2021). Quantification of tire wear particles in road dust from industrial and residential areas in Seoul, Korea. *Science of the Total Environment*, 784, Elsevier B.V., p.147177. [Online]. Available at: doi:10.1016/j.scitotenv.2021.147177.

Zakaria, M.P., Takada, H., Tsutsumi, S., Ohno, K., Yamada, J. and Kouno, E. (2002). Distribution of polycyclic aromatic hydrocarbons (PAHs) in rivers and estuaries in Malaysia: a widespread input of petrogenic PAHs. Environ. Sci. Technol. 36, 1907–1918.

References

Ziajahromi, S., Drapper, D., Hornbuckle, A., Rintoul, L. and Leusch, F. D. L. (2020). Microplastic pollution in a stormwater floating treatment wetland: Detection of tyre particles in sediment. Science of the Total Environment 713 136356.

Ziajahromi, S., Lu, H., Drapper, D., Hornbuckle, A. and Leusch, F. D. (2023). Microplastics and Tire Wear Particles in Urban Stormwater : Abundance, Characteristics, and Potential Mitigation Strategies. Environ. Sci. Technol. 57, 12829−12837.